Department of Molecular & Clinical Cancer Medicine

Deregulation of the folate pathway in respiratory tract cancer: Molecular and functional consequences

Thesis submitted in accordance with the requirements

of the University of Liverpool for the degree of Doctor in Philosophy by

Israa Abd Ali Al-Humairi

September 2017

Supervisors: Dr. Triantafillos Liloglou, Dr. Janet Risk, Mr. Richard Shaw & Prof. John K Field

Dedication

This thesis work is dedicated to my beloved parents for their spiritual support in all aspects of my life, my lovely husband Qasim for his great patience, support and understanding, my lovely sweet kids, Yusur and Mohammed for their smiles that encourage me to overcome the difficulties encountered in my pursuit of the PhD degree, my dearest brothers, sisters, mother and sisters in law whose love and support sustained me throughout.

Acknowledgements

First and foremost, enormous gratitude is due to my primary supervisor Dr. Triantafillos Liloglou who has been there for the whole four years of my study with his unstinting support and constructive critique. His guidance from the initial to the final step in this study, enabled me to develop my understanding on the subject and complete this thesis.

Many thanks are also due to my secondary supervisors Dr. Janet Risk, Mr. Richard Shaw and Prof. John K Field. I am highly indebted to Dr. Amelia Acha-Sagredo for her insightful comments, stimulation and encouragement throughout my study. A specific note of gratitude to Dr. Michael P.A. Davies and Dr. Michael W. Marcus for imparting their knowledge and expertise in this study. I would like to express thanks and gratitude to my colleagues Dr. Ahmed Al-Khafaji, Mrs Bubaraye Uko, Miss Ghaliah Alnefaie, Mr Ben Brown, Miss Beth Barnes, Mr Innocent Gerald, Miss Paschalia Pantazi, Mr Periklis Katapodis, Miss Vivian Dimou and all the members of the Liverpool Lung Project team for their help and support throughout these years. Special thanks to Mrs Beverley Green for taking care of all the administrative issues involved. Particular thanks must also be recorded to the International Support Team (IST) staff at the university, particularly Mr Christopher Bennett, Mr Christopher Fawn and Mrs Bev Sinclair. Finally, my thanks and appreciations also go to MHESR/IRAQ and the Roy Castle Lung Cancer Foundation. This study would not have been possible without their financial and moral support.

Disclaimer:

All of the work presented in this thesis, unless otherwise stated, is the work of the author.

Contents

Abstract

Respiratory tract (lung and head and neck) cancers constitute a significant public health burden, contributing greatly to the cancer-related mortality worldwide. Folate is an essential nutrient for genome stability through its role in regulating DNA biosynthesis, repair and methylation processes. The deregulation of specific genes encoding for enzymes in this pathway has been implicated in several types of cancer including respiratory tract cancer and might be critical for cancer cell growth. Certain folate-related genes are targets of very common anticancer drugs and their expression has been associated associated with the relevant chemotherapeutic response.

The current study sought to expand the current knowledge on folate pathway deregulation in respiratory tract cancer and shed light on as yet unexplored areas. In particular it aims to:

1) explore the expression profile of the core genes of the folate pathway in lung cancer.
2) investigate the potential of sensitising respiratory tract cancer cells to antifolates using well-known epigenetic drugs.
3) assess the impact of manipulating the activity of previously unexplored folate genes on cancer cell response to antifolates.

We evaluated the mRNA expression levels of MTR, AHCY, MAT2A, CBS, DHFR, MTHFR, TYMS, DNMT1 and SHMT1 genes in 104 primary non-small cell lung carcinomas (NSCLC) and adjacent normal tissues, utilising quantitative real time PCR (qPCR). Expression analysis revealed significant expression differences between normal and tumour lung tissues in only six of the examined genes (DHFR, DNMT1, SHMT1, CBS, TYMS and MTHFR) ($p=0.003$, $p<0.001$, $p=0.015$, $p=0.002$, $p<0.001$ and $p=0.014$) respectively. The relative expression of CBS and SHMT1 splice variants was assessed in 53 NSCLC, paired with

adjacent normal tissues using relative fluorescent quantification and qPCR, respectively. CBS variant 3 (CBSv3) and SHMT1 variant 2 (SHMT1v2) were found to be differentially expressed in NSCLC tumour samples compared to adjacent normal tissues.

A significant reduction was observed in the viability of A549 and SK-MES NSCLC cell lines when exposed to the HDAC inhibitor sodium valproate 48 hours prior to treatment with 5-Fluorouracil (5-FU), while no epigenetic sensitisation was established for methotrexate and pemetrexed.

Finally, SHMT1 expression was knocked down in the PE/CA-PJ15 head and neck squamous cell carcinoma (HNSCC) cell line, using short hairpin RNA (shRNA). SHMT1-low clones consistently showed increased sensitivity to the 5-FU anticancer drug in a n expression dose dependent manner. Inhibition of SHMT1 enzymatic activity by the selective inhibitor aminomethylphosphonic (AMPA) acid also potentiated 5-FU activity in the same cell line.

In conclusion, the data generated from this study provides compelling new evidence into the functional role of CBS and SHMT1 splice variants that might influence NSCLC pathogenesis. Moreover, this study uncovers a new role of SHMT1 as a potential modulator of 5-FU based chemotherapy and points to a new strategy for exploiting SHMT1 as a valuable metabolic target for precision 5-FU therapy.

Abbreviation Table

Symbol	Description
3'UTRs	3' Untranslated regions
3DCRT	Three-Dimensional Conformal Radiotherapy
5-FU	5-Fluorouracil
ABC	ATP-dependent Binding Cassette
AC	Atypical Carcinoid
AMPA	Amonimethyl Phosphonic Acid
APS	Adenosine 5' phosphosulfate
BCA	BicinChoninic Acid
BSA	Bovine Serum Albumin
Ct	Cycle-threshold
DAC	5-aza-2'-deoxycytidine (decitabine)
DHF	Dihydrofolate
DHFU	Dihydrofluorouracil
DNMTs	DNA Methyltransferases
DPD	Dihydropyrimidine dehydrogenase
DTYMK	Deoxythymidylate kinase
dTMP	Deoxythymidine Monophosphate
dTTP	Deoxythymidyne triphosphate
dUMP	Deoxyuridine Monophosphate
EBV	Epstein-Barr virus

EGFR	Epidermal Growth Factor Receptor
FDA	Food and Drug Administration
FdUMP	Fluorodeoxyuridine Monophosphate
FdUTP	Fluorodeoxyuridine Triphosphate
FOCM	Folate-Mediated One Carbon Metabolism
FPGS	Folylpolyglutamate synthase
FRs	Folate Receptors
FUTP	Fluorouridine Triphosphate
GGH	Gamma-glutamyl hydrolase
GWAS	Genome Wide Association Study
HBEC	Human Bronchial Epithelial Cells
HCY	Homocysteine
HDACi	Histone Deacetylase Inhibitor
HER2	Heregulin Receptor
HNSCC	Head and Neck Squamous Cell Carcinoma
HPV	Human Papilloma Virus
IMRT	Intensity-Modulated Radiotherapy
KRAS	Kirsten Rat Sarcoma viral gene
LA	locoregionally Advanced
LCNEC	Large Cell Neuroendocrine Carcinoma
LDCT	Low Dose Computed Tomography
LINES	Long Interspersed Nuclear Elements

LLP	Liverpool Lung Project
LLPi	Liverpool Lung Project Risk Projection Model for Lung Cancer Incidence
MET	Methionine
MRPs	Multidrug-Resistant Proteins
MTT	3-(4,5-Dimethylthiazol-2-Yl)-2,5-Diphenyltetrazolium Bromide
MTX	Methotrexate
MTX-PGs	Polyglutamated derivatives of MTX
NSCLC	Non-Small Cell Lung Cancer
OPSCC	Oropharyngeal Squamous Cell Carcinoma
PCFT	Proton coupled folate transporter
PcG	Poly-comb Group proteins
PLP	Pyridoxal Phosphate
PEM	Pemetrexed
PNECs	Pulmonary neuroendocrine cells
R/M	Recurrent/or Metastatic
RFC	Reduced folate carrier
RIN	RNA Integrity Number
ROS	Reactive Oxygen Species
rp	Ribosomal proteins
RQ	Relative Quantification
RTCs	Respiratory Tract Cancers

RTX	Raltitrexed
SABR	Stereotactic Ablative Radiotherapy
SAH	S-adenosylhomocysteine
SAHA	Suberoylanilide Hydroxamic Acid
SAM	S-adenosylmethionine
SCC	Squamous Cell Carcinoma
SCLC	Small Cell Lung Cancer
shRNA	Short hairpin RNA
shRNA	Short hairpin RNA
SINES	Short Interspersed Nuclear Elements
SNP	Single Nucleotide Polymorphism
T/N	Tumour/Normal
TC	Typical Carcinoid
THF	Tetrahydrofolate
TKIs	Tyrosine Kinase Inhibitors
TRAIL	Tumour necrosis factor-Related Apoptosis Inducing Ligand
TSGs	Tumour Suppressor Genes
UNG	Uracil DNA glycosylase
VNTR	Variable Number Tandem Repeat
VPA	Valproic Acid
ΔCt	Delta Cycle threshold

Chapter 1: Introduction

Respiratory tract cancers (RTCs) include lung and head and neck carcinomas, which, combined, represent the highest incidence and mortality rates among cancers world-wide. Almost 2.72 million people (representing 21% of all cancer cases) are affected, demonstrating a combined mortality rate of 28% of all cancer related deaths (Marcus et al. 2013).

1.1 Lung cancer

Lung cancer is one of the most life threatening medical conditions worldwide. For several decades, it has been the most common cancer in the world (Ferlay et al. 2015). In the UK (Figure 1.1), lung cancer is the third most commonly diagnosed cancer, accounting for 13% of all new cases. It has the second highest incident rate in males after prostate cancer with 24,769 diagnosed in 2014. While in females the figures are different; lung cancer has the second highest incidence rate following breast cancer with 21,634 new cases observed in the year 2014. The male: female ratio is around 11:10 (Cancer Research UK, 2014).

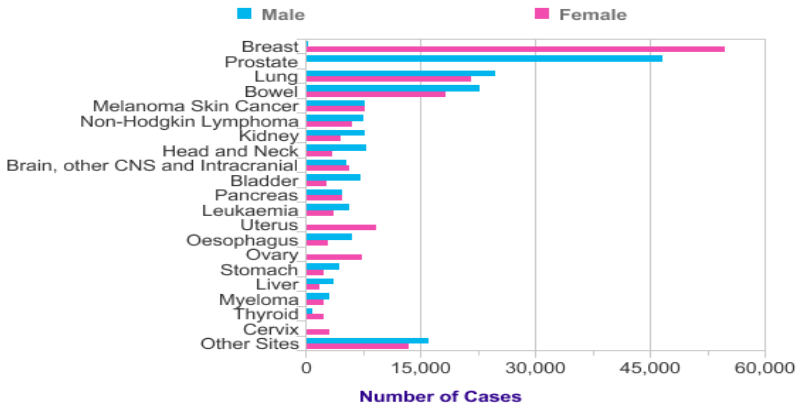

Figure 1.1: Incidence rates of the most frequently diagnosed cancers for the year 2014 in the UK. Number of cases includes both sexes. Taken from Cancer Stats, CRUK website (2014).

Lung cancer is by far the leading cause of cancer-related death worldwide. The lung cancer mortality rates are more than that of colon, prostate and breast combined (Marcus et al. 2013). In the UK, also, it was the most common cause of cancer related death with 35,900 deaths in 2014 accounting for 22% of all cancer deaths in that year (Figure 1.2). The mortality rate is higher in males (19,600 deaths) compared to females, with around 16,300 deaths in the UK. (Cancer Research UK, 2014).

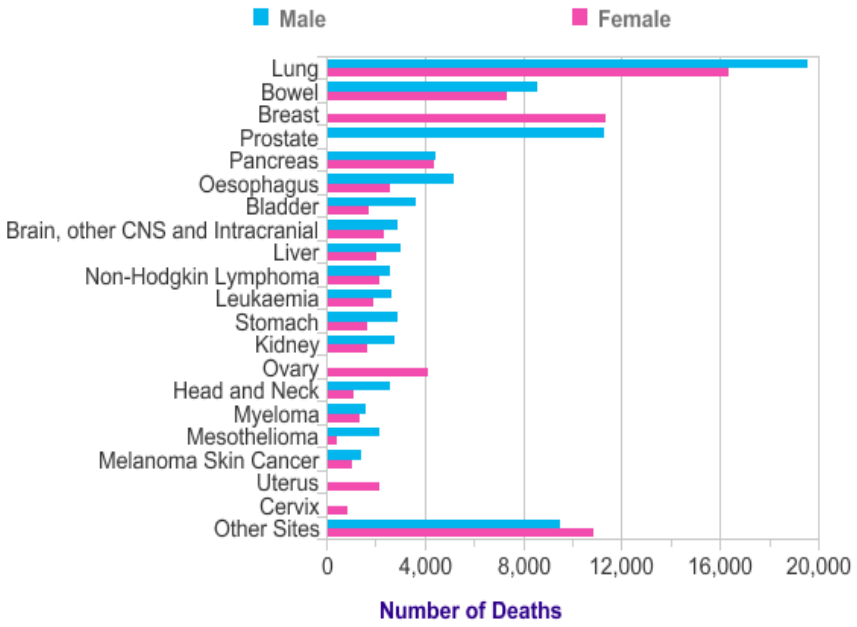

Figure 1.2: Mortality rates for the most common causes of cancer-related death for the year 2014 in the UK. Number of deaths includes both sexes. Taken from Cancer Stats, CRUK website, 2014.

1.1.1 Histological classification of lung cancer

The histological classification of lung cancer is very important, as it determines to a high degree the therapeutic and prognostic implications of the disease. Lung cancer is divided into three main categories: non-small cell lung carcinomas (NSCLC), small cell lung cancer (SCLC) and carcinoid tumours (Davidson et al. 2013). NSCLC is further divided into three major subgroups: adenocarcinoma, squamous cell carcinoma and large cell carcinoma. The 2015 World Health organisation (WHO) Classification of lung cancer is shown in Table (1.1) (Travis et al. 2015).

1.1.1.1 Adenocarcinoma

Adenocarcinoma is the most frequent histological subtype of NSCLC. It is a quite heterogeneous peripheral pulmonary tumour (Figure 1.3) and the prognosis primarily depends on several factors including histological subtype, molecular profile, type of surgical resection and tumour size (Beasley, Dembitzer, & Flores, 2016). The different histological subtypes of adenocarcinomas are shown in (Figure 1.3)(Cagle 2010).

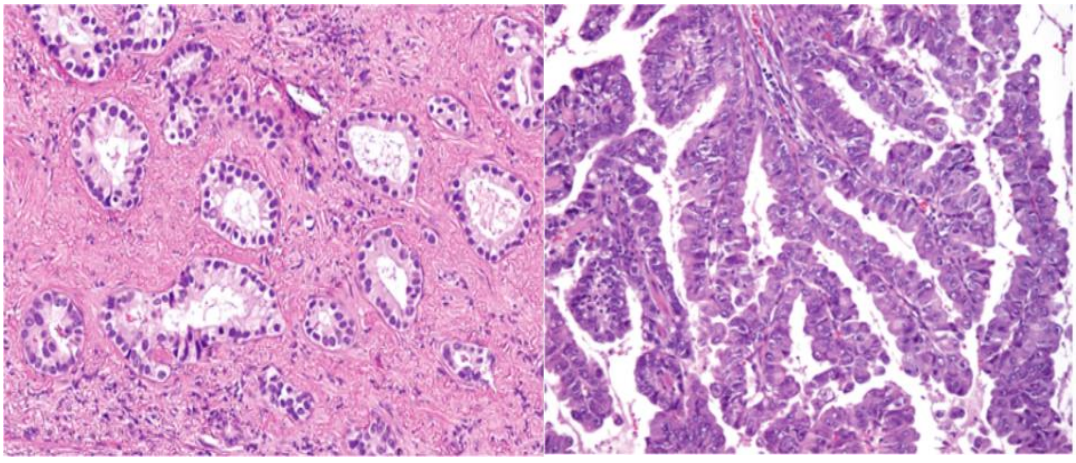

Figure 1.3: Histological presentation of acinar adenocarcinoma (left) and Papillary adenocarcinoma (right). Taken from Cagle (2010).

Table 1. 1: 2015 WHO Classification of malignant epithelial lung tumours. Taken from Travis et al. (2015).

- **Adenocarcinoma**
  - Lepidic adenocarcinoma
  - Acinar adenocarcinoma
  - Papillary adenocarcinoma
  - Micropapillary adenocarcinoma
  - Solid adenocarcinoma
  - Invasive mucinous adenocarcinoma
  - Mixed invasive mucinous and nonmucinous adenocarcinoma
  - Colloid adenocarcinoma
  - Foetal adenocarcinoma
  - Enteric adenocarcinoma
  - Minimally invasive adenocarcinoma
    - Nonmucinous
    - Mucinous
  - Preinvasive lesions
    - Atypical adenomatous hyperplasia
    - Adenocarcinoma insitu
      - Nonmucinous
      - Mucinous
- **Squamous cell carcinoma**
  - Keratinising squamous cell carcinoma
  - Non-keratinising squamous cell carcinoma
  - Basaloid squamous cell carcinoma
  - Preinvasive lesions
    - Squamous cell carcinoma insitu
- **Neuroendocrine tumours**
  - Small cell carcinoma
    - Combined small cell carcinoma
  - Large cell neuroendocrine carcinoma
    - Combined large cell neuroendocrine carcinoma
  - Carcinoid tumours
    - Typical carcinoid tumours
    - Atypical carcinoid tumours
  - Preinvasive lesions
    - Diffuse idiopathic pulmonary neuroendocrine cell hyperplasia
- Large cell carcinoma
- Adenosquamous carcinoma
- Sarcomatoid carcinomas
  - Pleomorphic carcinoma
  - Spindle cell carcinoma
  - Giant cell carcinoma
  - Carcinosarcoma
- Other and unclassified carcinomas
  - Lymphoepithelioma-like carcinoma
  - NUT cell tumour
- Salivary gland-type tumours
  - Mucoepidermoid carcinoma
  - Adenoid cystic adenoma
  - Epithelial-myoepithelial carcinoma
  - Pleomorphic adenoma
  - Papilloma
    - Squamous cell papilloma
      - Exophytic
      - Inverted
    - Glandular papilloma
    - Mixed squamous and glandular papilloma
  - Adenomas
    - Sclerosing pneumocytoma
    - Alveolar adenoma
    - Papillary adenoma
    - Mucinous cystadenoma
    - Mucous gland adenoma

1.1.1.2 Squamous cell carcinoma

Squamous cell carcinoma (SCC) is the second most common type of malignant lung tumour after adenocarcinoma. The typical presentation of squamous cell carcinoma involves a central endobronchial mass with haemoptysis, obstructive pneumonia or lobar collapse. Distant metastasis usually appears later in the course of the disease (Collin et al. 2007). Well-differentiated SCC is characterised by keratinisation with pearl formation and intracellular bridges, however, these features are usually lost in poorly differentiated SCCs. (Figure 1.4)(Drilon et al. 2012).

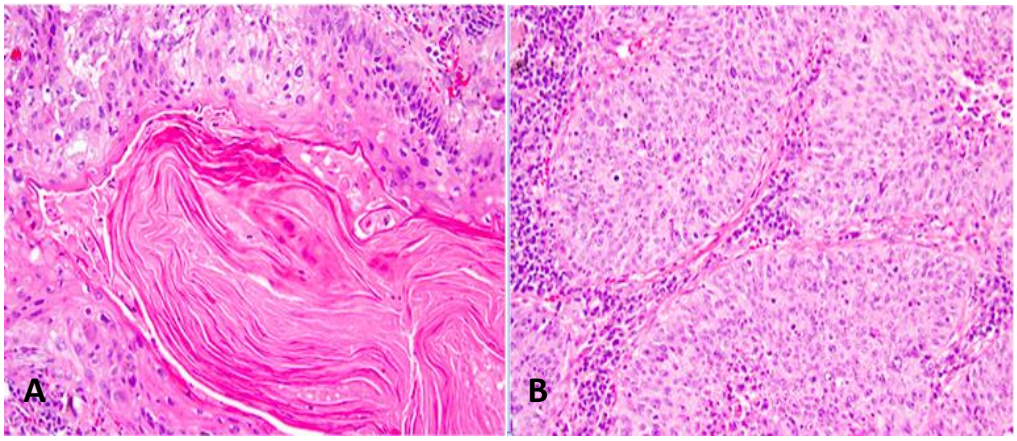

Figure 1.4: **Squamous cell carcinoma of lung. A-Keratinising, B-Non-Keratinising subtypes. Taken from Drilon et al. (2012).**

1.1.1.3 Large cell carcinoma

Large cell carcinomas (LCCs) are a heterogeneous group of lung neoplasms that lack the morphological features of adenocarcinoma, squamous cell carcinoma or small cell lung cancer, thus being referred to as a diagnosis of exclusion (Barbareschi et al. 2011). These poorly differentiated tumours often have a peripheral location, although they may also arise centrally. LCCs tend to be large partially necrotic tumours, composed of nests of large polygonal cells with vesicular nuclei and prominent nucleoli (Figure 1.5) (Travis et al. 2004).

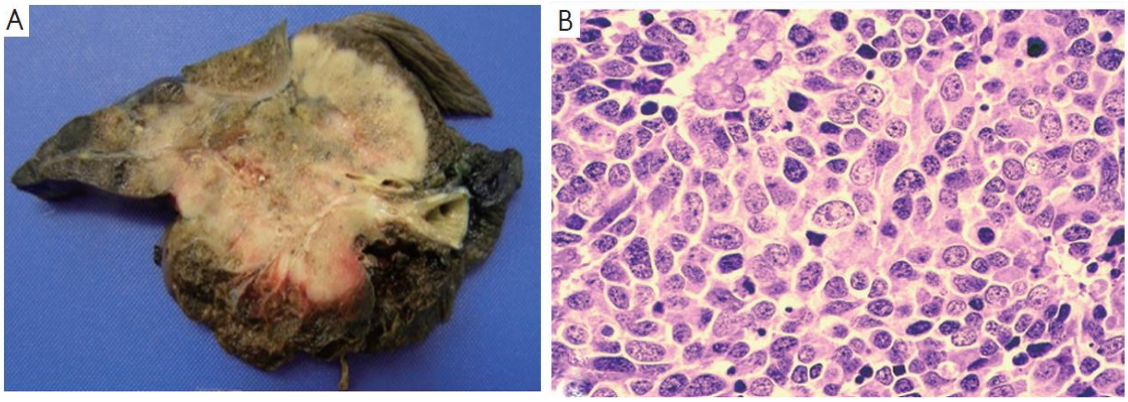

Figure 1.5: Large cell carcinoma of lung. The tumour is often large and partially necrotic (A) and composed of patternless nests of polygonal cells with no obvious histological differentiation. Taken from Travis et al. (2004).

1.1.1.4 Small cell carcinoma

Small cell lung cancer (SCLC) is a highly aggressive tumour with neuroendocrine properties and early development of metastasis (Gustafsson et al. 2008). It has a central location in the majority of cases (Davidson et al. 2013). The tumour cells are characteristically small with distinctive cytological features like an oval-shaped nucleus, scanty cytoplasm and fine granular chromatin (Figure 1.6)(Travis et al. 2004). SCLC has the highest association with cigarette smoking compared to other types of lung cancer (Tartarone et al. 2017). Generally, the prognosis is very poor with a median survival of less than 12 months in case of extensive SCLC (Gaspar et al. 2012).

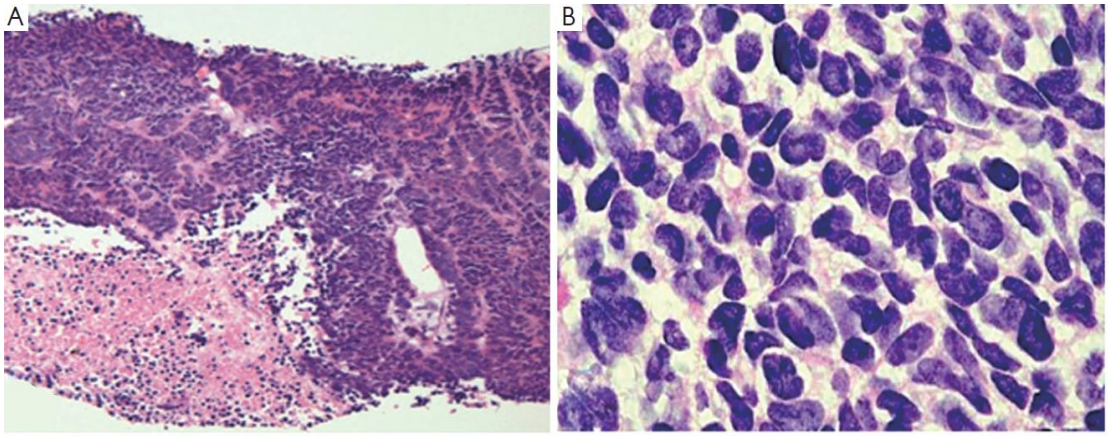

Figure 1.6: Small cell lung carcinoma with typical scanty cytoplasm and hyperchromatic nuclei at A- low B- high magnification. Taken from Davidson et al. (2013).

1.1.1.5 Carcinoid lung tumours

Lung carcinoids are rare neuroendocrine tumours arising from pulmonary neuroendocrine cells (PNECs)(Filosso et al. 2014). They include heterogeneous groups of malignancies that range from the well-differentiated low grade typical carcinoids (TC) and the intermediate grade atypical carcinoids (AC) to the poorly differentiated high grade large cell neuroendocrine carcinomas (LCNEC) and small cell lung carcinomas (SCLC)(Caplin et al. 2015). Histologically, TCs are characterised by their distinctive trabecular growth pattern as a highly vascularised stroma, while the punctuated necrotic (Comedo-like) appearance is the predominate feature of ACs (Figure 1.7)(Rekhtman, 2010).

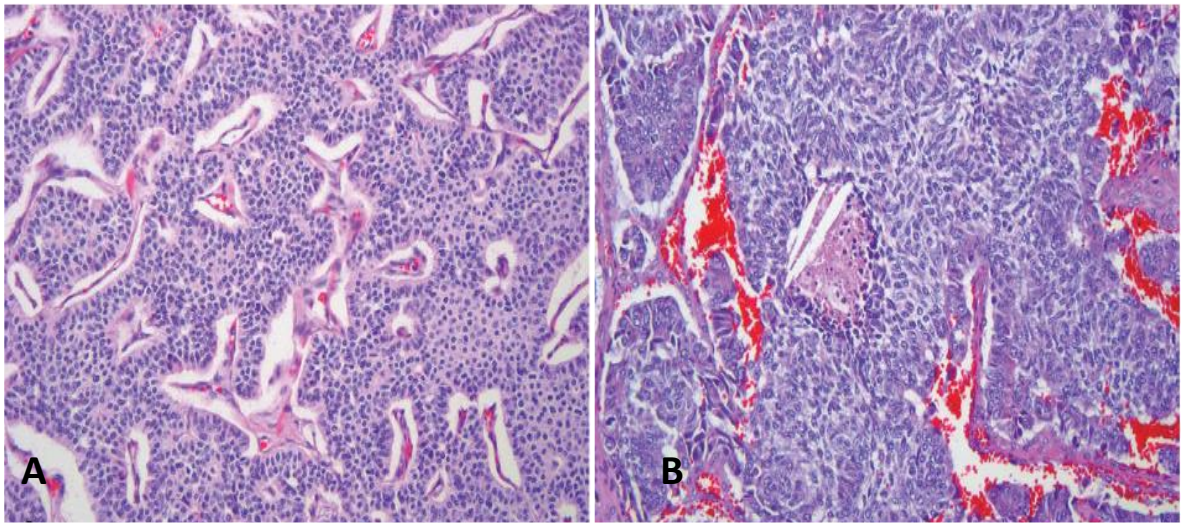

Figure 1.7: Low grade pulmonary carcinoids. A-Typical Carcinoid and B-Atypical Carcinoid. Taken from Rekhtman (2010).

1.1.2 Risk factors

The single most important risk factor for lung cancer is cigarette smoking (Furrukh 2013) . Smokers risk of developing lung cancer is estimated to be on average 10-fold higher than that of non-smokers. Although the overall aim in any lung cancer prevention strategy is to stop smoking, former smokers still have the potential to develop lung cancer years after breaking their cigarette habit (Szabo et al. 2013). In addition to tobacco smoking, important risk factors for lung cancer include age, male gender, a previous history of chronic obstructive pulmonary disease, a family history of early onset lung cancer and other malignancy elsewhere. All these factors are included in the Liverpool Lung Project Risk Projection Model for Lung Cancer Incidence (LLPi)(M. W. Marcus, Chen, Raji, Duffy, & Field, 2015) and are used currently in the UK lung cancer screening trial (UKLS) to identify individuals at high risk of lung cancer that would benefit from a low dose computed tomography (LDCT) scan (Brain et al. 2017).

There are also several lines of evidence suggesting that genomic susceptibility has the potential to modulate lung cancer risk. Genome wide association studies (GWAS) have reported certain loci to be associated with inherited patterns of lung cancer (Amos et al. 2008; Hung et al. 2008).

1.1.3 Therapeutic intervention in lung cancer

1.1.3.1 Surgery

Although not all lung carcinomas are operable at the time of presentation, surgery is still considered to be the cornerstone in the efficient treatment of lung cancer (Baltayiannis et al. 2013). Surgical resection remains the treatment of choice for patients with localised NSCLC (Cortés et al. 2015). The 5-year survival rates for stage I and stage II NSCLC patients treated with complete resection are between 60-80% (Baltayiannis et al. 2013). Due to the rapid development and early metastasis of SCLC, pulmonary resection alone is rarely an option, although a small minority of cases with limited disease may benefit from a combination of surgery and chemotherapy (Inoue et al. 2012; Veronesi et al. 2015).

1.1.3.2 Radiotherapy

Radiotherapy plays a major role in treating inoperable lung cancer patients, for instance elderly patients or those with cardiovascular problems (Oshiro & Sakurai, 2013). Another indication for radiation is widely metastasized incurable tumours, in which radiotherapy is mainly palliative (Shultz et al. 2014). More than 50% of lung cancer patients receive radiation therapy at some point during their treatment course. The ultimate goal of radiotherapy is to achieve a high rate of tumour control with minimal damage to the nearby normal tissue (Oshiro & Sakurai, 2013). Several irradiation techniques such as three-dimensional conformal radiotherapy (3DCRT) and intensity-modulated radiotherapy (IMRT) have been used in lung cancer. Moreover, Stereotactic ablative radiotherapy (SABR) has been approved as a standard care option for inoperable peripheral early stage NSCLC and has shown relatively high local tumour control (Hurst & Chetty 2014).

1.1.3.3 Chemotherapy

Several chemotherapeutic schemes are applied for the treatment of SCLC patients with both limited and extensive-stage disease, bur most patients relapse, despite initial responsiveness, because of the aggressiveness of the tumour and its metastasis at time of presentation (Arcaro 2015). Chemotherapeutic drugs have a significant role in the management of NSCLC, including being utilised either as neoadjuvant therapy (before surgery) or as adjuvant therapy (after surgery). While using adjuvant or neoadjuvant chemotherapy is still controversial, postoperative chemotherapy has become the regimen of choice in clinical practice (Cortés et al. 2015; McElnay & Lim 2014). The most common chemotherapeutic agents available for lung cancer treatment include: (i) Antimetabolites such as pemetrexed and methotrexate (Tomasini, Barlesi, Mascaux, & Greillier, 2016); (ii) Antimitotic drugs such as paclitaxel (Ferrara et al. 2016) and (iii) organometallics, for instance cisplatin (Fennell et al. 2016).

1.1.3.4 Targeted therapy

Novel approaches have been developed for the treatment of cancer patients over the last few years. The discovery of new generations of targeted therapies has revolutionised the management strategy for certain types of cancer including advanced NSCLC (Czarnecka-Kujawa & Yasufuku 2014; Hurvitz et al. 2014) . Several types of targeted therapy are available, including monoclonal antibodies, tyrosine kinase inhibitors and growth factor inhibitors (Arora & Scholar 2005). The most important molecular target in NSCLC is epidermal growth factor receptor (EGFR) mutation. EGFR-tyrosine kinase inhibitors (TKIs) have dramatically improved treatment outcomes in NSCLC patients harbouring these mutations (Milano 2015).

1.2 Head and Neck Squamous Cell carcinoma

The majority of head and neck malignancies (~90%) are squamous cell carcinomas (HNSCC), arising from the epithelial linings of the oral cavity, pharynx and larynx (Vigneswaran & Williams 2014).

1.2.1 Incidence and mortality

Worldwide, head and neck cancers represent the sixth most frequent cancers with around 630,000 new cases reported annually causing more than 350,000 deaths every year (Vigneswaran & Williams 2014). In the UK, head and neck cancers represent the eighth most commonly diagnosed cancer (accounting for 3% of cancer incidence) with 11,449 new cases reported in 2014 (7,918 males and 3,531 females)(Figure 1.1). Moreover, the mortality from several types of head and neck cancers was 3704 deaths in year 2014 in the UK. The figures are higher in men with 2604 cases compared to women with 1100 cases (Figure 1.2) (Cancer Research UK, 2014).

1.2.2 Risk factors

1.2.2.1 Tobacco and alcohol

Cigarette smoking and heavy alcohol consumption are the most important predisposing factors for HNSCC carcinogenesis (Lacko et al. 2014). More than moderate alcohol consumption appears to increase risk of HNSCC particularly cancers of larynx, oropharynx and hypopharynx. Alcohol has also been shown to act in a synergistic way with tobacco smoke resulting in magnifying the latter effects (Pai & Westra 2009). Furthermore, genetic predisposition may have a significant role in HNSCC pathogenesis, since even among heavy smokers, only a small proportion will eventually develop HNSCC (Lacko et al. 2014).

1.2.2.2 Human papilloma virus

Human papilloma virus (HPV) is an important independent risk factor for HNSCC, particularly oropharyngeal squamous cell carcinoma (OPSCC)(Gillison et al. 2000). HPV infection, specifically with the high risk HPV type 16, has been found to play a significant role in the tumourigenesis of OPSCC, often with distinct molecular and clinical criteria (Gillison et al. 2008; Ang et al. 2010; Ndiaye et al. 2014). Interestingly, several studies have shown that HPV positive OPSCC patients have a better prognosis than those with HPV negative smoking related cancers, despite using the same therapeutic intervention (Vigneswaran & Williams 2014; Marur & Forastiere 2016).

1.2.3 Histological description

HNSCCs present a spectrum of histopathological patterns that often develop through multistep processes and are governed by certain genetic and epigenetic alterations progressing from precancerous lesions, through to dysplasia and thence to the full-blown picture of HNSCC (BOŽENA 2016). Disappointingly, the disease is well documented to be highly associated with the development of second tumours, mainly in the lungs, oesophagus, or other parts of the head and neck according to what is called field cancerisation (Leemans et al. 2011). Several histological subtypes of HNSCC have been recognised, some of them have distinctive clinical and molecular features correlating with specific risk factors (Figure 1.8), these include: Human Papilloma virus associated squamous cell carcinoma (Figure 1.8A), Spindle cell carcinoma which is strongly associated with tobacco smoking and alcohol (Fig 1.8B) and Epstein-Barr virus (EBV) associated squamous cell carcinoma (Figure 1.8C) (Shah et al. 2014).

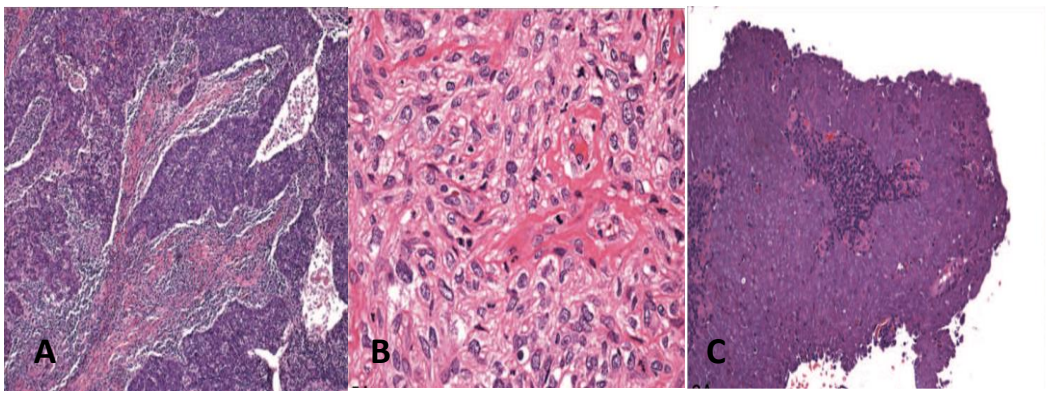

Figure 1 .8: Histological types of HNSCC (A) HPV associated HNSCC, (B) Spindle cell carcinoma, (C) Epstein Bar virus associated HNSCC. Taken from Shah et al. (2014).

1.2.4 Therapeutic Interventions

Therapeutic strategies for HNSCC basically depend on the stage and anatomical location of the tumour (Vermorken et al. 2008; Aung & Siu 2016). For early stage disease, a single modality treatment approach is often used with surgery or radiotherapy (Vermorken et al. 2008). Unfortunately, HNSCCs demonstrate highly malignant phenotypes and the majority of patients present clinically with locoregionally advanced disease (LA-HNSCC)(Pulte & Brenner 2010; Koontongkaew 2013; Safdari et al. 2014). For the best oncologic results, a multidisciplinary treatment regimen is required to manage advanced HNSCCs. In this setting, a combination of chemotherapy with radiotherapy or surgery is often used; however, concurrent cisplatin-based chemo-radiotherapy is the gold standard approach for controlling LA-HNSCC (Forastiere & Trotti 1999; Vermorken et al. 2008; Aung & Siu, 2016). Patients with recurrent and/or metastatic (R/M) HNSCC are not amenable to curative treatment and the therapeutic goal in this situation is mainly palliation. Platinum based chemotherapy is the cornerstone of palliative treatment, either as a single or combined chemotherapy and the most active paradigm of systemic palliative therapy is composed of platinum (cisplatin or

carboplatin) plus fluorouracil or taxanes (Sacco & Cohen 2015). Despite providing some benefit to R/M HNSCC disease patients, the toxicity of platinum based-combination therapy is higher than that with single agent chemotherapy and the prognosis remains dismal (Colevas 2006; Bernier et al. 2009). Recently, cetuximab, a chimeric monoclonal antibody directed against epidermal growth factor receptor (EGFR) has demonstrated some survival benefit in combination with platinum based therapy or as a single agent in platinum refractory patients (Vermorken et al. 2008; Price & Cohen 2012). So far, however, the EGFR inhibitors are the only targeted drugs to be approved and routinely used in the treatment of head and neck carcinomas (Rieke et al. 2016).

1.3 Folate metabolic pathway and cancer

1.3.1 Folate chemistry

In 1931, Lucy Willis, an honorary consultant pathologist at the Royal Free Hospital, made her discovery of a factor in yeast (Willis factor) that she used to treat pregnant women with megaloplastic anaemia (Wills 1931). A few years later, this Willis factor was recognised to be folate (Mitchell et al. 1941).

Folates are essential micronutrients, and include a group of water soluble B-vitamins occurring naturally in foods and as a synthetic form (folic acid). Folate encompasses a family of chemical compounds that have a similar core structure; the parent of this family is folic acid, which is the fully oxidised synthetic form of folates (Scaglione & Panzavolta 2014), and is composed of pteridine ring, para-amino benzoic acid (PABA) and glutamic acid (Figure 1.9)(Gazzali et al. 2016). Folic acid by itself, however, is biologically inactive and needs to be activated through several cellular metabolic steps to be reduced into dihydrofolate (DHF) and then converted to the metabolically active form tetrahydrofolate (THF)(Ducker & Rabinowitz

2016).

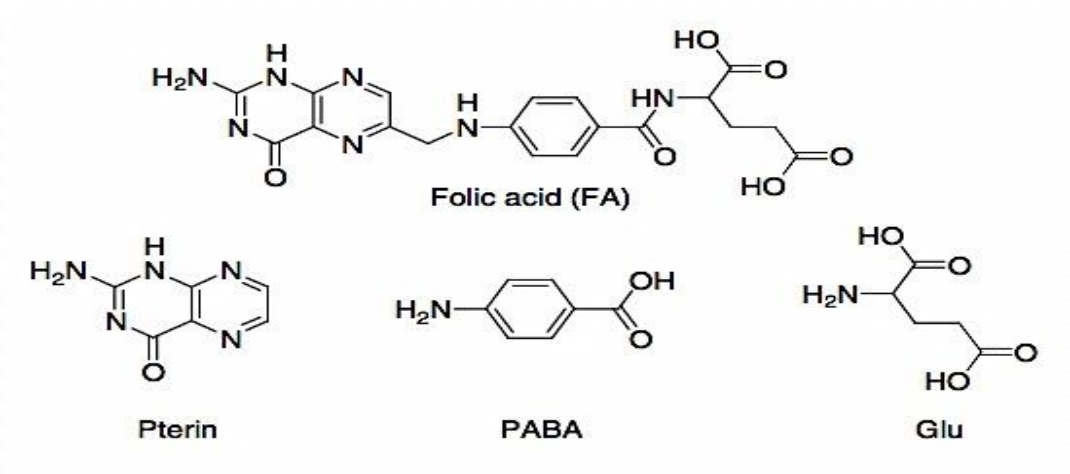

Figure 1.9: Molecular structure of folic acid. Taken from Gazzali et al. (2016).

1.3.2 Folate Metabolism and transport

Humans do not have the ability to synthesise folates. Instead, they primarily depend on intestinal absorption from nutritional sources, mainly green leafy vegetables, oranges and livers in the form of polyglutamates (Liu & Ward 2010; Scaglione & Panzavolta 2014). To be absorbed from the intestinal lumen, dietary polyglutamates must be converted into monoglutamates by the action of intestinal mucosal and the brush border gammaglutamyl-carboxypeptidase enzyme. Unlike dietary folates, folic acid is well absorbed from the intestine without deconjugation of the polyglutamate forms. The most efficient absorption of folates occurs primarily in the proximal small intestine (jejunum) at the cell surface acidic microenvironment by a carrier mediated, pH-dependent mechanism. Following enterocyte uptake, absorbed folate is biotransformed into 5-methyTHF, and then transported by the mesenteric vein to the portal circulation in order to be released in the liver and subsequently delivered to peripheral tissues via systemic circulation as polyglutamated folates (Figure 1.10)(Kim 2007a; Liu & Ward 2010).

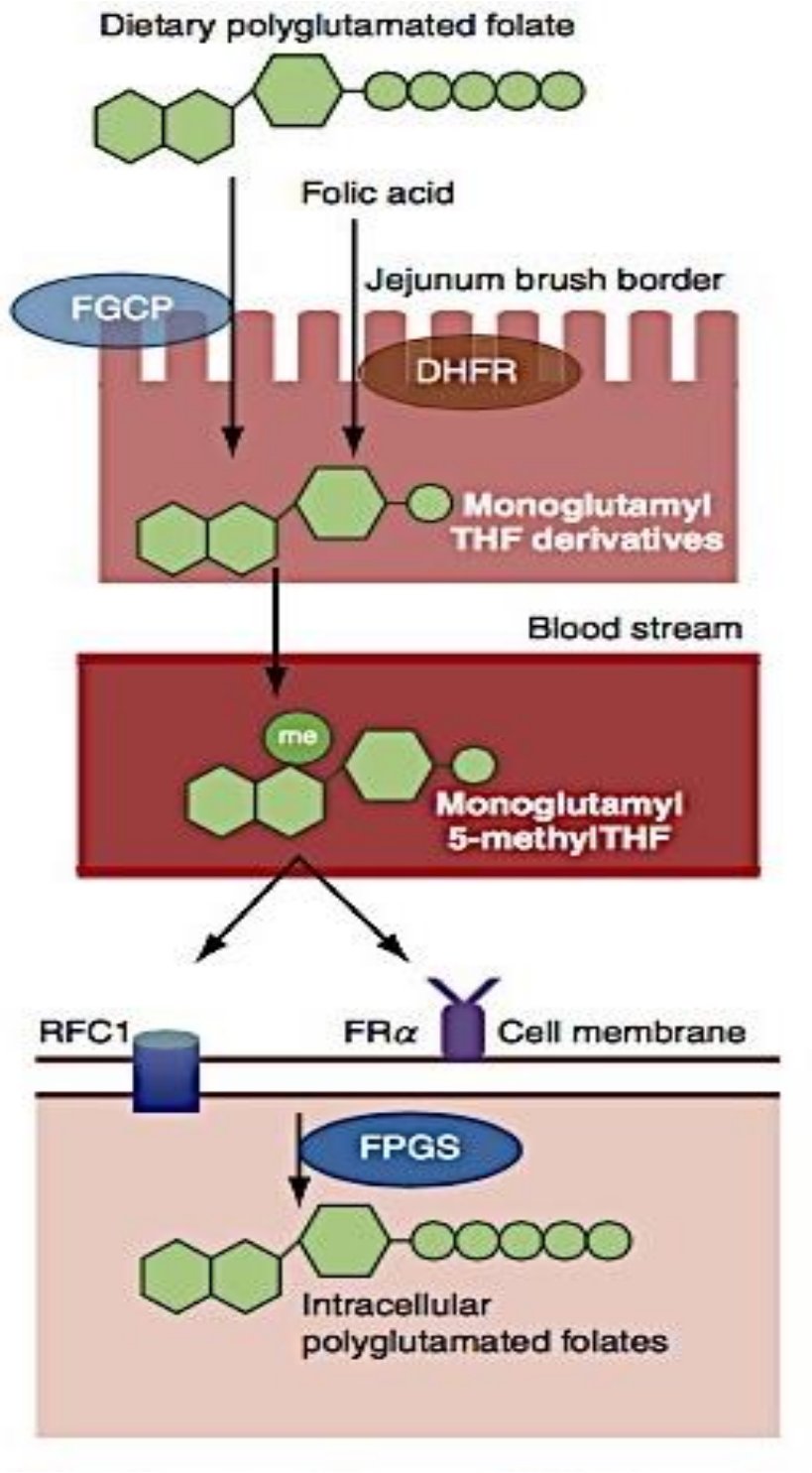

Figure 1.10: Folate absorption and transport. Taken from Liu & Ward (2010).

1.3.2.1 Cellular folate transporters

Folates are hydrophilic negatively charged molecules and therefore only have minimal ability to permeate the plasma membrane through passive diffusion. Instead, specific uptake systems are required for intestinal absorption and delivery of folate cofactors into the peripheral tissues (Zhao et al. 2013). To date, three folate specific transporters are known to facilitate folate cellular entry: (i) Reduced folate carrier (RFC) (ii) Proton coupled folate transporter (PCFT) and (iii) Folate receptors (FRs). RFC is the major folate transporter from blood to the peripheral tissues, relying on a bidirectional ion exchange mechanism to transfer folates across the plasma membrane. While FRs utilise endocytotic mechanism to facilitate folate cellular entry (Liu & Ward 2010). PCFT, the crucial transporter for intestinal folate absorption, functions as a unidirectional symporter, transporting folate as well as protons into cells (Qiu et al. 2006). The structural analogues of natural folate compounds (antifolate drugs) utilise folate transport systems in a similar way to enter the cell and produce their pharmacological effect; for example, RFC has been implicated as the primary transporter for methotrexate (MTX), raltitrexed (RTX) and pemetrexed (PEM) in both normal and neoplastic tissues (Matherly et al. 2007; Gonen & Assaraf 2012). RCF-mediated transport of MTX has been extensively documented as an important parameter for determining MTX inhibitory effect. Further, impaired MTX uptake by RFC results in drug resistance in several malignancies including ALL and osteogenic sarcoma (Zhao et al. 2003; Matherly et al. 2007; Gonen & Assaraf 2012). Although pemetrexed is an excellent substrate for both RFC and PCFT, it has shown higher affinity for the PCFT mechanism as a means to enter into tumour cells (Zhao et al. 2008).

1.3.3 Folate mediated one carbon metabolism

Folate-mediated one carbon metabolism (FOCM) is a complex network of interconnected metabolic pathways. Although it is highly compartmentalised, occurring mainly in the cytosol, nucleus and mitochondria, there is an interdependence of one carbon transfer reactions between these different cellular regions (Desai et al. 2016). Within the folate metabolic network, folate molecules function to activate and transfer one-carbon units obtained from amino acid catabolism (serine, glycine and methionine) for crucial cellular biological processes including methylation reactions, nucleotide biosynthesis and thymidylate and amino acid metabolism (Fox & Stover 2008). While mitochondrial derived formate provides the major supply of one carbons for cytosolic and nuclear FOCM (Fox & Stover 2008; Tibbetts & Appling 2010), direct cytoplasmic serine catabolism can be another source of one carbon moiety through the activity of cytosolic serine hydroxymethyltransferase 1 enzyme (SHMT1), which catalyses the conversion of serine to glycine and the formation of 5,10-methyleneTHF (Fox & Stover 2008; Ducker et al. 2016). Before entering the folate cycle, folic acid passes through a series of chemical transformations in order to be reduced to dihydrofolate, and then to the metabolically active form THF in a reaction catalysed by the critical enzyme dihydrofolate reductase (DHFR). At that point, the one-carbon groups can be carried at N-5 and N-10 positions of THF with different covalent bonds formed between (one-carbon), units and these nitrogen atoms giving rise to different folate coenzymes, these include 5,10-methylene THF, 5-methyl THF, 5-formyl THF and 10- formyl THF (Liu & Ward, 2010; Ducker et al. 2016). Each of those has specific biological roles except 5-formyl THF; instead, it functions as a (one-carbon) reservoir. Interestingly, the intracellular folate metabolism is at the branch of two metabolically interconnected pathways; thymidylate synthesis and homocysteine remethylation (Scaglione & Panzavolta, 2014). Hence, several drugs targeting folate

metabolising enzymes (Figure 1.11) have taken advantage of folates critical role in maintaining cellular growth and proliferation such as 5-FU, MTX and pemetrexed (Figure 1.11)(Robien et al. 2005).

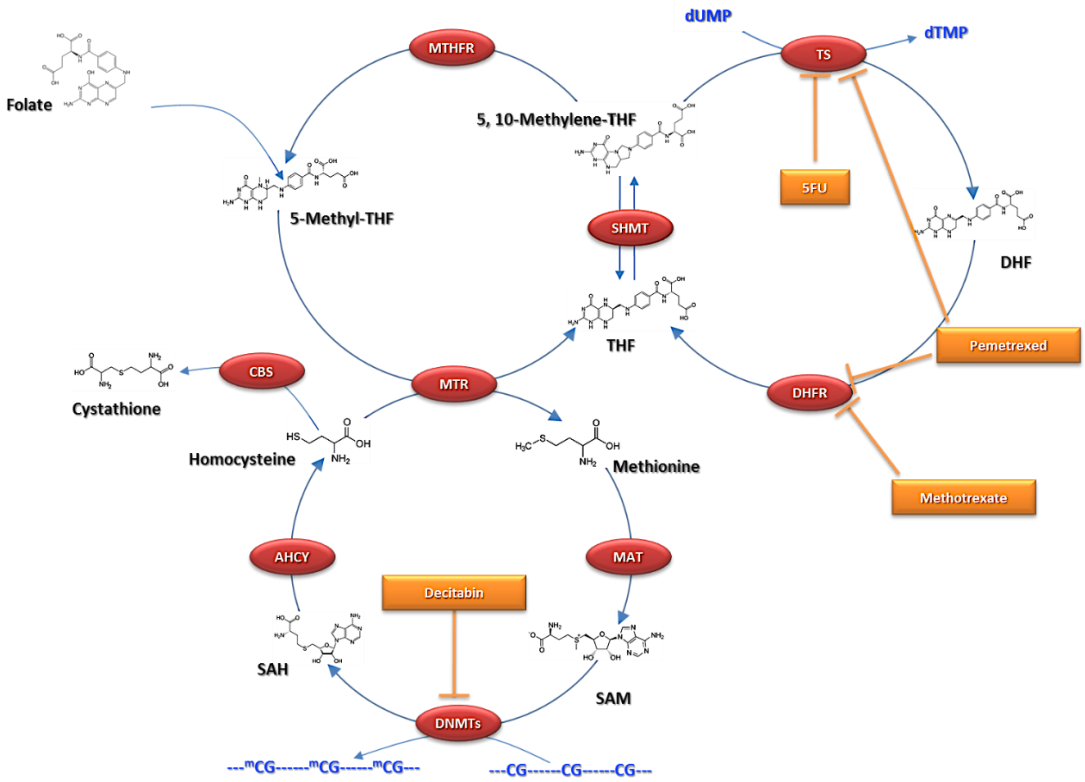

Figure 1.11: Graphic representation of part of the folate metabolic pathway illustrating its connections with the thymidylate biosynthesis pathway and the homocysteine metabolic pathway. Folate genes are shown as red ovals while yellow boxes denote folate targeting drugs.

1.3.3.1 Biochemistry of folate mediated one carbon metabolism

The one carbon transfer performed by folate coenzymes plays an important role in the fundamental cellular processes such as nucleotide biosynthesis and methylation reactions (Chon, Stover, & Field, 2017). 5,10 methylene THF has been implicated as the key player that is required for these important biosynthetic pathways (Ducker et al. 2016). Intracellular folates exist in numerous functionally distinct but metabolically interrelated pools (Figure 1.12)(Liu & Ward 2010).

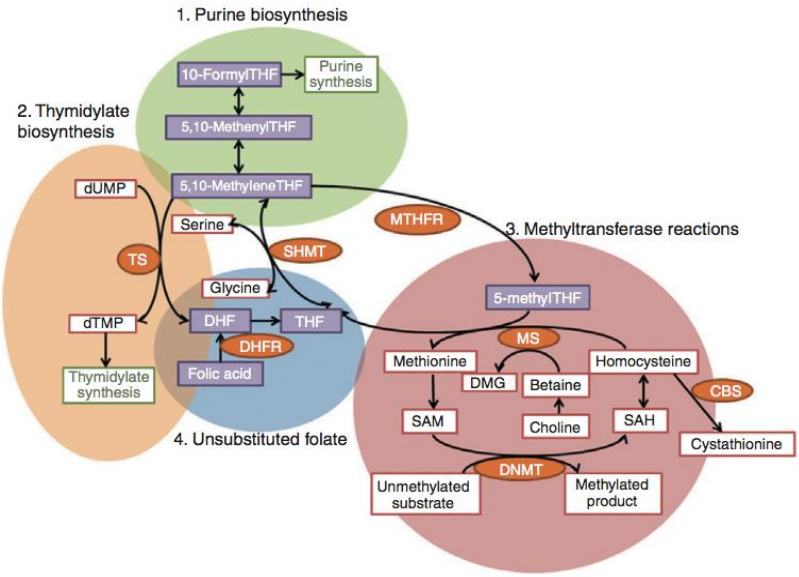

Figure 1.12: Folate metabolic pathway with the main intracellular folate pools. Taken from Liu & ward (2010).

Thymidylate biosynthesis

Folate dependent *de novo* thymidylate biosynthesis is catalysed by the thymidylate synthase enzyme (TYMS), which uses 5,10 methylene THF as a cofactor to methylate deoxyuridine monophosphate (dUMP) into deoxythymidine monophosphate (dTMP), resulting in oxidation

of the THF into DHF. Moreover, thymidylate synthesis is a rate limiting reaction for nucleotide synthesis and for maintaining the balanced pool of dNTPs pool that is crucial for DNA synthesis and repair (Lucock 2000). Given the importance of the thymidylate biosynthesis pathway, drugs targeting it, such as 5-FU, pemetrexed and RTX have had a significant impact on cancer treatment (Wright & Anderson 2012).

Purine biosynthesis

10-formyl THF plays an important role in purine synthesis by donating two one carbon groups to the purine ring at 2 and 8 carbon atoms positions. Two enzymes are required to perform this chemistry; glycinamide ribonucleotide transformylase (GAR Tfase) and aminoimidazolecarboxamide ribonucleotide transformylase (AICAR Tfase)(Scotti et al. 2013; Ducker & Rabinowitz 2016).

Methyltransferase reaction

The 5,10-methylene THF is reduced into 5-methyl THF by the cytosolic NADPH dependent methylene tetrahydrofolate reductase (MTHFR) enzyme. Then, the unique cellular fate of the most reduced folate form (5-methylTHF) is the synthesis of methionine (MET) from homocysteine (HCY) within the homocysteine remethylation cycle (Mudd et al. 2007). The HCY metabolic pathway has a significant physiological importance because it produces MET, the critical amino acid for protein synthesis initiation. Furthermore, MET is the precursor of S-adenosylmethionine (SAM), a general methyl group donor for the most important biochemical cellular reactions, including methylation reactions of RNA, phospholipids and chromatin (CpG islands in DNA and histone proteins)(Scotti et al. 2013). For instance, SAM is the substrate for DNA methyltransferases, which convert it into S-adenosylhomocysteine (SAH) after the transfer of methyl group to an acceptor substrate. SAH, in turn, is hydrolysed

by a SAH hydrolase enzyme into adenosine and HCY (Mentch & Locasale 2016). To this end, HCY is located at the branch point of the pathway, so it is either degraded into cysteine and cystathionine through the transsulfuration pathway or remethylated back to MET by methionine synthase (MS) enzyme (Stead et al. 2004; Mentch & Locasale 2016).

Unsubstituted folates

Unsubstituted folates include DHF and THF folate molecules. They do not have a direct contribution in the folate metabolic pathway but instead, receive one carbon units and transfer them towards either DNA biosynthesis or methylation processes. The MTX antifolate drug is an irreversible inhibitor of DHFR which is required for the reduction of folic acid and DHF into THF, thereby, inhibiting both nucleotide synthesis and methylation reactions (Liu & Ward 2010).

1.3.4 Deregulation of the folate metabolic pathway in human cancer

Given the metabolic importance of folate in maintaining genomic stability by regulating DNA synthesis, repair and methylation, folate depletion can have a potential role in promoting carcinogenesis. Further, folate deficiency has been associated with the development of pancreatic, breast, cervical, oesophageal, colorectal and gastric cancers (Choi & Mason 2000). Limited dietary folate affects normal cellular proliferation and accelerates tumourigenesis through several mechanisms (Figure 1.13)(Liu & Ward, 2010; Duthie, 2011), including:

(i) Impairment of thymidylate synthesis.

(ii) Impairment of purine synthesis.

(iii) Alteration of DNA methylation.

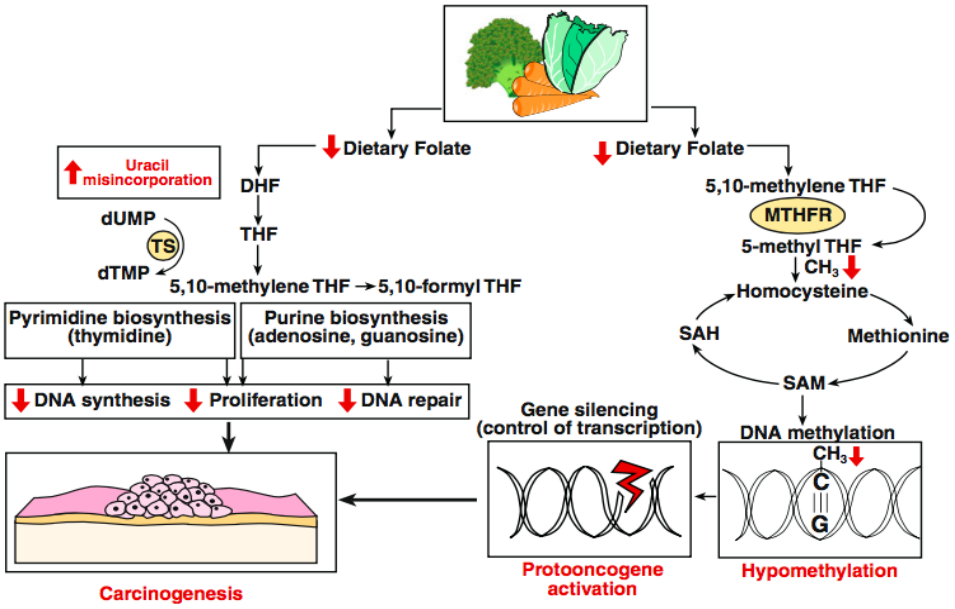

Figure 1.13: Consequences of folate depletion. Taken from Duthie (2011).

1.3.4.1 Impairment of DNA synthesis and repair

Low availability of 5,10-methylene THF retards thymidylate biosynthesis and results in the misincorporation of uracil into DNA instead of thymidine, which is normally removed by DNA repair enzymes. This creates a temporary single strand break in the DNA. If folate limitation continues, the cycle of DNA break and repair is continuously repeated and ultimately results in a double strand break in the DNA, chromosomal instability and cellular transformation (Blount et al. 1997). Excessive uracil content and double strand breakage of DNA have been demonstrated in folate deficient cultured tumour cells of human tissues and blood (Beetstra et al. 2005; Duthie et al. 2008). Likewise, reduced dietary folate perturbs *de novo* purine synthesis leading to alteration of purine and pyrimidine precursors balance and inhibiting normal DNA repair activity. Impaired dNTPs synthesis due to folate deficiency has been

suggested as inducing chromosomal aberration *in vitro*. Cultured cells grown in a folate-depleted media exhibit different patterns of chromosomal breaks, whereas, cells cultured in hypoxanthine supplemented folate deficient medium (hypoxanthine is a purine precursor that bypasses the need for folate in purine synthesis) demonstrate significantly less chromosomal damage (Libbus et al. 1990).

1.3.4.2 Alteration of DNA methylation

Folate deficiency has been associated with an aberrant DNA methylation pattern (Kim 2007).Specifically. Reduced availability of one carbon moieties leads to an attenuation of the homocysteine remethylation cycle, resulting in accumulation of homocysteine and inhibition of DNA methytransferases with subsequent DNA hypomethylation (Yi et al. 2000), disruption of gene regulation, protocogene activation and chromosomal instability (Duthie 2011). Moreover, the DNA damaging effect of folate depletion also includes regional promotor hypermethylation of specific genes, mainly tumour suppressor genes (James et al. 2003; Arasaradnam et al. 2008)

1.4 Molecular pathogenesis of lung cancer

The malignant transformation of normal lung cells passes through an orchestrated multistep process driven by several permanent genetic mutations, mainly point mutation, deletion and translocation, as well as dynamic epigenetic alterations, including abnormal DNA methylation, histone modification, chromatin remodelling and micro RNAs (mRNAs) (Risch & Plass 2008; Langevin et al. 2015). As in all types of cancer, the accumulation of these genetic and epigenetic changes gives rise to dysregulation of growth-promoting oncogenes and growth-suppressing genes and ultimately results in the initiation and progression of lung cancer (Figure 1.13) (Hanahan & Weinberg 2011; Mehta et al. 2015).

1.4.1 Lung Cancer Genetics

It is widely acknowledged that genetic aberrations are the key events in triggering lung carcinogenesis, affecting both oncogenes and tumour suppressor genes (Risch & Plass 2008; Cooper et al. 2013). Oncogenic activation of growth-promoting genes has been observed in >50% of adenocarcinoma subtypes of NSCLC (Yip et al. 2013).

1.4.1.1 Proto-oncogene activation

Genomic studies have identified the most frequently activated oncogenes in lung cancer including KRAS, one of RAS proto-oncogene family which encodes RAS proteins involved in regulation of cellular proliferation, differentiation and survival through controlling signal transduction pathway (Schubbert et al. 2007). KRAS mutation occurs in approximately 20% of all NSCLCs, most commonly in adenocarcinomas (25-40%)(Cooper et al. 2013). Interestingly, KRAS mutant NSCLC cell lines have shown a high level of dependency on folate metabolic pathway *in vivo* with enhanced response to pemetrexed and MTX antifolate drugs compared with wild-type ones (Moran et al. 2014). Deregulation of EGFR that encodes a transmembrane

tyrosine kinase is also involved in the pathogenesis of lung cancer (Fenizia et al. 2015). Active mutation of EGFR has been reported in 10-35% of NSCLC patients (Califano et al. 2015). Along with EGFR, human epidermal growth factor receptor 2 HER2 gene is frequently activated in lung carcinomas. HER2 gene amplification occurs in 20% of NSCLC cases and is also associated with poor outcome and short survival (Heinmöller et al. 2003). Other less frequent activated oncogenes that have been reported in lung cancer include BRAF (Schmid et al. 2009), MET(Engelman et al. 2006) and ALK (Choi et al. 2008).

1.4.1.2 Tumour suppressor genes inactivation

Tumour suppressor genes (TSGs) are crucial for regulating normal cell growth; hence, inactivation of TSGs is an essential mechanism for tumour initiation and progression (Cooper et al. 2013). *TP53* is one of the most notable tumour suppressor genes that plays a fundamental role in tumourigenesis (Gibbons et al.2014). The *TP53* gene encodes a critical transcription factor that regulates the expression of various genes involved in DNA repair, cell cycle progression and apoptosis. Levels of p53 proteins are induced in response to a variety of stress signals including hypoxia, DNA damage and oncogenic activation (Flöter et al. 2017). Consequently, p53 response triggers different types of cellular protective reactions including cell cycle arrest, DNA repair, senescence or apoptosis (Lazo 2017). *TP53* inactivating mutations have been implicated as the most significant genetic events in lung cancers (Cooper et al. 2013). Mutations mainly occur in SCLCs (70-80%) and to lesser extent in NSCLCs (50%) of cases, being more frequent in squamous cell carcinomas than adenocarcinomas (Campling & el-Deiry 2003; Viktorsson et al. 2005).

RB1 is another tumour suppressor gene that is widely disturbed in lung cancer and mostly altered by small deletion, splicing abnormalities and non-sense mutation and has been reported in more than 90% of SCLCs and 20-30% of NSCLCs (Osada & Takahashi 2002).

Less frequent tumour suppressor inactivated genes in lung cancer include the LKB1 whose encoded protein (a serine-threonine kinase) is involved in regulation of important cellular biological process such as cell polarity, cell cycle, chromatin remodelling and energy metabolism (Marignani 2005). LKB1 inhibition occurs in 11-30% of adenocarcinomas through a range of somatic mutation and deletion (Parrella et al. 2002; Matsumoto et al. 2007). In addition, inhibition of the PTEN tumour suppressor gene is seen in only 5% of NSCLCs and more frequently in squamous cell carcinoma than adenocarcinoma patients (Jin et al. 2010).

1.4.1.3 Deregulation folate pathway genes and cancer

Folate is an essential nutrient for preserving genomic stability and DNA methylation. Consequently, deregulation of folate pathway genes might influence cancer risk. Several studies have shown that variation in particular folate genes could be associated with lung cancer risk, including methylenetetrahydrofolate reductase (MTHFR) (Shen et al. 2005; Liu et al. 2008; Piskac-Collier et al. 2011), thymidylate synthase (TYMS) (Shi et al. 2005; Liu et al. 2008), serine hydroxymethyl transferase 1 (SHMT1) (Wang et al. 2007), and cystathionine betasynthase (CBS) (Shen et al. 2005).

1.4.1.3.1 Serine hydroxymethyl transferase

Serine hydroxymethyl transferase proteins encoded by SHMT genes have a key role in the metabolic reprogramming of cancer cells. It catalyses the interconversion of serine to glycine thereby providing the one carbon units for nucleotide biosynthesis and methylation reactions

(Paone et al. 2014). Two SHMTs are found in the human genome, cytoplasmic (SHMT1) and mitochondrial (SHMT2)(Stover et al. 1977; Garrow et al. 1993; Girgis et al. 1998). SHMT2 encodes for two transcripts; SHMT2 and SHMT2α. Interestingly, SHMT2α can not be imported to the mitochondria, and is thus localised mainly in the cytoplasm and nucleus together with SHMT1. The main function of SHMT2 is supporting cytosolic one carbon metabolism (Anderson & Stover 2009). The cytosolic isoform serine hydroxymethyl transferase1 that is encoded by SHMT1 gene is an important player in maintaining cell proliferation by using serine to generate cytosolic 5,10-methylene-THF; with the latter is poised to perform all the major cellular physiological tasks of 1C groups including thymidine synthesis, methylation reaction and purine biosynthesis (Ducker et al. 2016). SHMT1 is frequently deregulated in several types of cancers (Both et al. 2012; Davidson et al. 2014; Kim et al. 2014; Gupta et al. 2017) including lung cancer (Paone et al. 2014; Wu et al. 2016); probably because of its crucial role in sustaining one carbon homeostasis for fuelling essential nucleotides and amino acids as well as adjusting cellular methylation capacities of the rapidly proliferating malignant cells. Interestingly, there is some evidence to suggest that activated SHMT1 may act as a metabolic switch which offers high metabolic priority for thymidylate biosynthesis (Herbig et al. 2002; Anderson & Stover 2009). Moreover, genetic variants of SHMT1 have been found to be associated with increased risk of HNSCC (Zhang et al. 2005) and lung cancer (Wang et al. 2007). Recently, Paone et al. (2014) demonstrated that SHMT1 knockdown in lung cancer cells induces cell cycle arrest and promotes p53 dependent apoptosis, which is caused by uracil misincorporation into the genomic DNA during the DNA replication process. Based on these findings, SHMT1 might be a promising therapeutic target for the treatment of lung cancer patients.

1.4.1.3.2 Cystathionine-beta-synthase

Cystathionine-beta-synthase is a cytosolic enzyme encoded by the CBS gene. It is a member of the pyridoxal phosphate PLP dependant family of enzymes that use (PLP) as a coenzyme in their reactions (Jhee & Kruger 2005). Cystathionine-beta-synthase enzyme is allosterically activated by SAM (Miles & Kraus 2004; Jhee & Kruger 2005). Cystathionine beta-synthase catalyses the conversion of homocysteine to cystathionine through the transsulfuration pathway (Refsum et al. 2004). In addition to clearing homocysteine, CBS is also involved in the production of endogenous biological mediator hydrogen sulphide (H_2S), which is a tumour growth promoting factor that has been implicated in the pathogenesis of breast and ovarian cancer (Bhattacharyya et al. 2013; Sen et al. 2015). CBS expression is tightly regulated by transcriptional, post-translational and epigenetic mechanisms in addition to the hormonal control. CBS deregulation has been reported in numerous malignancies (Kim et al. 2009; Bhattacharyya et al. 2013; Sen et al. 2015; Gai et al. 2016). Moreover, Genomic studies on CBS SNPs have demonstrated a potential association between CBS genetic variants and the risk of developing lung cancer (Shen et al. 2005). The variant allele, rs2850146 (-8283G > C) showed a positive correlation with reduced CBS expression and, elevated levels of homocysteine, as well as increasing the liability for gene specific promoter hypermethylation in the pulmonary epithelium of smokers (Flores et al. 2012).

1.4.1.3.3 Thymidylate synthetase

Thymidylate synthase, the gene product of TYMS is a constitutive enzyme for maintaining cellular the dTMP pools essential for faithful DNA replication and repair through the methylation of deoxyuridylate into deoxythymidylate in the presence of 5,methyleneTHF as a cofactor (Carreras & Santi 1995). Given its importance as the unique source of cellular

thymidylate, TYMS has been of interest as a valuable target for several chemotherapeutic drugs, including 5-FU, MTX, PEM and RTX (Marsh 2005). High levels of TYMS expression have been correlated with resistance to these agents in advanced lung cancer *in vivo* (Shimizu et al. 2012; Wang et al. 2013) and *in vitro* (Oguri et al. 2005). Moreover, TYMS overexpression has been linked with poor outcomes in lung cancers (Grimminger et al. 2010; Ceppi et al. 2012; Sun et al. 2015). Along with other folate pathway genes, TYMS polymorphisms have been identified (Horie et al. 1995). In one case control study, the TS3'UTR variant was associated with an increased risk of lung cancer; however, gene-diet interaction evidence may necessitate further studies (Shi et al. 2005).

1.4.1.3.4 Dihydrofolate reductase

Dihydrofolate reductase enzyme which is encoded by DHFR gene converts the polyglutamated folate into tetrahydrofolate which is in turn loaded with the crucial one carbon units needed for subsequent cellular reactions (Salbaum & Kappen 2012). Diminished dihydrofolate reductase activity contributes to reduction of the cellular THF level and ultimately affects purine and pyrimidine synthesis and methylation processes (Askari & Krajinovic 2010). Dihydrofolate reductase is targeted by antifolate cancer chemotherapeutics including pemetrexed and MTX (Robien et al. 2005). Furthermore, DHFR overexpression is the most important mechanism for acquired resistance to these drugs (Ducker & Rabinowitz, 2016). Genetic studies have suggested that the DHFR genetic variant rs1650697 G>A is associated with favourable prognosis in NSCLC and might be a potential candidate biomarker in this type of lung cancer (Jin et al. 2010).

1.4.1.3.5 Methylenetetrahydrofolate reductase

The methylenetetrahydrofolate reductase that is encoded by the MTHFR gene, is the central enzyme in folate metabolism and homeostasis. It catalyses the irreversible conversion of 5,10-methylene-THF into 5-methyl-THF, the one carbon donor in the homocysteine remethylation reaction (Scotti et al. 2013). Methylenetetrahydrofolate reductase enzymatic activity is affected by several factors such as the potent inhibitor SAM; when present in high concentrations, SAM competitively inhibits methylenetetrahydrofolate reductase, affecting the flux of methyl group for homocysteine remethylation (Crider et al. 2012). Methylenetetrahydrofolate reductase enzymatic activity is also modulated by common MTHFR polymorphisms. The C677T MTHFR genetic variant has been reported to divert the one carbon group in the direction of the thymidine and purine synthesis pathway away from DNA methylation pathway (Quinlivan et al. 2005). Moreover, the most important biological effect of C677T mutation is the aberrant DNA methylation pattern, which is an exceedingly common finding in carcinogenesis (Stern et al. 2000). The MTHFR C677T polymorphism has been shown to be associated with numerous malignancies in (Kim 2007). The association with lung cancer is still controversial, however, with some studies reporting that this type of MTHFR genetic variant is significantly associated with an increased risk of lung cancer (Liu et al. 2013; Wang et al. 2015; Yang et al. 2016) while others have failed to reveal a considerable role of C677T mutation in lung carcinogenesis (Mao et al. 2008; Zhang et al. 2012; Yilmaz et al. 2014).

1.4.2 Lung cancer epigenetics

Epigenetic modifications are the heritable changes in gene expression that exist without alterations in the primary DNA sequence; they include DNA methylation, histone modification, chromatin remodelling and non-coding RNAs (Ong et al. 2012). The interplay of these mechanisms makes up an "epigenetic landscape" that controls the way the human genome expresses itself in different tissues, developmental stages and pathological disorders, including cancer (Sharma et al. 2010). Several studies have identified the role of epigenetic reprogramming in cancer cell initiation and progression (Sharma et al. 2010; Martin et al. 2011).

1.4.2.1 DNA methylation

DNA methylation is credited as the first and the most widely studied epigenetic modification (Holliday & Pugh 1975; Langevin & Kelsey 2013). It plays an important role in epigenetic regulation by controlling gene expression and chromatin architecture (Sharma et al. 2010; Lin et al. 2014). DNA methylation primarily occurs by the covalent addition of the methyl group on the fifth carbon position of cytosine residue (5mC) within the CpG dinucleotide sequence (Langevin & Kelsey 2013). CpG dinucleotides are under-represented and unevenly distributed across the genome, often found as small clusters called CpG islands that are located in the 5' end of genes occupying about 60% of human promoters (Saxonov et al. 2006). During development and differentiation, the genome is globally methylated, thereby maintaining genomic stability, while most promoter CpG islands (CGIs) remain predominately unmethylated (Liloglou et al. 2014). DNA methylation is accomplished by DNA methyltransferase enzymes (DNMTs) that catalyse the transfer of the methyl group from the universal methyl donor (SAM) into the cytosine residue. To date, five DNMTs have been

discovered: DNMT1, DNMT2, DNMT3a, DNMT3b and DNMT3L (Kulis & Esteller 2010). DNMT1, or maintenance methyltransferase enzyme, plays a major role in transmitting original DNA methylation patterns through multiple generations with high fidelity. In this context, DNMT1 is responsible for restoring the pre-existing methylation patterns onto the newly synthesised DNA following DNA replication process (Kulis & Esteller 2010; Liloglou et al. 2014; Subramaniam et al. 2014). While DNMT3a and DNMT3b are the *de novo* methyltransferases that are involved in *de novo* DNA methylation (Jones & Liang 2009). Interestingly, DNMT2 is mainly involved in RNA methylation instead of DNA (Okano et al. 1998). Although DNMT3L does not act as cytosine methyltransferase, it stimulates *de novo* methylation mediated by DNMT3a, as well as provoking transcriptional silencing through interaction with histone deacetalyse 1 (Chedin et al. 2002; Deplus et al. 2002). Moreover, the establishment of the DNA methylation machinery is mediated by the organised activity of DNMTs and associated factors such as poly-comb group proteins (PcG), which interact with DNMTs in the presence of the general methyl donor (SAM) (Robertson 2001). The DNA methylation process is generally associated with the cessation of gene expression (Figure 1.14) (Liloglou et al. 2014). This is achieved either by creating a physical barrier for some transcriptional factors such as AP-2, c-myc, CREB/ATF, E2F and NF-kB, thereby inhibiting the transcriptional factors binding to promoter binding sites, and ultimately blocking transcriptional activation (Kulis & Esteller 2010; Sharma et al. 2010) or by recruiting methyl binding proteins (MBPs) that in turn interact with histone deacetylases (HDACs), called repressive epigenetic modification enzymes, resulting in chromatin reorganisation so that it becomes compacted and no longer accessible for transcriptional machinery (Figure 1.15) (Lopez-Serra & Esteller 2008). In addition to mediating transcriptional suppression, DNA methylation has a profound impact on maintaining genomic stability through other

mechanisms, including inactivation of X-chromosome, genomic imprinting (Jones & Baylin 2007; Portela & Esteller 2010) as well as silencing of repetitive and parasitic DNA sequences that otherwise have a detrimental illegitimate effect on genetic stability by causing transcriptional deregulation of adjacent genes (Robertson 2005).

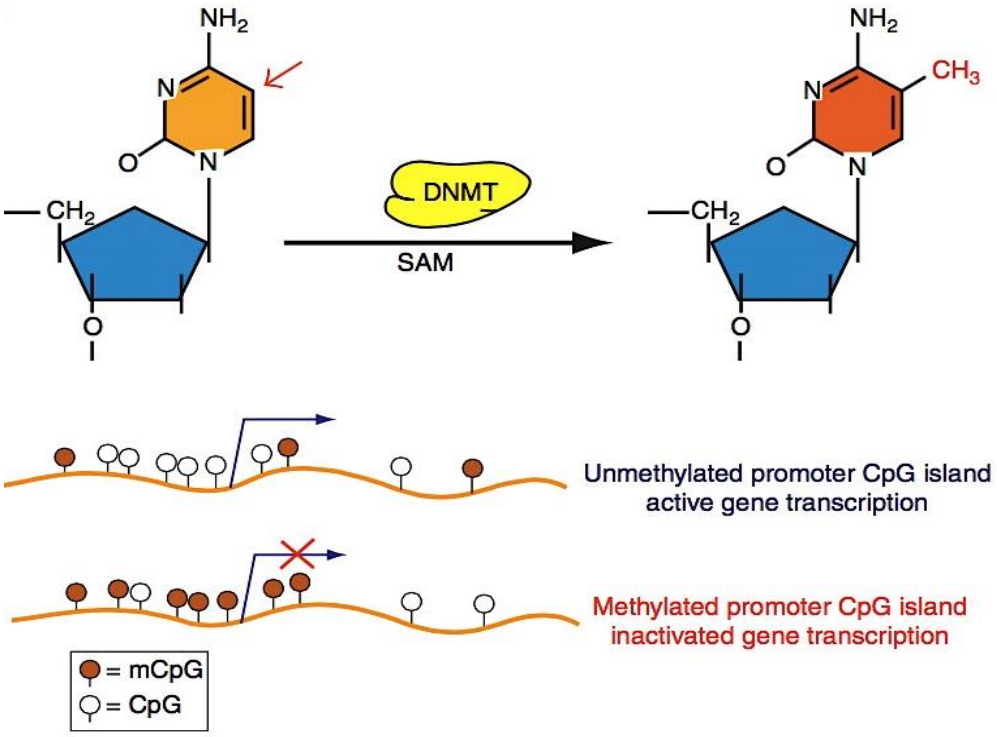

Figure 1.14: DNA methylation at 5-position of cytosine residue and associated gene silencing. Taken from Kulis & Esteller (2010).

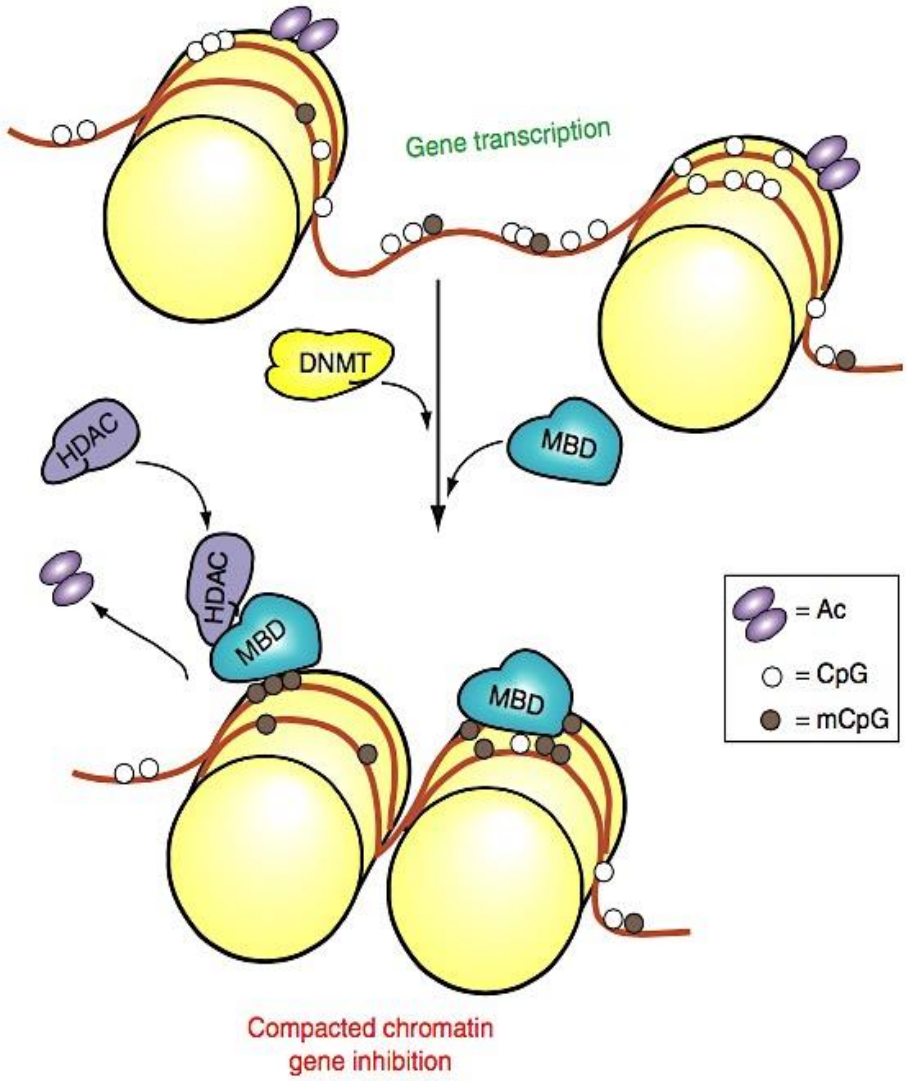

Figure 1.15: transcriptional repression mechanism induced by DNA methylation through recruitment of methyl binding domain proteins (MBD) with subsequent association with histone deacetylases (HDACs) resulting in chromatin reorganisation and inhibition of transcription machinery. Taken from Kulis & Esteller (2010).

1.4.2.1.1 DNA Methylation in lung cancer

The relationship between DNA methylation and cancer was first observed in 1983, when the genome of tumour cells was shown to be hypomethylated, compared to their normal counterparts (Feinberg & Vogelstein 1983). It is now well established that genomic methylation patterns are profoundly altered in tumour cells (Frigola et al. 2006; Wilson et al. 2007; Irizarry et al. 2009). Indeed, cancer cells methylome is quite different from that of normal ones; the fact that both genome-wide hypomethylation and regional promoter hypermethylation events occur concomitantly in cancer suggests the importance of epigenetic mechanisms in tumour initiation and progression (Baylin & Jones 2016). Studies on DNA methylation in lung cancer have strongly emphasised the importance of aberrant genomic DNA methylation in the pathogenesis of lung cancer (Heller et al. 2010; Heller et al. 2013). In this context, an increasing number of tumour suppressor genes (TSG) have been reported to be inactivated by hypermethylation of their promoter CpG islands during lung carcinogenesis (Li et al. 2013; Mehta et al. 2015). While regional promoter hypermethylation is a high incidence early event in lung carcinogenesis, global DNA hypomethylation is an equally common phenomenon in lung cancer. Genome-wide loss of methylation predominately affects repeated DNA sequences such as LINES (long interspersed nuclear elements), SINES (short interspersed nuclear elements), satellite repeats and imprinted genes (Kulis & Esteller 2010) and can result in genomic instability (Daskalos et al. 2009)

1.4.2.1.1.1 DNA methylation in the diagnosis of lung cancer

Several studies have suggested the potential of using aberrant DNA methylation patterns as a biomarker for the diagnosis and clinical monitoring of patients with lung cancer, particularly the aberrant methylation of promoter regions affecting the driver genes involved in critical cellular functions (Sandoval et al. 2013). In this context, numerous aberrantly methylated

genes have been identified in the tumour tissue, bronchioalveolar lavage, sputum, plasma and serum of lung cancer patients (Table 1.2) such as *RAR2* (Ponomaryova et al. 2011), SHOX2 (Kneip et al. 2011). (Dietrich et al. 2012). Over the last decade, a plethora of blood-based DNA methylation assays have been used in clinical research as a minimally invasive source of samples to detect aberrant DNA methylation signatures in cell free DNA (cfDNA) in plasma, serum (Begum et al. 2011) or peripheral blood leukocytes (Wang et al. 2010) in lung cancer (Balgkouranidou et al. 2013).

Table 1.2: DNA methylation biomarkers in diagnosis of lung cancer. Taken from Sandoval et al. (2013)

Epigenetic marker	Biological material	Diagnostic value
SHOX2	Bronchioalveolar lavages	78% Sn, 96% Sp
SHOX2	Plasma	60% Sn, 90% Sp
RARB2	Plasma (Csb-CirDNA)	70% Sn, 63% Sp
RARB2	Csb-CirDNA	63% Sn, 51% Sp
APC, CDH1, MGMT, RASSF1, DCC and AIM1	Serum	75% Sn, 73% Sp
Cir: Circulating; Csb: Cell surface-bound; Sn: Sensitivity; Sp: Specificity		

1.4.2.1.1.2 DNA methylation in lung cancer treatment

DNA methylation has been aggressively pursued as a promising therapeutic target for lung cancer (Liu et al. 2013). In fact, DNA methyltransferase inhibitors (DNMTi) are the most extensively studied agents (Mehta et al. 2015). The US Food and Drug Administration (FDA) has approved decitabine (5-aza'-2-deoxycytidine and azacytidine (5-azacytidine) hypomethylating agents for the treatment of myeloid malignancy (Issa 2007; Yang et al. 2010). Both drugs are cytidine analogues, incorporating themselves into the DNA of rapidly

growing tumour cells during replication and forming covalent adducts with DNA methyltransferases (DNMTs), and thereby specifically inhibiting these enzymes and inducing hypomethylation (Zeller & Brown 2010) and re-expression of previously silenced genes through promoter hypermethylation *in vitro* (Figure 1.16) (Sharma et al. 2010; Belinsky 2015)). Although both decitabine and azacytidine have the same biological mechanism of action, decitabine is considered to be a more potent DNA methylation inhibitor than azacytidine, since it is able to incorporate specifically into DNA, while 5-azacytidine is predominately integrated into RNA and can only bind DNA after conversion into 5-aza-2'-deoxycytidine (decitabine)(Navada et al. 2014; Mehta et al. 2015). Although they have shown substantial therapeutic potential in haematological malignancies, the effectiveness of decitabine and 5-azacytidine in solid tumours remains limited, however (Graham et al. 2009). Interestingly, these demethylating agents have demonstrated a promising response in lung cancer cell line models through inhibition of DNA methylation and reactivation of epigenetically silenced tumour suppressor genes (Merlo et al. 1995; Cantor et al. 2007; Fang et al. 2012). There is, therefore, a sound rationale for the use of 5-azacytidine and decitabine therefore in lung cancer treatment; as yet however, clinical studies employing hypomethylating drugs have not generally revealed an objective disease response (Digel & Lübbert 2005; Schrump et al. 2006).

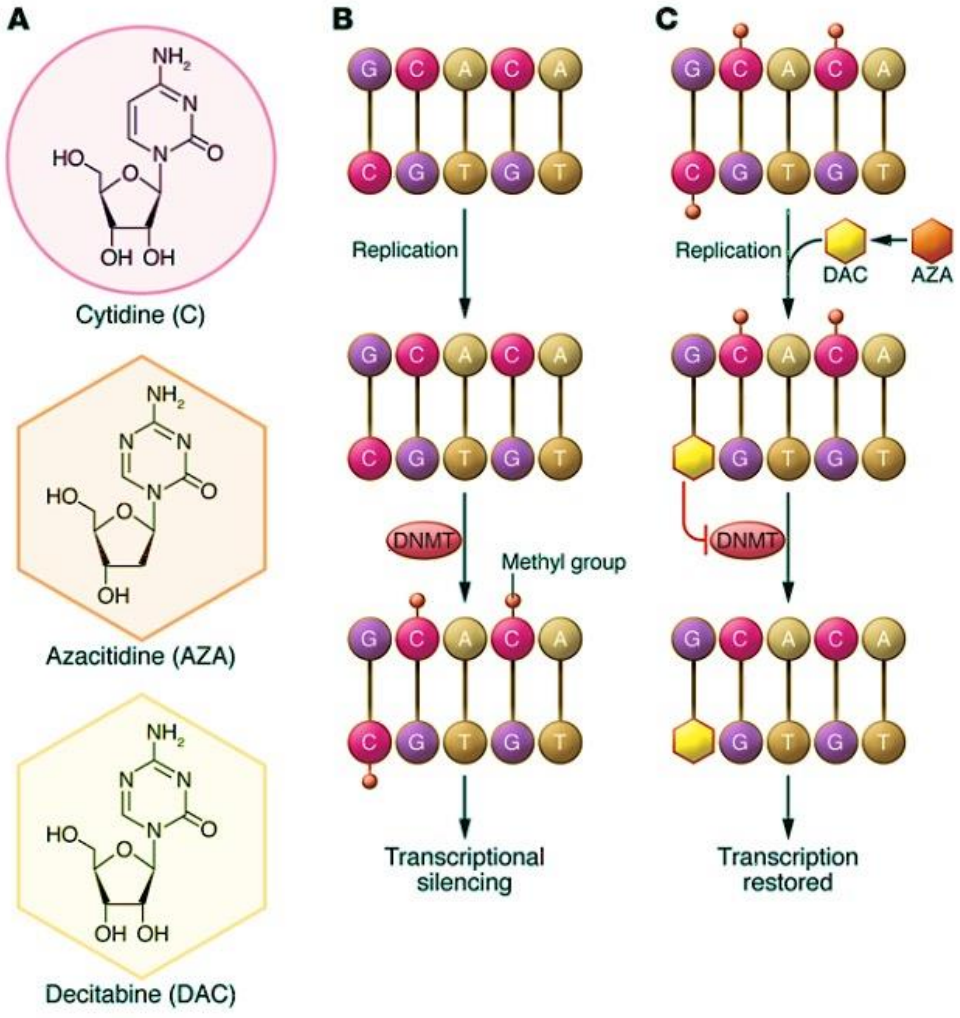

Figure 1.16: Mechanism of depletion of DNMTs for decitabine and 5-azacytidine. (A) Chemical structure of cytidine, azacytidine and decitabine (B) Gene promoter methylation of cytidine blocks transcriptional factor binding resulting in transcription repression and epigenetic silencing (C) During replication, azacytidine is converted into decitabine, and then integrated into DNA, substituting cytidine. Both drugs inactivate DNMTs, thereby blocking DNA methylation and resurrecting the expression of previously inactivated genes. Taken from Navada et al. (2014).

1.5 Epigenomic footprint of folate

Various epigenomic molecular modalities depend largely on DNA methylation reactions to define the activities of epigenetic factors, as well as for identifying the specific epigenetic mark (Salbaum & Kappen 2012). While the biological relevance of folate for epigenetic events has been derived from the view of folate involvement in the provision of SAM for methylation reactions and in maintaining the cellular methyl donor pool (Kim 2004; Kim 2005), a direct and positive link between DNA methylation status and folate level must be assumed given that folate is a rate-limiting factor for DNA methylation reactions. In this scenario, a high level of folate results in an increase in DNA methylation status; conversely, low folate levels lead to reduced DNA methylation. This prevailing view has changed dramatically recently, however (Salbaum & Kappen 2012). Evidence from several experimental studies has suggested a higher level of complexity in this relationship since folate deficiency could result in different aberrant DNA methylation patterns ranging from global DNA hypomethylation, global DNA hypomethylation associated with promoter hypermethylation for specific genes, global hypermethylation and no change at all in DNA methylation status (Kim et al. 1995; Duthie et al. 2000; Crott et al. 2008; Protiva et al. 2011). Indeed, the effect of folate deficiency on DNA methylation and subsequent tumourigenesis is more sophisticated, variable and influenced by several factors, including the cell and organ type, stage of transformation, extent and duration of folate limitation and genetic variants of folate pathway genes (Kim 2007). Moreover, folate has been found to have a significant effect on gene expression through mechanisms other than DNA methylation. Provita et al. (2011) for example, provided support for the notion that folate can significantly regulate gene expression without changing global or promoter DNA methylation status in colorectal cancer (Protiva et al. 2011).

As well as affecting DNA methylation, the epigenetic impact of folate involves other realms of the epigenome such as microRNA (Davis & Ross 2008; Shookhoff & Gallicano 2010) and histone methylation (Luka et al. 2011; Garcia et al. 2016). Overall, therefore, more complicated regulatory relationships need to be considered than were previously anticipated (Salbaum & Kappen 2012).

1.6 Folate pathway targeting therapy

Chemotherapeutics targeting folate metabolism are among the most successful drugs used in cancer treatment (Wright & Anderson 2012). They inhibit key enzymes in the folate metabolic pathway (Table 1.3) (Robien et al. 2005) namely TYMS, DHFR, MTHFR, B-glycinamide ribonucleotide transformylase (GARFT), 5-amino-4-imidazolecarboxamide ribonucleotide transformylase (AICARFT). The therapeutic effectiveness of drugs targeting folate metabolising enzymes is largely attributed to folate role in cellular replication, with disruption of folate resulting in the interruption of nucleotide biosynthesis as well as reduced growth and proliferation of neoplastic cells (Robien et al. 2005).

1.6.1 Thymidylate synthase inhibitors

TS targeting agents are well-established anticancer drugs used in the management of the most-difficult-to-treat haematological and solid malignancies, including NSCLC and colorectal and pancreatic carcinomas, either alone or in combination with other therapeutic regimens (Wilson et al. 2014). TS plays a key role in maintaining the proliferation and survival of cancer cells by providing the sole source of deoxythymidyne triphosphate (dTTP), the essential precursor for DNA replication and repair (Taddia et al. 2015). Additionally TS has been reported to repress p53 tumour suppressor gene activity (Ju et al. 1999) and demonstrate oncogenic-like behaviour when forcibly overexpressed in mammalian cells (Rahman et al. 2004). The TS enzyme is therefore a critical pinch-point for inhibition in cancer chemotherapeutics. The enzyme is a homodimer that contains binding sites for folate (5,10-CH2THF) and nucleotide (dUMP) substrates; hence, disruption of TS enzymatic activity is achieved by inhibitors binding to these sites. Agents targeting TS fall into two structurally different categories: fluoropyrimidine, which targets nucleotide binding sites, and antifolates, which target folate binding sites (Wilson et al. 2014).

Table 1.3: Clinically used folate antagonists and TYMS inhibitors. Taken from Robien et al. (2005)

Generic name	Target enzyme(s)	Approved clinical oncology use
Methotrexate	DHFR (primary), TYMS, MTHFR, GART, AICARFT	Leukemia, lymphoma (Burkitt and Non.Hodgkin), breast cancer, head and neck cancer, osteosarcoma.
Trimetrexate	DHFR	NSCLC, prostate and colorectal cancers
Edatrexate	DHFR	NSCLC, advanced braest cancer, head and neck cancers, soft tissue sarcomaand non. Hodgkin lymphoma
PT523	DHFR	NSCLC, cervical, breast and endometrial cancers
Lometrexol	GART (primary), AICARFT	NSCLC
5-Fluorouracil (5-FU)	TYMS	Colorectal, pancreatic, stomach, breast cancers, basal cell carcinoma
Capecitabine	TYMS	Colorectal and breast cancers
Pemetrexed	TYMS (primary), DHFR, GART	Malignant pleural mesothelioma, NSCL
Ralitrexed	TYMS	Colon cancer
Nolatrexed	TYMS	Hepatocellular carcinoma
Tegafur	TYMS	Breast, gall bladder, gastrointestinal, head and neck, liver and pancreatic cancers
Plevitrexed	TYMS	Gastric, pancreatic and ovarian cancers

1.6.1.1 Fluoropyrimidines

5-Fluorouracil (5-FU) is the best-known fluoropyrimidine, it was first synthesised by Heidelburger et al. in 1957 (Heidelberger et al. 1957), and continues to be one of the most widely used drugs in cancer therapy for numerous types of solid tumours (Table 1.3), such as head and neck, breast and pancreatic cancers (medlineplus.gov). Furthermore, several randomised clinical trials have demonstrated the effectiveness of 5-FU derivatives in the treatment of NSCLC (Kawahara et al. 2001; Ichinose et al. 2004; Kato et al. 2004). 5-FU has also shown a promising effect in mutant KRAS NSCLC cells *in vitro*, in combination with tumour necrosis factor-related apoptosis inducing ligand (TRAIL)(Wang et al. 2015).

1.6.1.1.1 Mechanism of 5-Fluorouracil action

5-FU is a uracil analogue with a flourine atom at the C-5 position instead of hydrogen. It enters the cell via a facilitated transport mechanism (Wohlhueter et al. 1980), then undergoes intracellular conversion into three main active metabolites, fluorodeoxyuridine monophosphate (FdUMP), fluorodeoxyuridine triphosphate (FdUTP) and fluorouridine triphosphate (FUTP). These 5-FU active metabolites interfere with RNA synthesis and TYMS activity. Also, they can be misincorporated into DNA, resulting in DNA strand breaks and eventually apoptotic cell death (Longley et al. 2003).

Approximately 80% of administered 5-FU is degraded in the liver by the action of dihydropyrimidine dehydrogenase (DPD) enzyme that converts 5-FU into dihydrofluorouracil (DHFU)(Figure 1.17)(Diasio & Harris 1989).

TYMS inhibition: Fluorodeoxyuridine monophosphate (FdUMP) metabolite forms a covalent ternary complex with the TYMS enzyme and 5,10 MTHF, thereby inhibiting dTMP synthesis by blocking dUMP binding (Sommer & Santi 1974). Depletion of dTMP causes deoxynucleotide pool imbalances and disrupts DNA synthesis and repair leading to lethal DNA damage (Yoshioka et al. 1987; Houghton et al. 1995). Furthermore, 5-FU induced TYMS inhibition results in dUMP accumulation that may subsequently result in increased dUTP levels (Mitrovskiet al. 1994; Aherneet al. 1996).

RNA misincorportaion: FUTP metabolite is extensively incorporated into RNA and interferes with normal RNA processing and function (Longley et al. 2003). 5-FU containing RNA has been shown to inhibit normal processing and maturation of mRNA, tRNA and rRNA precursors thereby potentially disrupting normal cell viability and metabolism (Cammico & Glazer 1979; Santi & Hardy 1987; Ghoshal & Jacob 1994; Mojard et al. 2013).

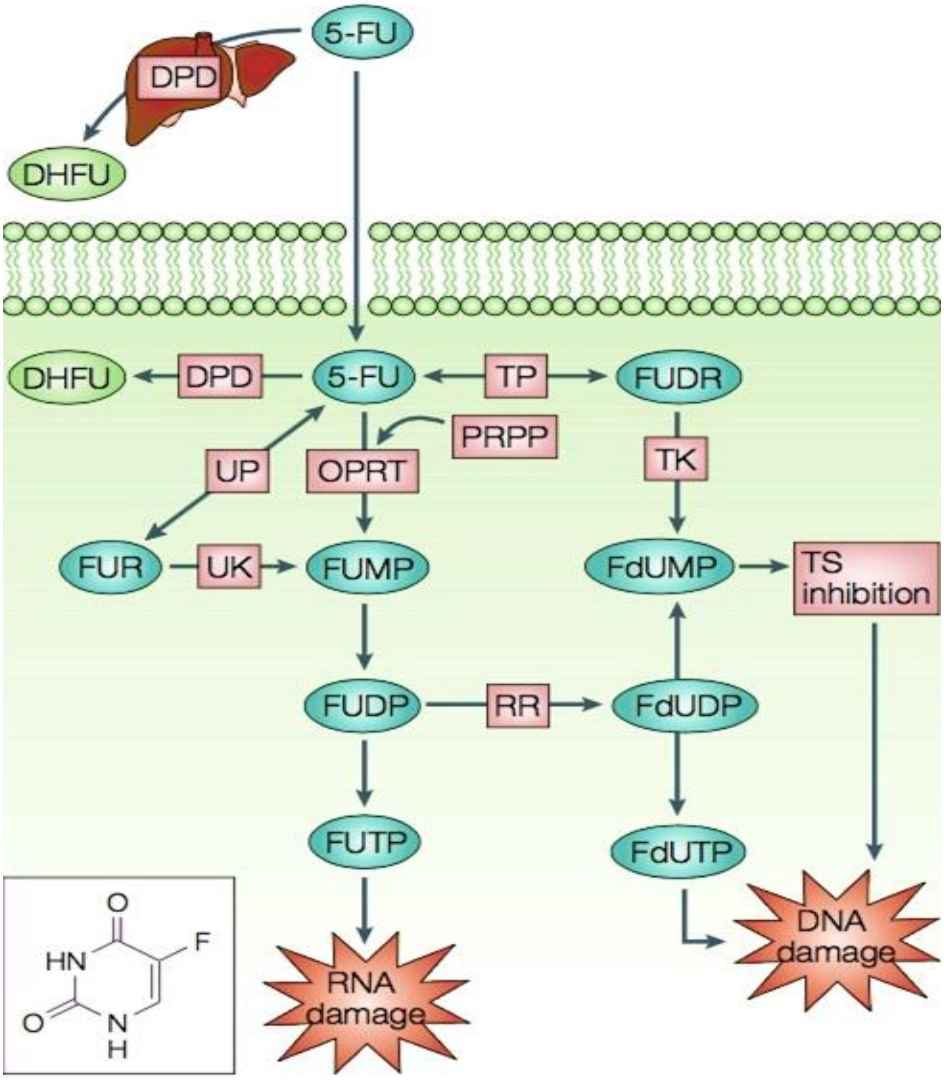

Figure 1.17: Structure and metabolism of 5-fluorouracil. The 5-FU activation pathway is either direct, through the action of orotate phosphoribosyl transferase (OPRT) using phosphoribosyl pyrophosphate (PRPP) as a cofactor, or indirect, through fluorouridine (FUR) by the activity of uridine phosphorylase (UP) and uridine kinase (UK) enzymes, thereby converting 5-FU into (FUMP), which is then phosphorylated to fluorouridine diphosphate (FUDP). In turn, (FUDP) can either be converted to fluorodeoxyuridine diphosphate (FdUDP) through the enzymatic activity of ribonucleotide reductase (RR) or phosphorylated to fluorouridine triphosphate (FUTP). The latter can in turn be phosphorylated or dephosphorylated, generating FdUTP and FdUMP active metabolites, respectively. An alternative pathway for 5-FU activation is through conversion into fluorodeoxyuridine (FUDR) in a thymidine phosphorylase dependent reaction. The latter is then phosphorylated into FdUMP by thimydine kinase (TK). Taken from Longley et al. (2003).

1.6.1.1.2 Resistance to 5-Fluorouracil

Despite its anticancer efficacy, resistance to 5-FU based chemotherapy remains an important reason for treatment failure, and a significant limitation on its use in clinical applications (Zhang et al. 2008). Several factors have been implicated in 5-FU resistance, such as cell cycle disorders, abnormal metabolism of target enzymes, mismatch repair deficiency, deregulation of drug transportation and apoptosis resistance; nonetheless, the molecular mechanism behind 5-FU resistance has yet to be fully understood (Deng et al. 2017). Overexpression of TS is widely acknowledged as the major mechanism for 5-FU resistance (van Triest et al. 1999; Oguri et al. 2005). Moreover, the efficacy of 5-FU treatment can also be changed as a result of TS mutation or polymorphism, leading to alteration of enzyme structure and possibly affecting the binding of 5-FdUMP. An increasing number of these alterations have been analysed, and particular attention has been paid to the presence of different 28-bp variable number tandem repeats (VNTR) in the 5'-UTR of TS (Scartozzi et al. 2011).

Similarly, high expression of dihydropyrimidine dehydrogenase DPD has been shown to be associated with a marked reduction in the antitumor effect of 5-FU (Salonga et al. 2000). The predictive role of DPD is still controversial, however, since several other studies have reported no statistical significance between DPD expression level and response rate to Fluoropyrimidine-based chemotherapy (Kodera et al. 2007; Meulendijks et al. 2015). Recently, microarray analyses have demonstrated that miRNAs play a vital role in reducing 5-FU efficiency through different molecular mechanisms in multiple cancer cell lines. Gotanda et al. (2013) and Li et al. (2015) found that TYMS is a target of *miR*-433 and *miR*-203, which modify the chemosensitivity of 5-FU in Hella cells and colonic cancer cells, respectively.

In addition, several other miRNAs have been implicated in 5-FU resistance, including *miRNA*-497 (Guo et al. 2013), *miRNA*-221 (Zhao et al. 2015), *miRNA*-141(Shi et al. 2015) and *miRNA*-137 (Xiao et al. 2014).

1.6.1.2 Antifolates

Folate antagonists are structural analogues of folate that use the same facilitative transporters as physiological folate for their cellular entry, namely folate receptors (FRs), reduced folate carrier (RFC) and proton coupled folate transporter (PCFT) (Zhao et al. 2013). In addition to inhibition of the thymidylate biosynthesis pathway, antifolates target other key enzymes in folate metabolism, such as DHFR, GARFT and AICARFT (Hagner & Joerger 2010). The interest in antifolates started in 1948 when Farber and Diamond noticed that administration of folic acid conjugates to children with acute leukaemia exacerbated the process of the disease, so they proposed that reversing this phenomenon might be achieved by treating leukaemic patients with a folic acid antagonist. Indeed, one of the earliest folate analogues, aminopterin, induced temporary remission of childhood leukaemia in 10 out of 16 children with acute leukaemia (Farber & Diamond 1948). Eventually, aminopterin homologue, or MTX, was established with an improved therapeutic index, (Goldin et al. 1955) and clinically introduced as a primary antifolate drug that is still successfully used in the treatment of numerous malignancies, including leukaemia, lymphoma, osteosarcoma, breast cancer and head and neck cancers (Hagner & Joerger 2010; Wilson et al. 2014). After that, several novel antifolate drugs with improved pharmacological properties have been developed including RTX, pemetrexed and pralatrexate (PTX)(Visentin et al. 2012).

1.6.1.2.1 Methotrexate

The antifolate drug MTX was introduced into clinical practice sixty years ago and is still widely used as a chemotherapeutic agent for several types of cancer, including lung and head and neck cancers (Wilson et al. 2014). It acts by interrupting folate homeostasis through inhibiting several critical folate metabolising enzymes (Kodidela et al. 2014). The major transporters for MTX entry into the tumour cell are RFC-1 or SLC19A1. Once inside the cell, MTX is polyglutamated by the enzyme folylpolyglutamyl synthase (FPGS) (Figure 1.18). The polyglutamated derivatives of MTX (MTX-PGs) are important determinants of its pharmacological activity (Genestier et al. 2000) since both MTX and MTX-PGs inhibit the DHFR enzyme, resulting in accumulation of dihydrofolates and depletion of tetrahydrofolate stores (Kodidela et al. 2014), thereby causing cessation of vital one-carbon dependent cellular processes (Zhao et al. 2013). Although DHFR is the primary target, the main cytotoxic driver of MTX is thymidylate depletion through potent competitive inhibition of TS by MTX-PGs (McBurney & Whitmore 1975; Moran et al. 1979). In addition, MTX has been found indirectly to inhibit the thymidylate synthesis reaction through impairment of 5,10-MTHF cofactor recycling, resulting in potent suppression of thymidylate synthesis and ultimately impeding DNA replication and repair (Hryniuk 1975). Moreover, polyglutamated forms of MTX inhibit other folate enzymes including GARFT, AICAR (thereby affecting purine *de novo* synthesis) and MTHFR, which is indirectly influenced by MTX mediated depletion of intracellular folate pools (Zhao et al. 2013; Kodidela et al. 2014). Consequently, malignant cells are unable to synthesise DNA or RNA, which affects their proliferation capacity and leads to further damage, eventually promoting cancer cell apoptosis (Hagner & Joerger 2010).

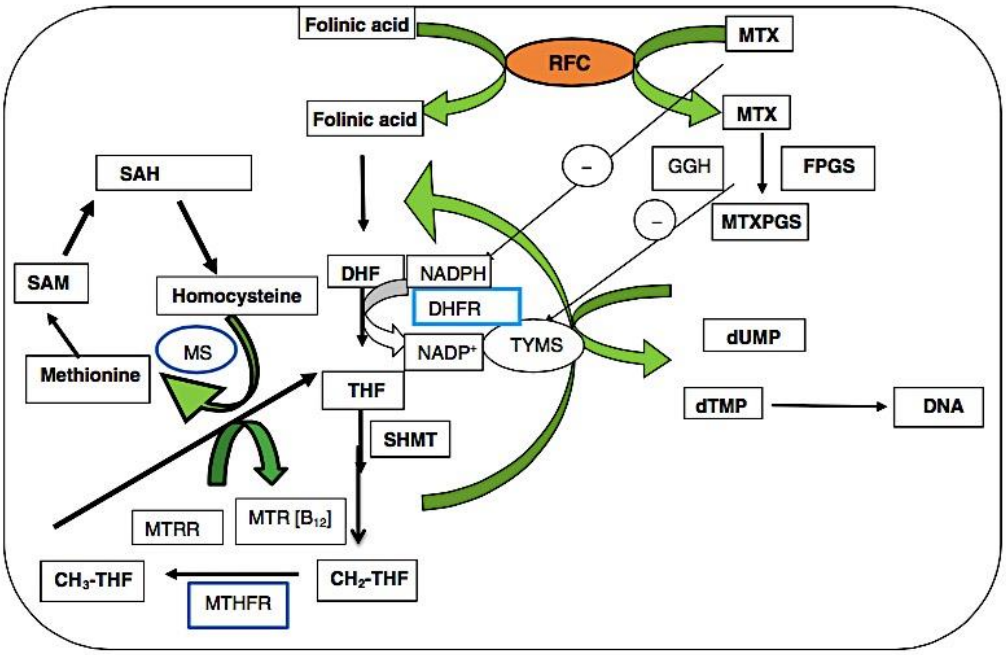

Figure 1.18: MTX cellular pathway. Taken from Kodidela et al. (2014)

1.6.1.2.2 Pemetrexed

Pemetrexed (PEM) is a multi-target antifolate drug that is approved by the U.S. Food and Drug Administration (FDA) for treatment of locally advanced and metastatic NSCLC (Cohen et al. 2005) and has been evaluated in a range of solid tumours, including head and neck carcinomas (Latz et al. 2006; Argiris et al. 2013). Interestingly, pemetrexed has an histology driven specificity for non-squamous NSCLC (Scagliotti et al. 2009; Scagliotti et al. 2011; Rijavec et al. 2013). Pemetrexed exerts its antitumour effect through disrupting folate dependent metabolic processes important for cellular replication and proliferation (Figure 1.19). The drug is transported into the tumour cell by three main folate transporters: Alpha folate receptor, reduced folate carrier (RFC) and Proton coupled folate transporter (PCFT). Once in the cell, pemetrexed is rapidly and extensively polyglutamated into its active derivatives by the action of folylpolyglutamate synthase. Polyglutamated metabolites have a longer half-life

and better affinity for target enzymes than the parent drug (Baldwin & Perry 2009). It plays a critical role in disturbing DNA synthesis through inhibition of the key enzymes for purine and pyrimidine synthesis, TS, DHFR, GARFT and AICART, thereby inducing cell cycle arrest. Several studies have demonstrated the potential predictive role of intratumoural expression of TS mRNA in respect to the response to pemetrexed therapy in patients with NSCLC (Shimizu et al. 2012; Wang et al. 2014; Olaussen & Postel-Vinay 2016; Yang et al. 2017).

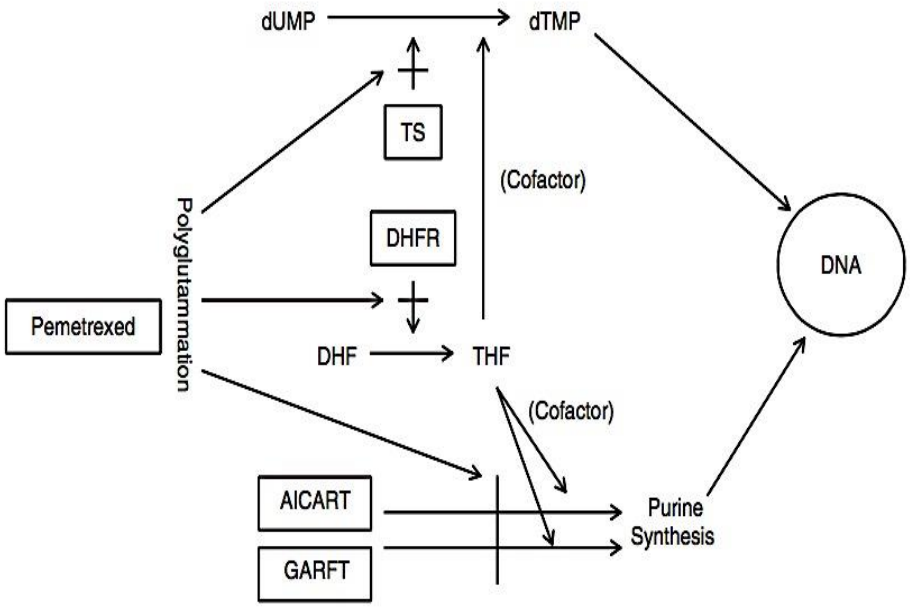

Figure 1.19: Mechanism of action of pemetrexed. Taken from Rijavec et al. (2013).

1.6.1.2.3 Molecular mechanisms underlying resistance to antifolate drugs in cancer

Various molecular mechanisms frequently provoke resistance to antifolate containing chemotherapy and hinder their therapeutic efficacy (Figure 1.20)(Gonen & Assaraf 2012). The documented mechanisms that render antifolate agents ineffective include:

(i) Impaired cellular uptake

RCF is the major transporter mediating antifolate cellular entry. A reduced transportation capacity of RFC is frequently associated with inactivated mutation, allele loss and reduced expression or silencing, thereby contributing to antifolate resistance (Visentin et al. 2012). Decreased RFC expression has been reported in several malignancies with resistance to MTX (Levy et al. 2003; Kastrup et al. 2008; Wang & Li 2014). To date, however, no mechanism of resistance associated with impaired membrane transport has been documented in pemetrexed resistant cells (Visentin et al. 2012).

(ii) Loss of FPGS function

Polyglutamylation is crucial for antifolate cellular retention and pharmacological activity; hence impaired FPGS activity is an important mechanism for polyglutamylation-dependent antifolate resistance. A large number of studies have documented a markedly reduced activity of FPGS in drug-resistant cancer cell lines following treatment with MTX, pemetrexed and RTX antifolates (Chéradame et al. 1999; Mauritz et al. 2002; Liani et al. 2003; Stark et al. 2009; Wojtuszkiewicz et al. 2016).

(iii) Overexpression of the target genes

The higher the expression level of the target enzymes for antifolates, the smaller the fraction of these enzymes required to sustain their normal metabolic function, and the higher the concentration of antifolate drugs required to fully block their action (Gonen & Assaraf 2012). In fact, DHFR amplification has been identified as one of the underlying mechanisms for MTX resistance in both cancer cell lines and tissue samples from cancer patients (Scionti et al. 2008; Morales et al. 2009). Likewise, increased expression of the primary target, TYMS, as well as other targets such as DHFR and GARFT, has been correlated with pemetrexed resistance in NSCLC cell lines (Giovannetti et al. 2005; Ozasa et al. 2010; Yang et al. 2014).

(iv) Overexpression of Gamma-glutamyl hydrolase (GGH)

GGH enzyme is responsible for hydrolysing the gamma-glutamyl chain of folates and folate antagonists and converting them into monoglutamates, thereby maintaining the cellular folate homeostasis (Raz et al. 2016). High GGH hydrolytic activity results in antifolates extruding out of the cell, reducing their efficacy and reducing intracellular folate pools (Schneider & Ryan 2006; Gonen & Assaraf 2012; Yoshida et al. 2016). Moreover, epigenetic modulation and SNPs of GGH promoter and coding regions have been identified as modulating GGH expression levels and antifolate responsiveness (Cheng et al. 2006; Adjei et al. 2010; Organista-Nava et al. 2010).

(v) Expansion of intracellular folate pools

The expansion of cellular folate THF cofactor pools has a significant impact on the instant competition between folates and antifolates in terms of polyglutamylation, target enzyme binding and efflux, leading to reduction in the pharmacological activity of antifolates (Zhao & Goldman 2003; Gonen & Assaraf 2012). In fact, increasing the folate pools is a well-established mechanism for resistance to antifolates (Jansen et al. 1999; Zhao et al. 2001)

(vi) Enhanced efflux of antifolates through overexpression of the ATP-driven MDR efflux transporters

Multidrug-resistant proteins (MRPs) are members of ATP-dependent binding cassette (ABC) efflux transporters that utilise ATP-driven energy to transport their substrates across the biological cell membrane. MRP1 (ABCC1) through to MRP5 (ABCC5) and BCRP (ABCG2) mediate folate and antifolate ATP-dependent efflux (Assaraf 2006; Sodani et al. 2012). Various studies have shown that elevated levels of MRPs1-4 and ABCG2 efflux pump can mediate antifolate resistance (Shafran et al. 2005; Bram et al. 2006; Hooijberg et al. 2014). Overexpression of these efflux transporters can also extrude THF cofactors out of the cell, however (Assaraf 2006) resulting in a decrease in intracellular folate pools and ultimately enhancing the chemotherapeutic effect of antifolates. Elevated MRPs and ABCG2 activity, therefore, would result in two opposing effects on antifolate chemosensitivity, and the net result depends on the affinity of that particular antifolate towards ABC transporters, as well as the impact of the cellular folate pool on antifolate anticancer activity (Gonen & Assaraf 2012).

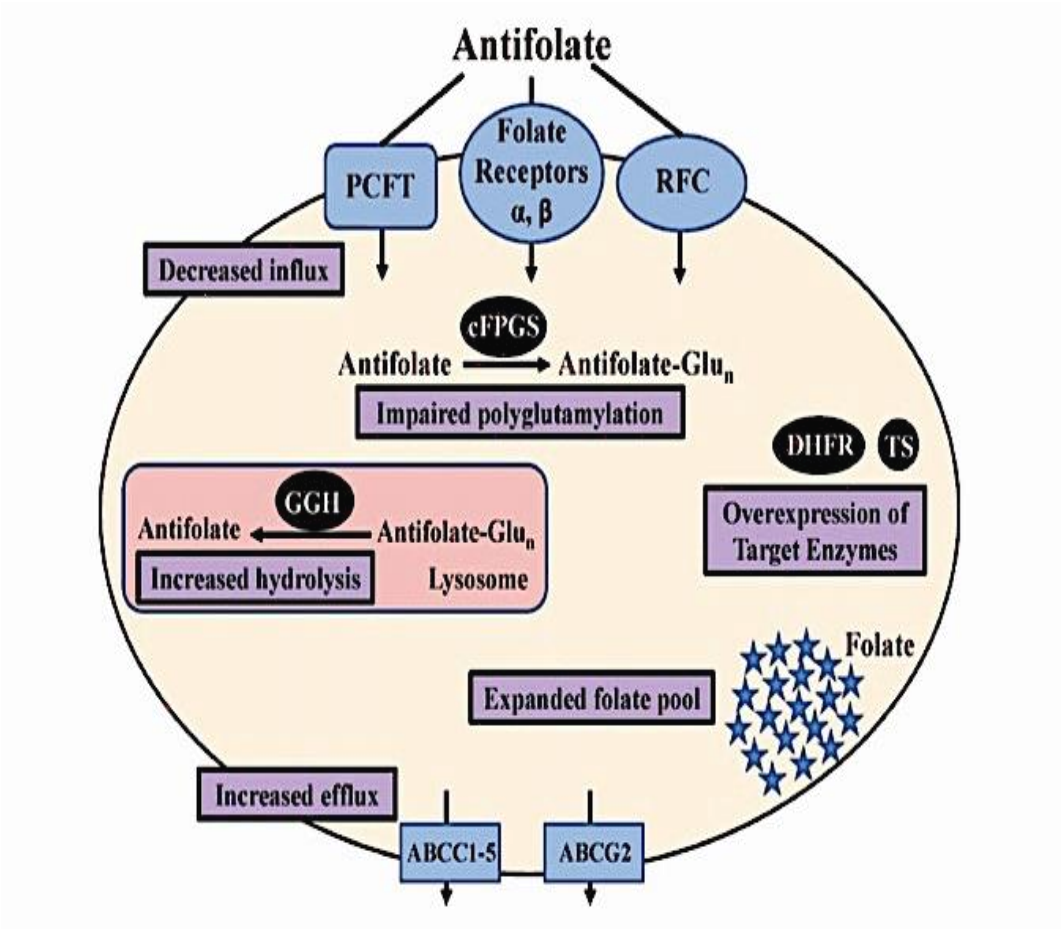

Figure 1.20: Molecular mechanisms of resistance to antifolates in cancer. Taken from Gonen & Assaraf (2012).

1.7 Aims and Objectives

The overarching aim of this thesis is to expand the current knowledge on folate pathway deregulation in respiratory tract cancers and deliver conclusions of translational significance, i.e. potential utilisation in the diagnosis, prognosis and therapy of the disease. The specific objectives are:

1- To explore the extent of the deregulation of core folate pathway genes in lung cancer

2- To examine the possibility of modifying the sensitivity of respiratory tract cell lines to antifolate drugs by using the potential epigenetic modifiers, Decitabine and VPA.

3- To investigate the modulation of the efficiency of antifolate drugs by individual genes of the pathway.

Chapter 2: Materials and methods

2.1 Human lung cancer tissue samples

All the clinical samples were sourced through the Liverpool lung project (LLP) biobank and appropriate ethical approval has been granted. One hundred and four (104) pairs of lung cancer and adjacent normal tissue were included in this study (49 adenocarcinomas, 53 squamous cell carcinomas, 1 large cell carcinoma and 1 unclassified NSCLC). Forty-one were from females (39%) and sixty-three were from males (61%). Patient ages ranged between 44 and 87 (mean =66). Most of our specimens were from the pT2 stage group (n=80) while pT1 and pT3 comprised 11 and 10 respectively, with only three from patients at an advanced pathological state (pT4).

2.2 Cell lines and growth conditions

Seven non-small cell lung cancer (A549, CALU6, COR-L23, LUDLU, SK-MES-1, SK-LU-1, H358) and three head and neck squamous cell carcinoma cell lines (BHY, PE/CA-PJ15 and PE/CA-PJ41) were used for folate gene expression experiments, in addition to the immortalised, non-tumourigenic human bronchial epithelial (HBEC-3KT) (Table 2.2). mRNA expression of HBEC-3KT cells was taken as a calibrator in each qPCR run. All of the cell lines included in this study were authenticated using the GenePrint 10 System (Catalogue no. B9510 - Promega)(Table 2.1) and verified as being mycoplasma free using the e-MycoTM plus Mycoplasma PCR Detection Kit (Catalogue no. 17341 - Intron Biotechnology). Cells were grown in Dulbecco Modified Eagle Medium DMEM: F12 medium, supplemented with L-glutamine and 5% foetal bovine serum (FBS) (Sigma-Aldrich), except for HBEC 3KT, which was cultured in Keratinocyte

serum free medium supplemented with Bovine Pituitary Extract (BPE) and human recombinant Epidermal Growth Factor (rEGF)(Life Technologies).

All cells were maintained at 37 ^{o}C in an incubator supplemented with 5% CO2.

Table 2.1: STR profiles of cell lines employed in this study.

	SK-MES-1	SKLU-1	CALU-6	A549	COR-L23	H358	LUDLU-1	HTB-182	DMS-53	H2073	CALU-1	HTB-59	HBEC-3KT	IMR-90	Lung-14	BHY	PE/CA-PJ15	PE/CA-PJ41
Amelogenin	X, Y	X	X	X, Y	X, Y	X, Y	X	X	X	X	X	X	X	X	X	X, Y	X, Y	X
CSF1PO	12	10	12	10, 12	11	11, 12	11	10	12	13	10	11	10, 11	11, 13	11, 12	10	10, 12	11, 13
D13S317	11	10	11	11	10, 11	8, 12	12	10, 11	10	13	11, 12	8	12, 13	11, 13	11, 12	12, 13	8, 10	11, 12
D16S539	13	8	13	11, 12	11, 13	12, 13	13, 14	8, 13	12, 13	12	11	11	9, 12	10, 13	11, 12	12	9, 13	11, 13
D5S818	11	11	11	11	10, 12	10, 12	12	12, 13	10, 11	12	10, 12	11	12	12, 13	10, 12	10	11, 13	12
D7S820	8	9	10	8, 11	9	10, 11	10, 12	8, 12	8, 11	12	9, 10	11, 12	8, 12	9, 12	10	11, 12	8, 12	9, 11
THO1	6, 9.3	7	9	8, 9.3	9	6	6	10	8, 9.3	6, 9.3	9, 9.3	8	9.3	8, 9.3	6, 9.3	9	6, 9.3	7
TPOX	8	8, 10	8	8, 11	8, 11	8, 9	8, 11	8	12	9	8	11	11, 12	8, 9	9, 10	8, 11	8, 11	8
vWA	14	16, 17	17	14	19	17	17, 19	18, 19	15, 17	17	15, 16	16	15, 17	16, 19	15, 16	15, 16	17, 19	15, 19

Table 2.2: Cell lines included in this study with their histological types and p53 status.

Cell line	Histological type	p53 status
NSCLC		
SK-MES-1	SCC	
SK-LU-1	Adenocarcinoma	
CALU6	Adenocarcinoma	
A549	Adenocarcinoma	[1]Wild type
COR-L23	Large cell carcinoma	
H358	Bronchioloalveolar adenocarcinoma	
LUDLU-1	SCC	
HTB-182	Squamous cell carcinoma	
DMS-53	Small cell carcinoma	
H2073	Adenocarcinoma	
CALU-1	Lung epidermoid carcinoma	
HTB-59	Squamous cell carcinoma	
Normal lung cell lines		
HBEC 3KT	Immortalised non tumourigenic normal bronchial epithelial cells	
IMR90	Normal lung fibroblast	
LUNG-14	Normal lung fibroblast	
HNSCC		
BHY	Oral SCC	
PE/CA-PJ15	Oral SCC	
PE/CA-PJ41	Oral SCC	

[1] Jia et al. (1997)

2.3 mRNA expression analysis

2.3.1 RNA extraction

RNA from cell lines and tissues was extracted using Direct-zol™ RNA MiniPrep Kit (Zymo Research). Primary tissue RNA was extracted from 10 µm thick tissue sections and 500 µl of TRIzol lysing reagent was used per approximately 50 mg tissue. Total cell line RNA extraction was performed by lysing the cells in the culture flask, the liquid medium was aspirated and cells were washed with Dulbecco phosphate buffer saline (PBS), then 600 µl of TRIzol reagent was added. The culture container was then briefly scraped with a plastic cell scrapper and TRIzol/cell lysate was collected and deposited into a 1.5 ml Eppendorf tube. Then, the lysate (tissue or cell lysates) was vortexed and an equal volume of ethanol (95-100%) was added to the homogenised lysate and mixed thoroughly by vortexing for 1 minute. The mixture was then loaded into a Zymo-Spin™ IIC Column in a collection tube and centrifuged at 16,000 x g for 30 seconds. The column was transferred into a new collection tube and the collection tube containing the flow-through was discarded. This was followed by DNAase I treatment which was prepared by adding 5 µl DNAase I (6U/µl) with 75 µl DNA digestion buffer in an RNase-free tube, then the DNase I incubation mix was added directly into the column matrix and incubated at room temperature for 20-30 minutes. 400 µl Direct-zol™ RNA PreWash buffer was added to the column and centrifuged for 30 seconds at 16,000 x g. The flow-through was then discarded. The previous stage was repeated twice. Subsequently, 700 µl RNA Wash Buffer was added to the column and centrifuged for 2 minutes at the same centrifugation speed. To ensure complete removal of the washing reagent, a dry spin was performed for an additional 4 minutes and the flow-through was discarded. The column was carefully transferred into an RNase-free tube then 40 µl of DNase/RNase-free water was added directly to the column matrix, incubated at room temperature for 1 minute then centrifuged at 16,000

x g for 2 minutes to elute the RNA. Aliquots from the extracted RNA samples were used for quality and quantity checking using a NanoDrop 2000 Spectrophotometer (Thermo Scientific) and Agilent chip analysis, while the remaining RNA was stored frozen at -80 °C for future use.

2.3.2 RNA quality control - Agilent RNA 6000 Nano kit

RNA quality and quantity was assessed by capillary electrophoresis on an Agilent 2100 RNA quality and quantity was assessed by capillary electrophoresis using an Agilent 2100 Bioanalyser (Agilent Technologies). In brief, 550 µl of Agilent RNA 6000 Nano gel matrix were placed into the top receptacle of a spin filter. The spin filter was centrifuged for 10 minutes at 1500 x g ± 20 % and 65 µl of filtered gel was used per each chip. RNA 6000 Nano dye concentrate was vortexed and 1 µl of RNA 6000 Nano dye concentrate was added to a 65 µl aliquot of filtered gel. The gel and dye mix was then vortexed thoroughly and spun for 10 minutes at room temperature at 13000 x g. 9.0 µl of the gel-dye mix were dispensed at the bottom of the well marked with a RNA Nano chip. The gel and dye mix was spread throughout the chip under air pressure using a syringe for 30 seconds. After 5 seconds, the plunger of the syringe was slowly pulled back, the chip priming station was opened and 9.0 µl of the gel-dye mix were pipetted into each of the marked wells. Subsequently 5 µl of the RNA 6000 Nano marker were pipetted into the well marked with the ladder symbol and each of the 12 sample wells. To minimise secondary structure, RNA ladder and samples were heat denatured at 70 °C for 2 minutes before loading onto the chip. 1 µl of the RNA ladder was pippeted into the well marked with the ladder symbol, and 1 µl of each sample into each of the 12 sample wells. The chip was placed horizontally in the adapter of the IKA vortex mixer and was vortexed for 60 seconds at 100 g. Finally, the chip was inserted in the Agilent 2100 Bioanalyzer and the run was started during the following five minutes.

2.3.3 Reverse transcription

A High-Capacity cDNA Reverse Transcription kit (Applied Biosystems) was used to synthesise single stranded cDNAs according to the manufacturer protocol. In brief, Reverse Transcription Master Mix was prepared by mixing 2 µl of 10x RT Buffer, 0.8 µl of dNTP Mix (100 mM), 2 µl of RT Random primers, 1 µl of MultiScribe™ Reverse Transcriptase and 4.2 µl of Nuclease-free H_2O. The premix was then mixed by brief vortexing and spinning before being placed on ice. 1 µg of total RNA (10 µl) was then added to the RT Master Mix with subsequent mixing by pipetting and brief centrifugation to remove any air bubbles. After that, a reverse transcription reaction was performed in a thermal cycler with the following reaction conditions: 10 min at 25 ^{o}C, 120 min at 37 ^{o}C and 5 sec at 85 ^{o}C. cDNAs were diluted five times with ddH2O and 3 µl were used for the subsequent quantitative PCR reactions.

2.3.4 Quantitative Real-Time PCR expression assays

Target selection was based on existing data obtained from a lung-cancer specific microarray (Almac platform) study undertaken by the lung group. The pilot validation study involved 120 NSCLC samples identifying folate genes with frequent deregulation in lung cancer. These genes were subsequently selected for comprehensive qPCR-based expression profiling in order precisely to determine their expression status in lung cancer. In an attempt to minimise the optimisation time, we used predesigned FAM-MGB labelled Taqman expression assays to investigate the expression levels of SHMT1, CBS, MTHFR, DHFR, DNMT1, AHCY, MTR, MAT2A and TYMS in lung cancer tissues and cell lines (Table 2.3).

Table 2. 3: IDs and dye of predesigned FAM-MGB labelled Taqman expression assays for the folate genes examined in this study

Gene	Assay ID	Dye
DHFR	Hs00758822_s1	FAM
MTHFR	Hs00195560_m1	FAM
CBS	Hs00163925_m1	FAM
TYMS	Hs00426586_m1	FAM
DNMT1	Hs00945875_m1	FAM
SHMT1	Hs00541045_m1	FAM
AHCY	Hs00898135-gH	FAM
MTR	Hs00165188_m1	FAM
MAT2A	Hs00428515_g1	FAM

ACTB was used as an endogenous control. The RT-qPCR primers and probe (labelled with TAMRA-BHQ2 reporter/quencher) were designed using the Primer Express v 3.0 software (Life technologies)(Table 2.4). ACTB was selected as a reference gene based on data from a microarray experiment (ALMAC platform 2009) that clearly showed similar levels of ACTB transcripts among lung normal and tumour samples. Validation experiments demonstrated very good linearity and therefore was qualified to be used as a reference (Figure 2.1).

Table 2.4: Designed Primers for detection of ACTB RNA sequence

Forward primer (5'→3')	Reverse primer (5'→3')	Probe (5'→3')
GGCACCCAGCACAATGAAG (58.7°C)	CATACTCCTGCTTGCTGATCCA (58.9°C)	CTCCTCCTGAGCGCAAGTACTCCGTG (68.8°C)

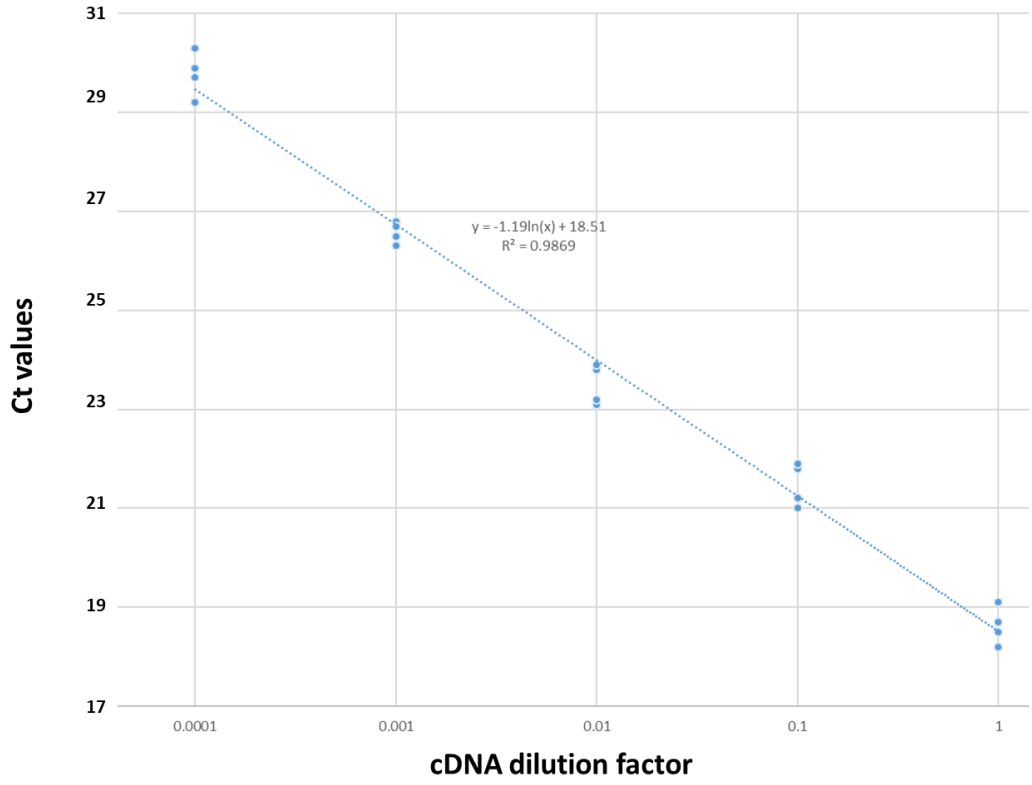

Figure 2.1: The 5-log dilution experiment for the ACTB qPCR assays. Ct=cycle threshold.

Assays were performed to a final reaction volume of 15 µl containing 7.5 µl of 2x QuantiTect® Probe PCR Master Mix (Qiagen), 900 nM of each primer and 250 nM probe (targets), 900 nM of each primer and 250 nM of the probe of the endogenous control ACTB TAMRA (Life Technologies), and 3 µl of cDNA were then added to the premix, following the universal real-time cycler conditions (95 ^{o}C for 15 min, followed by 45 cycles of 94 ^{o}C for 15 sec and 60 ^{o}C for 1 min) on an Applied Biosystems 7500 Fast Real-time PCR system. Data analysis was done utilising the 7500 Software v2.3 (Applied Biosystems). mRNA levels were expressed as relative quantification values (RQ) which were calculated as: $RQ=2^{(-\Delta\Delta Ct)}$, where the mRNA expression of HBEC-3KT cells was used as a calibrator in each run. The calibrator, or reference sample, was utilised as the basis for the comparative expression results with an RQ value=1. All assays were run in duplicate and the mean values were used for the analysis.

2.4 Detection of CBS/SHMT1 splice variants in human lung-derived cell lines

According to the CBS/SHMT1 splice variants schematic (Figure 3.10), primer assays were designed for the transcript variants using oligo 7.0 primer analysis Eurofins Genomics (Molecular Biology Insights, Inc., USA)(Table 2.5). Fifteen lung-derived cell lines were used for the preliminary expression assessment (A549, CALU6, CALU1, CALU3, COR-L23, HTB-182, DMS-53, H2073, HTB-59, LUDLU, SK-MES-1, SK-LU-1, H358, IMR-90 and LUNG-14) (Table 2.1). Endpoint PCR assays were performed to a final reaction volume of 20 µl containing 10 µl of 2X HotStarTaq Master Mix (Qiagen), 0.8 µl of each primer mixture (5 mM working concentration comprised 90 µl ddH2O, 5 µl of forward primers (stock solution, 100 mM), 5 µl of reverse primers (stock solution, 100 mM), and 3 µl of reverse transcription product (cDNA diluted five times) was then added with 6.2 µl ddH2O. The final reaction mixture was then briefly vortexed, spun down and thermal cycled. Endpoint PCR thermal profiles are shown in Table 2.6.

Table 2.5: CBS and SHMT1 transcript variants assay designed assays for endpoint PCR

Assay	Forward primer (5'→3')	Reverse primer (5'→3')	Annealing temperature (*x*° C)	PCR Product
CBSv1	CCTCTTTTCCATGTATCCGTCC (Exon 1)	CGGACAGATGGTGCTGACA (Exon 2)	61	v1 (100bp)
CBSv2/3	GTTTCAAGCTCATCAGTAAAGG (Exon 1)	TCTGTAAGGAGACGTGACAAC (Exon 2)	56	v2 and v3 (119bp)
CBSv3	CACGAGCAGATCCAGTACC (Exon 17a)	CTGGCCGACTTCTCTCTC (Exon 17b)	58	v1, v2 and v4 (392bp) v3 (178bp)
CBSv4	GTGTCTTTCGCTGCAGGG (Exon 1a-exon 1b junction)	CGGACAGATGGTGCTGACA (Exon 2)	60	v4 (132bp)

SHMT1v2	CCATTTGAACACTGCCAT (Exon 7)	TTAAATTCCAGAGTCATAGCTTG) (Exon 9)	56	v1 and v3 (245bp) v2 (128bp)
SHMT1v3	GCAGTTTTGGAGGCCCTA (Exon 3)	TTCCACCAGGGCAGTGT (Exon 5)	59	v1 and v2 (222bp) v3 (106bp)

Table 2.6: Thermal profile of CBS/SHMT1 splice variants Endpoint PCR reaction

Step	Temperature (°C)	Time	No of cycles
Taq Activation	95	15 min	
Denaturation	94	30 sec	
Annealing	X*	30 sec	40
Extension	72	30sec	
Final extension	72	10 min	

* (Table 2.5)

The quality and quantity of the PCR amplicons were then confirmed by 2% agarose gel electrophoresis and UV visualisation on a UVP VisionWorks LS instrument.

2.4.1 Relative fluorescence quantitation for CBS splice variants

Fluorescent quantification was performed in order to investigate the expression status of CBS transcripts in NSCLC tissue samples paired with adjacent normal counterparts. The customised expression CBS variants assays (Table 2.5)(with some modification of the CBSv3 forward primer by adding 5'-FAM (6- Carboxyfluorescein)), were used for the quantitative fluorescence PCR. The reaction mixture was prepared from 10 µl of 2X HotStarTaq Master

Mix (Qiagen), 0.5 µl of each primer mixture (which was prepared previously for expression assessment in lung cell lines), with 3 µl of lung cancer tissue cDNA. After that, the PCR reaction was performed in thermal cycler. The reaction conditions are shown in Table (2.7).

Table 2.7: Thermal profiles of CBS variants quantitative fluorescence PCR

Step	Temperature (°C)	Time	No of cycles
Taq Activation	95	15 min	
Denaturation	94	30 sec	
Annealing	59	30 sec	32
Extension	72	30sec	
Final extension	72	30 min	

In preparation for fluorescence quantitation, the PCR products were mixed with 9.5 µl formamide and 0.5 µl Allelic ladder (500 or 1000 ROX size standard). The mixture was denatured at 95 °C for 2 min, cooled on ice, and loaded on to a 3130 Genetic Analyzer (Applied Biosystems, USA) for capillary electrophoresis. The Peak Scanner Software v2.0 (Applied Biosystems, USA) was used for data analysis.

2.4.2 Quantitative Real-Time PCR for expression of SHMT1 splice variants

SHMT1 splice variants expression analysis was conducted using Quantitative real-time PCR expression assays. SHMT1 transcripts assays were specifically designed to target SHMT1v2 and SHMT1 (v1+3) sequences (Figure 3.10)(Table 2.8).

Table 2.8: Real time PCR primers and probes designed for the quantitation of the expression of SHMT1 splice variants

Primer/Probe	(5'→3') sequence	Position (Figure 3.10)	5' fluorescent dye
Forward primer	GAACACTGCCATGTGGTGA	(Exon 7)	-
Reverse primer	CCAGAGTCATAGCTTGCTTCA	(Exon 9)	-
(v1+v3) probe	CAGGCCAGGGAACACAGCAGA	(Exon 8)	6-FAM (518 nm)
v2 probe	CACAGCAACCCCTTTCCTGTAGAAGA	(Exon 7-exon 9 junction)	TAMRA (582 nm)

RQ values of SHMT1 v2 (Ct) values were normalised to (v1+v3) Ct values and expressed as fold changes relative to a calibrator, which is one of the non-tumour normal tissue samples (254N). When TATAA-box binding protein (TBP) was included as a reference gene, SHMT1 variant 2 (v2) and combined variants 1 and 3 (v1+v3) cycle-threshold (Ct) values were normalised with TBP Ct values and expressed as a fold change relative to parental cells.

2.5 Cellular exposure to chemotherapeutic agents

2.5.1 Examination of cell growth and phenotypic characteristics

An Eclipse TS100 inverted microscope (Nikon) was used for phenotypic examination of cell lines in addition to monitoring cell growth, confluence and the formation of clonal colonies.

2.5.2 Cell growth curves

Cell growth curves were performed in order to define the growth characteristics of each cell line involved in drug treatment experiments. The cells were plated at a density of 0.1 x 10^6 cells per well in a flat-bottomed 12-well plate in four replicates, cultured in 2 ml growth medium (as discussed in 2.2) and allowed to adhere for the subsequent viability assessment

using the MTT method. MTT assays were undertaken every 24 hours for four successive days. The curve was constructed using the average values of the replicates.

2.5.3 Treatment of cell lines with chemotherapeutics

Depending on the proliferation rate of each cell line, (5-8) × 10^4 cells were plated in each well of a flat-bottomed 48-well plate in six replicates and cultured in a 500 µl growth medium. Following overnight incubation, the medium was replaced with media containing a range of concentrations (0-1mM) of 5-Fluorouracil (Catalogue No. F6627- Sigma-Aldrich), (0.125-8 µM) Methotrexate (Catalogue No. M9929- Sigma-Aldrich) and (0.5-64 µM) Pemetrexed (pemetrexed)(Catalogue No. 456180010- Acros Organics). Cells were incubated for 72 hours with replenishment of the medium with fresh drugs at 36 hours.

For DNA methylation/ histone acetylation inhibition experiments, the most resistant cell lines to the aforementioned drugs were treated with the corresponding IC50 concentrations combined with 100 nM of Decitabine (5-Aza-2'-deoxycytidine)(Catalogue No. A3656-Sigma) and pre-treated with 1 mM Valproic acid (VPA)(Catalogue No. P4543-Sigma).

For SHMT1 inhibition experiment, PJ15 cells were exposed to 25 mM of Amonimethyl phosphonic acid (AMPA)(Catalogue No. 324817-Sigma) synchronously with seven different concentrations of 5-FU ranging from (0-1 mM). Cells were incubated for 72 hours and the culturing medium was changed every 24 hours with fresh drugs.

2.5.4 MTT assay

MTT assays were used in this study to assess cell metabolic activity. Viable cells with active metabolism are capable of reducing the tetrazolium dye MTT 3-(4,5-dimethylthiazol-2-yl)-2,5-diphenyltetrazolium bromide into a purple-coloured formazan product with a maximum absorbance near 570 nm. Since dead cells have no ability to convert MTT into its insoluble

formazan, colour formation serves as a useful marker of viable cells only (Berridge et al. 2005). Cells already seeded and/or exposed to the chemotherapeutic drugs in 48 well plates for the appropriate time course were washed with PBS and incubated (at 37 °C supplemented with 5% CO2) with MTT (3-(4,5-dimethy1–2-thioazoyl) 2,5-diphenyltetrazolium bromide)(Catalogue No. M5655 - Sigma-Aldrich) made up in a fresh medium to a final concentration of 0.75 mg/ml for 3-4 hours (or until purple precipitates became visible). Then, the medium was discarded and the converted formazan crystals were solubilised by lysing the cells with 200 µl of 0.04 M HCl in isopropyl alcohol. Five minutes later, the quantity of formazan quantity (presumably proportional to the number of viable cells) was determined by recording changes in absorbance using a GENios plate reader (Tecan Austria GmBH), which records the optical density (O.D.) at 590 nm with a 630 nm reference absorbance.

2.6 DNA methylation analysis

2.6.1 DNA extraction

Total cell line DNAs were extracted using a DNeasy® Blood and Tissue Kit (QIAGEN) (Spin column protocol). Briefly, cells were seeded in 75 cm^2 until they reached 75%-80% confluence. The cells were lysed in the culture flask, the liquid medium was aspirated and the cells were washed with PBS, then 500 µl of ATL lysis buffer with 10 µl proteinase K (Qiagen) were added. The adherent cells were then scraped off the culture flask using a plastic cell scraper. 500 µl of AL lysis buffer was then added and the entire cell lysate was thoroughly mixed and transferred into clean 2 ml microcentrifuge tubes. The cell suspension-containing tubes were then incubated at 56 °C for 15-60 minutes. After the incubation time, 500 µl of ethanol (96–100%) were added to the sample and mixed thoroughly by vortexing. The

mixture was then transferred into the DNeasy Mini spin column (which carries a silica based membrane) placed in a 2 ml collection tube, and centrifuged at 16000 x g for 1 min. 700 µl of Buffer AW1 was added, and the sample was centrifuged for 1 min at 16000 x g . 680 µl of Buffer AW2 was then added and the sample was centrifuged for 1 min at 16000 x g. The second washing step was repeated and the columns were then spun for an additional 4 minutes in order to dry the DNeasy membrane. The DNeasy mini spin column was then placed in a 1.5 ml microcentrifuge tube and the DNA was recovered into 50 µl Buffer AE and left to stand for 5 minutes at room temperature. Then, elution of the sample DNA was completed by centrifuging the columns at 16000 x g for 1 min. DNA quality and quantity were then assessed by spectrophotometry at a wavelength of 260/280 nm.

2.6.2 Bisulphite treatment of DNA

In order to explore the DNA methylation status of CBS and SHMT1 knockdown clones relative to their parental controls, we performed bisulphite genomic sequencing using the EZ DNA Methylation-Gold™ Kit (Catalogue Nos. D5005 & D5006-ZymoResearch) following the manufacturer protocol. The CT Conversion Reagent was prepared by adding 900 µl of water, 300 µl of M-Dilution buffer and 50 µl M-Dissolving Buffer in that exact order. Then, the mixture was vortexed for about 2 minutes and left on a rotating mixer for another 8 minutes. The M-Wash Buffer was prepared by adding 24 ml of 100% ethanol to the 6 ml M-Wash Buffer concentrate *(D5005)* or 96 ml of 100% ethanol to the 24 ml M-Wash Buffer concentrate *(D5006)* before use. Then a conversion reaction was performed by mixing 130 µl of CT Conversion Reagent with 20 µl of each DNA sample (1 µg) in a PCR tube strip, and samples were mixed by flicking the tube or pipetting up and down, before the liquid was briefly centrifuged to the bottom of the tube. After that, the sample tubes were placed in the thermal

cycler and the following steps were performed: 98 °C for 10 minutes, 64 °C for 2.5 hours. In the bisulphite conversion reaction, unmethylated Cytosine (C) is converted to Uracil (U), whereas methylated Cytosine (^{m}C) remains unchanged.

2.6.3 Reaction clean up

Following the conversion reaction, the converted bisulphite samples were transferred to a 1.5 ml tube containing 600 µl of M-Binding Buffer, and pipetted very well. The resulting mix was then transferred into a Zymo-Spin™ IC Column placed on a provided collection tube. The tubes were centrifuged at >10000 x *g* for 1 minute and the flow-through was discarded. 200 µl of M-Wash Buffer were added to the column and centrifuged at >10000 x *g* for 1 minute. 200 µl of M-Desulphonation Buffer was then added to the column and the mixture was left at room temperature (20°C–30°C) for 15-20 minutes. Following the incubation period, the columns were centrifuged at full speed for 30 seconds and the flow-through was discarded. Then, 300 µl of M-Wash Buffer was added and the columns were centrifuged at full speed for 30 seconds. Another 300 µl of M-Wash Buffer were added and centrifuged for additional 4 minutes to ensure complete removal of alcohol traces. Next, Zymo-Spin™ IC Columns were placed onto a 1.5 ml microcentrifuge tube and 35 µl of the M-Elution Buffer, pre-warmed to 65 °C, was added directly into the column matrix. The columns were then incubated at room temperature for 5 minutes and spun down at full speed for 1 minute to elute the DNA.

2.6.4 Preparation of Pyrosequencing samples

The first part of our LINE1 pyrosequencing process was started with the preparation of the samples that were to be sequenced. The targeted DNA sequence was amplified by PCR using LINE 1 assay (Genbank accession no M80343). Primers were designed by the assay design

software (PyroMark assay design 2.0 software) with one of the two PCR primers being biotinylated (Table 2.9).

Table 2. 9: Designed Primers for LINE-1 pyrosequencing assays. BIO: biotinylated end.

Promoter	Forward primer (5'→3')	Reverse primer (5'→3')	Sequencing primer (5'→3')
LINE-1	BIOTAGGGAGTGTTAGATAGTGG	AACTCCCTAACCCCTTAC	CAAATAAAA CAATACCTC

PCR amplifications were performed using Qiagen HotStarTaq Plus Master Mix Kit, 5 µM biotinylated primer with 10 µM non-biotinylated primer and 3 µl (approximately 60 ng) of bisulphite-treated DNA were used. The thermal profile of the LINE1 amplification is shown in (Table 2.10).

Table 2. 10: Thermal profile for LINE-1 amplification PCR reactions.

Step	Temperature (°C)	Time	No of cycles
Taq Activation	95	5 min	
Denaturation	94	30 sec	
Annealing	58	45 sec	40
Extension	72	45 sec	
Final extension	72	10 min	

Following the amplification reaction, the PCR product quality was checked in 2% agarose gel and visualised on a UVP VisionWorks LS instrument. At the end of the PCR reactions, Uracil (U) is amplified to Thymine (T), whereas methylated Cytosine (^{m}C) is amplified to Cytosine (C). Discrimination between ^{m}C and C is thereby achieved by transforming ^{m}C and C to appear as a C/T SNP (Figure 2.2).

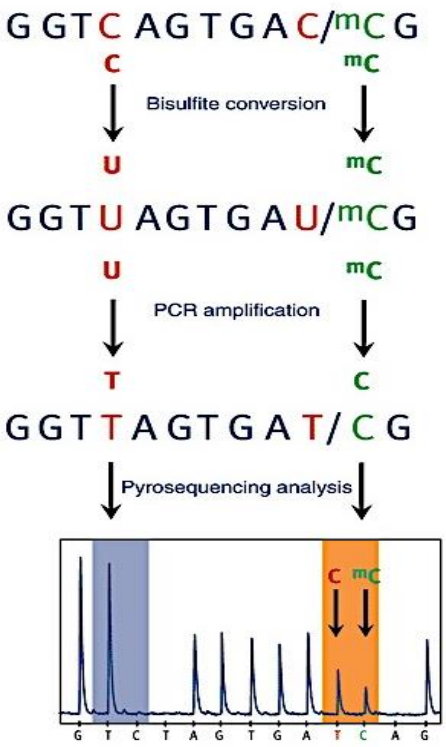

Figure 2.2: An example of a DNA sequence illustrating the principle of sequence based methylation analysis. The methylated C (green) and unmethylated C (red) are differentiated by PCR and bisulphite conversion reactions. Subsequently, pyrosequencing measures the unmethylated C and methylated C as the relative content of T and C at the CpG sequence, respectively. The figure is taken from the Qiagen website.

2.6.5 Pyrosequencing analysis

The LINE1 methylation status of PE/CA-PJ15 and H358 knockdown clones was evaluated using the SQA kit following the suppliers protocol (Qiagen) and the reaction was performed on a 96MA Pyrosequencer (Qiagen). Briefly, the amplified product was mixed with 75 µl of pyrosequencing binding mix (which contains 50 µl of Pyromark Binding Buffer, 23 µl of ddH2O and 2 µl of streptavidin-coated sepharose beads. The whole mixture was then directly transferred into a 96-well pyrosequencing plate. With the help of a vacuum preparation tool,

the beads, in which the desired PCR product was bound, were held against a filter, thereby capturing and holding them during the subsequent purification steps. The tips of the filters were then immersed (for 5 seconds) in three successive baths, containing 70% ethanol, NaOH and wash solution, respectively. NaOH denatures and separates the strands, while the wash buffer neutralises the immobilised strand. As a result, at the end of the above procedure, only the streptavidin beads with the biotinylated strand of the PCR products remained in the tool. The beads were then released by gentle shaking into a new 96-well pyrosequencing plate containing 45 µl of the annealing mix per well (the annealing mix was composed of 43.5 µl of PyroMark Annealing Buffer and 1.5 µl of LINE1 pyrosequencing primers). The sequencing plate was then incubated at 80 °C for 2 minutes and left at room temperature for 2 minutes to cool down. Meanwhile, nucleotides, substrates and enzyme reagents were dispensed onto the appropriate wells of the pyrosequencing cartridge. After the pyrosequencing plate and cartridge were loaded inside the pyrosequencer instrument, the template DNA, together with the annealed sequencing primer, were incubated with the enzymes DNA polymerase, ATP sulphurylase, luciferase and apyrase, in addition to the enzyme substrates adenosine 5' phosphosulphate (APS) and luciferin. The four triphosphates (dNTPs) were injected into the reaction one at time repeatedly in a cyclic manner. DNA polymerase catalyses the incorporation of the first dNTP into the DNA strand if it forms a base pair with the template strand. Each incorporation event is accompanied by release of inorganic pyrophosphate (PPi) in an equivalent quantity to the amount of incorporated nucleotide. PPi serves as a substrate for the enzyme ATP sulphurylase that converts PPi to ATP in the presence of APS. This ATP drives the luciferin to oxyluciferin, which generates visible light signal in amounts that are proportional to the amount of the ATP. The light produced in the luciferase-catalysed reaction was detected by a charge coupled device (CCD) camera and seen as a peak in a pyrogram. The

height of each peak (light signal) is proportional to the number of nucleotides incorporated (Figure 2.2). The apyrase enzyme helps to remove the unincorporated nucleotides along with ATP. This nucleotide degradation process in between base additions is essential for coordinated DNA synthesis. As the process continues, the complementary DNA strand is built up and the nucleotide sequence is determined from the signal peaks in the pyrogram (Figure 2.3).

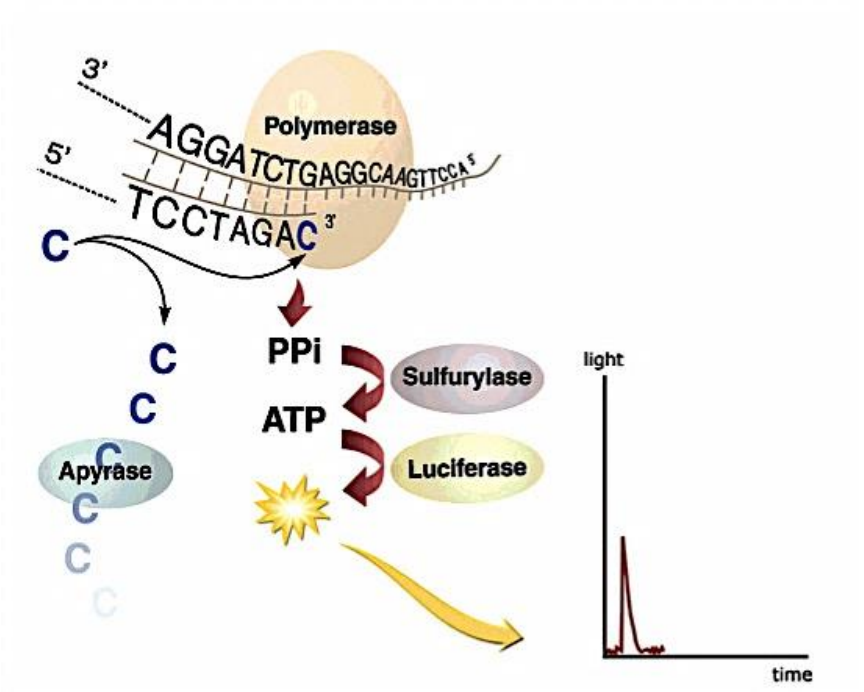

Figure 2.3: Schematic representation of pyrosequencing technology principles. Taken from Russom et al. (2005)

2.7 Transfection

2.7.1 SHMT1 and CBS knockdown by shRNA

Three different constructs were used to target SHMT1 and CBS mRNA expression (Table 2.11), belonging to type TRC2-pLKO-puro Vector along with a scrambled control construct, which was MISSION TRC2 pLKO.5-puro Non-Mammalian shRNA Control Plasmid DNA (Sigma-Aldrich) (Figure 2.4).

Table 2. 11: SHMT1 and CBS genes knock down constructs from the MISSION shRNA library (Sigma)

Clone ID	Clone legacy number	Target sequence	Target region
SHMT1			
TRCN0000034764	NM_004169.3-1141s1c1	CCGGGCAAGCTATGACTCTGGAATTCTCGAGAATTCCAGAGTCATAGCTTGCTTTTTG	CDS
TRCN0000034765	NM_004169.3-715s1c1	CCGGCCCAGATACTGGCTACATCAACTCGAGTTGATGTAGCCAGTATCTGGGTTTTTG	CDS
TRCN0000034767	NM_004169.3-1456s1c1	CCGGCCACTTTATTCACAGAGGGATCTCGAGATCCCTCTGTGAATAAAGTGGTTTTTG	CDS
CBS			
TRCN0000045360	NM_000071.1-409s1c1	CCGGCTTGCCAGATATTCTGAAGAACTCGAGTTCTTCAGAATATCTGGCAAGTTTTTG	CDS
TRCN0000045361	NM_000071.1-1604s1c1	CCGGCCGTCAGACCAAGTTGGCAAACTCGAGTTTGCCAACTTGGTCTGACGGTTTTTG	CDS
TRCN0000045362	NM_000071.1-600s1c1	CCGGACACGATTATCGAGCCGACATCTCGAGATGTCGGCTCGATAATCGTGTTTTTTG	CDS

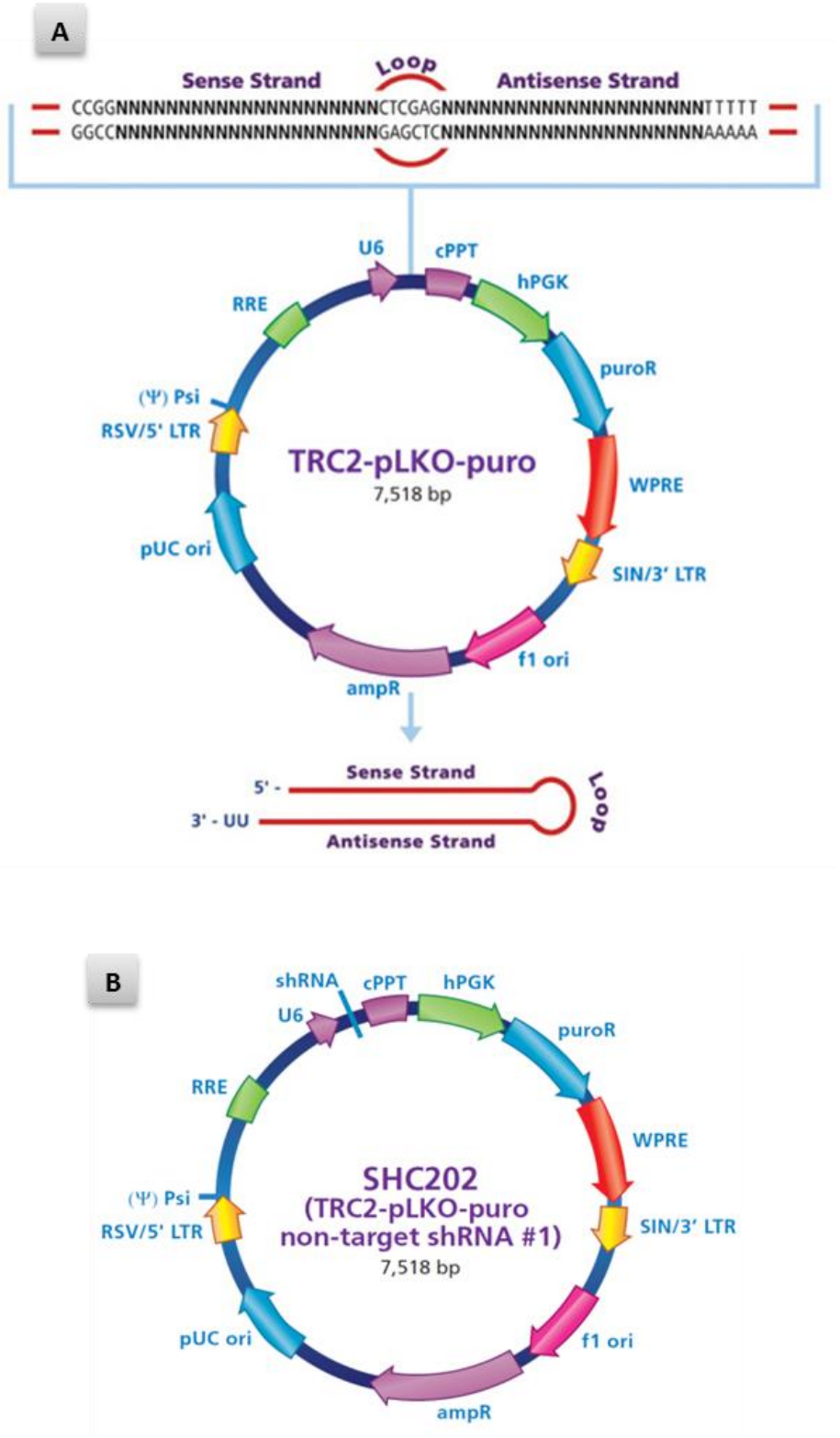

Figure 2.4: Graphic maps of TRC2-pLKO-puro plasmid with the shRNA insert (A) and MISSION TRC2 pLKO.5-puro Non-mammalian shRNA Control Plasmid DNA (B). Both figures were taken from the Sigma-Aldrich website.

2.7.2 Propagation of MISSION short hairpin RNA (shRNA) constructs

The MISSION shRNA constructs utilised in this study were propagated in an LB medium. 1 ml of construct was inoculated in 150 ml of LB medium supplemented with 100 µg/ml of Ampicillin and left overnight at 37 °C in a shaking incubator at 150 rpm. Isolation of the plasmid was performed the next day.

2.7.3 shRNA constructs DNA isolation

The plasmids of the shRNA constructs were extracted using Zyppy™ Plasmid Maxiprep Kit (Catalogue No. D4027& D4028-Zymo Research) according to the manufacturer instructions. In brief, 150 ml of fresh bacterial culture was split into 3 x 50 ml Falcon tubes and spun at 3,400 x g for 10 minutes. The supernatant was then discarded in a beaker with triagene. 15 ml of P1 Buffer (Red) was then added to the bacterial cell pellet (5 ml for each 50 ml tube), completely re-suspended by vortexing and combined in a single tube. Then 15 ml of P2 Buffer (Green) was added and immediately mixed by inverting the tube 4-6 times, and the tube was then let to stand for one minute to lyse the cells completely. 20 ml of P3 Buffer (Yellow) were added and thoroughly mixed until a homogenous colour was achieved; the mixture was then incubated on ice for 5 minutes. The Zymo-Maxi Filter™/Zymo-Spin™ VI column assembly was placed onto a vacuum manifold and the entire mixture was added directly into the Blue Maxi Filter column. After the cell debris floated to the surface, the vacuum was turned on until all of the liquid had passed completely through both columns. The blue Zymo-Maxi Filter™ column was removed and discarded from the top of the Zymo-Spin™ VI column. The columns were then placed in 50 ml tubes and centrifuged at 5000 x g for 1 minute to remove any mixture left in the column walls. After that, the columns were placed back onto the vacuum

manifold and 10 ml of Endo-Wash Buffer were added to the Zymo-Spin™ VI column and the vacuum was turned on. After the Endo-Wash Buffer had completely passed through the Zymo-Spin™ VI column, 10 ml of Zappy Wash Buffer were added and the vacuum was turned on. The Zymo-Spin™ VI column was then transferred into a clean 50 ml tube and centrifuged at full speed for 1 minute. The 50 ml tubes were then discarded and columns were placed into new 50 ml tubes. 2 ml of Zyppy-Elution Buffer, pre-warmed to 65 °C, was then added directly to the column matrix and incubated at room temperature for 5 minutes. Following the incubation period, the columns were centrifuged for 1 minute at 5000 x g to elute the plasmid DNA that subsequently was transferred to a clean 2 ml microcentrifuge tube. The plasmid DNA quality and quantity were assessed by spectrophotometry at a wavelength of 260/280 nm.

2.7.4 Transfection of Cell lines

PE/CA-PJ15 and H358 cell lines were transfected with SHMT1 and CBS shRNA constructs using two different transfection protocols. For TRCN0000045360, TRCN0000045361, TRCN0000045362, TRCN0000034765 and TRCN0000034764, we utilised Xfect^{TM} Transfection Reagents (Clontech) following the manufacturer protocol. Briefly, 60 mm of tissue culture dish was seeded with 5 x 10^5 cell/ml and cultured in 3 ml of culture medium containing serum and antibiotics. Cells were incubated under normal growth conditions (37 ^{o}C and 5% CO_2) until they reached 60%-70% confluent. On the day of transfection, 5 µg of plasmid DNA were diluted with Xfect Reaction Buffer to a final volume of 100 µl and mixed by vortexing for 5 seconds at high speed. 1.5 µl of Xfect Polymer was then added to the diluted plasmid DNA and mixed by vortexing at high speed for 10 seconds. The entire mixture was then incubated

at room temperature for 10 minutes to allow the nanoparticle complexes to form. Meanwhile, the medium from the cells was gently aspirated, the culturing disk was washed with 4 ml PBS and 3 ml fresh medium (containing 1% serum and antibiotics) were added to the cells. Subsequently the transfection complex was spun down for 1 second and added drop-wise onto the cells culture medium and the dish was gently swirled to ensure uniform distribution of the transfection complexes before the cells were incubated for 24 hours. Then, the Xfect complex was removed from the cells by gentle aspiration and replaced with 3 ml fresh complete growth medium and the dish returned back to the incubator under their normal growth conditions.

For the transfection of cells with (TRCN0000034767) shRNA construct we used the *FuGENE HD* Transfection Reagent (Promega) following the manufacturer protocol. One day prior to the transfection, cells were seeded at 5 x 10^5 cell/ml in a 10 cm^2 dish and cultured in 8 ml fresh growth medium supplemented with 5% serum and antibiotic. The transfection was performed at approximately 50% confluence,. Following 10-15 minutes incubation at room temperature, 24 µl *FuGENE® HD* Transfection Reagent were mixed with 8 µg of plasmid DNA diluted with fresh culture medium, so that the final volume of *FuGENE®* Transfection Reagent/DNA mixture was 400 µl. The mixture was then briefly vortexed, spun down and incubated at room temperature for 7 minutes. While complex formation took place, the medium from the cells was gently aspirated, the dish was washed with 10 ml PBS and then 2 ml of fresh medium (containing serum and antibiotics) was added to the cells. The entire mix was then added drop wise to different areas of the dish containing the plated cells with a gentle rocking back and forth motion to ensure even distribution of the transfection mixture. Subsequently, the culture dish was incubated at normal growth conditions (37 ^oC and 5% CO_2) for 48 hours.

2.7.5 Generation of PE/CA-PJ15-SHMT1 and H358-CBS down regulated stable cell line clones

PE/CA-PJ15 and H358 cells were transfected with the shRNA constructs that are able to efficiently silence the expression of the aforementioned genes. These short hairpin constructs carry the puromycin resistance gene. In order to determine the optimal concentration of puromycin, we examined the kill curve of PJ15 and H358 cells in the presence of various concentrations of puromycin. The lowest concentration of puromycin that promoted complete death of PJ15 and H358 cell lines was determined as 0.5 μg/ml and 3 μg/ml, respectively. 24-48 hours after transfection of cells with CBS/SHMT1 shRNAs and scramble plasmids, cells were grown in a complete growth medium containing puromycin. The growth medium and antibiotic was replenished every 2-3 days. After 2 weeks of selection, colonies were isolated using cloning cylinders, trypsinised and grown in new flasks under normal growth conditions and in the presence of puromycin selection antibiotic. CBS and SHMT1 downregulation was checked at both mRNA (qPCR) and protein (western blot) levels. Clones demonstrating >50% knockdown efficiency were grown and used for further functional analysis.

2.8 Western blot

2.8.1 Protein extraction

PE/CA-PJ15 parental and knockdown cells were seeded in 25 cm^2 until they reached 75%-80%. The culture medium was then aspirated, and the culture flask was placed on ice and cells were washed twice with ice-cold PBS. After that, the cells were lysed with Protein Extraction Buffer

(PEB)(25 µl per 1 cm^2 of growth area) supplemented with Protease inhibitor cocktail and PMSF (0.3M in DMSO) (Table 2.12).

Table 2.12: Reagents used for preparation of Protein Extraction Buffer

Solution	ml	Provider	Cat. no.
1M Tris-HCl pH=7.4	12.5	Fisher Scientific	BP152-1
Glycerol	12.5	Sigma-Aldrich	G5516
Deoxycholate 6.25%	5	Sigma-Aldrich	D6750
5M NaCl	2.5	Sigma-Aldrich	S9625
0.5M EDTA, pH= 7.4	1	AnalaR	100935V
Triton X-100	1.25	Sigma-Aldrich	T8787
SDS 20%	0.625	Sigma-Aldrich	L3771
ddH20	64.625		
Supplements			
Protease inhibitor cocktail	0.1	Sigma-Aldrich	S8830
PMSF (0.3M in DMSO)	0.0035	Sigma-Aldrich	P7626

The adherent cells were then scraped off the culture flask using a cold plastic cell scraper, and the cell lysate was gently transferred into a pre-cooled microcentrifuge tube. Subsequently, the tubes containing the cell suspension were incubated on an ice bath for 15 minutes. An additional lysis step was performed by sonication using a Bioruptor Sonication System (Catalogue no. B01010001 (UCD 200 TM) - Diagenode) following the manufacturer instructions. In brief, The Bioruptor sonicator was pre-cooled with ice-chilled water to keep it at 4 ^oC throughout the sonication time. Cell lysate tubes were placed in the tube holder and sonication cycle conditions were 15 sec. on/15 sec. off for 3 minutes. Next, sonicated cell lysates were centrifuged at 12000 x g for 15 min at 4 ^oC to remove any remaining insoluble

material. Then, the supernatants containing soluble proteins were carefully transferred to new 1.5 ml tubes and aliquots were taken for quantification, with the remaining protein extracts being stored at -20 for further analysis.

2.8.2 Protein quantitation with BicinChoninic Acid (BCA) assay

2.8.2.1 Preparation of bovine serum albumin (BSA) standard curve

In order to generate the standard curve, a set of seven standard concentrations of BSA (0.125, 0.25, 0.5, 1, 2, 4, and 8) mg/ml was prepared from 20 mg/ml stock (Catalogue no. A7906 - Sigma-Aldrich) using the same diluent as the samples (PEB). The BCA working reagents were prepared according to the manufacturer instructions. 1 unit of reagent B: 50 units of reagent A) were mixed and briefly vortexed (reagent A catalogue no.23228, reagent B catalogue no. 23224 - Thermo Fisher Scientific). Then, 4 µl of each BSA dilution was mixed thoroughly with 80 µl BCA working reagent by vortexing. The mixture was then incubated at 37 ^{o}C for 30 minutes and left at room temperature for an additional 5 minutes. The BSA standard curve was then plotted, and concentrations of unknown protein samples were measured using the NanoDrop 2000 Spectrophotometer (Thermo Fisher Scientific) according to the User Manual V1.0.

2.8.3 Electrotransfer, immunoblotting and detection.

2.8.3.1 Protein samples preparation for electrophoresis

In order to prepare the samples for SDS polyacrylamide gel electrophoresis, 20 µg of total protein from PJ15 cells and down regulated clones were mixed together with 2.5 µg of (4x) NuPAGE® LDS Sample Buffer (Catalogue no. NP0008 - Life Technologies), 1 µl of (10x) NuPAGE

Reducing Agent (Catalogue no. NP0004 - Life Technologies) and ddH_20, up to a total reaction volume of 10 µl. The entire mixture was then denatured by incubation at 70 ^oC for 10 minutes.

2.8.3.2 NuPAGE® Gels electrophoresis for proteins

For total protein electrophoresis, NuPAGE Novex Bis-Tris-Acetate (SDS-PAGE) Mini gels (Catalogue no. NP0321PK2 - Novex) were used. The comb was removed and gel wells were rinsed twice with 1x NuPAGE Tris-Acetate SDS running buffer (Catalogue no. LA0041 - Invitrogen). After removing the white tape near the bottom, the gels were placed in the XCell SureLock™ Mini-Cell gel running tank (Catalogue no. EI0001 - Invitrogen). The upper chamber was filled with 200 ml of 1x NuPAGE Tris-Acetate SDS running buffer mixed with 500 µl of NuPAGE Antioxidant (Catalogue no. NP0005 - Invitrogen), while the lower chamber was filled with 600 ml of 1x NuPAGE Tris-Acetate SDS running buffer. Then, the denatured protein samples were loaded on the gels together with SeeBlue® Plus2 Pre-Stained Standard (Catalogue no. LC5925 - Invitrogen). The gels were run at 200 V (110-125) mA/ gel for 45 minute.

2.8.3.3 iBlot Western Detection

For blotting of the electrophorised proteins we used the iBlot® Dry Blotting System (Catalogue no. IB1001 Invitrogen). Following electrophoresis, the gels were released from the cassette plates. The first gel was rinsed with ddH2O (3X 5 minutes), stained with Commassie Blue (e.g. Simple Blue SafeStain by Invitrogen), destained with water (3x 5 minutes), and photographed with the aid of a UVP VisionWorks LS instrument. The second gel was used for blotting. It was placed onto the PVDF blotting surface of an Anode iBlot Gel Transfer Stack (Catalogue no. IB8010-01 - Novex) and covered with pre-soaked (in deionised water) iBlot filter paper. The Cathode iBlot Gel Transfer Stack was then placed on the top of the filter paper and toped over

with side facing up and aligned to the right edge. The air bubbles were removed using a blotting roller. A disposable sponge with a metal contact was placed on the upper right corner of the lid. The lid was securely closed and the iBlot Dry Blotting System was switched on at program P3 for 9 min. Subsequently, the iBlot Gel Transfer Stacks were disassembled and the PVDF blotting membrane was then blocked in 5 ml 1x iBind™ Buffer supplemented with 1x iBind™ additive for 5 minutes at room temperature. The iBind Western System (Life Technologies) was employed to apply the binding primary and secondary antibodies (at dilutions of 1:1000) and the washing steps. Rabbit monoclonal primary antibodies to SHMT1 (Catalogue no. 80715S - Cell Signaling Technology), and β-actin (Catalogue no. 8457S - Cell Signaling Technology) were used as primary antibodies, while Anti-rabbit IgG HRP-linked antibody (Catalogue no. 7074S - Cell Signaling Technology) served as secondary antibodies. Both antibodies were used as recommended by the manufacturer protocol and, since they worked well, no further calibration was required. The immune complexes were detected using the Chemiluminescence Imaging System- GENE*Sys* (SYNGENE).

2.9 Statistical analysis

Differences in the expression of folate pathway genes between tumour and adjacent non-tumour samples were evaluated using Wilcoxon signed rank test, the non-parametric statistical test for paired analysis. Overexpression for a tumour sample was designated based on the 95% reference range of normal tissues (mean + 2x SD). The study characteristics were examined using descriptive statistics. Categorical variables were compared using the chi-squared test and continuous variables were examined using the Mann-Whitney test because of non-normality. The correlation (*r*) between the mRNA expression of the six folate genes was assessed by means of bivariate analysis (Spearman test).

Overall survival time was calculated from the date of surgery to the date of death or last follow-up date. All statistical analyses were performed using IBM® SPSS® statistics for Windows, software version 24.0 (Armonk, NY: IBM Corp). The IC50 values were determined using Prism 6.0 (GraphPad), which is able to fit a dose response curve with log concentration values (on the X axis), while the response was plotted on the Y axis. Prism calculates IC50s using nonlinear regression log (inhibitor) vs. normalised response equation.

$P<0.05$ was considered statistically significant.

Chapter 3: Deregulation of folate pathway genes in NSCLC

This chapter describes the experimental work undertaken in human lung cancer tissue samples and cell lines in order to ascertain a detailed mRNA expression profile of major genes related to folate metabolism. The aim of this part of the project was to identify which are the important targets of deregulation in this pathway, and to investigate potential relationships with clinicopathological data. In addition, based on this data, we decided which would be the most interesting gene targets to manipulate genetically (Chapter 5) in order to test their function in the cancer phenotype and for drug resistance. Finally, the relative expression of CBS and SHMT1 splice variants, which were qualified as major targets for reasons discussed below, was also determined in NSCLC surgical tissues and cell lines, as well as three HNSCC cell lines.

3.1 Expression status of folate genes in primary lung tumours

The quality of the RNA from all the primary lung cancer tissue samples included in this study was confirmed using the 2100 Agilent Bioanalyser using RIN (RNA integrity number) value ≥ 7 as an inclusion criterion. Initially, we investigated the mRNA expression of nine folate genes (AHCY, MAT2A, MTR, SHMT1, TYMS, CBS, DHFR, DNMT1 and MTHFR) in 54 frozen lung tumours and paired adjacent normal tissues. Gene expression analysis demonstrated significant expression differences between normal and tumour tissues in six of the examined genes (SHMT1, TYMS, CBS, DHFR, DNMT1 and MTHFR) (Figure 3.1). This finding was subsequently validated in a new set of 50 pairs of NSCLC samples and adjacent normal lung

tissue. For all 6 genes in the new set the difference in expression between normal and tumour tissues remained statistically significant. mRNA expression levels of DNMT1, CBS, DHFR SHMT1 and TYMS were significantly higher in lung cancer tissue than paired adjacent normal tissue (Wilcoxon test $p<0.001$, $p<0.002$, $p=0.003$, $p=0.015$ and $p<0.001$ respectively) while the MTHFR gene demonstrated significant downregulation in the same set (Wilcoxon test, $p=0.014$)(Figure 3.2).

The original plan of this project included mRNA expression screening for these genes in HNSCC tumours as well, however few good quality specimens were available, due to the loss of frozen specimens because of a freezer fault. It was therefore decided to proceed with NSCLC tissue samples only.

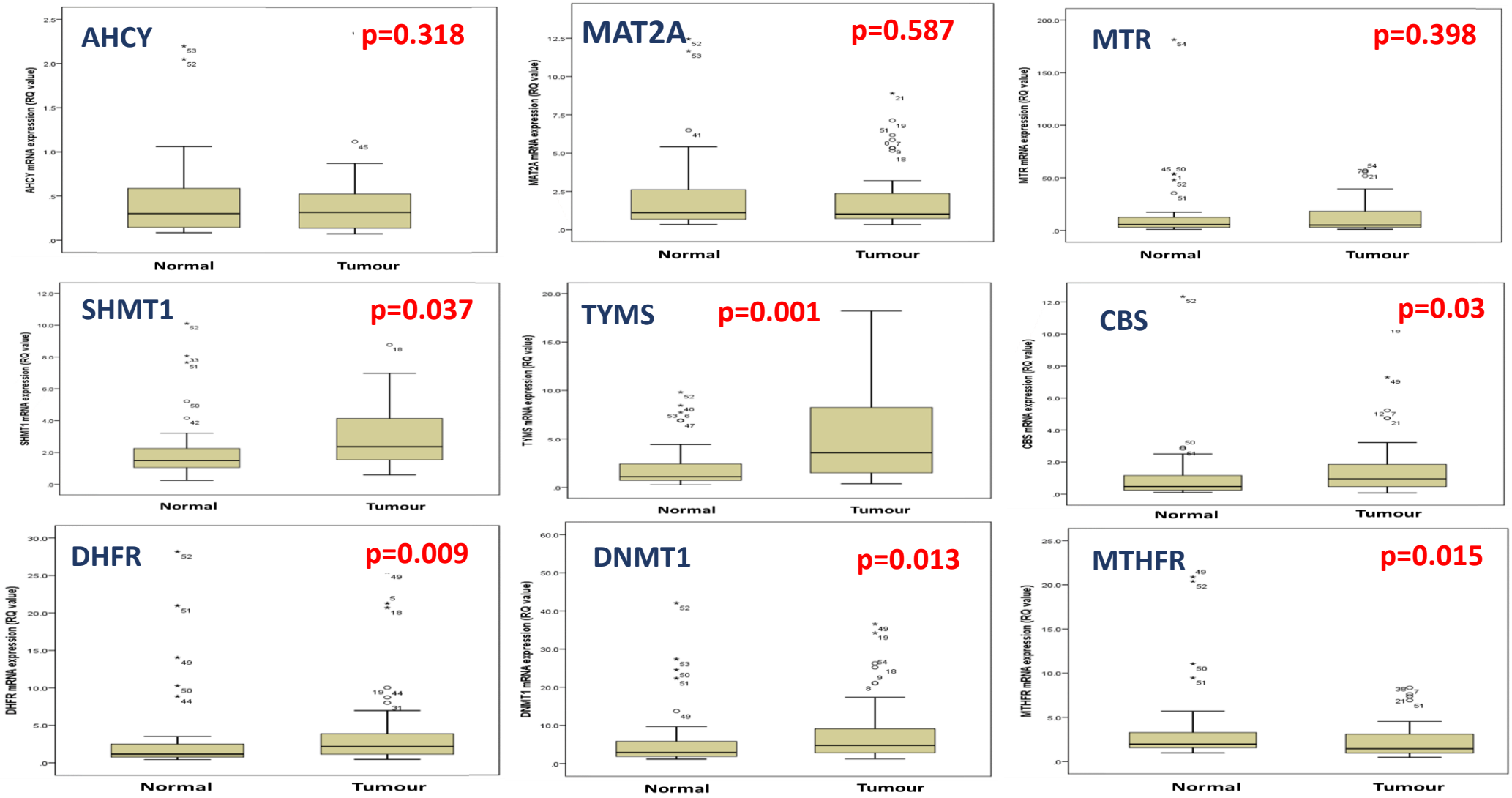

Figure 3.1: Preliminary analysis of mRNA expression in 54 pairs of NSCLC tumours and adjacent normal lung tissues. P-values were derived from the Wilcoxon signed ranked test. RQ values were calculated using the HBEC-3KT cell line as a calibrator. RQ=relative quantification

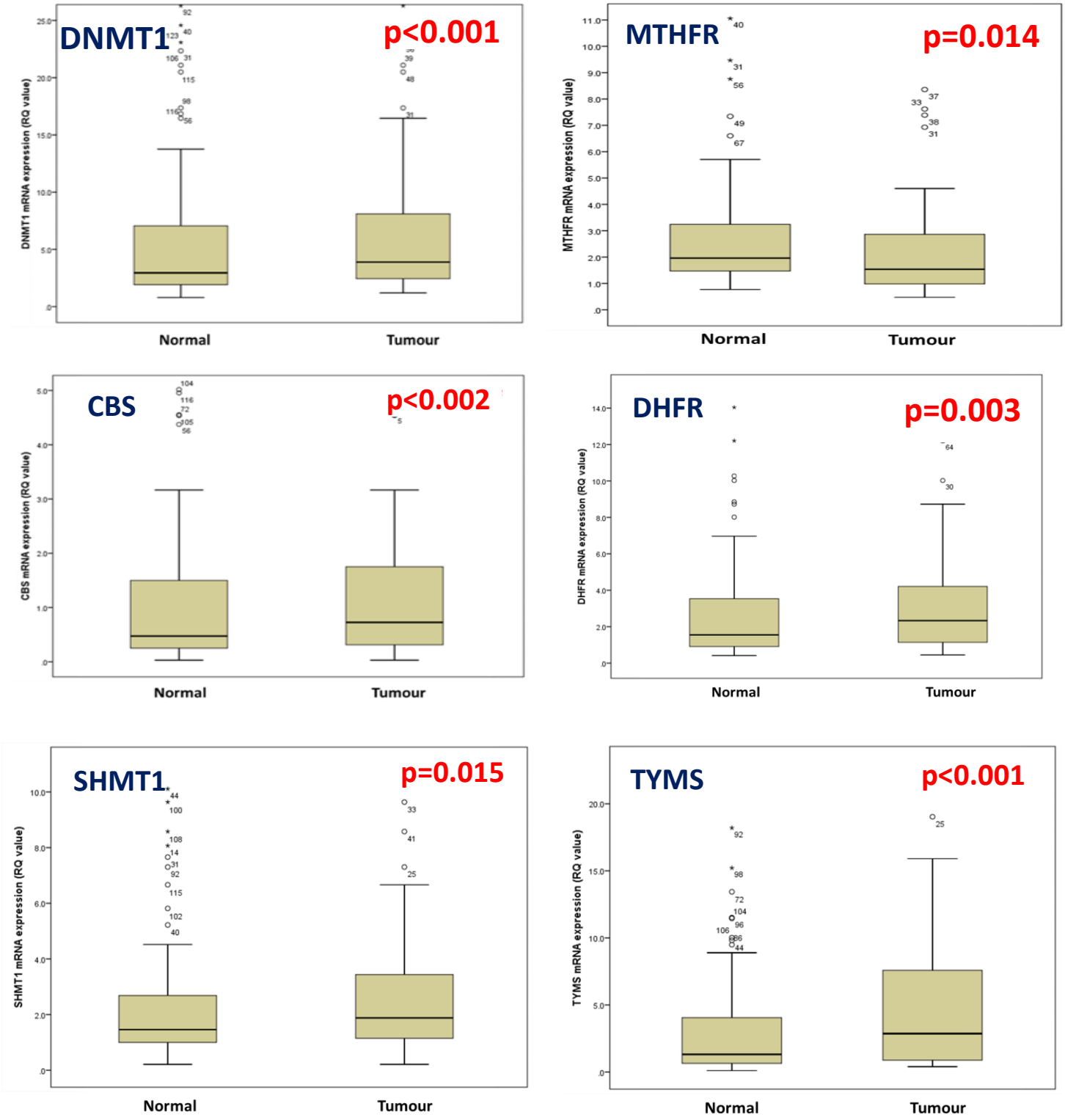

Figure 3.2: Validation of mRNA expression analysis of the top six genes from the preliminary analysis round, in an independent set of 50 pairs of NSCLC tumours and adjacent normal lung tissue. P-values were derived from the Wilcoxon signed ranked test. RQ values were calculated using the HBEC-3KT cell line as a calibrator. RQ= Relative quantification.

Having established the significant difference in both independent sets of samples, we combined the data of the two sets in order to investigate associations with clinicopathological parameters, utilising a larger sample (104 T/N pairs) and therefore potentially increasing the statistical power. Ahead of this analysis, we explored the potential correlation between the expression of the six highly deregulated genes. Spearman correlation showed a significant relationship between DNMT1 and DHFR ($r=0.708$, $p=4.1\times10^{-17}$) as well as between DNMT1 and TYMS ($r=0.67$, $p= 4.4\times10^{-15}$); relationships that both stood true after Bonferroni correction (i.e. multiplied by 6 to adjust for six independent comparisons).

In order to facilitate comparative analysis to clinicopathological features, we dichotomised the expression to normal (within the 95% prediction interval[1] = mean±2xSD, based on the values of normal lung tissues) or abnormal (outside the 95% PI). The analysis only demonstrated trends for MTHFR overexpression in adenocarcinoma (chi-square test, $p=0.029$) and DNMT1 and nodal status (chi-square test, $p=0.059$) (Figure 3.3). No other significant relationship to clinical or epidemiological association (age, gender, differentiation or T-stage, overall survival) was observed.

[1] Also referred to as the "Reference Range"

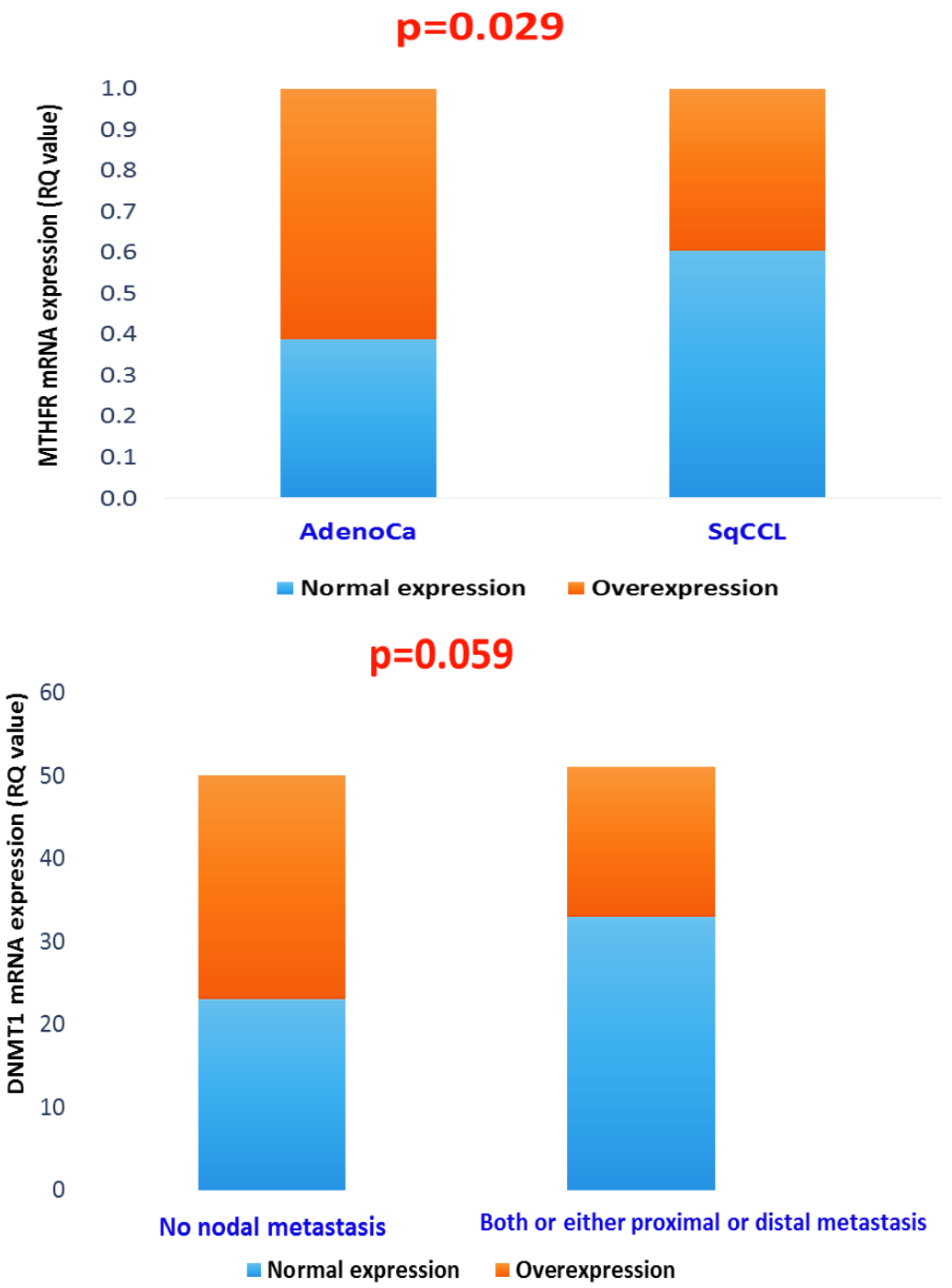

Figure 3.3: Histograms demonstrating the distribution of abnormal and normal expression of MTHFR in adenocarcinomas and squamous carcinomas (top) and DNMT1 in samples with no nodal involvement compared to those with positive nodes (bottom). P-values were derived from the Pearson chi square test. RQ=relative quantification, AdenoCa=adenocarcinoma, SqCCL=Squamous cell carcinoma.

3.2. Expression profiling of folate genes in respiratory tract cell lines

DHFR, MTHFR, CBS, SHMT1, TYMS, DNMT1 gene expression profiles were also evaluated in a panel of seven NSCLC and three HNSCC cell lines, along with the immortalised normal human bronchial epithelial cells (HBEC-3KT). The HNSCC cell lines included in this study were of oral squamous cell carcinoma origin, while NSCLC cell lines were derived from different histological origins including adenocarcinoma, squamous cell carcinoma and large cell carcinoma. Gene expression analysis of the six folate genes in the ten investigated cell lines in comparison to a normal bronchial epithelial cell line (HBEC), using RT-qPCR, revealed consistent overexpression of TYMS and DNMT1 (Figure 3.4 and Figure 3.5). Expression of DHFR was elevated in most of the tumourigenic cells with borderline reduction in CALU6, SKLU1 and SKMES (Figure 3.6). Likewise, most of the RTCs cell lines demonstrated upregulated SHMT1 mRNA, with the exception of SKLU1, SK-MES, CORL23 and BHY (Figure 3.7). The MTHFR expression level was consistently lower than that of HBEC-3KT in both the NSCLC and HNSCC cell lines, however (Figure 3.8). The CBS mRNA level was also downregulated among the tested cancer cell panel ecept for the LUDLU and H358 cells lines (Figure 3.9).

These findings correlate with the tissue expression results for the DHFR, MTHFR, SHMT1, TYMS and DNMT1 genes, except for CBS, which was downregulated in the RTCs cell lines and overexpressed in the lung cancer tissues.

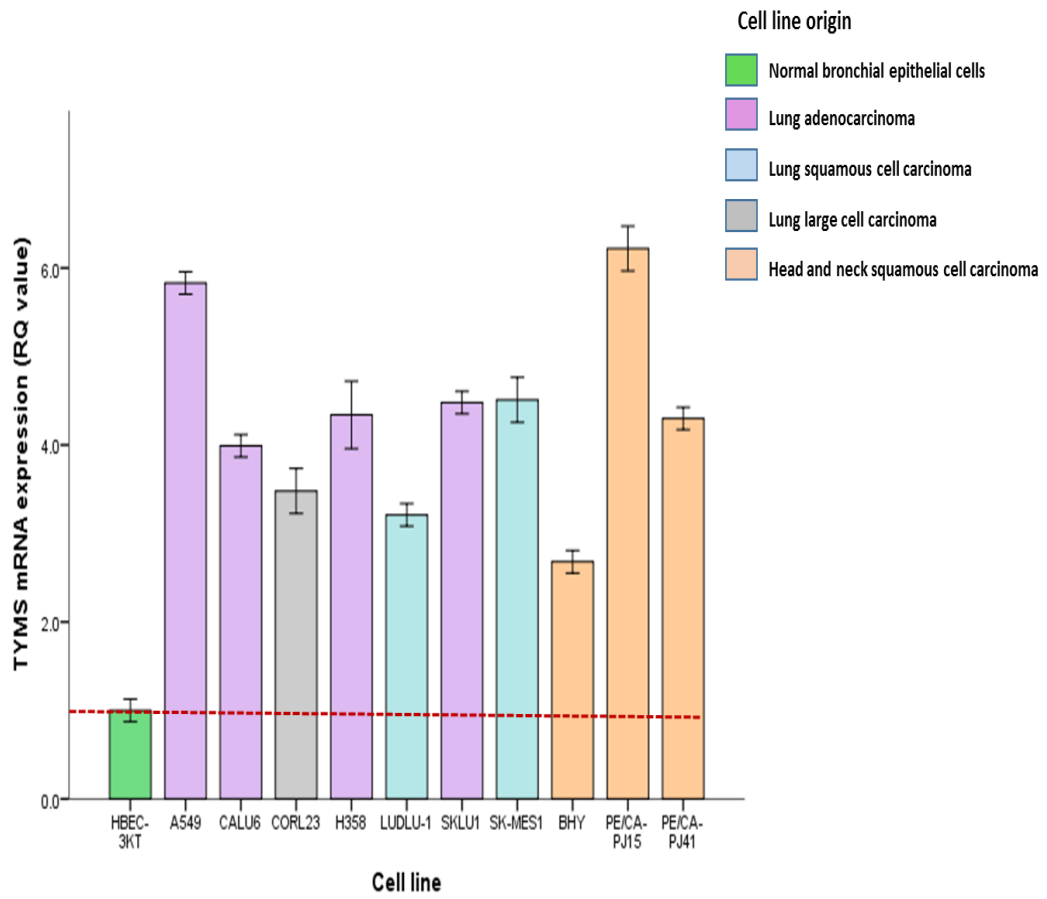

Figure 3.4: TYMS mRNA expression in NSCLC, HNSCC and non-tumorigenic human bronchial epithelial cells (HBEC-3KT). TYMS demonstrated significantly higher mRNA expression levels among NSCLC and HNSCC cell lines compared to that of HBEC-3KT. Bars represent the mean values of three technical repeats and error bars represent standard error of the mean. HBEC-3KT was used as a calibrator. RQ=relative quantification.

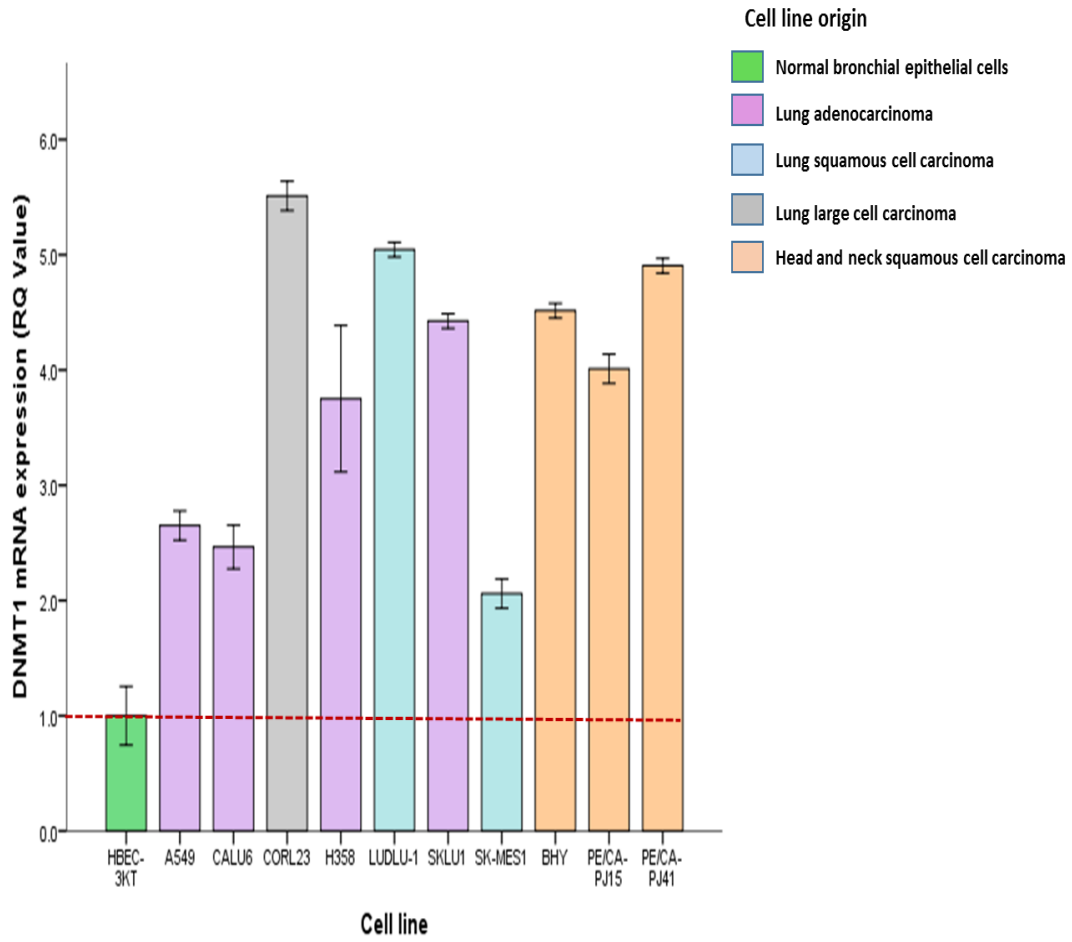

Figure 3.5: DNMT1 mRNA expression in NSCLC, HNSCC and non-tumorigenic human bronchial epithelial cells (HBEC-3KT). DNMT1 demonstrated significantly higher mRNA expression levels among NSCLC and HNSCC cell lines compared to that of HBEC-3KT. Bars represent the mean values of three technical repeats and error bars represent standard error of the mean. HBEC-3KT was used as a calibrator. RQ=relative quantification.

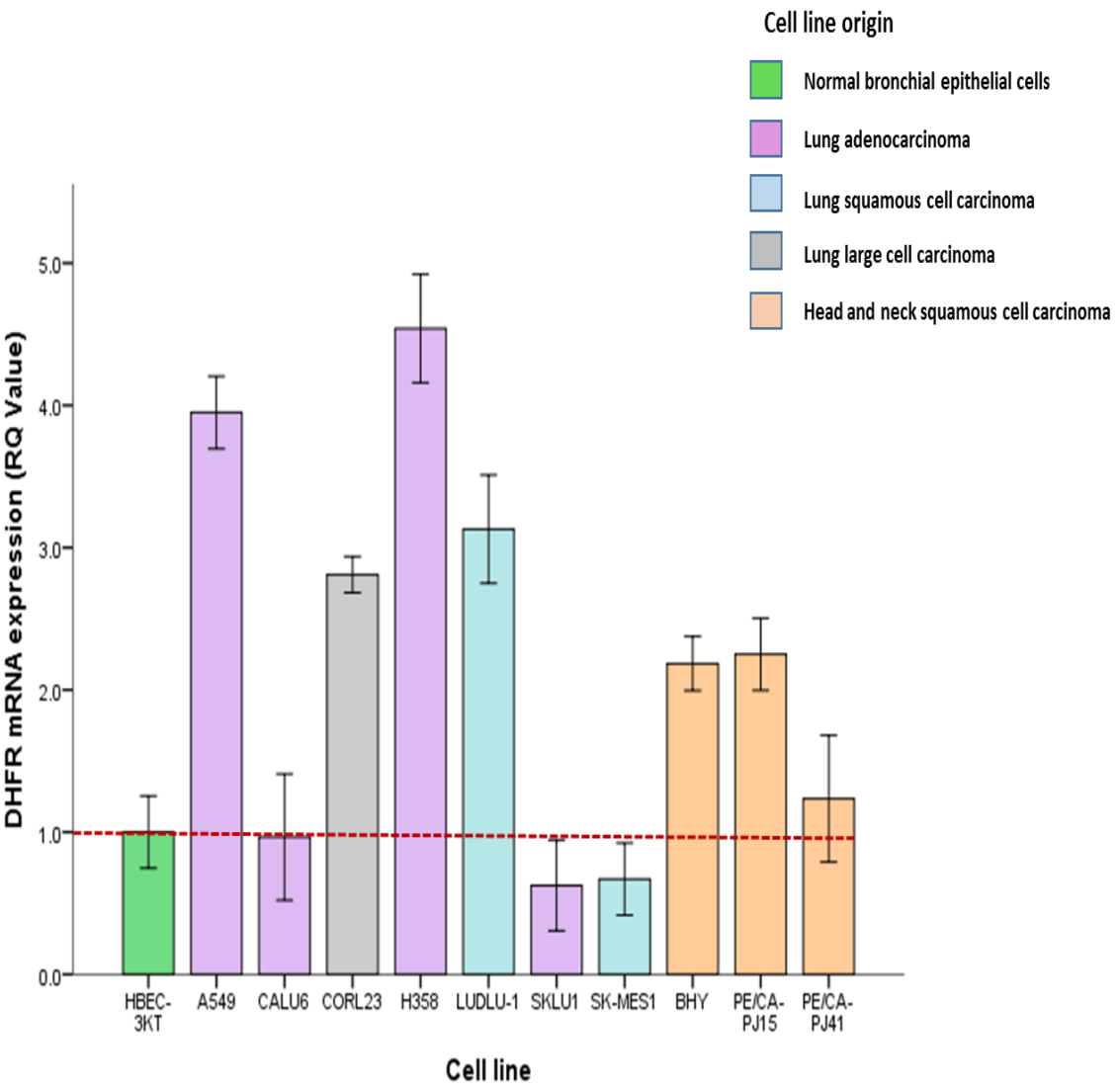

Figure 3.6: DHFR mRNA expression in NSCLC, HNSCC and non-tumourigenic human bronchial epithelial cells (HBEC-3KT). DHFR was overexpressed in seven out of ten NSCLC and HNSCC cell lines compared to immortalised normal bronchial epithelial cell lines. Bars represent the mean values of three technical repeats and error bars represent standard error of the mean. HBEC-3KT was used as a calibrator. RQ=relative quantification.

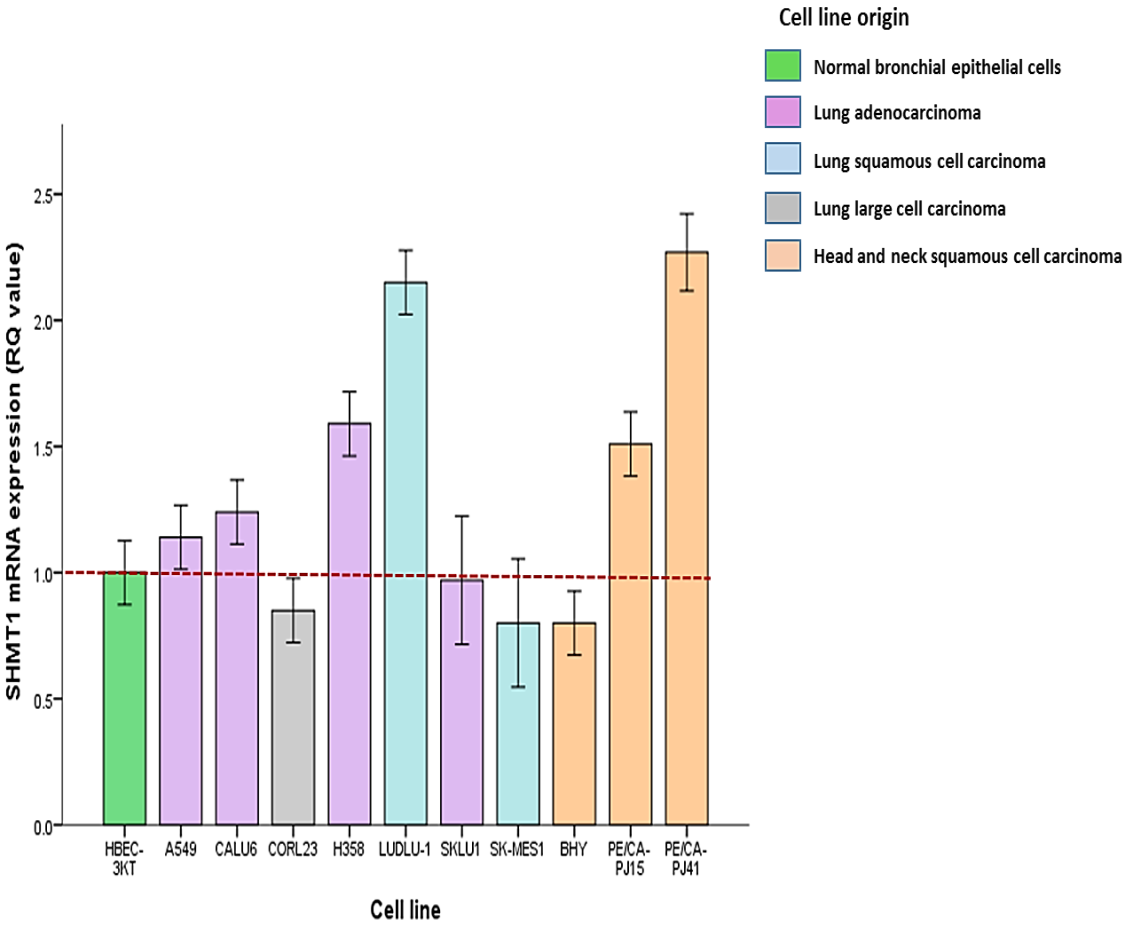

Figure 3.7: SHMT1 mRNA expression in NSCLC, HNSCC and non-tumorigenic human bronchial epithelial cells (HBEC-3KT). An upregulation of SHMT1 was observed in seven cell lines with a border line reduction in the remaining three (CORL23, SK-MES1 and BHY) compared to immortalised normal bronchial epithelial cell lines. Bars represent the mean values of three technical repeats and error bars represent standard error of the mean. HBEC-3KT was used as a calibrator. RQ=relative quantification.

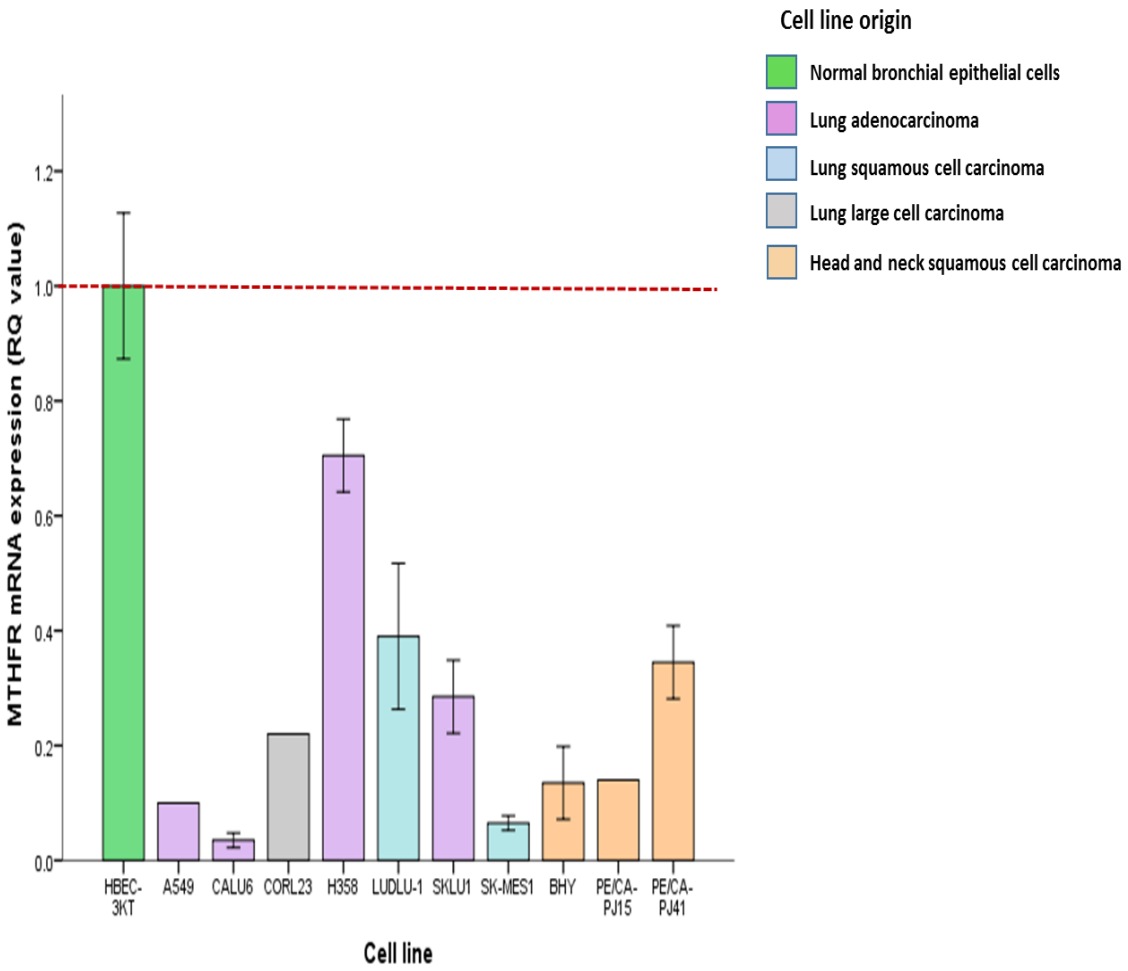

Figure 3.8: MTHFR mRNA expression in NSCLC, HNSCC and non-tumourigenic human bronchial epithelial cells (HBEC-3KT). The examined cell lines express MTHFR at different levels, however consistently lower than that of the non-tumourigenic human bronchial epithelial cell line. Bars represent the mean values of three technical repeats and error bars represent standard error of the mean. HBEC-3KT was used as a calibrator. RQ=relative quantification.

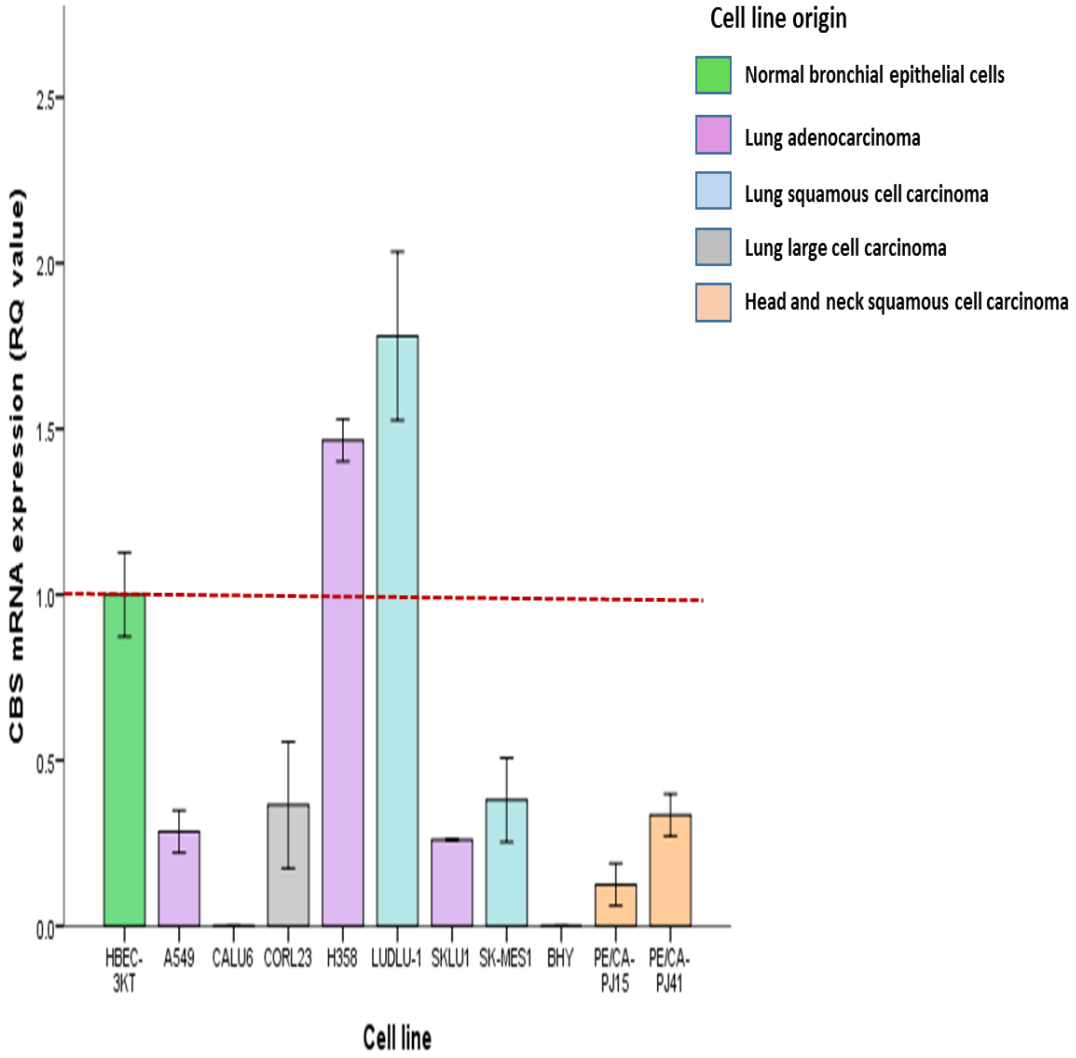

Figure 3.9: CBS mRNA expression in NSCLC, HNSCC and non-tumourigenic human bronchial epithelial cells (HBEC-3KT). The expression levels of CBS varied among the investigated cancer cell lines panel being highest in LUDLU-1 and H358 and lowest (undetermined) in BHY and CALU6 cell lines. Bars represent the mean values of three technical repeats and error bars represent standard error of the mean. HBEC-3KT was used as a calibrator. RQ=relative quantification.

3.3 Splicing variant expression profiles of SHMT1 and CBS in NSCLC

Following the establishment of deregulation of the six folate genes in lung cancer, a strategic decision was taken to focus on the SHMT1 and CBS genes, since there is negligible information in the literature in respect to their involvement in human cancer. Splicing variation was the first aspect to investigate. While there is a large body of experimental data about splicing isoforms of folate metabolic genes, CBS and SHMT1 splicing is currently less studied.

Utilising Genbank entries for the identified splice variants of these genes (Figure 3.10), endpoint PCR assays were designed (as in the Materials and Methods), initially to ascertain the presence of four CBS and three SHMT1 splice variants in 13 human lung cancer cell lines and two normal embryonic lung fibroblast cell lines: IMR90 and LUNG14. The results showed that all of the splice variants are expressed in the examined cell lines except SHMT1 variant 3 (SHMT1v3)(Figure 3.11A). Additional screening for this variant was therefore undertaken on four pairs of NSCLC tumour and adjacent normal tissue samples, which revealed its expression, albeit at a very low level (Figure 3.11B).

Figure 3.10: Schematic representation of (A) CBS and (B) SHMT1 splice variants. Exons are depicted with blue boxes and numbered in italic form 1-17 for CBS and from 1-12 for SHMT1 (not drawn to scales). The green boxes represent coding sequences CDS. Base 1 of the CBS transcripts corresponds to base 43053190 of the complement 43053190...43076868 (NCBI reference sequence NC_000021.9) while base 1 of the SHMT1 transcripts corresponds to base 18327860 of the complement 18327860...18363563(NC_000017.11). R=reverse primer, F=forward primers, P= RT probe. Taken from ncbi.nim.nih.gov; ensembl.org; Sultan et al. (2008)

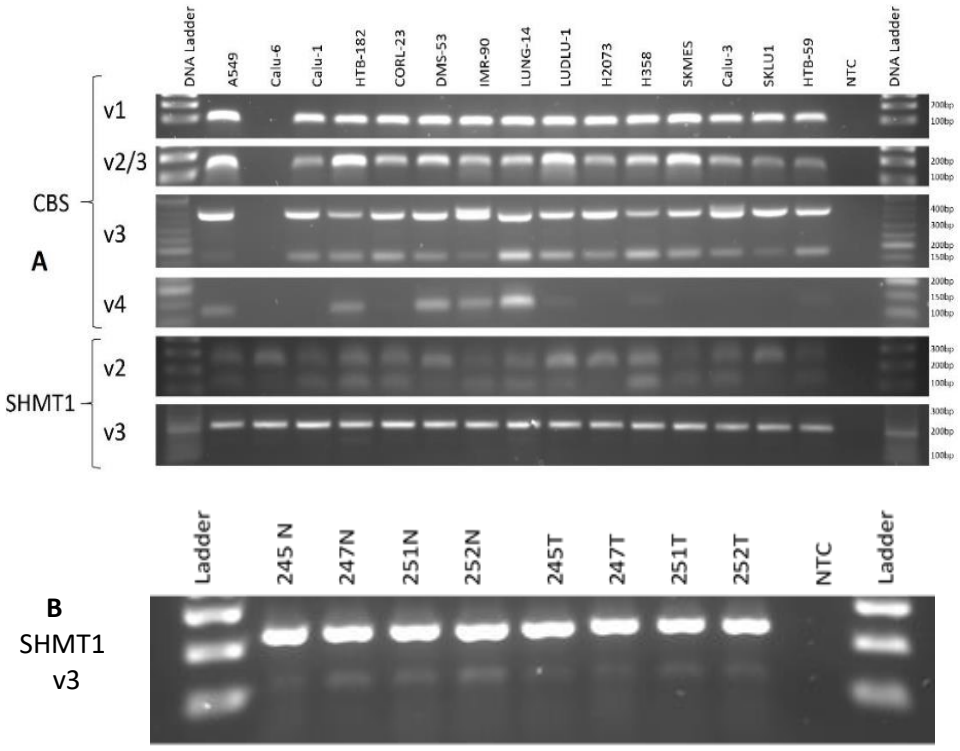

Figure 3.11: Endpoint PCR- based expression of candidate CBS and SHMT1 splice variants in fifteen lung derived cell lines. PCR products were separated on a 2% agarose gel. Gel picture analysis suggests the presence of CBSv1, v2, v3 and v4 and SHMT1 v2 splice variants. While SHMT1 v3 was undetectable in lung cell lines with scarce or barely evident expression (lower of two bands) in four NSCLC tumour/normal pairs. N=normal, T=tumour.

For quantitative analysis of CBS and SHMT1 variants in NSCLC, assays that could detect two or more transcript variants were designed for SHMT1 (qPCR -Taqman) and CBS (quantitative fluorescent fragment analysis on a 3130 sequencer).

CBSv3 exhibits higher expression in primary lung NSCLC tumours compared to normal adjacent lung tissues in a set of 53 normal/tumour pairs (Wilcoxon signed ranked test, p=0.032)(Figure 3.12A). In addition, SHMT1v2 demonstrated significant downregulation in NSCLC tumours compared to the non-tumour samples in 52 tumour/normal pairs (Wilcoxon signed ranked test, p=0.002)(Figure 3.12B).

The expression of these two variants (CBSv3 and SHMT1v2) was comparatively analysed with

the clinicopathological data in the studied samples set. CBSv3 was found to be expressed at a higher level in squamous cell carcinomas compared to adenocarcinomas (Mann-Whitney test, p=0.001)(Figure 3.13A). Furthermore, squamous cell carcinoma demonstrates a high mRNA level of CBSv3 with respect to the adjacent normal counterparts, whereas the case is not the same for adenocarcinoma (Figure 3.13B). Apart from that, there was no significant association between CBSv3 and SHMT1v2 transcripts expression and clinicopathological features (age, gender, nodal metastasis or differentiation) of NSCLC patients included in this study. When CBS/SHMT1 splice variants expression was analysed in relation to the overall mRNA profiles of these two genes, a weak association was shown (Spearman rank test, correlation coefficient between -0.3 and +0.3). Taken together, our data suggest that CBS and SHMT1 alternative splicing events might be independent of their upregulated mRNA level in NSCLC.

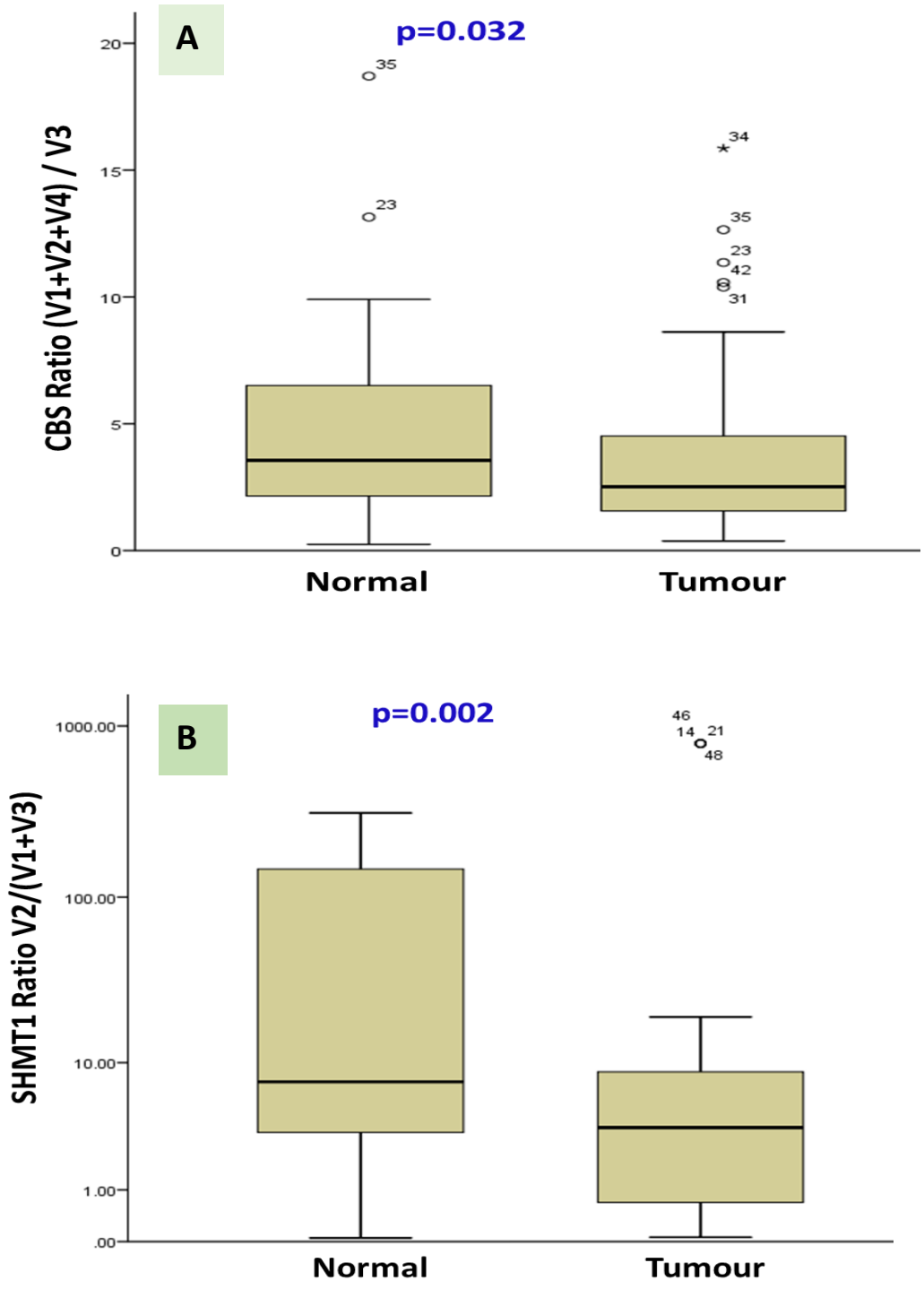

Figure 3.12: qPCR analysis of CBS and SHMT1 splice variants expression in NSCLC.

(A) Relative quantification (RQ) of CBS splice variants mRNAs, cycle threshold (Ct) was normalised to CBSv3 values and expressed as fold changes in relation to (254N) non-tumour sample in 53 normal/tumour NSCLC samples. CBSv3 was overexpressed in (34/53) tumour samples in comparison with normal ones.

(B) SHMT1 transcripts expression. SHMT1v2 Ct values were normalised to (v1+v3) Ct values. SMT1v2 demonstrates lower expression level in tumour samples (36/52) relative to their normal counterparts. P values were returned from the Wilcoxon signed ranked test.

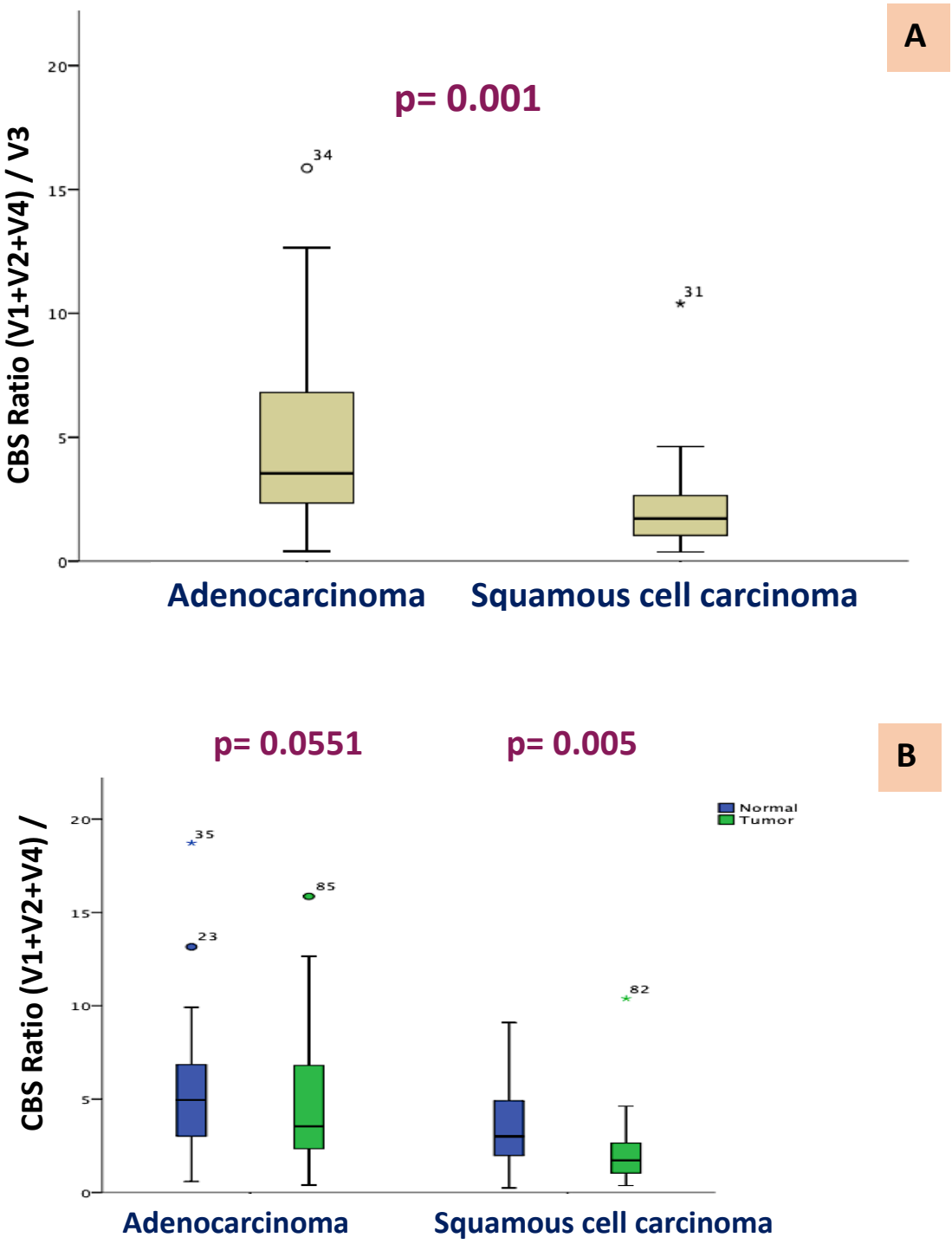

Figure 3.13: Boxplot representation of CBS transcript variants expression in adenocarcinoma versus squamous cell carcinoma. (A) CBSv3 exhibits marked overexpression in squamous cell carcinoma compared to adenocarcinoma in 51 tumour samples. CBS (v1+2+4) were normalised to CBSv3.
(B) CBSv3 expression difference between normal and tumour tissues in both adenocarcinoma and squamous cell carcinoma. Squamous cell carcinoma expresses CBSv3 at significantly higher level than adjacent normal tissues. This was not true for adenocarcinoma, however. P-values were returned from the Mann-Whitney test.

The uniqueness of CBSv3 with spliced out 3'-UTR (Figure 3.10) was also examined through exploration of predicted miRNA regulation. miRNA target prediction search revealed that CBS 3'-UTR region is a potential target of several miRNAs (Table 3.1)(Figure 3.14)(miRBase database)(Kozomara & Griffiths-jones 2014).

Table 3.1: Predicted microRNAs targeting CBS 3'-UTR region

Predicted microRNA	Alignment of CBS mRNA to mature miRNAs	Score[1]	E-value[2]
hsa-miR-6850-5p	CBS (+) 5'GUCCGGAGCGCUGGGCGGUGCG 3' || |||| |||||| ||| ||| hsa-miR-6850-5p 5'GUGCGGAACGCUGGCCGGGGCG 3'	74	3.0
hsa-miR-663a	CBS (+) 5'GGCGGUGCGGAGCGGGCCCGC 3' ||||| ||| ||||| |||| hsa-miR-663a 5'GGCGGGGCGCCGCGGGACCGC 3'	69	7.9
hsa-miR-4480	CBS (-) 5'UAAUGUAACUUCCUCUUAG 3' ||| ||||||||| ||| | hsa-miR-4480 3'UAAAGUAACUUCCACUUGG 5'	68	2.1
hsa-miR-675-5p	CBS (+) 5'GUGCGGAGCGGGCCCGC 3' |||||||| |||||| | hsa-miR-675-5p 5'GUGCGGAGAGGGCCCAC 3'	67	2.6
hsa-miR-5703	CBS (-) 5'CCUUGCCCACUUCUCCU 3' |||| || ||||||||| hsa-miR-5703 3'CCUUCCCGACUUCUCCU 5'	67	2.6
hsa-miR-5088-5p	CBS (-) 5'CUCCUUCGCUUUCCUGAGCCCU 3' |||| ||	|||||||||| hsa-miR-5088-5p 3'CUCCAUCCAAUCCCUGAGCCCU 5'	65	3.8
hsa-miR-6821-3p	CBS 5'CUGGGCGGUGCGGAGCGGGC 3' ||| |||| |||||| || | hsa-miR-6821-3p 3'CUGUGCGGAGCGGAGAGGUC 5'	64	5.1
hsa-miR-4259	CBS (-) 5'UCCUGAGCCCUAAACACA 3' |||||| ||||| || || hsa-miR-4259 3'UCCUGACCCCUAGACCCA 5'	63	5.6
hsa-miR-4664-5p	CBS (-) 5'UGCGGAGCGGGCCCGCCA 3' ||||||| ||||	||| hsa-miR-4664-5p 3'UGCGGAGUGGGCACCCCA 5'	63	5.6
hsa-miR-4268	CBS 5'CUUCCUCUUAGGAUGU 3' | |||||| ||||||| hsa-miR-4268 5'CCUCCUCUCAGGAUGU 3'	62	7.5
hsa-miR-210-5p	CBS (+) 5'CCCUGCACACGGCACA 3' |||||| ||| ||||| hsa-miR-210-5p 5'CCCUGCCCACCGCACA 3'	62	6.8
hsa-miR-7974	CBS (+) 5'GCUUUCCUGAGCCC 3' ||| |||||||||| hsa-miR-7974 5'GCUCUCCUGAGCCC 3'	61	8.3
hsa-miR-6884-3p	CBS (+) 5'UCCGUCUCCCCU 3' |||||||||||| hsa-miR-6884-3p 5'UCCGUCUCCCCU 3'	60	10.0

[1]Numerical description of alignment quality.

[2]Number of distinct alignments expected by chance.

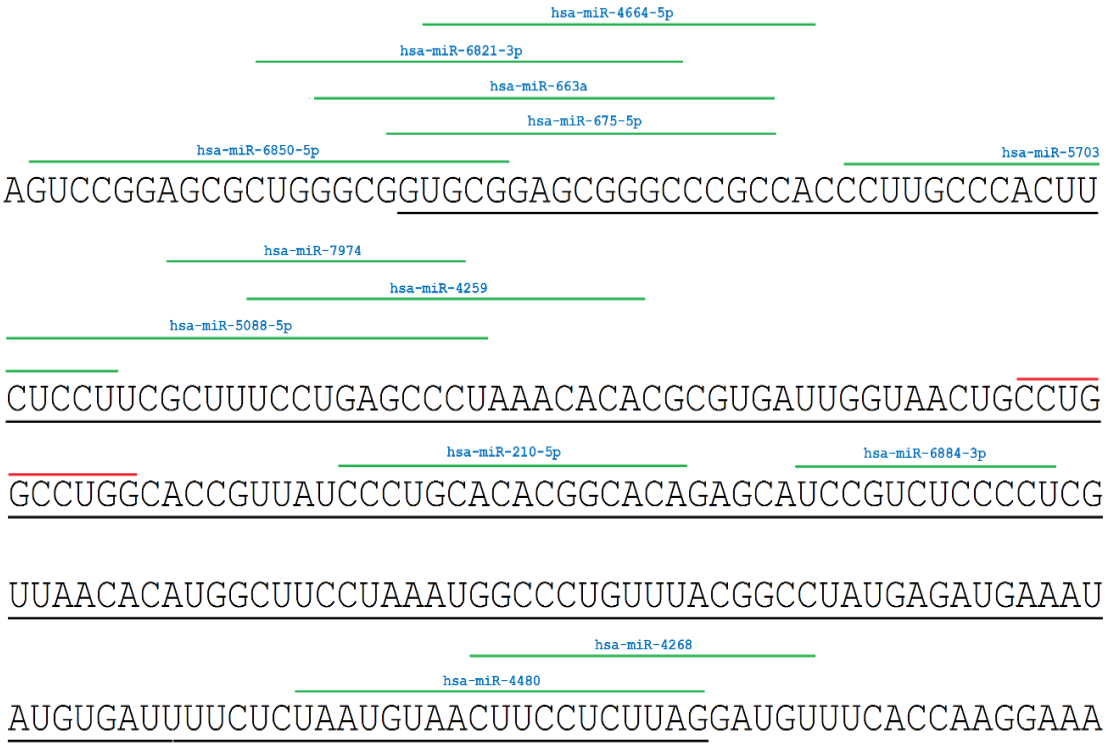

Figure 3.14: microRNAs predicted to target CBS 3'-UTR. Only portion of the CBS mRNA 3'-UTR region (Exon 17) is shown. The spliced out sequence of CBSv3 is underlined with black lines. Green lines show regions involved in Crick-Watson base pairing with the miRNAs (blue text) while untargeted pentanucleotide Short Tandem Repeats (STR) are marked with red lines.

3.4 Discussion

3.4.1 Deregulation of folate genes in lung cancer

The folate metabolic pathway plays an important role in maintaining genomic stability through feeding into, among other pathways, crucial biological processes such as DNA synthesis, repair and DNA methylation. Equilibrium imbalances incurred due to deregulation of specific genes in this pathway might therefore be critical for cancer growth and development. Most of the relevant published studies have examined the possible effect on lung cancer development of SNPs in folate pathway genes, while information regarding the expression of folate pathway gene members in this devastating neoplasia is limited. Nonetheless, mRNA overexpression of DNMT1, CBS, TYMS, DHFR and SHMT1 have been reported in several types of human tumours using different techniques (Mutze et al. 2011; Szabo et al. 2013; Koumarianou et al. 2014; Sun et al. 2016; Nakano et al. 2017).

Our study provides comprehensive qPCR-based expression profiling in order precisely to determine the expression status of the folate genes in a large number of NSCLC tissues and paired normal counterparts. Analysis of this expression profiling demonstrated overexpression of TYMS, SHMT1, DNMT1, CBS and DHFR, and downregulation of MTHFR in NSCLC tissues when compared to the normal adjacent tissues. These results are largely in accordance with previously published data that have documented upregulation of TYMS (Kotoula et al. 2012), SHMT1 (Paone et al. 2014) and DNMT1 (Pastuszak-Lewandoska et al. 2015) in lung cancer. We also demonstrated that the expression level of the investigated folate genes varied between different respiratory tract cancer cell lines, including NSCLC cell lines, but that this variation consistently matched the NSCLC tissue expression results, except for CBS, which exhibits a markedly reduced expression in the tested cell lines panel. A similar CBS downregulation pattern has been reported in the A549 NSCLC cell line (Zhang et al. 2005).

Given the importance of the CBS gene in promoting cancer cells proliferation, bioenergetics and migration through production of hydrogen sulphide (H_2S) (Hellmich et al. 2014), the lack of correlation between CBS expression patterns in lung cancer tissues and cell lines would be a great paradox since one might expect to see increased CBS expression level in both. Indeed, analysis of human colon cancer biopsy and colon cancer derived cell lines have shown selective CBS upregulation with increased H_2S production in both tissue and cell lines samples (Szabo et al. 2013). In the same way, CBS overexpression has been reported in primary epithelial ovarian cancer samples and ovarian cancer cell lines (Bhattacharyya et al. 2013). Nonetheless, it must be noted that this human enzyme has multiple and complex levels of regulation that vary from one cell type to another (Singh & Banerjee 2011). CBS downregulation has been demonstrated in prostatic cancer cell lines by post-transcriptional modification in response to testosterone (Prudova et al. 2007), while in a seminal article, Kabil et al. (2006) identified that CBS is a target for cellular sumoylation under both *in vitro* and *in vivo* conditions. This modification might serve to relocate the CBS gene to the nucleus in an attempt to meet the rising glutathione demand of the rapidly proliferating cancer cells (Markovic et al. 2007). In addition, modulation of CBS activity is a crucial mechanism for tuning the cellular response to adverse environmental conditions, including oxidative stress, where sulphur traffic through trans-sulphuration pathways is increased (Singh & Banerjee, 2011). Together, these suggestions could explain the inconsistent CBS expression results observed in lung cancer tissues and cell lines; although the biological relevance of this discrepancy in NSCLC clearly needs to be addressed.

Our current study demonstrated a general consistency of folate gene deregulation across the clinicopathological characteristics of NSCLC cancer patients. This indicates that this deregulation (a) occurs rather early in development and (b) is potentially critical in sustaining

tumour development across histologies. As minor exceptions, MTHFR and DNMT1 demonstrated statistical trends with histology and nodal involvement respectively, however it is unclear at the moment whether this is a circumstantial finding, or whether if the sample size were to be increased it would be found to be of more significance.

The correlation between DNMT1 and DHFR and TYMS expression levels is significant, however. This may suggest a need for concerted expression changes in order to maintain an increased cycle output, given the different enzymatic processitivity of all the involved enzymes. Such a coordinated molecular response might influence the vital cellular processes, including DNA methylation, repair and synthesis (Krushkal et al. 2016). Of course, this is a complicated biochemical network and it is well acknowledged that mRNA expression is by no means the only determinant of enzymatic activity. Nonetheless, the establishment of such relationships may assist in hypotheses and relevant future studies that are beyond of the scope of this thesis.

In summary, the data generated from this study (a) confirm the significant distortion of the mRNA expression profile among folate pathway genes in lung cancer, (b) provide new comprehensive information on SHMT1 and CBS1 as major targets for further research in NSCLC, as there is limited information on their relationship to lung cancer to date, (c) demonstrate folate cycle deregulation as a potential global mechanism for cancer development, and (d) indicate some degree of interdependence between the expression levels of different genes of the pathway in order to sustain its effect in cancer.

In view of the current use of a number of antifolate drugs in cancer management, this study provides evidence for the need for further research on the pathway in anticipation of identifying molecular modulators of resistance that might be used as clinical tools for improving drug efficacy and therefore patient survival.

3.4.2 Splicing variants expression profiles of SHMT1 and CBS genes in NSCLC

Alterations in alternative splicing of cancer-related genes may have a significant impact on lung cancer cell biology (Schwerk & Schulze-Osthoff 2005). Although SHMT1 and CBS encode important enzymes for normal physiology, no comprehensive attempt has been made so far to investigate splicing profiles in human disease. Our results demonstrate that all SHMT1/CBS variants are expressed in lung derived cell lines and NSCLC tissue samples, pointing out their importance for cell growth following high numbers of duplication in a culture environment. The unique, and very important, discovery in this study is that CBS variant 3 (CBSv3) is upregulated in NSCLC tissues, while SHMT1 variant 2 (SHMT1v2) exhibits significant downregulation with respect to adjacent non-tumorous tissues. This opens up a new research question regarding the functional role of these variants in cell growth and phenotype sustainability. The association of the differential expression of CBSv3 with the squamous phenotype is also of interest.

The reasons behind this splicing variant difference are currently unclear. Current evidence is insufficient to explain if this is because of a *de novo* expression difference, a difference in splicing rates or post-maturation mechanisms, such as the miRNA function, given that there is evidence of post-transcriptional modification by microRNAs (miRNAs) (Passetti et al. 2009). miRNAs are a group of small regulatory RNAs (~ 22 nucleotides) involved in post-transcriptional gene silencing through incorporation into the RNA-induced gene silencing complex (RISC), which binds the complementary sequence motifs of the target mRNA, mostly at the 3' untranslated regions (3'UTRs) (Betel et al. 2010; Jansson & Lund 2012) resulting in gene silencing, either by degradation or translational repression of the target mRNA (Filipowicz et al. 2008). Data from several studies have reported that alternative splicing in proliferating cancer cells might generate isoforms with deleted or shortened 3'UTR that

exhibit more mRNA stability with increased protein expression through a lack of miRNAs-mediated repression (Mayr & Bartel 2009; Hayes et al. 2014). Based on our data, however, CBSv3 lacks 3' UTR compared to other CBS splice transcripts employed in this study, hence a possible explanation for the CBSv3 upregulation in NSCLC might be the absence of 3' UTR that renders CBSv3 mRNA insensitive to miRNAs regulation.

Data generated from this study have also shown SHMT1v2 downregulation in NSCLC tissue compared to adjacent normal ones. As can be seen in Figure 3.10, SHMT1v2 lacks 1 additional α-helix, 3 β-sheets in comparison to isoform 1. The absence of these secondary structures as a result of a cleavage event might negatively affect the stability of the enzyme homotetramer by interfering with pyridoxal 5'-phosphate (PLP) binding (through Schiff base linkage) to the active site lysine, and thereby exposing this region to an external solvent (Liu et al. 2001; Giardina et al. 2015). Furthermore, the lack of exon 8 from the SHMT1v2 variant (Figure 3.10) might disrupt the enzyme amino-terminal domain, since exon 8 specifically encodes for the lysine that binds the active site PLP (Liu et al. 2001) and ultimately diminishes the enzyme catalytic activity. Collectively, this postulation may justify the decreased expression level of SHMT1v2 with the resultant attenuation of the enzyme catalytic activity in NSCLC samples.

To our knowledge, this is the first study to explore CBS and SHMT1 alternative splicing profiles in NSCLC. Our results suggest that the alteration of alternative splicing events affecting CBS/SHMT1 genes may have a potential mechanistic role in lung tumourigenesis. It remains a significant challenge, however, to identify whether these alterations in splicing profiles have the kind of direct role in lung carcinogenesis to make them potential biomarkers and/or therapeutic targets, as opposed to simply being bystanders occurring in lung cancer cells. Further investigations are therefore required in order to evaluate their impact in NSCLC pathogenesis.

Chapter 4: Epigenetic sensitisation to antifolates in respiratory tract cancer cells.

This chapter describes the experimental work undertaken to test the response of respiratory tract cancer cells to anticancer drugs that target folate metabolism and to explore the potential for epigenetic sensitisation of cell lines resistant to these agents.

4.1 Chemosensitivity of respiratory tract cancer cells to 5-Fluorouracil, methotrexate and pemetrexed

We measured the sensitivity to three commonly used anticancer drugs, 5-fluorouracil (5-FU), methotrexate (MTX) and pemetrexed (PEM), in a panel of ten respiratory tract cancer cell lines SK-MES-1, SK-LU-1, CALU6, A549, COR-L23, H358, LUDLU-1, BHY, PE/CA-PJ15, PE/CA-PJ41. The chemosensitivity of tumour cells was determined by estimating their half maximal inhibitory concentration (IC50), which is the drug concentration required to inhibit 50% of the cellular growth in comparison to untreated cells. Cell growth was measured by MTT assay and IC50 values were calculated using GraphPad Prism software version 6.0. As expected, a range of sensitivities were demonstrated among the studied cell lines. In general, all tested drugs reduced cellular viability in a concentration dependent manner, however, MTT analysis showed that the effectiveness of pemetrexed and MTX was moderate compared to that of 5-FU. Analysis of IC50 values at 95% confidence intervals following treatment with (1-64 µM) pemetrexed demonstrated that H358, A549 and SKLU1 were the most sensitive cancer cell lines (Table 4.1) while LUDLU and CALU6 were the most resistant ones (Figure 4.1). Following 72 hours treatment with 0.125-8 µM MTX, the studied respiratory tract cancer cell lines exhibited lower MTT absorbance readings compared to that of pemetrexed, with IC50 values

being highest in LUDLU and CALU6 and lowest in PE/CA-PJ41 cancer cell lines (Figure 4.2)(Table 4.1). The greatest reduction in cell viability was observed following (0.015-1mM) 5-FU exposure in most of the studied cancer cell lines, except A549 and SK-MES-1, with IC50 values of 0.765 and 0.339 mM respectively. The lowest MTT absorbance readings of 5-FU was spotted in SK-LU-1 with an IC50 value of 0.031 mM (Figure 4.3)(Table 4.1). Furthermore, the obtained IC50s were compared with publicly available data for 5-FU and MTX (cancerrxgene.org).

Table 4.1: IC50 values and their respective 95% confidence intervals in NSCLC and HNSCC cell lines exposed to 5-FU (0.015-1 mM), MTX (0.125-8 µM) and pemetrexed (1-64 µM) compared with the publically available data.

Cell line	5-FU (mM)	95% C.I	Available data	MTX (µM)	95% C.I	Available data	PEM (µM)	95% C.I	Available data
A549	0.76	*0.6-0.96*		3.78	*2.62-5.47*	2.84	45.89	*31.1-67.7*	
BHY	0.19	*0.16-0.21*	0.034	7.30	*5.31-10.05*				
CALU6	0.11	*0.09-0.13*	0.0133			0.402			
CORL23	0.11	*0.08-0.15*		7.18	*5.19-9.94*	0.0817			
H358	0.16	*0.12-0.22*	0.0113	5.70	*4.05-8.02*	0.251			
LUDLU	0.22	*0.18-0.28*							
PJ15	0.25	*0.18-0.35*	0.0559	2.40	*1.81-3.202*	2.73			
PJ41	0.21	*o.16-0.28*		0.88	*0.6291-*				
SKLU1	0.031	*0.02-0.04*	0.102	2.56	*1.71-3.81*		48.87	*31.61-75.57*	
SK-MES	0.33	*0.22-0.46*	0.061	8.38	*6.72-10.47*	1.4			

No significant correlation was observed between the sensitivity of the cell lines to 5-FU, MTX, pemetrexed drugs (represented by IC50) and corresponding mRNA expression levels of CBS, SHMT1, TYMS, MTHFR, DHFR and DNMT1 genes (Chapter 3)(Spearman test, p value> 0.05).

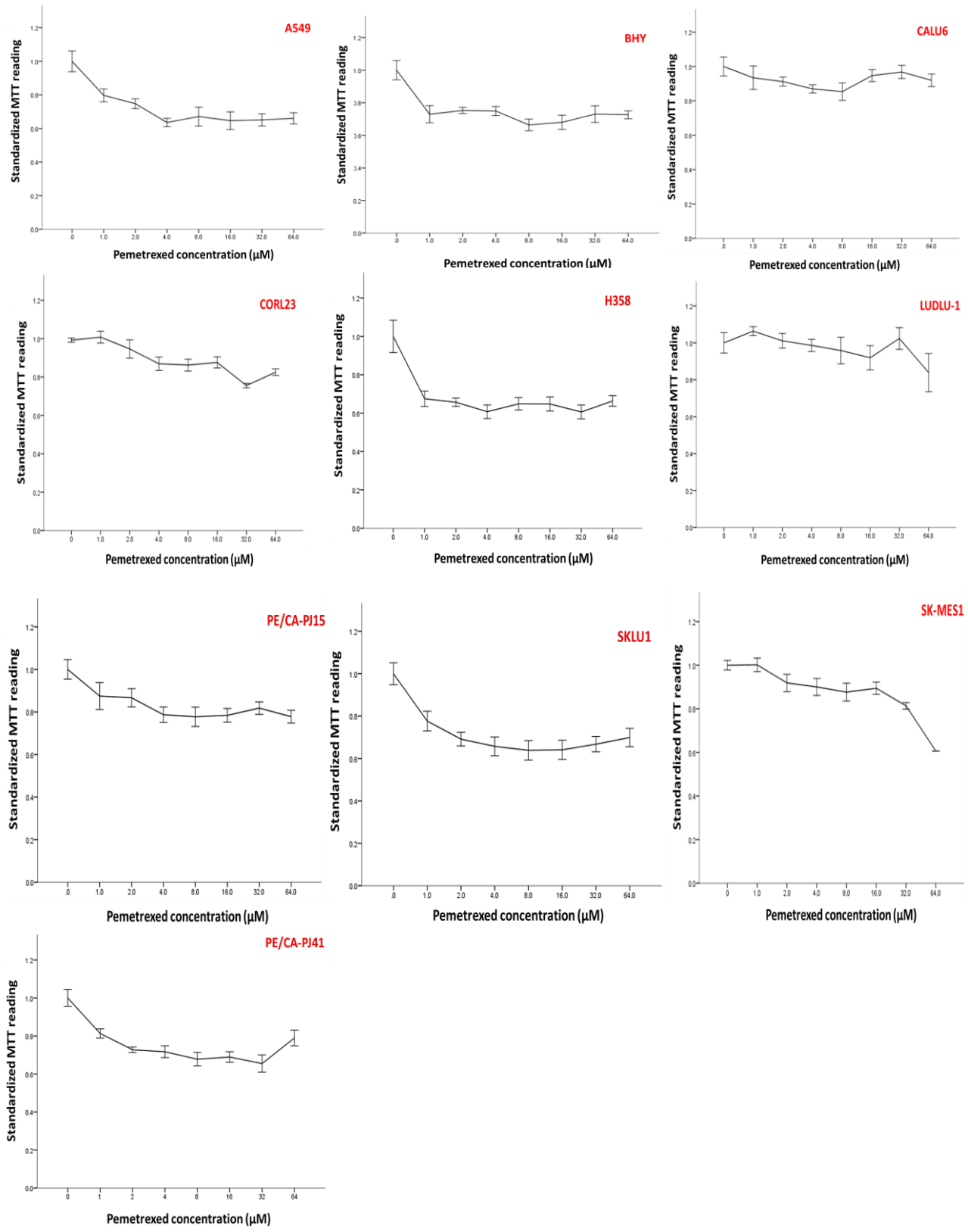

Figure 4.1: The effect on the cell viability of respiratory tract cancer cell lines of exposure to pemetrexed for 72 hours. The mean and error values in all graphs are for six technical replicates, and error bars represent 95% confidence intervals.

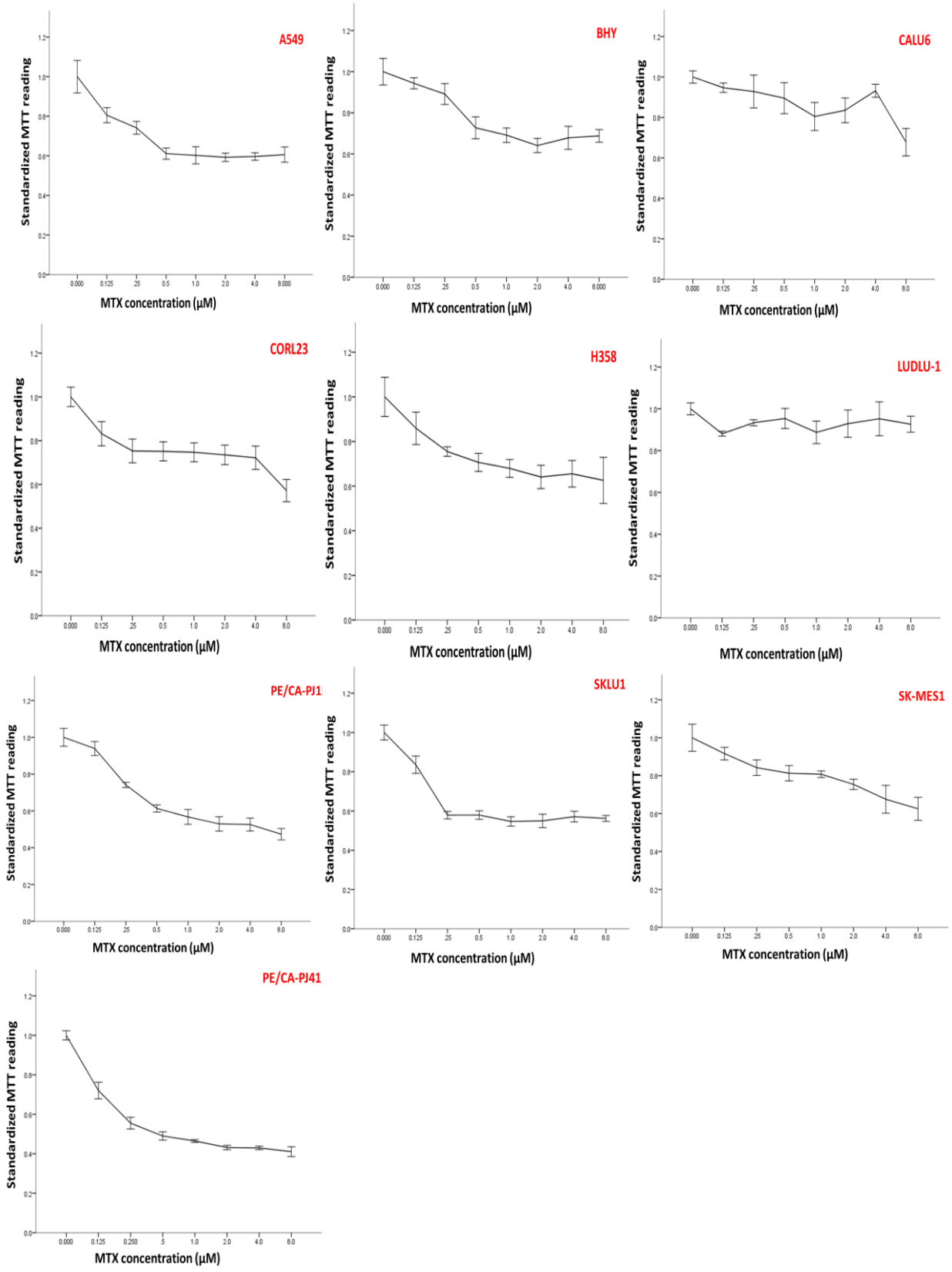

Figure 4.2: Heterogeneous response of the examined respiratory tract cancer cell lines following 72 hours MTX incubation. The mean and error values in all graphs are for six technical replicates, and error bars represent 95% confidence intervals.

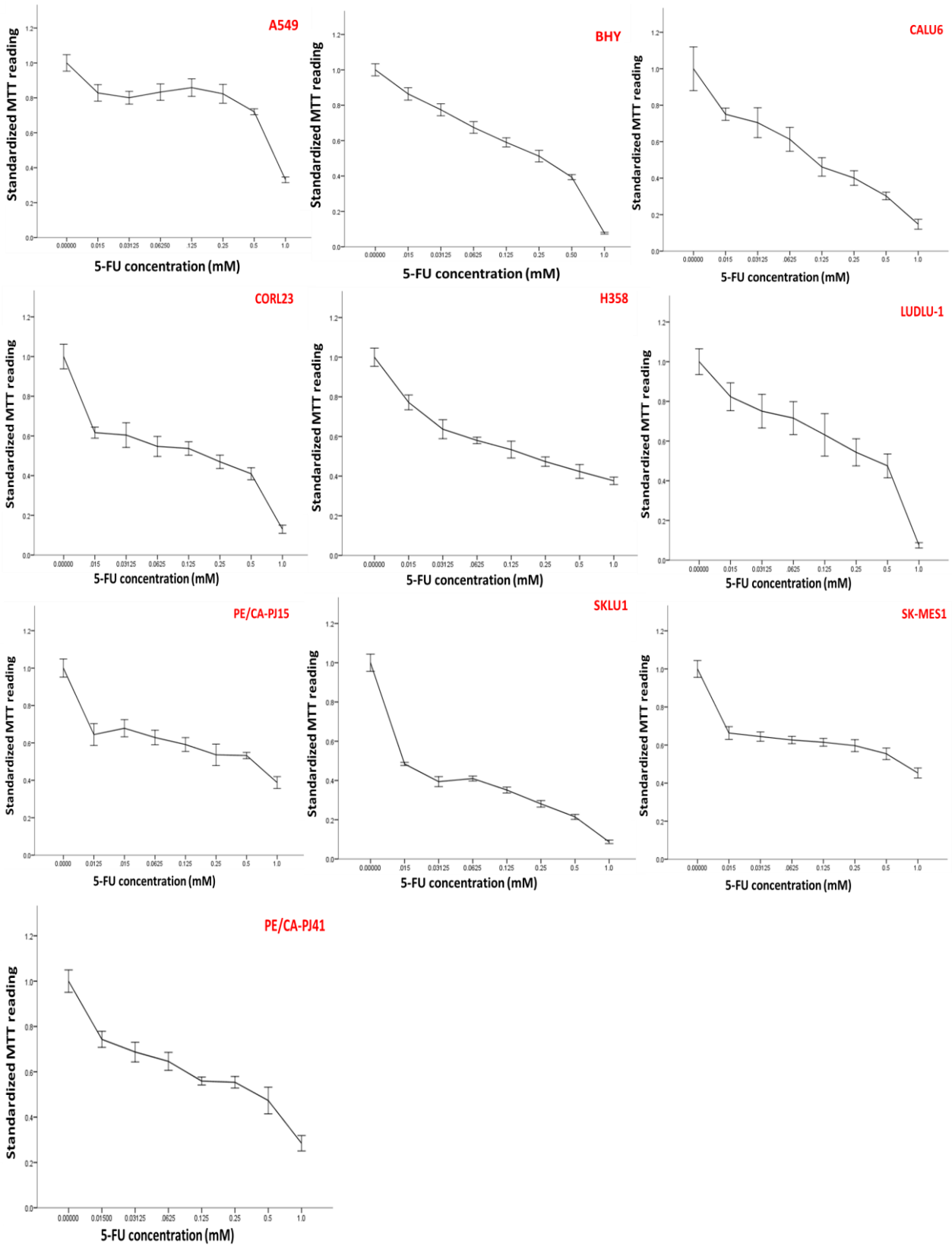

Figure 4.3: Dose response curves for the examined respiratory tract cancer cell lines following exposure to 5-FU for 72 hours. The mean and error values in all graphs are for six technical replicates, and error bars represent 95% confidence intervals.

Since 5-FU has demonstrated superior inhibition of cancer cell viability, with the exception of A549 and SK-MES-1, our next step was to evaluate the clinical significance of folate related genes in 5-FU resistant NSCLC cells. We employed quantitative real time PCR (qPCR) to assess the expression of TYMS, DHFR, MTHFR, SHMT1, CBS and DNMT1 at the mRNA levels in A549 and SK-MES cell lines following 24 and 72 hours exposure to three different doses; 0.5 mM, 0.25 mM and 0.0625 mM of 5-FU (Figure 4.4). Analysis of the TYMS mRNA level revealed increased expression across 5-FU non-responsive NSCLC cell lines compared to non-treated ones, nonetheless TYMS upregulation was not obvious in the first 24 hours of exposure in both resistant cell lines (Figure 4.4A). We also found that the expression level of MTHFR was upregulated early during 5-FU challenge at a concentration of 0.5 mM in both A549 and SK-MES-1 cell lines, and remained at similar levels (specially for SK-MES) for the whole incubation time (Figure 4.4B). This observation suggests that MTHFR overexpression may be an early response to high dose 5-FU therapy. Interestingly, DNMT1 expression showed significant reduction in A549 and the opposite was observed in SK-MES cells, with marked upregulation relative to that of the control, at 0.0625mM 5-FU seen late in the treatment course (Figure 4.5C). When the alteration of DHFR mRNA levels in response to 5-FU treatment was compared between the two studied cell lines, A549 was shown to express DHFR at a significantly lower level than its untreated counterpart throughout the whole time course, while SK-MES-1 displayed an upregulated DHFR activity which was more obvious in the subsequent 72 hours of 5-FU exposure (Figure 4.5D). Generally, SHMT1 (Figure 4.6E) and CBS (Figure 4.6F) mRNA levels were variable across the 5-FU resistant cell lines, but consistently lower than that of non-treated cells.

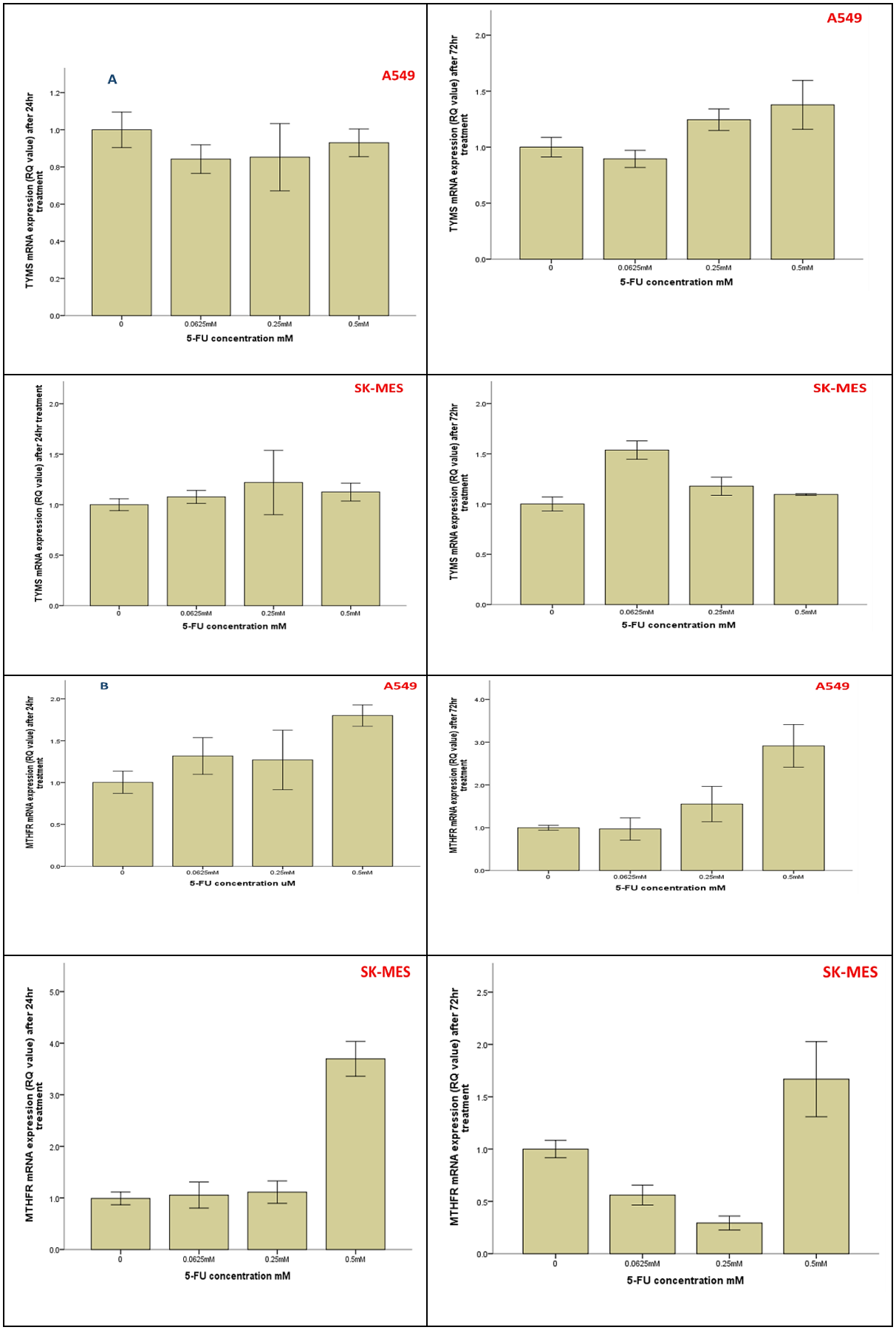

Figure 4.4: Bar charts representing the mRNA expression profile of TYMS (A) and MTHFR (B) in A549 and SK-MES following 24 and 72 hours incubation with 0.5, 0.25 and 0.0625 mM 5-FU. Error bars represent 95% confidence intervals.

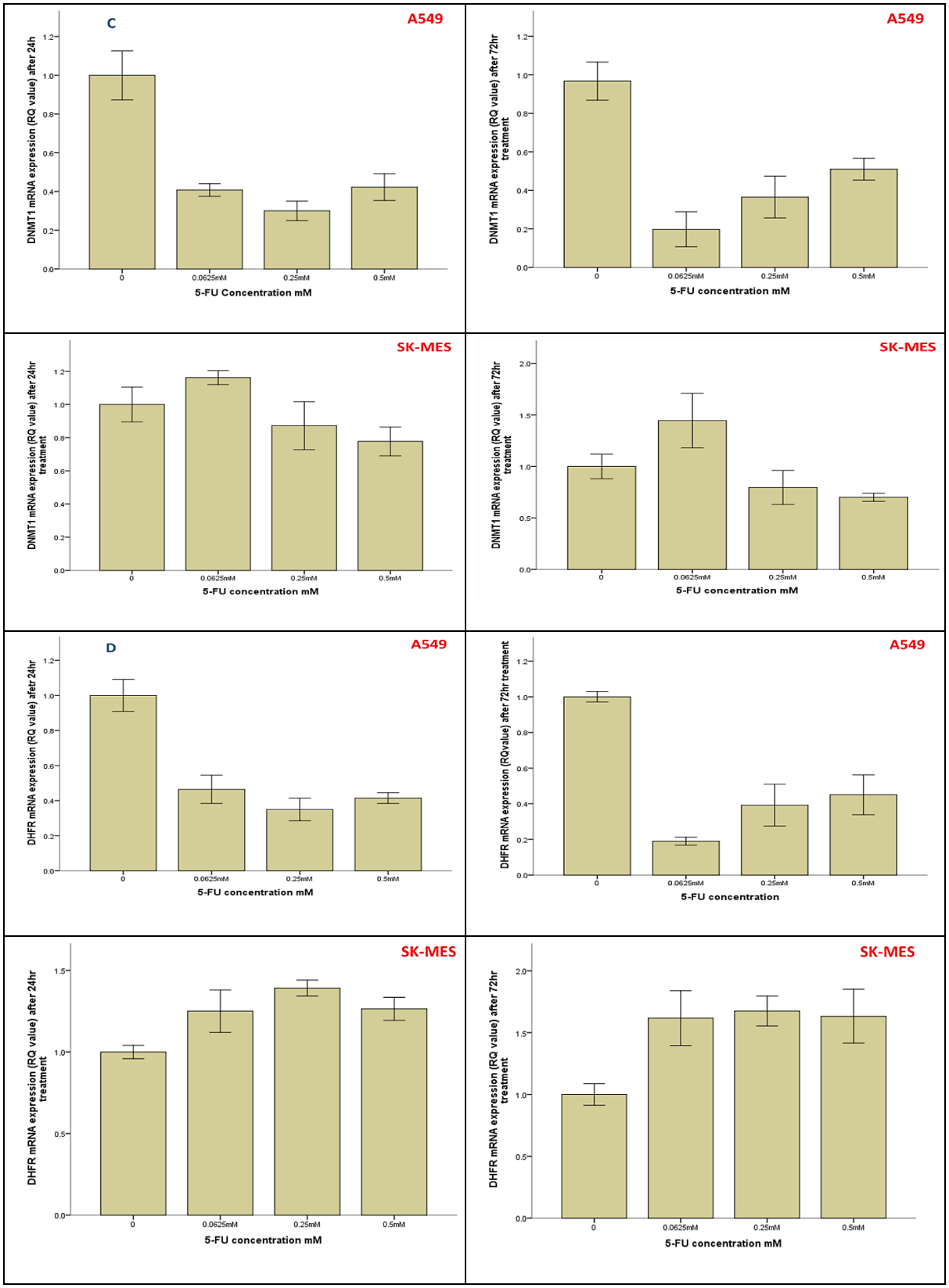

Figure 4.5: Bar charts representing the mRNA expression profile of DNMT1 (C) and DHFR (D) in A549 and SK-MES following 24 and 72 hours incubation with 0.5, 0.25 and 0.0625 mM 5-FU. Error bars represent 95% confidence intervals.

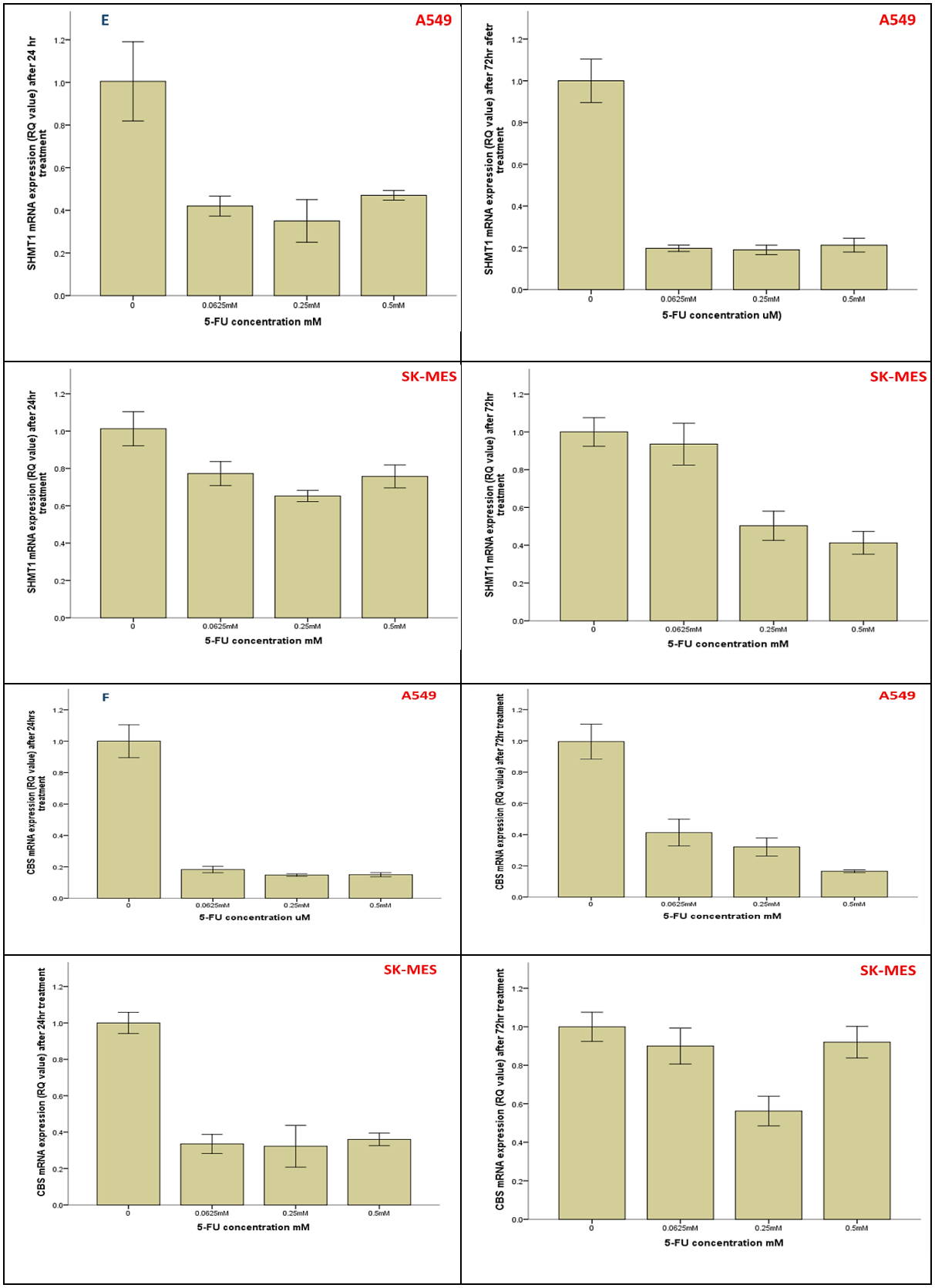

Figure 4.6: Bar charts representing the mRNA expression profile of SHMT1 (E) and CBS (F) in A549 and SK-MES following 24 and 72 hours incubation with 0.5, 0.25 and 0.0625 mM 5-FU. Error bars represent 95% confidence intervals.

4.2 Epigenetic sensitisation of non-small cell lung cancer cell lines to folate targeted drugs

Since epigenetic deregulation has been associated with cancer cell aggressiveness and chemoresistance (Steinhardt & Gartenhaus 2013), we hypothesised that aberrant epigenetic mechanisms, including DNA methylation and histone acetylation may contribute to resistance to folate pathway targeting drugs in NSCLC. Our hypothesis was founded on previous studies that have shown the potential efficacy of combining epigenetic-based therapy with these agents in several types of cancers (Kanda et al. 2005; Morita et al. 2006; Leclerc et al. 2010; Iwahashi et al. 2011; Bufalo et al. 2014). In this instance, we investigated the epigenetic influence on the reversal of 5-FU, MTX and pemetrexed resistance in NSCLC cell lines. Two well-known epigenetic modifiers, histone deacetylase (HDAC) class I inhibitor Valproic acid (VPA) and the DNA methyltransferase1 (DNMT1) inhibitor Decitabine (DAC), were utilised to test the sensitisation of the two most resistant cell lines (with the highest IC50 values, Table 4.1); A549 and SK-MES-1 to 5-FU, CALU6 and LUDLU to MTX and pemetrexed. Based on the preliminary results obtained from previous pilot experiments, cell lines were exposed to a tissue culture final concentration of 100 nM DAC and 1mM VPA with the corresponding IC50 doses of 5-FU, MTX and PEM (Table 4.1). Our results demonstrated a significant reduction of MTT absorbance readings for the subsequent 72 hours when A549 and SK-MES cell lines were exposed to VPA treatment 48 hours prior to the addition of 5-FU (Figure 4.7A &B). In contrast, VPA pretreatment did not change the MTT absorbance values of the normal human embryonic lung fibroblast IMR90 cell line following 5-FU exposure (Figure 4.7C). Synchronous treatment of DAC and 5-FU significantly reduced A549 cell viability as compared to 5-FU treatment alone (Figure 4.8A), whereas the MTT absorbance values of the SK-MES cell line demonstrated a minor effect in response to DAC and 5-FU concomitant treatment (Figure

4.8B). In addition, the combination of DAC/VPA with MTX did not markedly change the absorbance readings for the latter in the LUDLU or CALU6 cell lines (Figure 4.9 A&B). Similarly, no obvious difference in cell viability with pemetrexed treatment was seen in the same NSCLC cancer cell lines following synchronous treatment with DAC or prior VPA exposure (Figure 4.10 A&B).

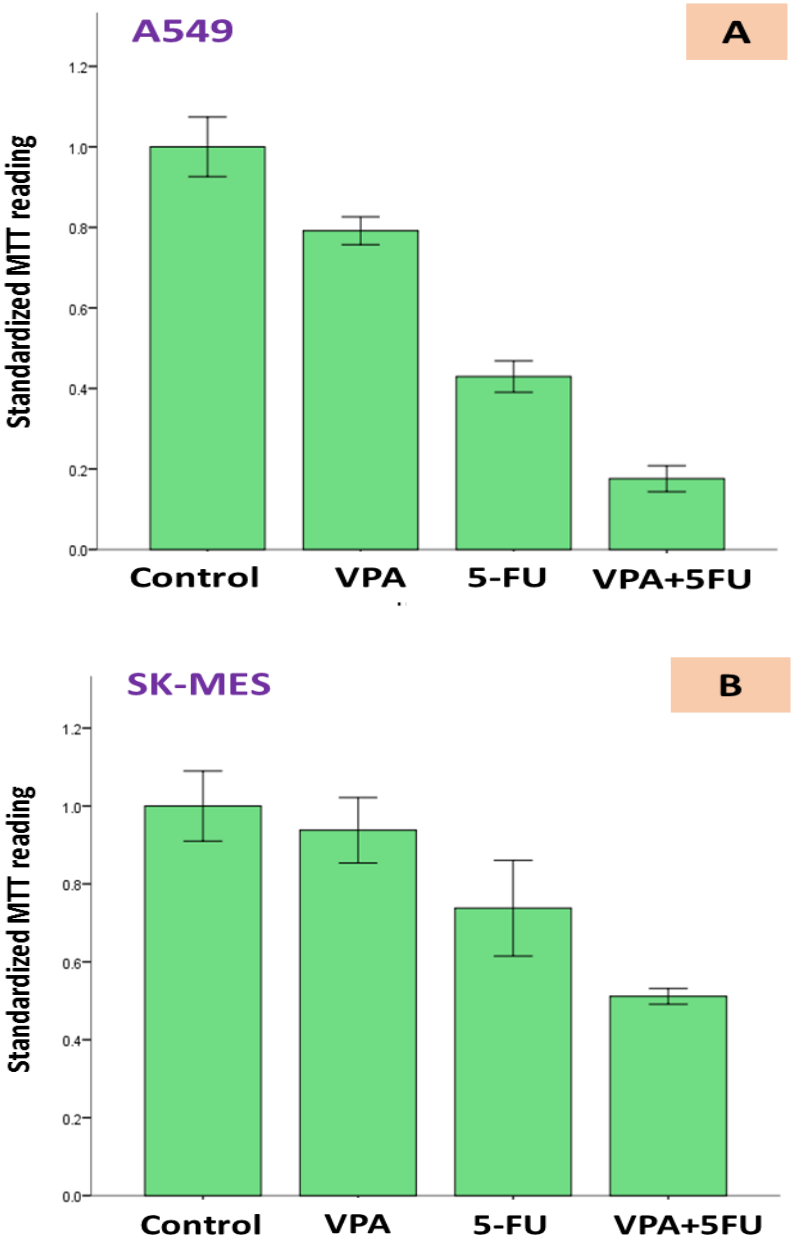

Figure 4.7: Bar charts representing MTT absorbance readings following 48 hours pretreatment with VPA followed by 72 hours 5-FU exposure in (A) A549 and (B) SK-MES cell lines. Error bars represent 95% confidence intervals.

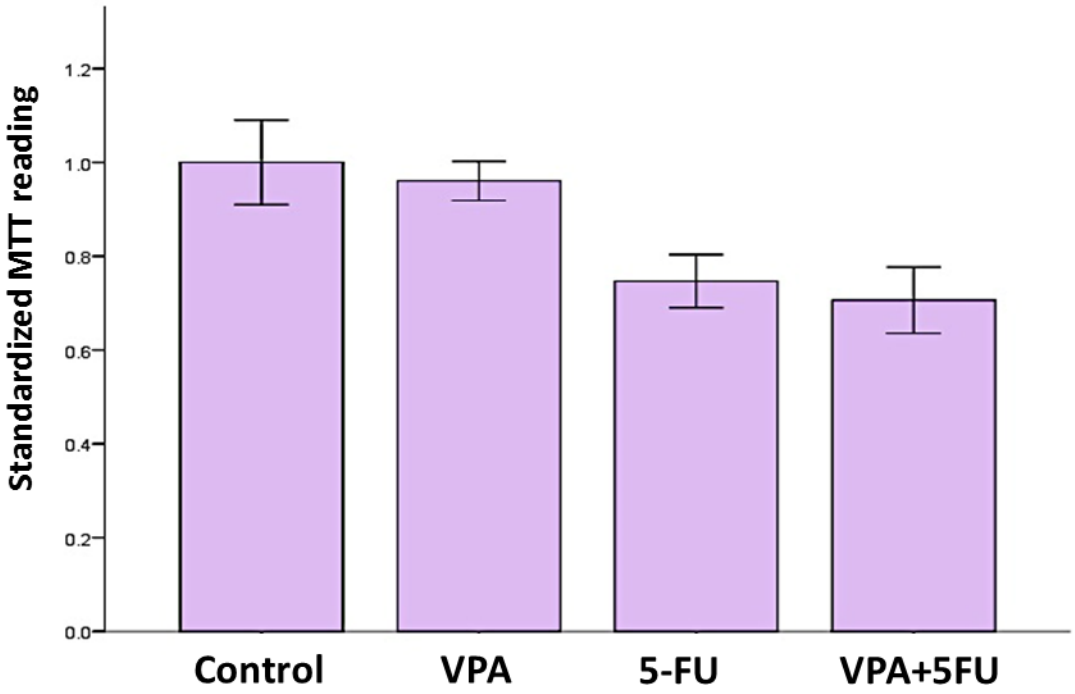

Figure 4.7 C: Bar charts representing the MTT absorbance readings of the IMR90 foetal lung fibroblast cell line with 5-FU treatment preceded by 48 hours incubation with VPA. Error bars represent 95% confidence intervals.

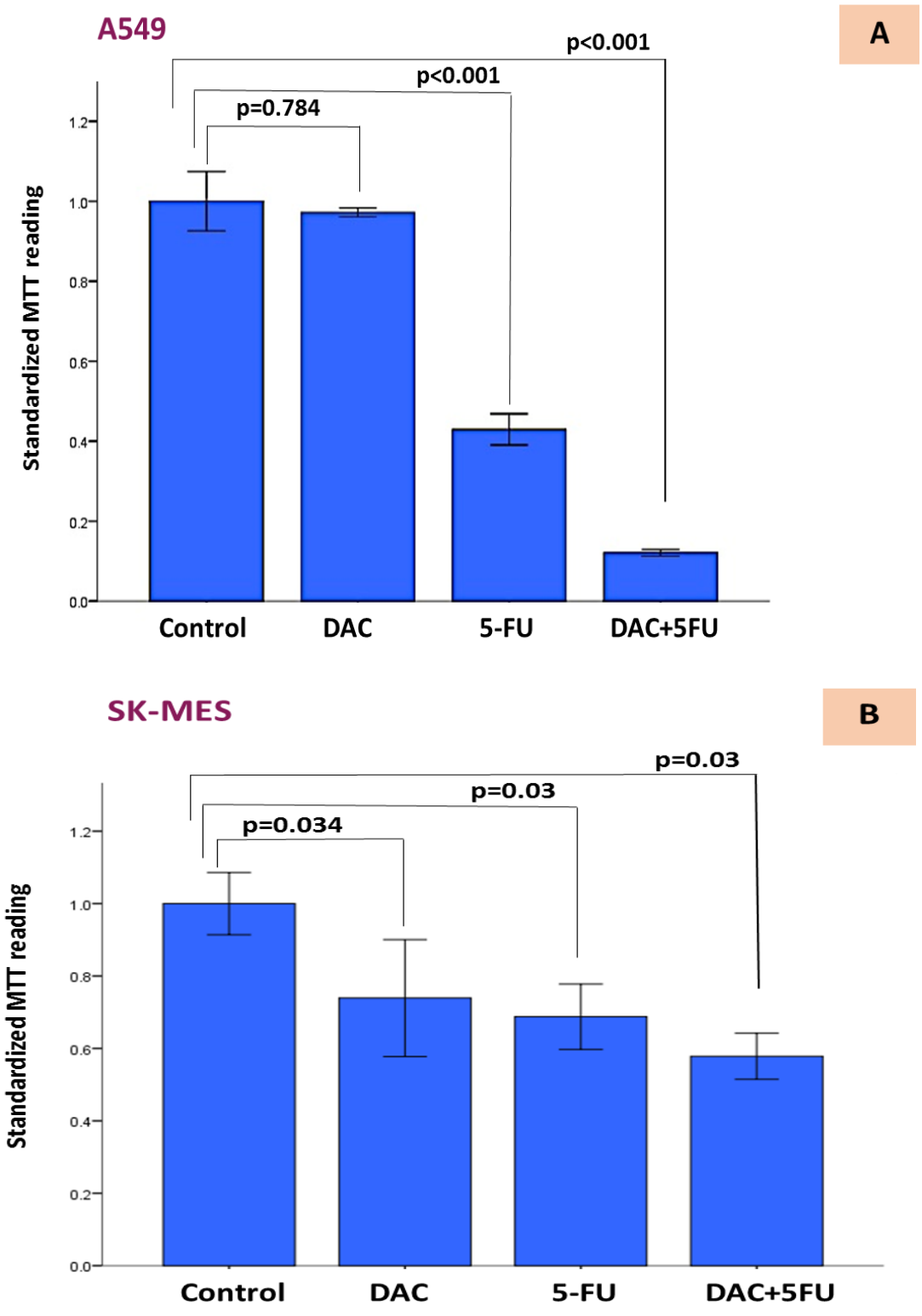

Figure 4.8: Effect of 72 hours 5-FU and DAC combination on viability of A549 (A) and SK-MES (B) cell lines. Error bars represent 95% confidence intervals. Bars represent the mean of four technical replicates. P values were derived from One-Way ANOVA, Post Hoc, Dunnett T3 tests.

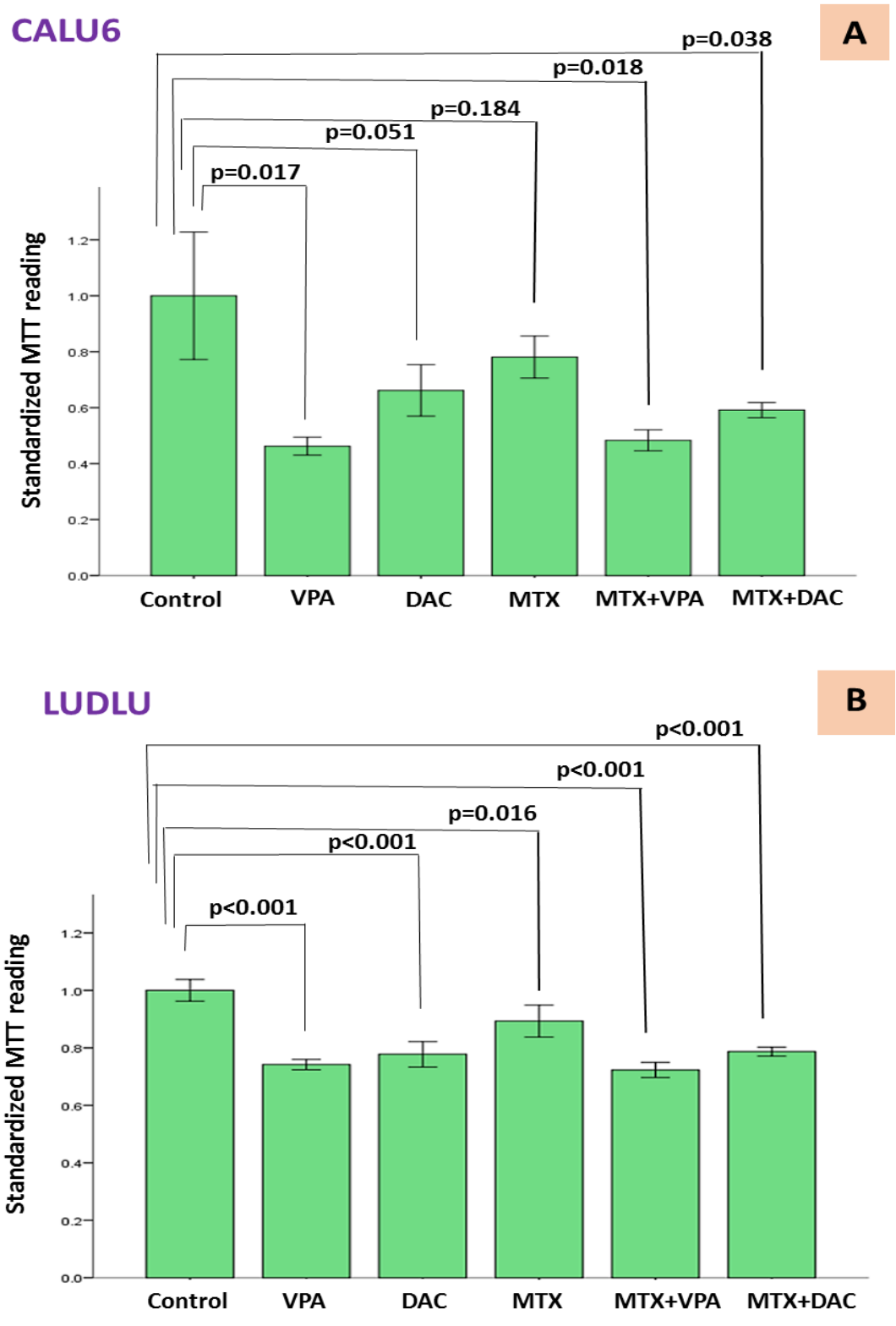

Figure 4.9: Bar charts representing the MTT absorbance reading of CALU6 (A) and LUDLU (B) cell lines following exposure to VPA and DAC combination with MTX. Error bars represent 95% confidence intervals. The results represent the mean of four technical replicates. P-values were derived from One-Way ANOVA, Post Hoc, Dunnett T3 tests.

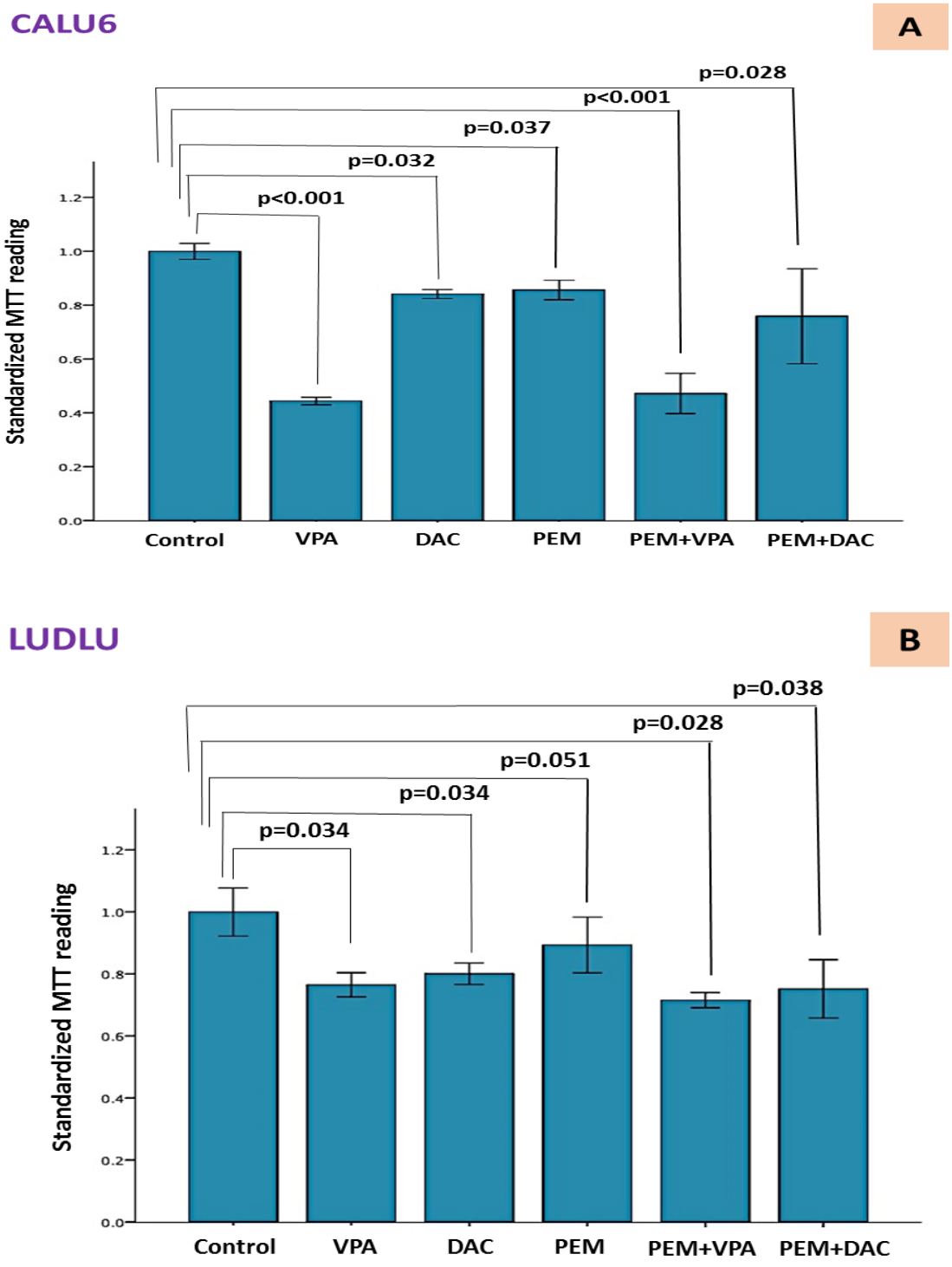

Figure 4.10: Bar charts representing the MTT absorbance readings of CALU6 (A) and LUDLU (B) cell lines following exposure to VPA and DAC combination with pemetrexed. Error bars represent 95% confidence intervals. The results are the mean of four technical replicates. P-values were derived from One-Way ANOVA, Post Hoc, Dunnett T3 tests.

In order to explore the potential mechanisms behind the enhancement of 5-FU antitumor effect against NSCLC cell lines following VPA exposure, we quantified the expression levels of our usual six folate target genes in A549 and SK-MES cell lines following 48 hours exposure to VPA incubation (Figure 4.11). Gene expression analysis by real time PCR demonstrated the ability of VPA to downregulate TYMS mRNA level in 5-FU unresponsive NSCLC cells in comparison with non-treated controls (Figure 4.11A). Similar to the TYMS response data, DNMT1 was found to be suppressed as a result of VPA treatment (Figure 4.11B). A consistent but borderline reduction of SHMT1 expression level was spotted across VPA treated A549 and SK-MES cells (Figure 4.11C). Furthermore, there was no alteration in MTHFR or CBS expression profiles in VPA treated A549, whereas SK-MES was observed to display these two folate genes at a significantly higher level than that of untreated counterparts (Figure 4.11D and Figure 4.11E). Interestingly, there was a significant reduction of DHFR mRNA expression in SK-MES cells exposed to VPA for 48 hours, however A549 expressed the same gene with only a borderline increment under the same reaction conditions (Figure 4.11F).

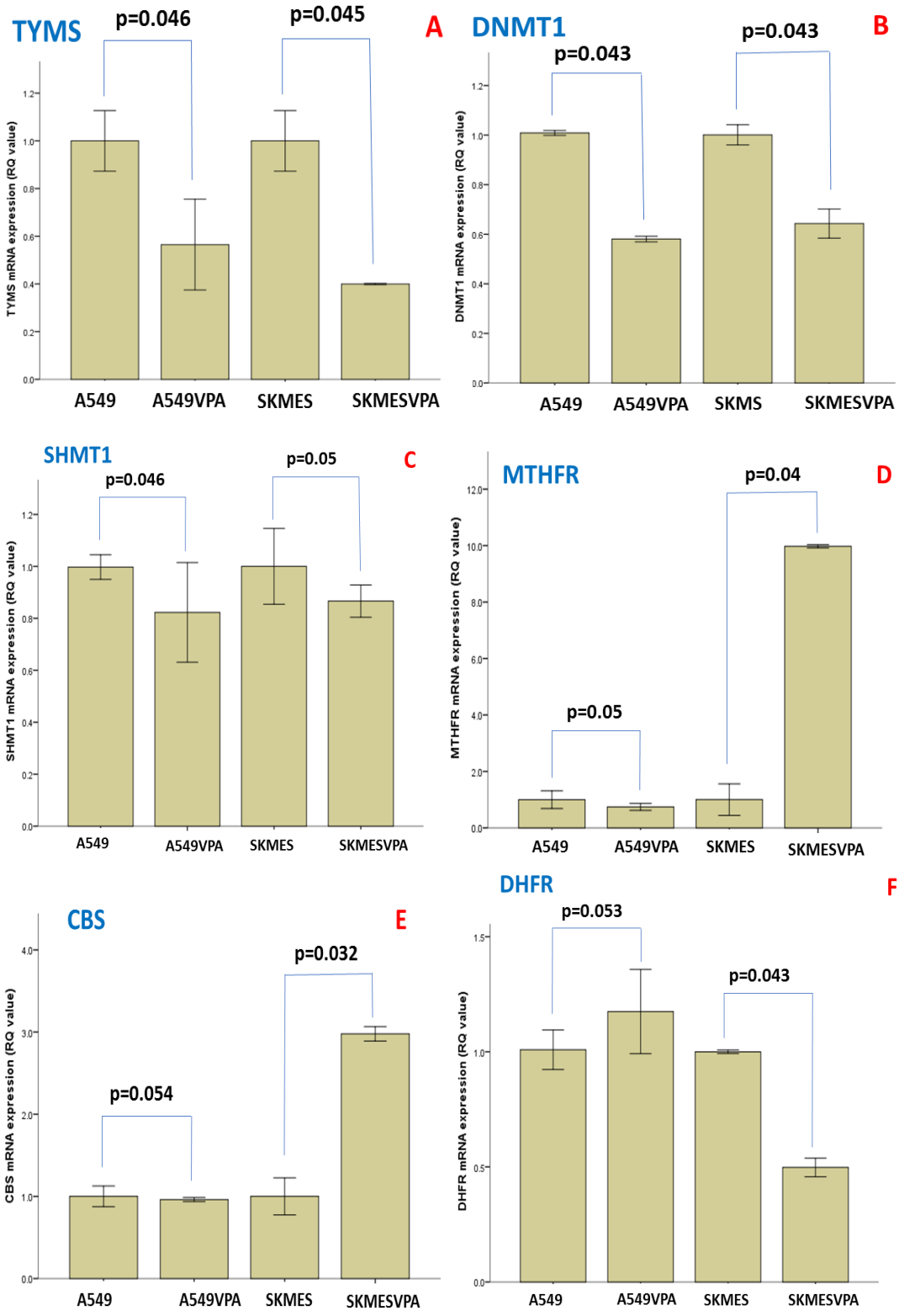

Figure 4.11: Altered mRNA expression of TYMS (A), DNMT1 (B), SHMT1 (C), MTHFR (D), CBS (E) and DHFR (F) A549 and SK-MES cell lines treated with VPA for 48 hours compared to untreated controls. The results are the mean values of two technical replicates. Error bars represent 95% confidence intervals. RQ=relative quantification. P-values were derived from Mann-Whitney tests.

4.3 Discussion

4.3.1 Chemosensitivity of respiratory tract cancer cells to 5-fluorouracil, methotrexate and pemetrexed

Folate metabolism is a typical example of a biological pathway with critical pharmacological relevance. It has been an attractive target for key chemotherapeutics that are widely used in medical oncology for several types of malignancies, including respiratory tract cancers (Ulrich & Robien, 2002). This study demonstrated a dose dependent reduction of cell viability across respiratory tract cancer cells in response to 5-FU, MTX and pemetrexed exposure, with the lowest MTT absorbance readings being achieved following 5-FU treatment. In contrast, MTT analysis showed a high degree of resistance against MTX and pemetrexed antifolates drugs among the cancer cell lines studied. Because of their high response rates combined with low toxicity, both MTX and pemetrexed are favourable drugs for the palliative treatment of HNSCC and NSCLC respectively (Cohen et al. 2005; Schuler et al. 2010) but our results showed poor response levels for these antifolates with several cancer cell lines. As already described in the introduction chapter, the chemotherapeutic efficiency of these anticancer agents is frequently hampered by the development of drug resistance. Clinical and preclinical studies have identified a plethora of mechanisms by which cancer cells develop resistance to these antifolate drugs (Gonen & Assaraf 2012). In addition, cell lines are usually established from tumour biopsies of patients who might be treated with antifolates, or those who may have a recurrent disease. It is therefore reasonable to notice some lack of responsiveness to antifolates in some of the investigated cell lines. In terms of IC50 values, 5-FU displayed low MTT absorbance values in eight out of ten RTCs cell lines. It is worth noting that we have observed a marked difference between some of 5-FU and MTX IC50 values generated from this study when compared with publicly available data. This might be attributed to the

different experimental conditions. In addition, it is widely accepted that cancer cell lines evolve genetically too fast through hundreds of thousands of duplications that have undergone in each lab. Another point is that they can be phenotypically different and do not relate to the original cell line.

In the general effort towards identifying the potential mechanisms behind 5-FU resistance, we explored the expression profiles of folate pathway related genes in cell lines that were less responsive to 5-FU.

So far, the majority of pharmacogenetic studies related to 5-FU have focused on TYMS expression as a key determinant of 5-FU antiproliferative effect, stating that an increase in TYMS mRNA expression has been a prominent feature for 5-FU resistance (Leichman et al. 1977; Johnston et al. 1995). In agreement with these reports, we found that the survival of A549 cells following treatment with three different concentrations of 5-FU for 48 hours, seems to depend on a high TYMS expression. In fact, there is even a trend of expression being associated with the dose. Additional supporting information comes from our epigenetic sensitisation experiments. VPA sensitises A549 cells to 5-FU. Interestingly, VPA results in a reduction of TYMS expression at both 24 and 72 hours of exposure. Although it is highly probable that other potential regulators contribute to 5-FU resistance, including FPGS, GGH, UNG, UMP kinase and DTYMK (Muhale et al. 2011), our data strengthens the case for the involvement of TYMS expression in 5-FU resistance. This finding was less clear cut in SK-MES cells, however. While at low 5-FU doses, the result resembled that for A549, at higher doses we observed a reduction in the effect. Based only on current data, this is not easy to explain, however it clearly reflects the clinical problem in respect to cancer heterogeneity in treatment response, and it is most likely due to the different histological origin of the cell lines, and their individual molecular profile.

We observed that MTHFR expression was higher in surviving cells following 5-FU exposure, in both A549 and SK-MES cell lines and in a dose-dependent manner at 72 hours. This has also been shown previously (Scartozzi et al. 2011; Wang et al. 2014). A probable explanation for this is that MTHFR is a key enzyme involved in intracellular folate haemostasis, through catalysing the irreversible conversion of 5,10 methylene tetrahydrofolate (CH2FH4) into 5-methyltetrahydrofolate (CH3FH4). 5-FU exerts its antitumor effect through binding of 5-fluorodeoxyuridine monophosphate to TYMS, thereby forming an inactive ternary complex together with CH2FH4. The stability of that complex is primarily based on a high CH2FH4 level (Scartozzi et al. 2011; Wang et al. 2014). One can therefore hypothesise that cancer cells exhibiting an increased MTHFR activity might be refractory to 5-FU treatment by minimising the bioavailability of CH2FH4, and that this might be an early event in the development of 5-FU resistance.

In the case of MTHFR, results from VPA exposure were less conclusive, however. MTHFR expression does not change in A549 after VPA treatment, while in SK-MES VPA leads to MTHFR overexpression, apparently contradicting the potential role of MTHFR in 5-FU resistance. One has to keep in mind, however, that VPA, as with every HDAC inhibitor, triggers expression changes in hundreds of genes and 5-FU resistance can be modulated by multiple genes within or outside the folate pathway.

DNMT1 mRNA expression following 5-FU treatment demonstrated an interesting profile. A549 cells surviving at 72 hours demonstrated lower DNMT1 expression compared to control cells. A marginal increase observed from lower to higher 5-FU dose does not change this trend. SK-MES cells demonstrated a puzzling overexpression at low level exposure, but, at higher doses, this reverts to under expression compared to unexposed cells. Interestingly, DNMT1 expression was reduced in the presence of VPA, suggesting this gene as another

potential mediator of epigenetic sensitisation to 5-FU. In the absence of any published report connecting DNMT1 expression and sensitivity to 5-FU, this data is unique, but very difficult to interpret with confidence. This is especially because of DNMT1 role as a global DNA methylation maintenance enzyme, affecting therefore the expression of many genes.

A rather inconclusive result was derived for the potential association of DHFR and 5-FU. Reduced DHFR expression was observed in the surviving A549 cells following 5-FU exposure, while the exact opposite was shown for SK-MES. Combining the lack of DHFR expression change in the VPA experiment for A549 and the downregulation of the gene by VPA in SK-MES increases the uncertainty regarding the role of this gene in 5-FU resistance. Furthermore, to date, there is no published work on this aspect.

SHMT1 and CBS gene expression patterns showed a remarkable reduction in the surviving A549 and SK-MES cells exposed to 5-FU. As we will see in Chapter 5, SHMT1 knock down in PJ15 head and neck cancer cells results in sensitisation to 5-FU, apparently contradicting these results. Once again, there is no published information on the role of SHMT1 in regulating drug resistance. The discrepancy of results between the two experiments could be explained by the different origin and molecular profile; however, it is fair to state that it is currently not understood what may be mediating the potential action of SHMT1 on 5-FU resistance and the different effects may be subject to its variable availability in the different cell lines. This is discussed further in Chapter 5.

Overall, the expression data in 5-FU resistant NSCLC cell lines demonstrated a substantial heterogeneity of responses and potential survival contingencies to gene expression. While the role of TYMS, MTHFR and DNMT1 in 5-FU resistance is strengthened, at this point, little can be concluded for the remaining genes. Nonetheless, this data offers a good baseline for further research.

4.3.2 Epigenetic sensitization of non-small cell lung cancer cell lines to folate targeted drugs

In this study, we also examined the potential of VPA and DAC epigenetic modifiers to act as chemosensitisers to 5-FU, MTX and pemetrexed in NSCLC cell lines. Pretreatment of A549 and SK-MES with VPA for 48 hours sensitised these cells to 5-FU, while no such sensitising effects were seen in MTX or pemetrexed resistant cells. Thus, our data showed the potential synergistic effect of the combined treatment with 5-FU and VPA in 5-FU resistant lung cancer cell lines. These findings are in accordance with Noro et al. (2010), who established that combined therapy of 5-FU and another HDAC inhibitor (SAHA) enhances 5-FU response in resistant NSCLC cell lines. The potentiation of 5-FU anticancer activity when combined with different types of HDACi has been reported in gastric (Lee et al. 2006), colorectal (Abaza et al. 2014), hepatic (Ocker et al. 2005), pancreatic and cholangiocarcinoma (Iwahashi et al. 2011). To our knowledge, this is the first report to show that VPA enhances the therapeutic effect of 5-FU in NSCLC cell lines.

The present study also demonstrated that DAC demethylating agent produced a pronounced reduction in the viability of A549, with a minor effect in the SK-MES cell line when treated simultaneously as compared with 5-FU alone. Similar results have been previously reported in breast cancer cell lines (Mirza et al. 2010) and hepatoma and pancreatic cancer cell lines (Kanda et al. 2005). While DAC was not efficient in reducing chemoresistance to MTX or pemetrexed in our data, epigenetic reprogramming and enhancement of 5-FU sensitivity among tumour cells following the addition of DAC might be achieved through breaking the silence and reactivation of transcriptional activity of certain genes involved in 5-FU metabolic pathway following aberrant promoter hypermethylation at specific sites (Humeniuk et al. 2009). Up to now, however, almost nothing is known about the effect of DNA demethylating

agents in 5-FU resistance in lung cancer, therefore the synergistic antineoplastic action of combined 5-FU chemotherapy with DAC observed in our experiments merits further investigation.

The toxicity profile of DAC has been linked with numerous issues when used in combination with chemotherapeutic agents in cancer clinical trials. For example, myelosuppression has been reported as the major side effect (Momparler et al. 1997), in addition to the limited capacity to reactivate enough tumour suppressor genes through inhibition of DNA methylation (Stephan & Momparler 2015). On the other hand, VPA has been a relatively safe and commonly prescribed antiepileptic and mood stabiliser for decades (Detich et al. 2003). We therefore chose to further pursue the synergistic antitumor promise observed when combining 5-FU based chemotherapy with VPA in A549 and SK-MES cell lines. For this, we investigated the influence of VPA treatment against the mRNA expression profiles of 5-FU metabolism-related genes in drug resistant NSCLC cell lines. Importantly, VPA exposure of A549 and SK-MES cells led to a marked reduction of TYMS mRNA expression levels, as discussed before. This observation suggests that VPA induced TYMS downregulation, the primary target for 5-FU, may serve as one of the mechanisms involved in the tumour inhibitory effect of the 5-FU and VPA combination. Indeed, TYMS has been reported as one of the predictive biomarkers for 5-FU response in lung cancer (Longley et al. 2003; Oguri et al. 2005). Similar results were observed with DNMT1, suggesting that VPA is a downregulator and potent inducer of DNMT1 degradation (Zhou et al. 2008).

It is worth noting that the effect of VPA treatment on CBS expression patterns was markedly different between the tested cell lines, with significant overexpression in SK-MES but not in A549. As we mentioned before, DHFR transcriptional activity was reduced to approximately 50% following VPA incubation in SK-MES, while no significant alteration was observed in A549

under the same experimental conditions. Still, it is unclear if this downregulation is a major consequence of VPA treatment as a result of cell cycle arrest, or simply a passive observation in response to reduced cellular viability. Furthermore, the cell specificity in terms of gene expression changes in response to VPA challenge observed in this study might be attributed to differences in the molecular, phenotypic characteristics, or in the histology and growth rate between the two NSCLC cell lines.

Collectively, we have identified potential synergistic interaction between 5-FU and VPA that may point the way to a novel therapeutic regime allowing for lower doses of each drug to be administered to NSCLC patients with less chemotherapeutic toxicity, while maintaining the same therapeutic effect. Further research is warranted in order to adapt this combination therapy successfully in clinical studies. Comparative gene expression (VPA treated vs. untreated) data of folate genes in 5-FU resistant NSCLC cell lines indicates an alteration of mRNA profiles that might be related to mechanisms of lung cancer-drug sensitivity and could be useful predictive biomarkers for epigenetic sensitisation of NSCLC to 5-FU based chemotherapy.

Chapter 5: CBS and SHMT1 involvement in respiratory tract cancer cell line response to 5-FU.

In the previous chapters, CBS and SHMT1 were found among the folate pathway genes with the most highly deregulated expression in lung cancer. It was intriguing that there is so little information regarding these two genes and cancer development, and virtually nothing on lung cancer. We therefore set their further investigation as a major priority in this study. The main objectives of this part of the study were:

(1) To investigate the role of CBS and SHMT1 expression in the respiratory tract cancer cell line phenotype.

(2) Most importantly, to assess if CBS and SHMT1 expression can modulate the resistance of cancer cells to antifolates.

(3) To further investigate the mRNA expression pattern of CBS and SHMT1 splice variants in order to gain preliminary evidence of potential post-transcriptional involvement.

5.1 CBS and SHMT1 downregulation in respiratory tract cancer cells

Following the observations regarding deregulated expression profiles of folate genes in lung cancer tissues and respiratory tract cancer cell lines (chapter three), we picked two genes; SHMT1 and CBS for genetic manipulation and response modulation to folate pathway targeting chemotherapeutics. Based on the mRNA expression profiles of SHMT1 and CBS in respiratory tract cancer cell lines included in this study (chapter three), representative cells

with the highest mRNA levels of each gene were selected as models for genetic manipulation experiments, utilising a small hairpin (shRNA) mediated gene silencing approach. LUDLU, PJ15 and PJ41 were selected for SHMT1, with LUDLU and H358 for CBS knock down experiments. Individual transfections were performed with two shRNAs for SHMT1 and three shRNA constructs for CBS. These constructs are known to be effective at knocking down the mRNA expression of the aforementioned genes. Stable cell transfectants were therefore achieved from the TRCN0000034765 SHMT1 silencing construct in PJ15 and three CBS-targeting constructs (TRCN0000045360, TRCN0000045361 and TRCN0000045362) in the H358 cell line. RT-qPCR based mRNA expression analysis confirmed the manipulated SHMT1 and CBS down regulation across their derivative clones.

The knock down efficiency of SHMT1 transcript expression in PE/CA-PJ15 cells was approximately 46%-73% (Figure 5.1) while that of CBS was 52%-60% (Figure 5.3). Suppression of SHMT1 expression in PJ15 derived clones was also validated by western blotting analysis (Figure 5.2). We decided to proceed to the subsequent experiments with clones demonstrating > 50% knocking down efficiency.

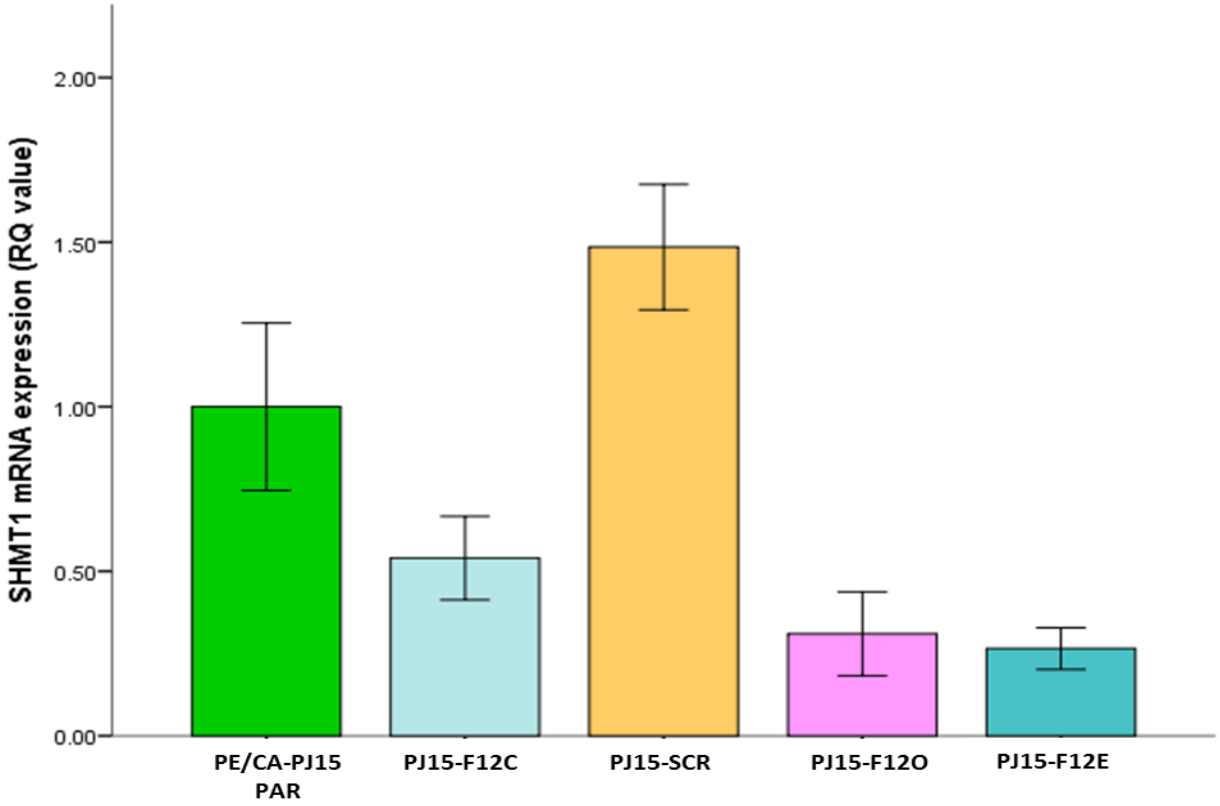

Figure 5.1: Real time PCR analysis of SHMT1 mRNA expression in PE/CA-PJ15 derived knockdown clones. shRNA mediated silencing was variable among the knockdown clones, being >73% reduction PJ15-F12E, 69% in PJ15-F12O while PJ15-F12C exhibited ~50% reduction. The expression levels were normalised to ACTB and depicted as a fold change relative to PE/CA-PJ15 PAR. Error bars represent 95% confidence intervals. RQ= relative quantification, PAR=parental, SCR=scramble

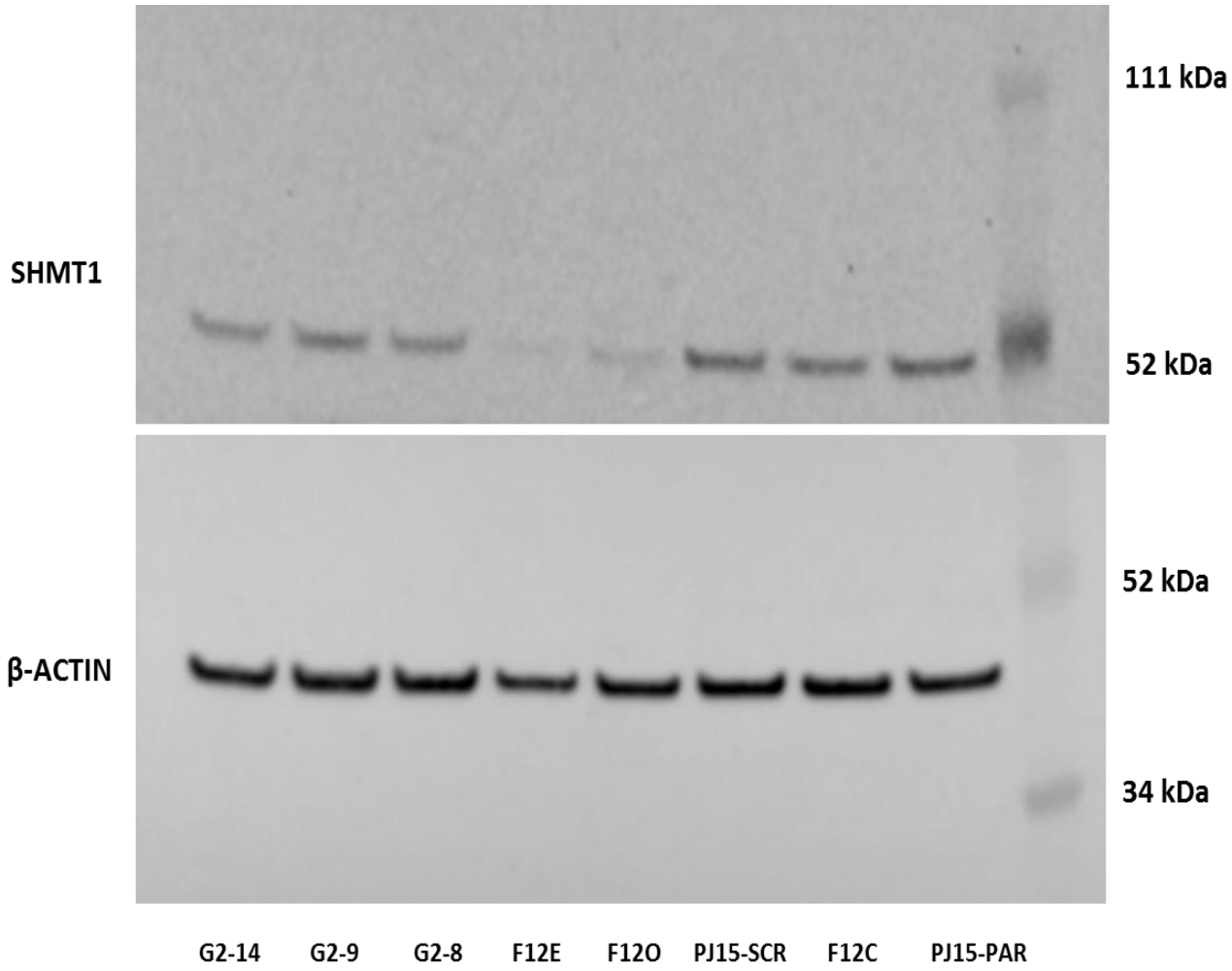

Figure 5.2: Representative western blotting of SHMT1 protein expression in PE/CA-PJ15 parental, scramble and knockdown clones. Blotting analysis showed a significant reduction of the SHMT1 protein level in the downregulated clones relative to that of scramble and parental ones. β-ACTIN was used as an endogenous control.

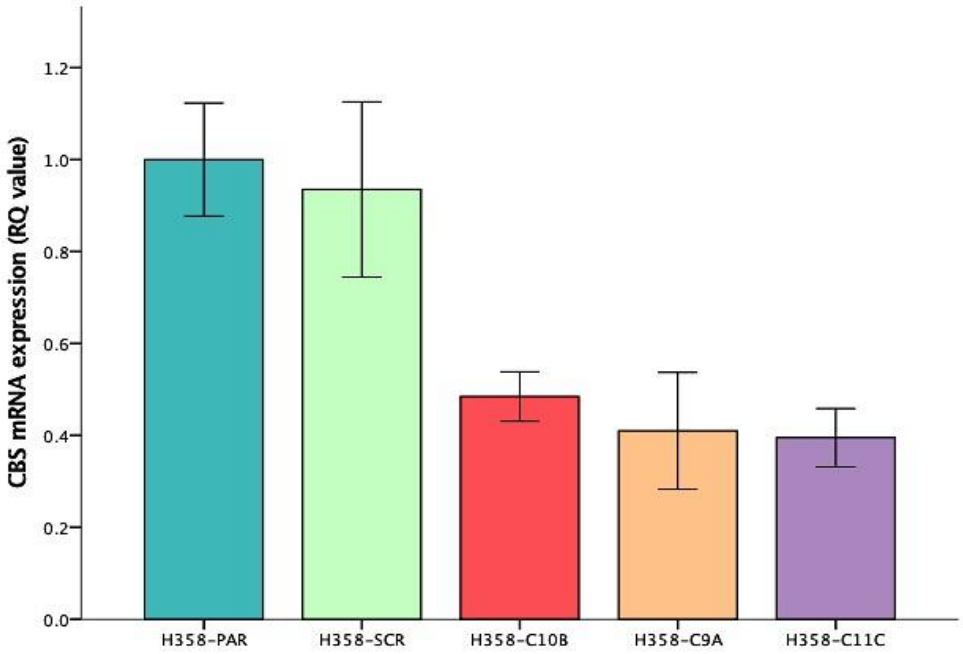

Figure 5.3: CBS mRNA expression profiles in H358-derived CBS knockdown clones. The expression levels were normalised to ACTB and depicted as a fold change relative to H358-PAR. Error bars represent 95% confidence intervals. RQ=relative quantification, PAR=parental, SCR=scramble

In order to assess the phenotypic effect of SHMT1 and CBS suppression, growth rates were analysed using MTT assay for four successive days. Both CBS and SHMT1 knocked down clones exhibited reduced MTT absorbance readings compared to the parental and scramble cells (Figure 5.4 and Figure 5.5).

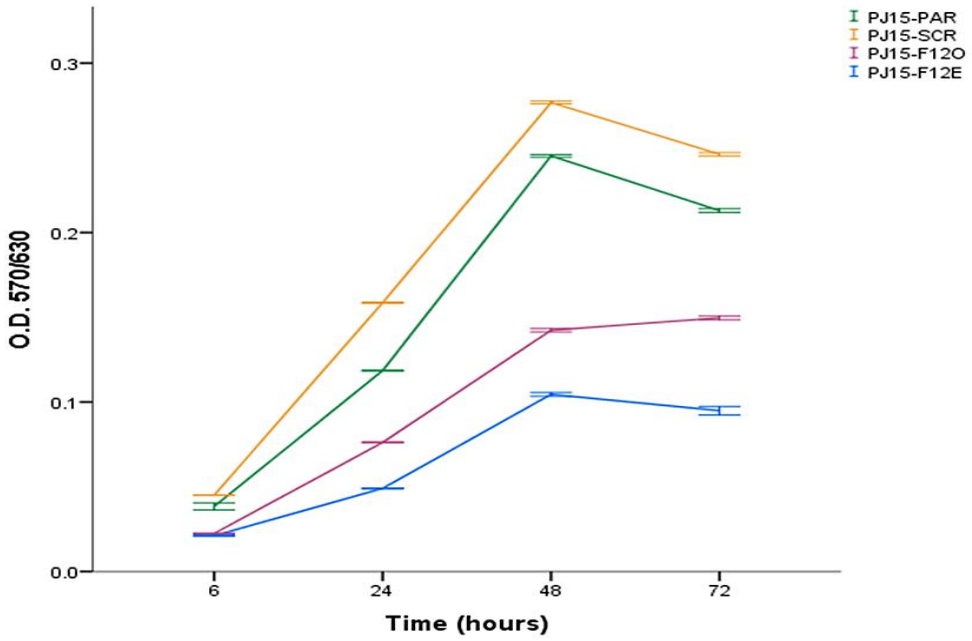

Figure 5.4: Exponential growth curves of SHMT1 silenced PE/CA-PJ15 cell line. It seems that shRNA-mediated knockdown of SHMT1 expression significantly attenuates viability of PE/CA-PJ15 derived clones relative to that of parental and scramble controls. O.D=optical density, PAR=parental, SCR=scramble

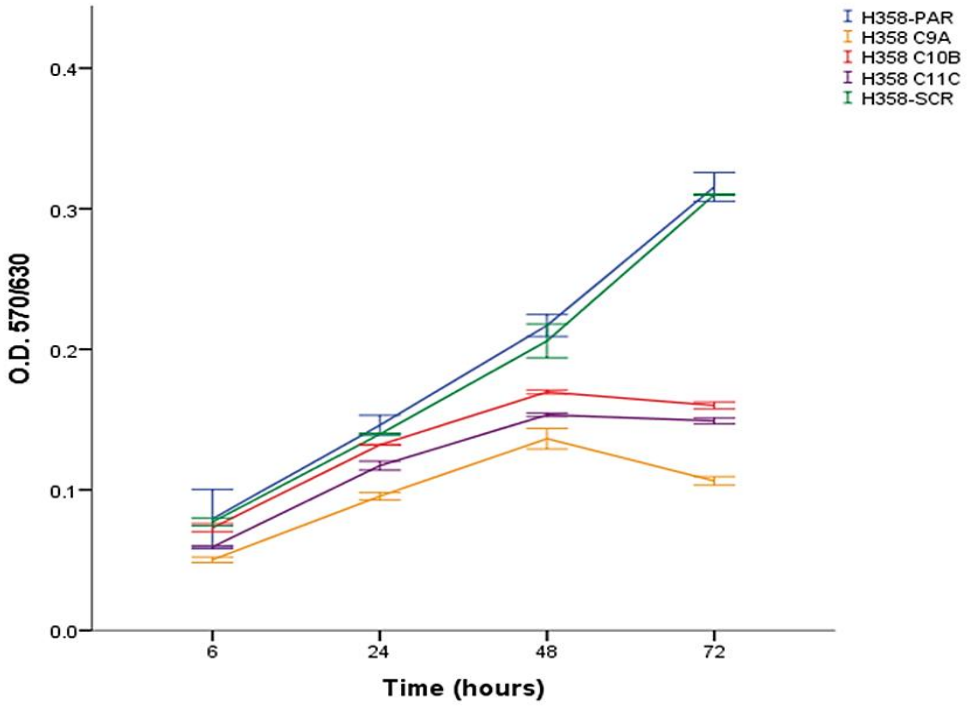

Figure 5.5: Effect of CBS knockdown on the viability of H358 cell line. A significant reduction in MTT absorbance readings was observed in CBS downregulated clones compared to parental and scramble controls. O.D=optical density, PAR=parental, SCR=scramble

Next, we examined the functional significance of SHMT1/CBS silencing on respiratory tract cancer cell sensitivity to chemotherapeutic drugs. Our results showed that SHMT1 suppression significantly decreased cellular viability in PJ15-F12O and PJ15-F12E knockdown derived clones treated with an IC25 dose of 5-FU with respect to parental and scramble cells (Figure 5.6A). Similarly, treatment of SHMT1 knockdown clones with an IC25 concentration of MTX resulted in a prominent reduction in clonogenic MTT absorbance readings when compared with the parental and scramble lines (Figure 5.6B). Pemetrexed exposure data, however, demonstrated that SHMT1 silencing did not sensitise the PE/CA-PJ15 cell line to an IC25 dose of multitarget pemetrexed treatment (Figure 5.6C).

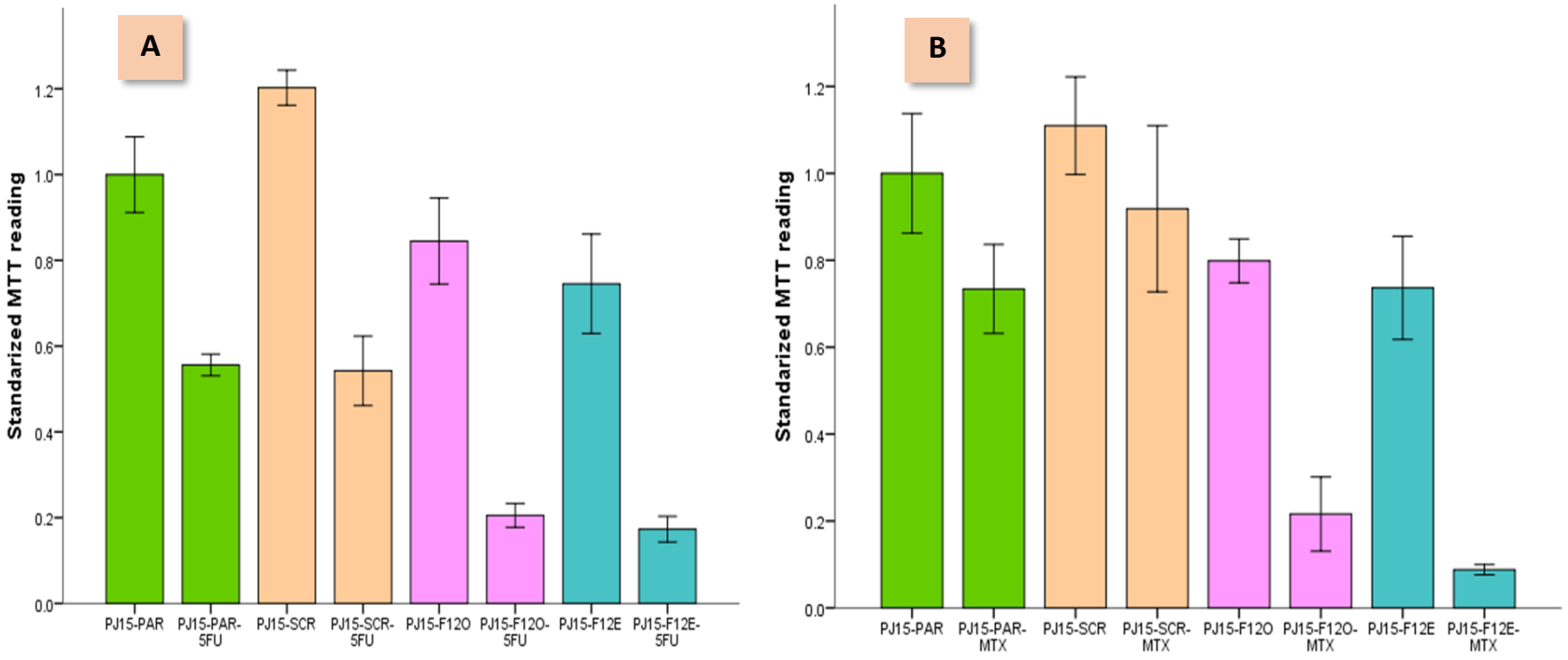

Figure 5.6: Bar chart representing the response of SHMT1 knockdown clones to an IC25 dose of 5-FU (A) and MTX (B). Down regulation of SHMT1 expression seems to sensitise PE/CA-PJ15 line to 5-FU and MTX as indicated by reduction of MTT absorbance values when compared to that of parental and scramble controls. The results represent the mean values of six technical replicates. Error bars represent 95% confidence intervals. PAR= parental, SCR= scramble.

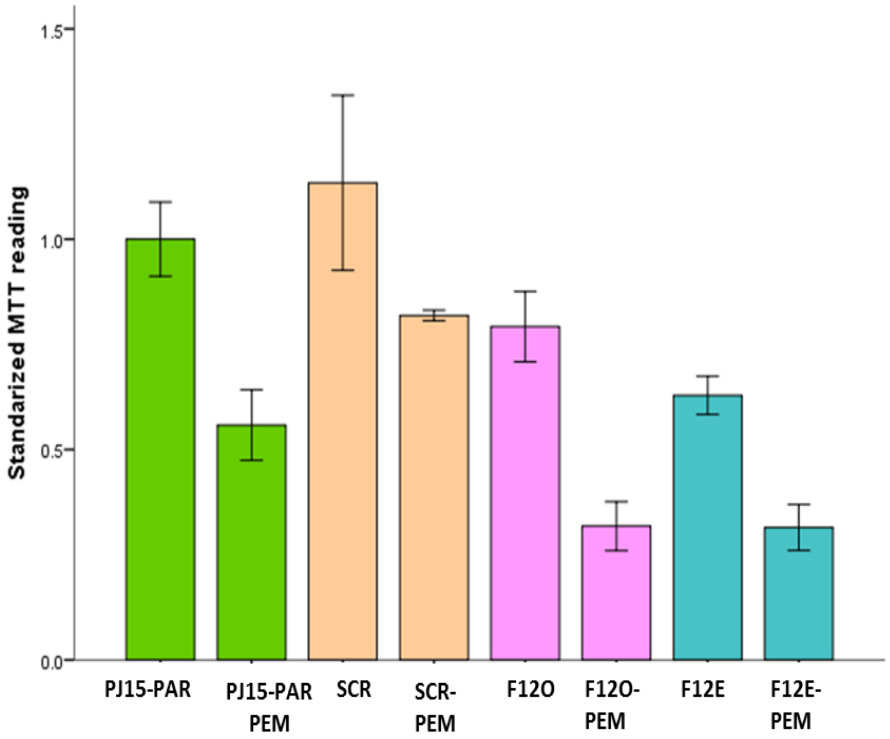

Figure 5.6 C: Effect of SHMT1 silencing on the response of the PE/CA-PJ15 cell line to an IC25 dose of pemetrexed. No significant reduction of MTT absorbance values was observed in PE/CA-PJ15 derived SHMT1 knockdown clones with respect to that of parental and scramble controls. The results represent the mean of six technical replicates. Error bars represent 95% confidence intervals. PAR= parental, SCR= scramble.

Based on these results, SHMT1 downregulated clones were then exposed to a range of seven different doses of 5-FU (0.015-1 mM) and MTX (0-8 µM), applied for 72 hours, along with the parental and scramble cells. MTT analyses showed lower values of 5-FU relative IC50 in PJ15-F12O and PJ15-F12E than those noted in the parental and mock (scramble) cells (Table 5.1) in a manner directly correlating with the level of SHMT1 suppression (Figure 5.7). These findings indicate that SHMT1 knockdown affords a possibility of a significant reduction of cell viability following 5-FU treatment in the PE/CA-PJ15 HNSCC cell line. This result was not replicated for MTX, however. Although SHMT1 silencing in PJ15-F12O and PJ15-F12E resulted in a reduction

of IC50 values for MTX (Table 5.1), we did not observe a significant change in drug sensitivity relative to that of parental and shRNA control. In fact, MTX exposure line graphs show an overlapping response (Figure 5.8). These results suggest that SHMT1 has no contributory role in sensitising PE/CA-PJ15 head and neck cancer cell lines to MTX treatment.

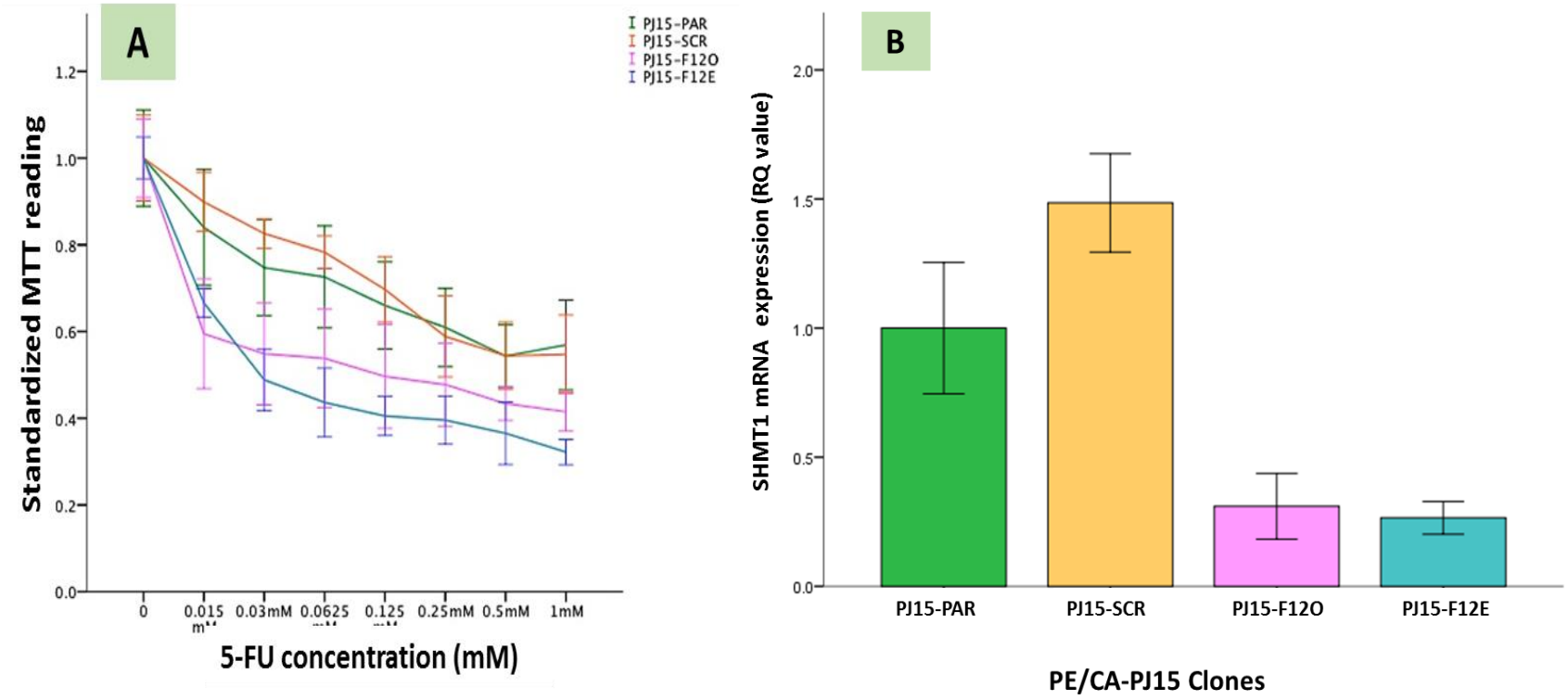

Figure 5.7: Effect of SHMT1 silencing in PE/CA-PJ15 cell line sensitivity to 5-FU. (A) Knocking down of SHMT1 expression resulted in significant reduction in cell viability of the PE/CA-PJ15 derived knockdown clones reflected by MTT absorbance readings relative to the SHMT1 suppression levels (B). Results represent the mean of six technical replicates. Error bars represent 95% confidence intervals. RQ=relative quantification, PAR= parental, SCR= scramble.

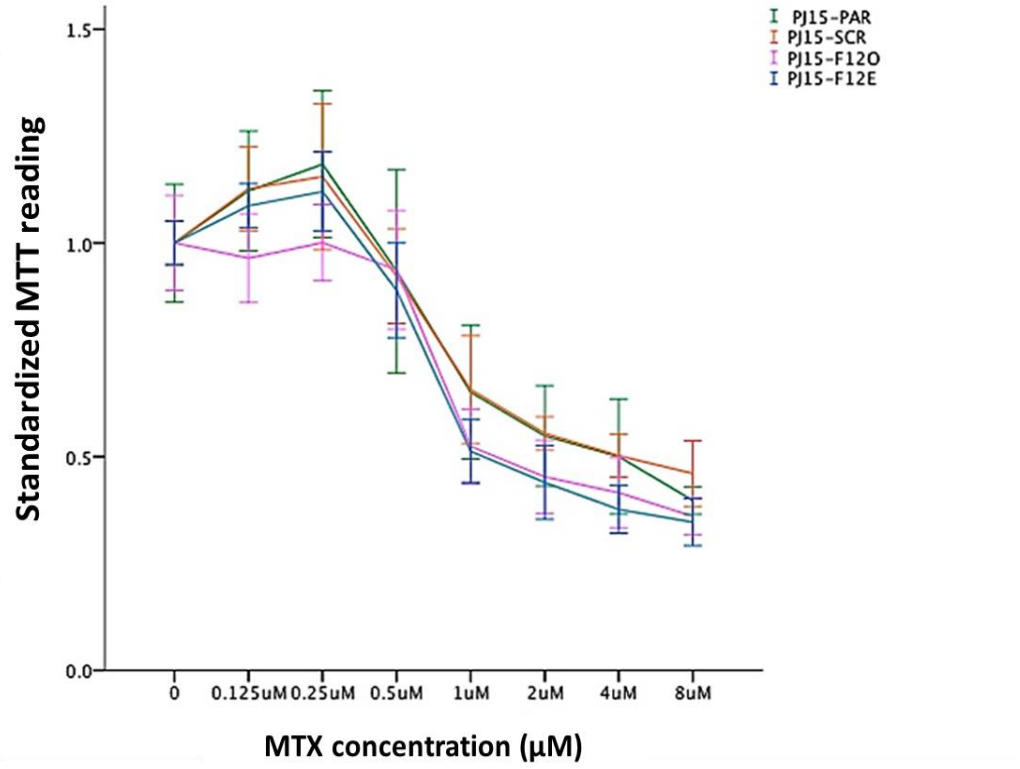

Figure 5.7: Effect of SHMT1 silencing in PE/CA-PJ15 cell line sensitivity to MTX. Knocking down of SHMT1 expression did not have a significant effect in reducing PE/CA-PJ15 derived knockdown clones viability following MTX exposure as reflected by their MTT absorbance readings. Results represent the mean of six technical replicates. Error bars represent 95% confidence intervals. PAR= parental, SCR= scramble.

Table 5.1: IC50 values, with their respective 95% confidence intervals, in PE/CA-PJ15 parental, scramble and SHMT1 knockdown clones following treatment with 0-1 mM 5-FU and 0-8 µM MTX.

Clone	IC50-5FU mM	95% C.I	IC50-MTX µM	95% C.I
PJ15-PAR	0.491	*0.35 to 0.68*	3.734	*2.639 to 5.284*
PJ15-SCR	0.519	*0.40 to 0.66*	4.018	*2.982 to 5.415*
PJ15-F12O	0.126	*0.08 to 0.19*	2.355	*1.854 to 2.993*
PJ15-F12E	0.066	*0.047 to 0.09*	2.274	*1.737-2.976*

Furthermore, our data demonstrated that artificial suppression of CBS induced by specific shRNAs did not sensitise H358 cells to 5-FU (Figure 5.9). The same is true for the MTX and pemetrexed response among CBS knockdown H358 derived clones (data not shown). We therefore decided to continue with the PE/CA-PJ15 cell line and 5-FU anticancer drug for the subsequent functional analysis experiments.

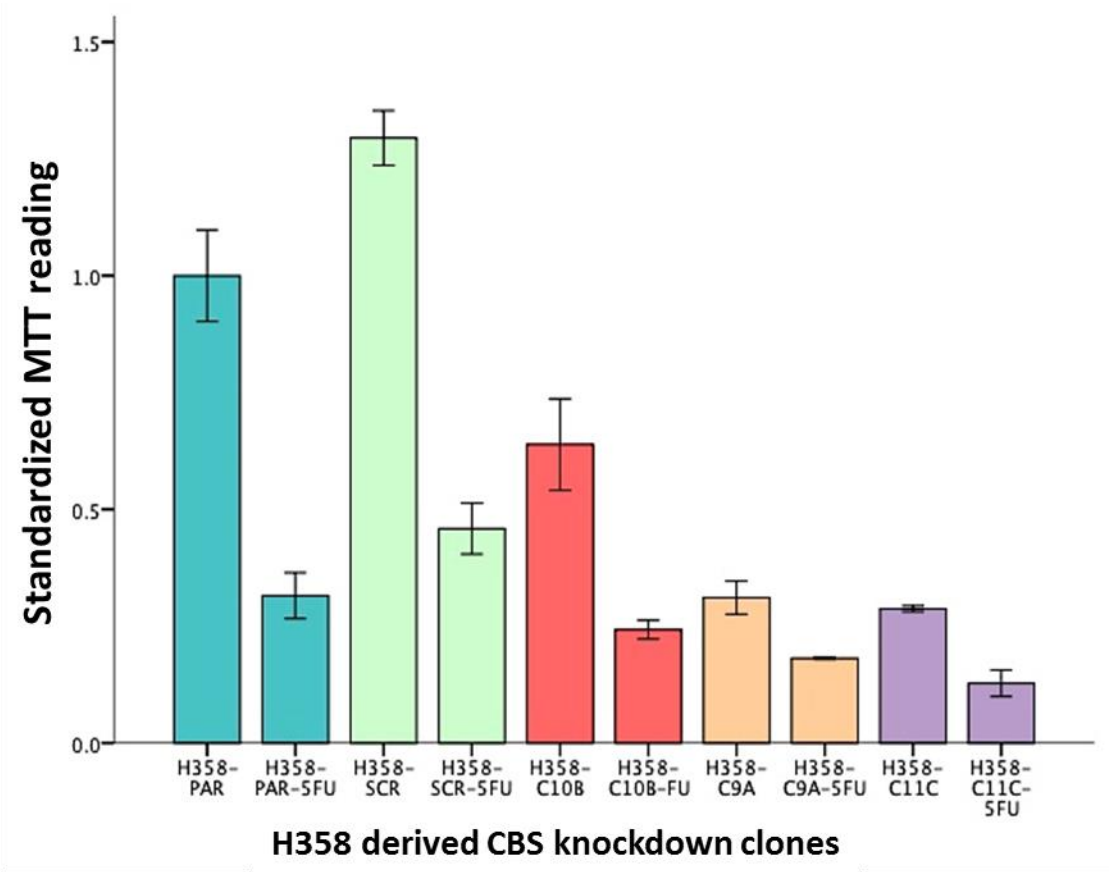

Figure 5.9: Effect of CBS knockdown on the response of H358 cells to an IC25 dose of 5-FU chemotherapy. No significant reduction in the viability of CBS downregulated clones with respect to that of parental and scramble control was observed. Error bars represent 95% confidence intervals. PAR=parental, SCR=scramble.

In order to confirm the link between SHMT1 and 5-FU sensitivity in PE/CA-PJ15 HNSCC cells, we next utilised a different shRNA construct (TRCN0000034767) effective at knocking down SHMT1 mRNA expression. Of several independent PJ15 clones generated, three (PJ15-G2-8, PJ15-G2-9 and PJ15-G2-14) demonstrated ~60% reduction in SHMT1 mRNA levels as determined by qPCR analysis (Figure 5.10B). Suppression of SHMT1 expression in the new PE/CA-PJ15 derived clones was also validated by western blotting analysis (Figure 5.2). Consistently with our previous findings, PJ15-G2-8, PJ15-G2-9 and PJ15-G2-14 clones exhibited a marked drop in absorbance readings following 5-FU exposure in comparison to that of parental or scrambled controls (Figure 5.10A). MTT analyses have shown lower values of 5-FU relative IC50 in PJ15-G2-8 and PJ15-G2-9 and PJ15-G2-14 downregulated clones than those noted in the parental and mock (scramble) cells (Table 5.2). These findings imply that SHMT1 knockdown in PE/CA-PJ15 cells enhances their sensitivity to 5-FU.

Table 5.2: IC50 values with their 95% confidence intervals of 5-FU therapy in PE/CA-PJ15-derived SHMT1 silenced clones (with G2 shRNA constructs) compared to that of the parental (PAR) and scramble (SCR) control.

PJ15 Clones	5-FU IC50 (mM)	95% CI
PJ15-PAR	0.446	*0.365 to 0.544*
PJ15-SCR	0.639	*0.559 to 0.731*
PJ15-G2-8	0.178	*0.143 to 0.221*
PJ15-G2-9	0.133	*0.101 to 0.174*
PJ15-G2-14	0.156	*0.125 to 0.195*

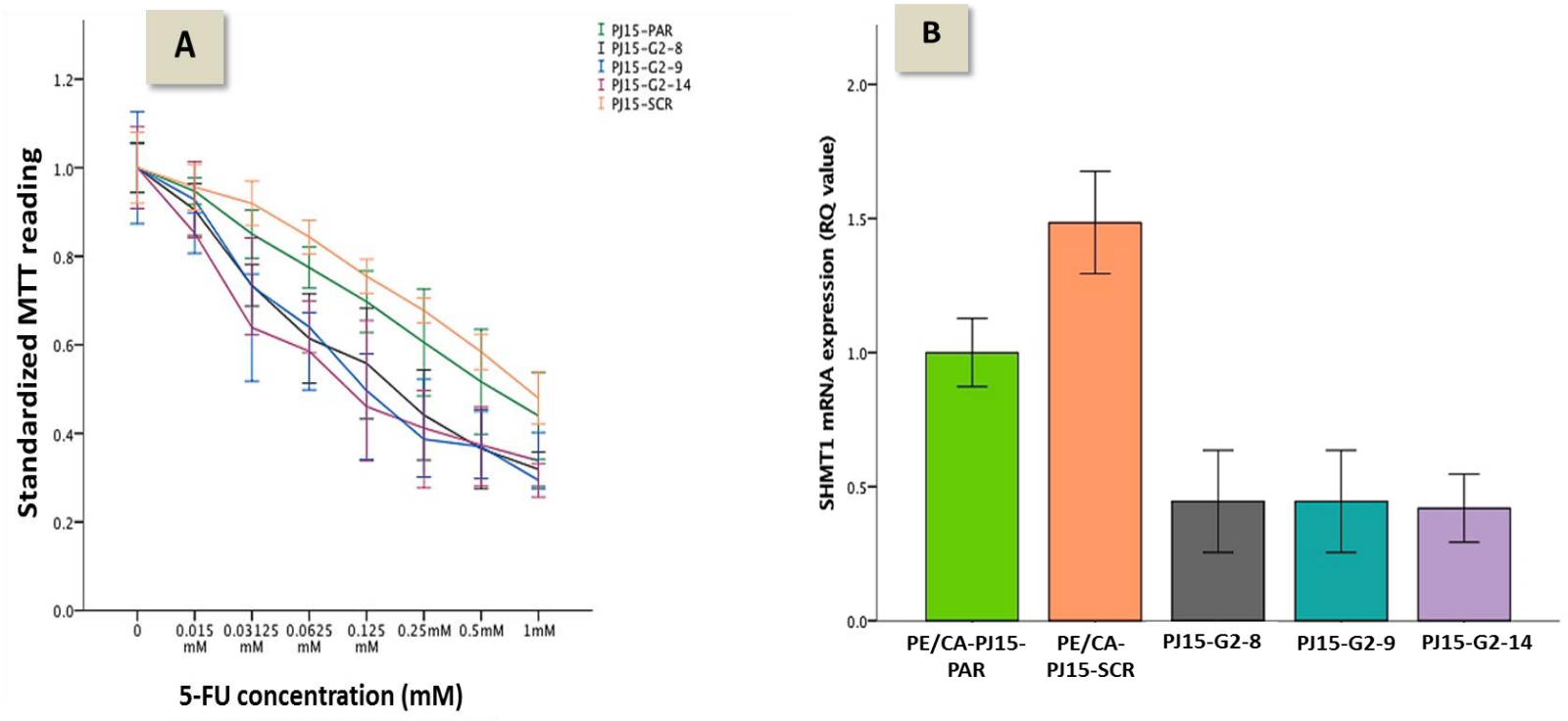

Figure 5.10: Effect of SHMT1 silencing (with different shRNA construct) in PE/CA-PJ15 cell line sensitivity to 5-FU. Knocking down of SHMT1 expression resulted in a significant reduction of PE/CA-PJ15 derived knockdown clones viability as reflected by their MTT absorbance readings (A) relative to the SHMT1 suppression levels (B). Results represent the mean of six technical replicates. Error bars represent 95% confidence intervals. RQ=relative quantification, PAR= parental, SCR= scramble.

To further confirm the influence of SHMT1 expression on 5-FU drug sensitivity in HNSCC, aminomethyl-phosphonic acid (AMPA), a known effective SHMT1 inhibitor, was used to investigate cancer cell growth response to SHMT1 suppression induced by this glycine analogue. According to previous optimisation experiments, 25 mM was determined as an optimal concentration of AMPA to be used in this study. When the PE/CA-PJ15 cell line was exposed to a combination of 25 mM AMPA with s IC50 concentration of 5-FU, a significant enhancement of 5-FU anticancer effect was observed (Figure 5.11A). The cell line was then treated with seven variable concentrations of 5-FU (0-1 mM) in combination with 25 mM AMPA. MTT analysis demonstrated a significant reduction of absorbance readings with a 5-FU-AMPA combination compared to the PE/CA-PJ15 cell line treated with 5-FU only (Figure 5.11B) and an associated marked drop in the IC50 value (Table 5.3).

Table 5.3: IC50 values and their respective confidence intervals (95%) in PJ15 cells after treatment with 0-1 mM of 5-FU in the presence of 25 mM AMPA

Treatment	5-FU IC50 (mM)	95% CI
5-FU only	0.957	0.813 to 1.126
5-FU+AMPA	0.327	0.250 to 0.427

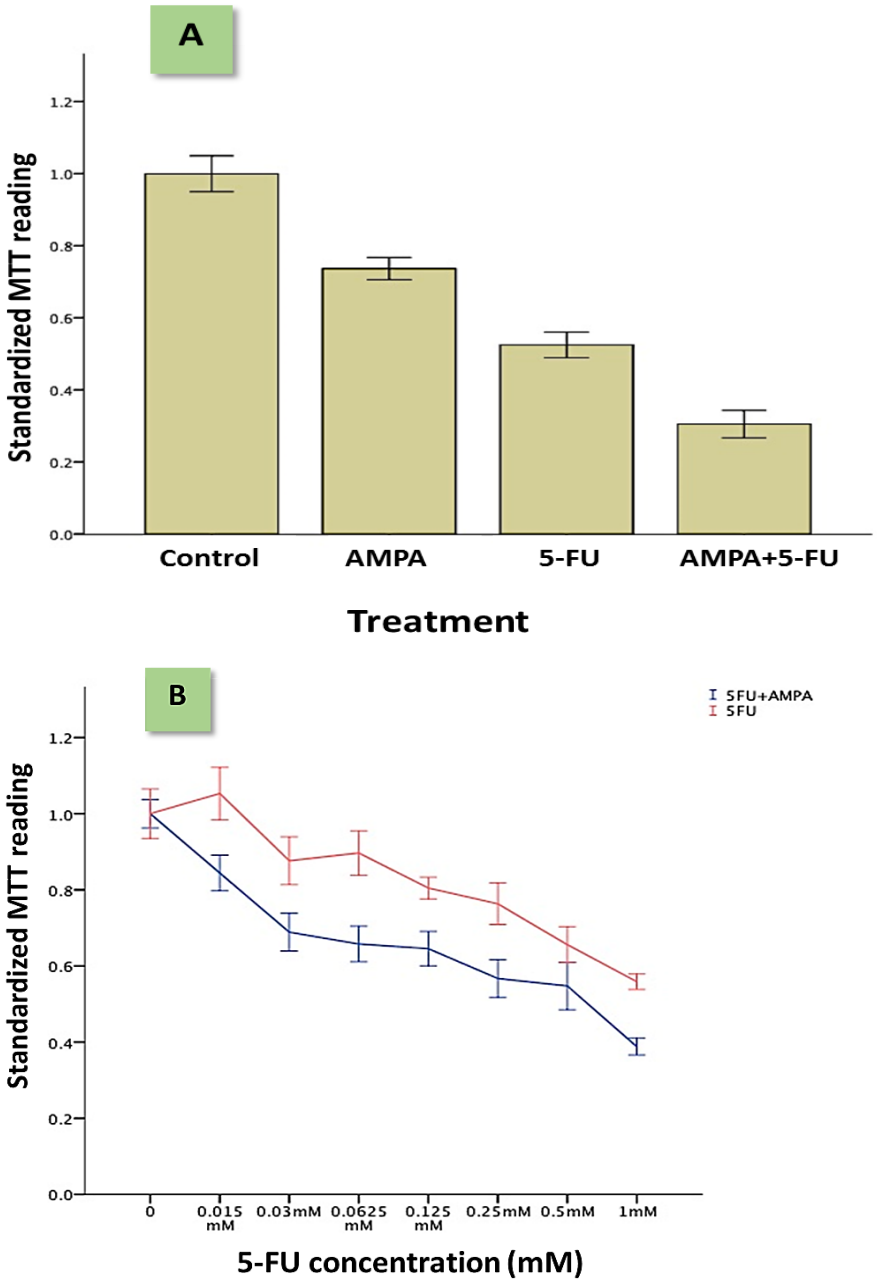

Figure 5.11: Sensitivity of PE/CA-PJ15 cells to 5-FU treatment in the presence of an SHMT1 inhibitor (AMPA). PE/CA-PJ15 cell line was treated with a combination of (A) an IC50 concentration, (B) a range of seven different doses of 5-FU with 25mM AMPA for 72hours. In both graphs, AMPA seems to cooperate with 5-FU as reflected by MTT absorbance values. The results represent the mean of six technical replicates. Error bars represent 95% confidence intervals.

5.2 SHMT1 and CBS Splice variants expression profiles in their knock down clones

In order to investigate whether shRNA mediated knockdown of SHMT1 and CBS genes can specifically target splice variant sequences, we assessed the relative expression of different CBS/SHMT1 splicing isoforms (previously discussed in chapter three) in the knockdown derived clones using quantitative RT-PCR. Expression profile analysis revealed depletion of SHMT1v2 in PJ15-F12O, PJ15-F12E (which showed an increased sensitivity to the 5-FU based anticancer agent) as well as PJ15-F12C, which demonstrated a 46% reduction of SHMT1 expression at the mRNA level (Figure 5.13). Similarly, CBSv3 was found to be downregulated in H358-C9A, H358-C10B and H358-C11C CBS knockdown clones (Figure 5.14). We reasoned that mRNA levels of CBS/SHMT1 splicing isoforms that were underrepresented in the knockdown clones might be attributed to specific targeting by the short hairpin RNA that was utilised to downregulate the CBS/SHMT1 expression in these clones. To test this hypothesis, we next checked the shRNA target regions using *The Genetic Perturbation Platform web portal* (portals.broadinstitute.org). As shown in Table 5.4, the shRNA mediated CBS/SHMT1 silencing employed in this study targets exons that are present in all splice variants (CBS exons 4, 5 or 15 and SHMT1 exon 6). These data potentially exclude the possibility of specific splice targeting through RNA interference in SHMT1 and CBS genes. Furthermore, analysis of the minimum free energy (data not shown) and predicted centroid secondary structures (rna.tbi.univie.ac.at) (Package et al. 2011) demonstrated a subtle difference in the CBS/SHMT1 shRNA target regions (Figure 5.12), suggesting that variation in RNA conformations might not justify the differential knockdown across downregulated clones.

Table 5.4: shRNA constructs utilised in CBS and SHMT1 knockdown assays

Assay	Knock-down clone	Clone ID	Oligosequence*	Target region	Match (%)
CBSv3	H358-C9	TRCN0000045360	CCGGCTTGCCAGATATTCTGAAGAACTCGAGTTCTTCAGAATATCTGGCAAGTTTTTG	Exon 4	100
	H358-C10	TRCN0000045361	CCGGCCGTCAGACCAAGTTGGCAAACTCGAGTTTGCCAACTTGGTCTGACGGTTTTTG	Exon 15	100
	H358-C11	TRCN0000045362	CCGGACACGATTATCGAGCCGACATCTCGAGATGTCGGCTCGATAATCGTGTTTTTTG	Exon 5	100
SHMT 1v2	PJ15-F12	TRCN0000034765	CCGGCCCAGATACTGGCTACATCAACTCGAGTTGATGTAGCCAGTATCTGGGTTTTTG	Exon 6	100

* **The 5' stem region is highlighted with red while its reverse complement is green**

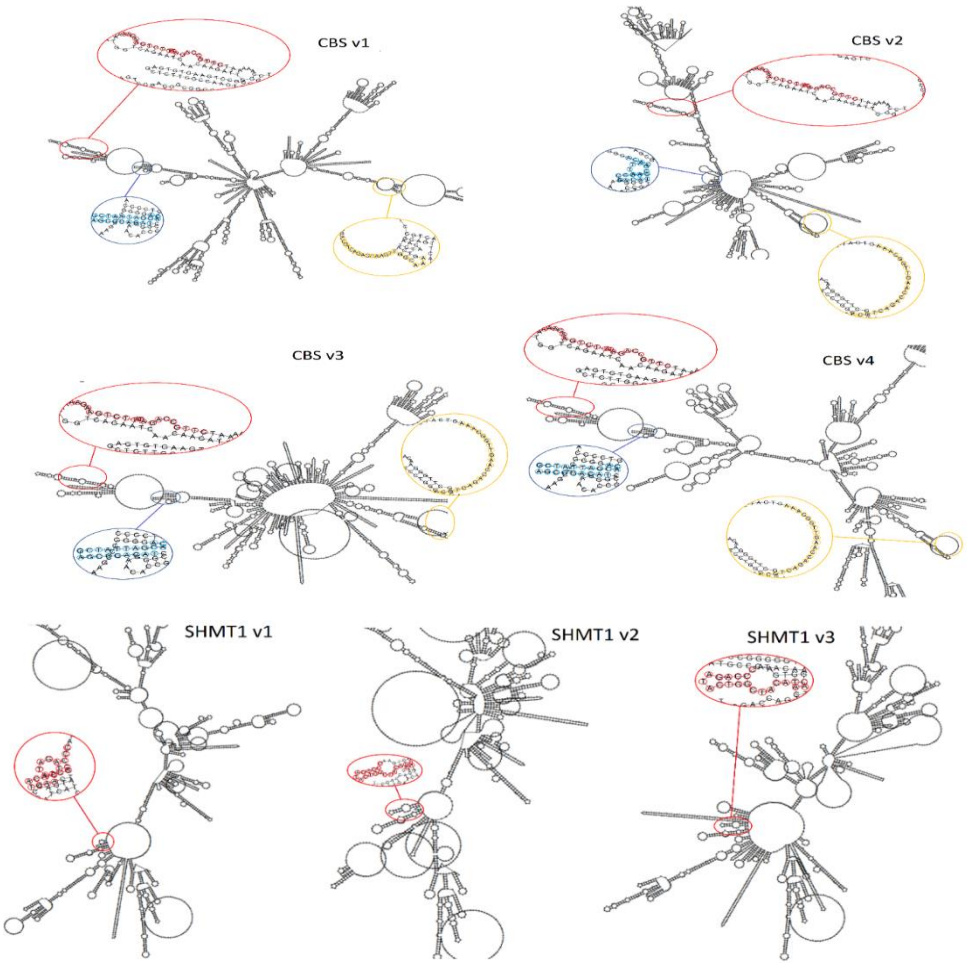

Figure 5.12: Predicted RNA secondary structures of CBS and SHMT1 splice variants. Subtle differences were observed between CBS and SHMT1 knockdown targets. Target regions in CBS Exon 4 and SHMT1 Exon 6 are shown as red insets while yellow and blue ones denote targets in CBS Exon 15 and 5 respectively. shRNA nucleotide sequences are presented as circles within the insets.

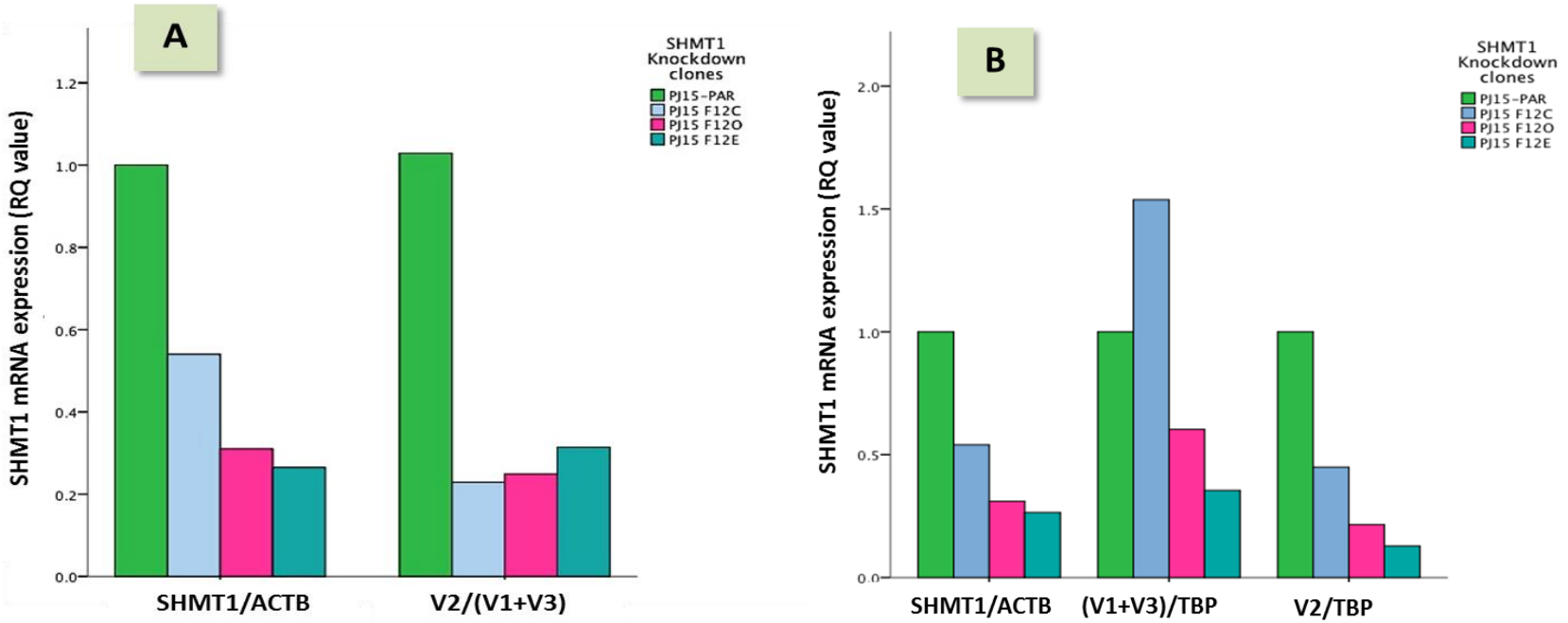

Figure 5.13: qPCR-based analysis mRNAs of SHMT1 and its splice variants in SHMT1 knockdown clone derivatives. (A) SHMT1 (left panel) and SHMT1v2 (right panel) demonstrated downregulation across the PJ15-derived knockdown clones. Results from all samples were normalised to ACTB and SHMT1 (V1+V3) respectively and presented as a fold change relative to that of PJ15-PAR cell population. (B) Variable expression levels of SHMT1(v1+v3) and SHMT1v2 alternative transcripts in SHMT1 downregulated clones (middle and right panels) as compared to decreased expression of SHMT1 (all variants, the left panel) in the same clones. Quantification of SHMT1 gene was normalised to that of ACTB whereas (V1+V3) and V2 splice isoforms data were separately normalised to TATAA-box binding protein (TBP). PJ15-PAR was used as an internal calibrator.

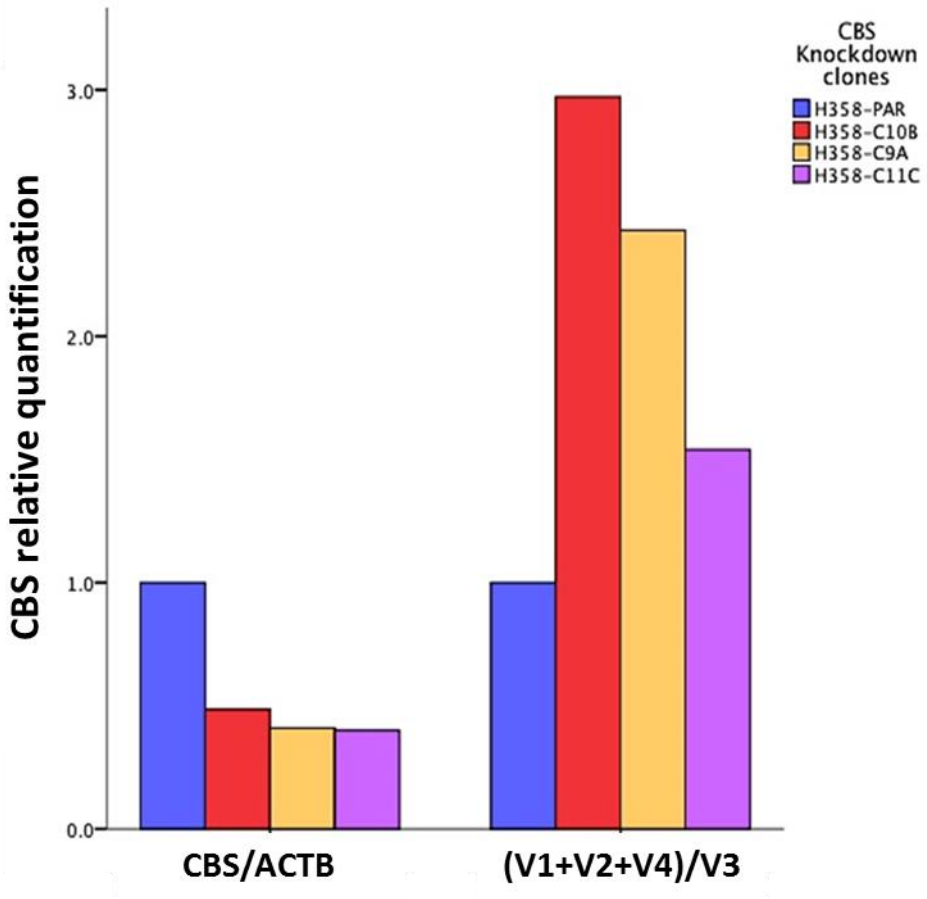

Figure 5.14: Fluorescent quantification-based analysis of the mRNA expression of the CBS gene and its splice variants in H358-derived CBS knockdown clones. Results show downregulation of the CBS gene (left panel) and CBSv3 (right panel) across H358 clones. The H358-PAR cell population was used as a technical calibrator. RQ values of the CBS transcript and CBS (v1+v2+v4) mRNAs of all samples were normalised to that of ACTB and CBSv3 respectively.

5.3 Discussion

5.3.1 CBS and SHMT1 downregulation in respiratory tract cancer cell lines

The *de novo* thymidylate biosynthesis pathway is essential for maintaining cellular dTTP pools and ensuring faithful replication of cellular DNA. SHMT1 is a critical player in this pathway, which also includes SHMT2α, TYMS and DHFR (MacFarlane et al. 2011). Among these enzymes, SHMT1 is the only one that has not currently been extensively studied (Paone et al. 2014). Moreover, the impact of SHMT1 suppression on cancer growth and progression has not been sufficiently investigated (Pandey et al. 2014). Our study highlighted the relevant role of SHMT1 expression in controlling cancer cell growth and viability. We demonstrated that shRNA induced suppression of SHMT1 reduces cancer cell viability in the PE/CA-PJ15 HNSCC cell line. This is in line with recent reports on SHMT1 silencing in xenograft mice (Pandey et al. 2014), lung (Paone et al. 2014) and ovarian cancer cell lines (Gupta et al. 2017). Moreover, we used Kaplan Meier estimator software in order to assess the biological relationship between SHMT1 expression and lung cancer patients survival (Győrffy et al. 2013). As shown in Figure 5.15, high SHMT1 expression is associated with low survival among lung cancer patients, especially those not receiving chemotherapy. This provides a further line of evidence for the role of SHMT1 in disease progression and, ultimately, patient survival.

Importantly, we showed for the first time, that artificial suppression of SHMT1 produced a cell sensitisation phenotype to 5-FU treatment. Our data demonstrated that shRNA-based knockdown of SHMT1 expression increases 5-FU response in the PJ15 HNSCC cell line. SHMT1 is a critical player in the *de novo* synthesis of thymidylate; its chief function is to catalyse the reversible conversion of serine to glycine, thereby generating the one-carbon donor essential for the methylation of dUMP to dTMP. In addition, it acts as a scaffold protein for the thymidylate synthesis metabolic complex (Anderson et al. 2012). Consequently, SHMT1

activity is correlated with the increased nucleotide biosynthesis demand evidenced in rapidly proliferating cancer cells. In line with this, we observed SHMT1 upregulation in lung cancer tissue and respiratory tract cancer cell lines (Chapter 3). TYMS inhibition has been established as the main mechanism of 5-FU anticancer action through formation of a covalent ternary complex involving 5-FU metabolite 5-fluoro-2'-deoxyuridine (FdUMP), TYMS and 5,10 MTHF (Santi & McHenry 1972). Moreover, 5-FU can also be converted through a complex intracellular metabolic network into 5-fluorouridine monophosphate (FUMP), which is the precursor of two cytotoxic 5-FU metabolites: 5-fluorouridine triphosphate (5-FUDR) and deoxyuridine triphosphate (dUTP). Following DNA incorporation, dUTP causes irreparable DNA damage, while 5-FUDR misincorporates into ribosomal RNA (rRNA) molecules, thereby disturbing rRNA processing, resulting in the induction of cell cycle arrest/or apoptosis in a p53 dependent manner. SHMT1 is a limiting factor in thymidylate biosynthesis reactions; hence suppression of SHMT1 expression causes disruption of these reactions leading to dUTP misincorporation within DNA during the DNA replication process, and ultimately cell cycle arrest and apoptosis. A recent study demonstrating that knockdown of SHMT1 in lung cancer cell lines induces p53 dependent apoptosis supports this contention (Paone et al. 2014). In the same direction, Anderson & Stover (2009) reported an abnormal uracil accumulation in mice lacking SHMT1. Accordingly, we may conclude that the synergistic apoptotic effect imparted by concurrent SHMT1 silencing and 5-FU treatment confers potent chemosensitisation of PE/CA-PJ15 cells.

We further present evidence that combined treatment with the SHMT1 inhibitor AMPA potentiates the effect of 5-FU in PE/CA-PJ15 HNSCC cell line. Although co-treatment with 5-FU and AMPA has not been attempted yet, AMPA has been identified as inhibiting proliferation and promote apoptosis in prostatic cancer cells *in vitro* (Li et al. 2013) and *in vivo*

(Parajuli et al. 2016). These findings align with the present data of manipulated SHMT1 expression in PE/CA-PJ15PJ15 cell line.

To our knowledge, this is the first report to demonstrate the *in vitro* efficacy of SHMT1 knockdown and the marked reduction in cell viability achieved when combined with 5-FU treatment in PE/CA-PJ15 HNSCC cells.

We have also examined the effect of shRNA mediated down regulation of CBS on NSCLC cells. Our data have shown that CBS knock down clones displayed reduced MTT absorbance values in the H358 cell line as compared with parental control. A similar observation has been reported in colonic (Hellmich et al. 2014) and ovarian cancer cells (Bhattacharyya et al. 2013). Of course, due to the important role of CBS-derived H2S in promoting bioenergetic fuel for the rapidly proliferating cancer cells, silencing/inhibition of this mammalian gene contributes to energy starvation of tumour cells thereby impairing their growth and proliferation (Hellmich et al. 2014).

Moreover, we also demonstrated that CBS genetic silencing did not influence the growth inhibitory effect of 5-FU, pemetrexed or MTX anticancer drugs in H358 knocked down clones as compared with the parental or scrambled cells. On the contrary, Pagliara et al. (2016) reported that CBS silencing was associated with a remarkable increase in 5-FU mediated anticancer effect in colon cancer cell lines lacking p53. They assume that 5-FU treatment induces nuclear stress and activates some ribosomal proteins (rp), specifically rpL3, which binds CBS and represses its activity at transcriptional and post-translational levels along with induction of the mitochondrial apoptotic pathway in colonic cancer cells lacking functional p53. Another recent report from the same group demonstrated that rpL3 has the potential to promote the antitumour effect of 5-FU effect through downregulation of CBS and NFkB transcription factor in p53 mutated lung cancer cell lines (Russo et al. 2016). This

inconsistency probably exists because of a difference in the p53 expression or mutational status of the cancer cell line examined. Further studies are needed to investigate the therapeutic potential of CBS modulation in respiratory tract cancer.

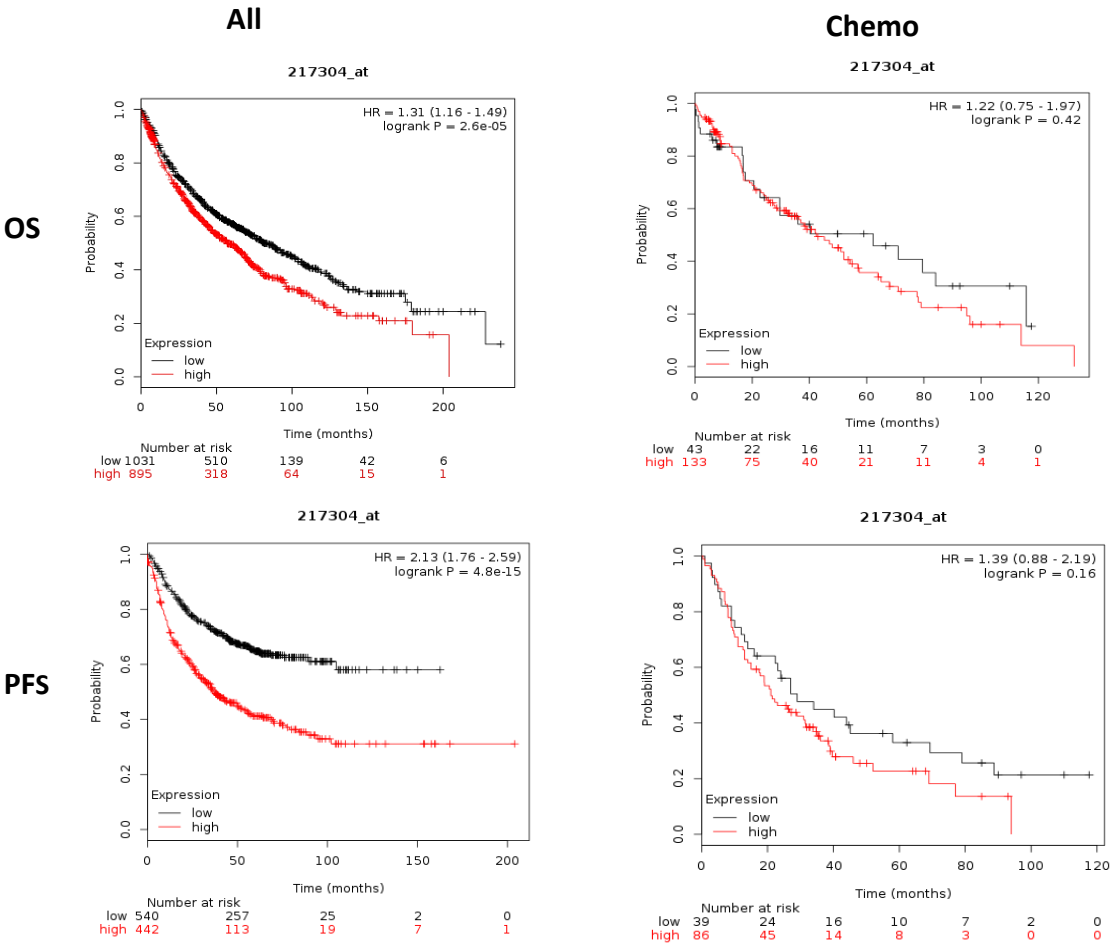

Figure 5.15: Kaplan Meier survival analysis of lung cancer patients in relation to SHMT1 mRNA expression comparing OS and PFS results in the presence and absence of treatment history. OS= Overall survival, PFS= Progression free survival, Chemo=Chemotherapy. Taken from Kaplan Meier- Plotter software (Lung cancer).

5.3.2 SHMT1 & CBS Splice variants expression profiles in SHMT1 and CBS knock down clones

In the current study, we also analysed SHMT1 and CBS splice variants expression levels in their corresponding knockdown clones. Both SHMT1v2 and CBSv3 have relatively lower mRNA levels in all of the three PJ15 and H358 knockdown clones, respectively. Furthermore, we fail to provide evidence for differential silencing of specific SHMT1/CBS mRNA isoforms, either by unique exon or via RNA conformation. These data suggest that splice variants controlling mechanisms might be independent of those involved in mRNA regulation (Doriguzzi et al. 2016). An alternative suggestion is that a change occurs in the alternative splicing of CBS/SHMT1 following the knocking down event. This might lead to variation in the splicing pattern with induced production of a specific mRNA isoform over the others (Grosso et al. 2008; Wang et al. 2008). Additional studies are necessary on the regulatory mechanisms that govern CBS/SHMT1 splicing processes in respiratory tract cancer.

In summary, the current study provides new information regarding the *in vitro* efficacy of SHMT1 as a potential enhancer for 5-FU activity. Our findings suggest that SHMT1 might have a clinical relevance in 5-FU based chemotherapeutic regimens in respiratory tract cancer and underline the need for further evaluation. In addition, we report for the first time the expression profiles of SHMT1/CBS splice transcripts in their respective knockdown clones. Our results might raise the possibility of specifically targeting aberrant respiratory tract cancer associated splicing isoforms. Detailed experiments to assess the CBS/SHMT1 knockdown effect on their corresponding splicing events would be crucial for this scenario.

Overall study discussion and final conclusion

The folate metabolic pathway has long been an attractive target for cancer therapy given its importance to DNA synthesis, methylation and repair. The development of drug resistance has, however, posed a major obstacle to clinical success. A full understanding of the mechanisms of resistance to these anticancer agents has yet to be achieved. Furthermore, development of rationally-based novel strategies that could overcome cancer cells chemoresistance remains an attractive objective for both the academia and the pharmaceutical industry.

The overarching aim of this study was to expand the knowledge around the folate pathway in respiratory tract cancer and explore potential new, less studied, targets for therapeutic exploitation. In this respect, our starting point was the expression profiling of the "core genes" of the folate pathway in primary respiratory tract cancer. Unfortunately, the head and neck samples available proved to be of insufficient quality; a possibility we had in mind as they were stored in a freezer that failed some time ago. Profiling was therefore undertaken only in RNA from NSCLC samples. Using a two-phase approach (training and validation in independent sample sets) we acquired a detailed expression profile of TYMS, DHFR, MTHFR, CBS, SHMT1 and DNMT1 in NSCLC tissue compared to normal tissue from the adjacent lung. Our results revealed a significant distortion of the mRNA profile among folate pathway genes. TYMS, DHFR, CBS and SHMT1 showed significant overexpression in lung tumours, while MTHFR gene showed downregulation in the same tumour set. Expression profiling in a panel of ten respiratory tract cancer cell lines demonstrated similar results TYMS, DHFR, MTHFR and SHMT1 (upregulation) and MTHFR (downregulation) compared to a non-tumorigenic

bronchial epithelial cell line (HBEC). The CBS gene, however, exhibited downregulation in most of the studied cell lines relative to the non-tumorigenic bronchial epithelial cells (HBEC-3KT). While this is not understood currently, one can hypothesize that low CBS may provide a selective advantage under culture conditions. At the end of this part of the project we decided to focus on the deregulated genes in SHMT1 and CBS as they were the least studied, with very few reports on their involvement in cancer and hardly anything in respect to lung cancer.

Several previous studies have underlined the critical impact of irregular splicing in cancer development but, to date, very little, if anything, exists on CBS and SHMT1. To our knowledge, this report represents the first attempt to explore the relative expression of the splice variants of these two genes in lung cancer. Our data show that CBS/SHMT1 variants are expressed in lung-derived cell lines and NSCLC tissue samples, demonstrating their importance in maintaining growth and biological activities in the cellular context. More importantly, CBS variant 3 (CBSv3) is upregulated in NSCLC tissues, being more prominent in squamous carcinomas, while SHMT1 variant 2 (SHMT1v2) exhibits significant downregulation with respect to adjacent non-tumorous tissues. This is an important observation that opens the way for further research to provide mechanistic evidence for (a) what drives this irregular splicing and (b) the differential function of those splice variants in cancer development. No solid hypotheses can be drawn currently as there is virtually no information on the function of those splice variants, but our attempt to model the structural configuration of the mRNAs from the different variants may be a helpful start.

Having identified the significant distortion in the mRNA expression levels of the key players in folate metabolism, our next step was to examine the potential sensitisation of respiratory tract cancer cell lines to 5-FU, MTX and pemetrexed; these are very common drugs, used

today as routine treatment for many cancer types, including respiratory ones. The first step in this route was to test well-known epigenetic modifiers (VPA to inhibit histone deacetylation and DAC for the induction of global DNA hypomethylation) and to investigate whether folate gene expression alterations might coincide with the sensitivity levels of cell lines to these epigenetic modifiers. Despite the fact that several studies employed other HDACi for potentiating 5-FU antitumour effect in lung, colorectal, gastric, hepatic, pancreatic and cholangiocarcinoma cell lines, the role of VPA in modulating lung cancer cells response to 5-FU has remained unexplored. As a subsidiary technical finding, we demonstrated for the first time that pretreatment (as opposed to concurrent treatment) of A549 and SKMES cell lines with VPA 48 hours prior to 5-FU addition significantly enhanced the efficiency of the latter. We also demonstrate the ability of VPA to downregulate TYMS and DNMT1 mRNA while, in a separate experiment, these two genes presented a high expression in the 5-FU 72-h exposure surviving NSCLC cells. This triangle of evidence suggests, apart from the profound benefit of VPA in 5-FU sensitisation, certain molecular routes leading to this epigenetic sensitisation.

Given the importance of the SHMT1 gene in the metabolic reprogramming of cancer cells, we hypothesised that this gene may have a critical role in 5-FU based chemotherapy in respiratory tract cancer. To explore this possibility, we developed shRNA-mediated knockdown clones from PE/CA-PJ15 HNSCC cell lines. Our data demonstrated that SHMT1 knockdown in PE/CA-PJ15 cell line was associated with decreased cell viability and, more importantly, sensitised tumour cells to 5-FU anticancer drug. The synergistic antitumor benefit of concurrent SHMT1 silencing and 5-FU treatment in PE/CA-PJ15 cells was further validated using the SHMT1 selective inhibitor AMPA. This is the first study uncovering the marked potentiation of 5-FU activity via SHMT1.

In conclusion, this study was successful in adding detail to existing information and producing significant new evidence demonstrating the potential exploitation of folate genes as targets to improve antifolate-based therapy for cancer. The three key findings, i.e. irregular CBS and SHMT1 splice isoforms in NSCLC, VPA-based epigenetic sensitisation to 5-FU through TYMS and DNMT1 repression, and SHMT1-mediated sensitisation to 5-FU, provide important new insights into the molecular basis of 5-FU based therapy, and pave the way for further research for clinical utilisation in respiratory, and potentially other, cancer types.

Future directions

SHMT1 appears to be a good candidate target for enhancing the efficiency of 5-FU *in vitro*. Although the present study provided important data regarding the role of SHMT1 expression in PE/CA-PJ15 cancer cell line response to 5-FU anticancer effect, there are a number of issues that should be investigated further.

Knocking down of SHMT1 expression should be performed in at least three NSCLC and HNSCC cell lines to establish whether it produces a similar result on a different genetic background, or it only affects a subset of cell lines, i.e. it is contingent to pre-existing genetic changes. Following establishment of SHMT1 knockout derivative clones with multiple shRNA constructs, cell sensitivity to 5-FU should be measured. If a positive outcome is obtained, rescue experiments should be undertaken in the SHMT1 knockdown clones. The re-expression of SHMT1 would further establish the relationship between this gene and 5-FU antitumour effect. Furthermore, this rescue experiment would demonstrate whether the indication that SHMT1 knockdown leads to sensitisation of respiratory tract cancer cell line to 5-FU anticancer drug is true or not.

We also provide evidence for the potential synergy between 5-FU and VPA in A549 and SK-MES NSCLC cell lines. Cell apoptosis assays would determine whether the VPA-dependent sensitisation to 5-FU is due to apoptosis reactivation or an alternative mechanism.

In addition, the observed alteration of CBS and SHMT1 alternative splicing in NSCLC tissues should be investigated further. CBS and SHMT1 splice variants mRNA and protein expression could be studied in a large cohort, together with investigation of the functional role of these variants in cancer phenotype and drug response in order to evaluate their impact in cancer development and response to chemotherapeutic agents.

References

Abaza, M. I., Bahman, A., & Al-attiyah, R. A. J. (2014). Valproic acid , an anti-epileptic drug and a histone deacetylase inhibitor , in combination with proteasome inhibitors exerts antiproliferative , pro-apoptotic and chemosensitizing effects in human colorectal cancer cells : Underlying molecular mechanisms. *International Journal of Molecular Medicine*, 513–532. https://doi.org/10.3892/ijmm.2014.1795

Adjei, A., Mandrekar, S., Dy, G., Molina, J., Adjei, A., Gandara, D., … Zinner, R. (2010). Phase II trial of pemetrexed plus bevacizumab for second-line therapy of patients with advanced non-small-cell lung cancer: NCCTG and SWOG study N0426. *J Clin Oncol.*, *28*(4), 614–9.

Aherne, G., Hardcastle, A., Raynatd, F., & Jackman, A. (1996). Immunoreactive dUMP and TTP Pools as an Index of Thymidylate Synthase Inhibition ; Effect of Tomudex (ZD1694) and a Nonpolyglutamated Quinazoline Antifolate (CB30900) in L12 10 Mouse Leukaemia Cells. *Biochemical Pharmacology*, *51*, 1293–1301.

Amos, C., Wu, X., Broderick, P., Gorlov, I., Gu, J., Eisen, T., … Houlston, R. (2008). Genome-wide association scan of tag SNPs identifies a susceptibility locus for lung cancer at 15q25.1. *Nat Genet.*, *40*(5), 616–22.

Anderson, D. D., & Stover, P. J. (2009). SHMT1 and SHMT2 are functionally redundant in nuclear de novo thymidylate biosynthesis. *PLoS ONE*, *4*(6). https://doi.org/10.1371/journal.pone.0005839

Ang, K., Harris, J., Wheeler, R., Weber, R., Rosenthal, D., Nguyen-Tân, P., … Gillison, M. (2010). Human papillomavirus and survival of patients with oropharyngeal cancer. *N Engl J Med.*, *363*(1), 24–35.

Arasaradnam, R., Commane, D., Bradburn, D., & Mathers, J. (2008). A review of dietary factors and its influence on DNA methylation in colorectal carcinogenesis. *Epigenetics.*, *3*(4), 193–8.

Arcaro, A. (2015). Targeted therapies for small cell lung cancer: Where do we stand? *Critical Reviews in Oncology/Hematology*, *95*(2), 154–164. https://doi.org/10.1016/j.critrevonc.2015.03.001

Argiris, A., Pennella, E., Koustenis, A., Hossain, A. M., & Obasaju, C. K. (2013). Pemetrexed in head and neck cancer: A systematic review. *Oral Oncology*, *49*, 492–501.

Arora, a, & Scholar, E. M. (2005). Role of tyrosine kinase inhibitors in cancer therapy. *J Pharmacol Exp Ther*, *315*(3), 971–979. https://doi.org/10.1124/jpet.105.084145.have

Askari, B. S., & Krajinovic, M. (2010). Dihydrofolate reductase gene variations in susceptibility to disease and treatment outcomes. *Current Genomics*, *11*(8), 578–83. https://doi.org/10.2174/138920210793360925

Assaraf, Y. G. (2006). The role of multidrug resistance efflux transporters in antifolate resistance and folate homeostasis. *Drug Resistance Updates*, *9*, 227–246.

Aung, K. L., & Siu, L. L. (2016). Genomically personalized therapy in head and neck cancer.

Cancers of the Head & Neck, 1–10. https://doi.org/10.1186/s41199-016-0004-y

Baldwin, C. M., & Perry, C. M. (2009). Pemetrexed A Review of its Use in the Management of Advanced Non-Squamous Non-Small Cell Lung Cancer Claudine. *Drugs*, *69*(16), 2279–2302.

Balgkouranidou, I., Liloglou, T., & Lianidou, E. S. (2013). Lung cancer epigenetics: emerging biomarkers. *Biomarkers in Medicine*, *7*(1), 49–58. https://doi.org/10.2217/bmm.12.111

Baltayiannis, N., Chandrinos, M., Anagnostopoulos, D., Zarogoulidis, P., Tsakiridis, K., Mpakas, A., … Zarogoulidis, K. (2013). Lung cancer surgery: An up to date. *Journal of Thoracic Disease*, *5*(SUPPL.4). https://doi.org/10.3978/j.issn.2072-1439.2013.09.17

Barbareschi, M., Cantaloni, C., Vescovo, V. Del, Cavazza, A., Monica, V., Carella, R., … Tirone, G. (2011). Heterogeneity of Large Cell Carcinoma of the Lung An Immunophenotypic and miRNA-Based Analysis. *Anatomic Pathology*, *136*(5), 773–782. https://doi.org/10.1309/AJCPYY79XAGRAYCJ

Baylin, S., & Jones, P. (2016). Epigenetic Determinants of Cancer. *Cold Spring Harb Perspect Biol.*, *8*(9).

Beasley, M. B., Dembitzer, F. R., & Flores, R. M. (2016). Surgical pathology of early stage non-small cell lung carcinoma. *Ann Transl Med*, *4*(12). https://doi.org/10.21037/atm.2016.06.13

Beetstra, S., Thomas, P., Salisbury, C., Turner, J., & Fenech, M. (2005). Folic acid deficiency increases chromosomal instability, chromosome 21 aneuploidy and sensitivity to radiation-induced micronuclei. *Mutation Research - Fundamental and Molecular Mechanisms of Mutagenesis*, *578*(1–2), 317–326. https://doi.org/10.1016/j.mrfmmm.2005.05.012

Begum, S., Brait, M., Dasgupta, S., Ostrow, K., Zahurak, M., Carvalho, A., … Sidransky, D. (2011). An epigenetic marker panel for detection of lung cancer using cell-free serum DNA. *Clin Cancer Res.*, *17*(13), 4494–503.

Belinsky, S. A. (2015). Unmasking the Lung Cancer Epigenome. *Annual Review of Physiology*, *77*(1), 453–474. https://doi.org/10.1146/annurev-physiol-021014-072018

Bernier, J., Bernier, J., Bentzen, S. M., & Vermorken, J. B. (2009). Molecular therapy in head and neck oncology. *Nat. Rev. Clin. Oncol*, *6*(May), 266–277. https://doi.org/10.1038/nrclinonc.2009.40

Betel, D., Koppal, A., Agius, P., Sander, C., & Leslie, C. (2010). Comprehensive modeling of microRNA targets predicts functional non-conserved and non-canonical sites. *Genome Biology*, *11*(8).

Bhattacharyya, S., Saha, S., Giri, K., Lanza, I. R., Nair, K. S., Jennings, N. B., … Mukherjee, P. (2013). Cystathionine Beta-Synthase (CBS) Contributes to Advanced Ovarian Cancer Progression and Drug Resistance. *PLoS ONE*, *8*(11). https://doi.org/10.1371/journal.pone.0079167

Blount, B. C., Mack, M. M., Wehr, C. M., MacGregor, J. T., Hiatt, R. a, Wang, G., … Ames, B. N. (1997). Folate Deficiency Causes Uracil Misincorporations into Human DNA and

Chromosome Breakage: Implications for Cancer and Neuronal Damage. *Proceedings of the National Academy of Sciences of the United States of America*, *94*(7), 3290–5. https://doi.org/10.1073/pnas.94.7.3290

Both, J., Wu, T., Bras, J., Schaap, G., Baas, F., & Hulsebos, T. (2012). Identification of novel candidate oncogenes in chromosome region 17p11.2-p12 in human osteosarcoma. *PLoS One*, *7*(1).

BOŽENA, S. (2016). SPECIFICS OF HISTOPATHOLOGICAL ANALYSIS OF HEAD AND NECK CANCER. *Lib Oncol*, *44*, 31–35.

Brain, K., Carter, B., Lifford, K. J., Burke, O., Devaraj, A., Baldwin, D. R., … Field, J. K. (2017). Impact of low-dose CT screening on smoking cessation among high-risk participants in the UK Lung Cancer Screening Trial. *Thorax.*, 912–918. https://doi.org/10.1136/thoraxjnl-2016-209690

Bram, E., Ifergan, I., Shafran, A., Berman, B., Jansen, G., & Assaraf, Y. (2006). Mutant Gly482 and Thr482 ABCG2 mediate high-level resistance to lipophilic antifolates. *Cancer Chemother Pharmacol.*, *58*(6), 826–34.

Bufalo, D. Del, Desideri, M., Luca, T. De, Martile, M. Di, Gabellini, C., Monica, V., … Trisciuoglio, D. (2014). Histone deacetylase inhibition synergistically enhances pemetrexed cytotoxicity through induction of apoptosis and autophagy in non-small cell lung cancer. *Molecular Cancer*, 1–16.

Cagle, P. (2010). *Advances in Surgical Pathology: Lung Cancer*. (P. Cagle & T. Allen, Eds.). Philadelphia: Lippincott William and Wilkins. Retrieved from https://books.google.co.uk/books?id=ud0PAAAAQBAJ&pg=PT72&lpg=PT72&dq=lung+cancer,+histological+classification,+beasley,+2005&source=bl&ots=iKoRLzN_oR&sig=zT-V70eVoLJAYyfBfwa3SmBk-jI&hl=en&sa=X&ved=0ahUKEwjy0LetisLSAhVLCcAKHTh_BAY4ChDoAQgtMAc#v=onepage&q=l

Califano, R., Abidin, A., Tariq, N. ul A., Economopoulou, P., Metro, G., & Mountzios, G. (2015). Beyond EGFR and ALK inhibition: Unravelling and exploiting novel genetic alterations in advanced non small-cell lung cancer. *Cancer Treatment Reviews*, *41*(5), 401–411. https://doi.org/10.1016/j.ctrv.2015.03.009

Cammico, C., & Glazer, R. (1979). Effect of 5-Fluorouracil on the Synthesis and Translation of Polyadenylic Acid-containing RNA from Regenerating Rat Liver. *Cancer Reasearch*, *39*, 3694–3701.

Campling, B., & El-Deiry, W. (2003). Clinical implications of p53 mutations in lung cancer. *Methods Mol Med.*, *75*, 53–77.

Cantor, J., Iliopoulos, D., Rao, A., Druck, T., Semba, S., Han, S., … Huebner, K. (2007). Epigenetic modulation of endogenous tumor suppressor expression in lung cancer xenografts suppresses tumorigenicity. *Int J Cancer*, *120*(1), 24–31.

Caplin, M. E., Baudin, E., Ferolla, P., Filosso, P., Garcia-Yuste, M., Lim, E., … Zheng-Pei, Z. (2015). Pulmonary neuroendocrine (carcinoid) tumors: European Neuroendocrine Tumor Society expert consensus and recommendations for best practice for typical and

atypical pulmonary carcinoids. *Annals of Oncology*, *26*(8), 1604–1620. https://doi.org/10.1093/annonc/mdv041

Carreras, C., & Santi, D. (1995). The catalytic mechanism and structure of thymidylate synthase. *Annu Rev Biochem.*, *64*, 721–62.

Ceppi, P., Rapa, I., Lo Iacono, M., Righi, L., Giorcelli, J., Pautasso, M., … Scagliotti, G. V. (2012). Expression and pharmacological inhibition of thymidylate synthase and Src kinase in nonsmall cell lung cancer. *International Journal of Cancer*, *130*(8), 1777–1786. https://doi.org/10.1002/ijc.26188

Chedin, F., Lieber, M., & Hsieh, C. (2002). The DNA methyltransferase-like protein DNMT3L stimulates de novo methylation by Dnmt3a. *Proc Natl Acad Sci U S A. 2002*, *99*(26), 16916–21.

Cheng, Q., Cheng, C., Crews, K., Ribeiro, R., Pui, C., Relling, M., & Evans, W. (2006). Epigenetic regulation of human gamma-glutamyl hydrolase activity in acute lymphoblastic leukemia cells. *Am J Hum Genet.*, *79*(2), 264–74.

Chéradame, S., Chazal, M., Fischel, J., Formento, P., Renée, N., & Milano, G. (1999). Variable intrinsic sensitivity of human tumor cell lines to raltitrexed (Tomudex) and folylpolyglutamate synthetase activity. *Anticancer Drugs.*, *10*(5), 505–10.

Choi, S.-W., & Mason, J. B. (2000). Folate and Carcinogenesis: An Integrated Scheme. *The Journal of Nutrition*, *130*, 129–132.

Choi, Y., Takeuchi, K., Soda, M., Inamura, K., Togashi, Y., Hatano, S., … Mano, H. (2008). Identification of novel isoforms of the EML4-ALK transforming gene in non-small cell lung cancer. *Cancer Res*, *68*(13), 4971–4976. https://doi.org/10.1158/0008-5472.CAN-07-6158

Chon, J., Stover, P. J., & Field, M. S. (2017). Targeting nuclear thymidylate biosynthesis. *Molecular Aspects of Medicine*, *53*, 48–56. https://doi.org/http://dx.doi.org/10.1016/j.mam.2016.11.005

Cohen, M., Johnson, J., Wang, Y., Sridhara, R., & Pazdur, R. (2005a). FDA drug approval summary: pemetrexed for injection (Alimta) for the treatment of non-small cell lung cancer. *Oncologist.*, *10*(6), 363–8.

Cohen, M., Johnson, J., Wang, Y., Sridhara, R., & Pazdur, R. (2005b). FDA drug approval summary: pemetrexed for injection (Alimta) for the treatment of non-small cell lung cancer. *Oncologist.*, *10*(6), 363–8.

Colevas, A. D. (2006). Chemotherapy options for patients with metastatic or recurrent squamous cell carcinoma of the head and neck. *Journal of Clinical Oncology : Official Journal of the American Society of Clinical Oncology*, *24*(17), 2644–52. https://doi.org/10.1200/JCO.2005.05.3348

Collins, L. G., Haines, C., Perkel, R., & Enck, R. E. (2007). Lung cancer: Diagnosis and management. *American Family Physician*, *75*(1), 56–63. https://doi.org/10.1378/chest.12-2345.

Cooper, W. A., Lam, D. C. L., O'Toole, S. A., & Minna, J. D. (2013). Molecular biology of lung

cancer. *Journal of Thoracic Disease*, *5*(SUPPL.5). https://doi.org/10.3978/j.issn.2072-1439.2013.08.03

Cortés, Á., Urquizu, L., & Cubero, J. (2015). Adjuvant chemotherapy in non-small cell lung cancer: state-of- the-art. *Transl Lung Cancer Res*, *4*(2), 191–197.

Crider, K. S., Yang, T. P., Berry, R. J., & Bailey, L. B. (2012). Folate and DNA Methylation : A Review of Molecular Mechanisms and the Evidence for Folate ' s Role. *American Society for Nutrition*, *3*(14), 21–38. https://doi.org/10.3945/an.111.000992.Figure

Crott, J., Liu, Z., Keyes, M., Choi, S., Jang, H., Moyer, M., & Mason, J. (2008). Moderate folate depletion modulates the expression of selected genes involved in cell cycle, intracellular signaling and folate uptake in human colonic epithelial cell lines. *J Nutr Biochem*, *19*(5), 328–35.

Czarnecka-Kujawa, K., & Yasufuku, K. (2014). Molecular alterations in non-small-cell lung cancer: Perspective for targeted therapy and specimen management for the bronchoscopist. *Respirology*, *19*(8), 1117–1125. https://doi.org/10.1111/resp.12377

Daskalos, A., Nikolaidis, G., Xinarianos, G., Savvari, P., Cassidy, A., Zakopoulou, R., … Liloglou, T. (2009). Hypomethylation of retrotransposable elements correlates with genomic instability in non-small cell lung cancer. *Int J Cancer.*, *124*(1), 81–7.

Davidson, B., Abeler, V. M., Forsund, M., Holth, A., Yang, Y., Kobayashi, Y., … Wang, T.-L. (2014). Gene expression signatures of primary and metastatic uterine leiomyosarcoma. *Human Pathology*, *45*(4), 691–700. https://doi.org/10.1016/j.pestbp.2011.02.012.Investigations

Davidson, M. R., Gazdar, A. F., & Clarke, B. E. (2013). The pivotal role of pathology in the management of lung cancer. *Journal of Thoracic Disease*, *5*. https://doi.org/10.3978/j.issn.2072-1439.2013.08.43

Davis, C., & Ross, S. (2008). Evidence for dietary regulation of microRNA expression in cancer cells. *Nutr Rev*, *66*(8), 477–82.

Deng, J., Wang, Y., Lei, J., Lei, W., & Xiong, J. P. (2017). Insights into the involvement of noncoding RNAs in 5-fluorouracil drug resistance. *Tumor Biology*, *39*(4), 101042831769755. https://doi.org/10.1177/1010428317697553

Deplus, R., Brenner, C., Burgers, W., Putmans, P., Kouzarides, T., de Launoit, Y., & Fuks, F. (2002). Dnmt3L is a transcriptional repressor that recruits histone deacetylase. *Nucleic Acids Res*, *30*(17), 3831–8.

Desai, A., Sequeira, J. M., & Quadros, E. V. (2016). The metabolic basis for developmental disorders due to defective folate transport. *Biochimie*, *126*, 31–42. https://doi.org/10.1016/j.biochi.2016.02.012

Detich, N., Bovenzi, V., & Szyf, M. (2003). Valproate induces replication-independent active DNA demethylation. *J Biol Chem.*, *278*(30), 27586–92.

Diasio, R., & Harris, B. (1989). Clinical Pharmacology of 5-Fluorouracil. *Clinical Pharmacokinetics*, *16*, 215–237.

Digel, W., & Lübbert, M. (2005). DNA methylation disturbances as novel therapeutic target in lung cancer: preclinical and clinical results. *Crit Rev Oncol Hematol.*, *55*(1), 1–11.

Doriguzzi, A., Salhi, J., & Sutterlüty-Fall, H. (2016). Sprouty4 mRNA variants and protein expressions in breast and lung-derived cells. *Oncol Lett.*, *12*(5), 4161–4166.

Drilon, A., Rekhtman, N., Ladanyi, M., & Paik, P. (2012). Squamous-cell carcinomas of the lung: Emerging biology, controversies, and the promise of targeted therapy. *Lancet Oncology*, *13*(10), 418–426. https://doi.org/10.1016/S1470-2045(12)70291-7

Ducker, G. S., Chen, L., Morscher, R. J., Ghergurovich, J. M., Esposito, M., Teng, X., … Rabinowitz, J. D. (2016). Reversal of Cytosolic One-Carbon Flux Compensates for Loss of the Mitochondrial Folate Pathway. *Cell Metabolism*, *24*(4), 640–641. https://doi.org/10.1016/j.cmet.2016.09.011

Ducker, G. S., & Rabinowitz, J. D. (2016). One-Carbon Metabolism in Health and Disease. *Cell Metabolism*, *25*(1), 27–42. https://doi.org/10.1016/j.cmet.2016.08.009

Duthie, S. (2011). Folate and cancer: How DNA damage, repair and methylation impact on colon carcinogenesis. *Journal of Inherited Metabolic Disease*, *34*(1), 101–109. https://doi.org/10.1007/s10545-010-9128-0

Duthie, S. J., Mavrommatis, Y., Rucklidge, G., Reid, M., Duncan, G., Moyer, M. P., … Bestwick, C. S. (2008). The response of human colonocytes to folate deficiency in vitro: Functional and proteomic analyses. *Journal of Proteome Research*, *7*(8), 3254–3266. https://doi.org/10.1021/pr700751y

Engelman, J. a, Luo, J., & Cantley, L. C. (2006). The evolution of phosphatidylinositol 3-kinases as regulators of growth and metabolism. *Nature Reviews. Genetics*, *7*(8), 606–619. https://doi.org/10.1038/nrg1879

Farber, S., & Diamond, L. (1948). Temporary remissions in acute leukemia in children produced by folic acid antagonist, 4-aminopteroyl-glutamic acid. *N Engl J Med.*, *238*(23), 787–93.

Feinberg, A., & Vogelstein, B. (1983). Hypomethylation distinguishes genes of some human cancers from their normal counterparts. *Nature*, *301*(5895), 89–92.

Fenizia, F., De Luca, A., Pasquale, R., Sacco, A., Forgione, L., Lambiase, M., … Normanno, N. (2015). EGFR mutations in lung cancer: from tissue testing to liquid biopsy. *Future Oncology (London, England)*, *11*(11), 1611–23. https://doi.org/10.2217/fon.15.23

Fennell, D. A., Summers, Y., Cadranel, J., Benepal, T., Christoph, D. C., Lal, R., … Ferry, D. (2016). Cisplatin in the modern era: The backbone of first-line chemotherapy for non-small cell lung cancer. *Cancer Treatment Reviews*, *44*, 42–50. https://doi.org/10.1016/j.ctrv.2016.01.003

Ferlay, J., Soerjomataram, I., Dikshit, R., Eser, S., Mathers, C., Rebelo, M., … Bray, F. (2015). Cancer incidence and mortality worldwide : Sources , methods and major patterns in GLOBOCAN 2012. *Int J Cancer*, *136*(5). https://doi.org/10.1002/ijc.29210

Ferrara, R., Pilotto, S., Peretti, U., Caccese, M., Kinspergher, S., Carbognin, L., … Bria, E. (2016). Tubulin inhibitors in non-small cell lung cancer: looking back and forward. *Expert Opin*

Pharmacother., *17*(8), 1113–29.

Filipowicz, W., Bhattacharyya, S., & Sonenberg, N. (2008). Mechanisms of post-transcriptional regulation by microRNAs: are the answers in sight? *Nat Rev Genet.*, *9*(2), 102–14.

Filosso, P., European Society of Thoracic Surgeons (ESTS), N. T. of T. L. W.-G., Committee, S., Asamura, H., Brunelli, A., Filosso, P., … Thomas, P. (2014). Knowledge of pulmonary neuroendocrine tumors: where are we now? *Thorac Surg Clin.*, *24*(3), ix–xii.

Flores, K. G., Stidley, C. A., Mackey, A. J., Picchi, M. A., Stabler, S. P., Siegfried, J. M., … Leng, S. (2012). Sex-specific association of sequence variants in CBS and MTRR with risk for promoter hypermethylation in the lung epithelium of smokers. *Carcinogenesis*, *33*(8), 1542–1547. https://doi.org/10.1093/carcin/bgs194

Flöter, J., Kaymak, I., & Schulze, A. (2017). Regulation of Metabolic Activity by p53. *Metabolites*. https://doi.org/10.3390/metabo7020021

Forastiere, A. A., & Trotti, A. (1999). Radiotherapy and Concurrent Chemotherapy : a Strategy. *Journal of the National Center Institute*, *91*(24).

Fox, J. T., & Stover, P. J. (2008). Folate-Mediated One-Carbon Metabolism. *Vitamins & Hormones*, *79*, 1–44. https://doi.org/10.1016/S0083-6729(08)00401-9

Frigola, J., Song, J., Stirzaker, C., Hinshelwood, R., Peinado, M., & Clark, S. (2006). Epigenetic remodeling in colorectal cancer results in coordinate gene suppression across an entire chromosome band. *Nat Genet*, *38*(5), 540–9.

Furrukh, M. (2013). Tobacco Smoking and Lung Cancer. *Sultan Qaboos Univ Med J.*, *13*(3), 345–358.

Gai, J. W., Qin, W., Liu, M., Wang, H. F., Zhang, M., Li, M., … Ma, H. S. (2016). Expression profile of hydrogen sulfide and its synthases correlates with tumor stage and grade in urothelial cell carcinoma of bladder. *Urologic Oncology: Seminars and Original Investigations*, *34*(4), 166.e15-166.e20. https://doi.org/10.1016/j.urolonc.2015.06.020

Garcia, B., Luka, Z., Loukachevitch, L., Bhanu, N., & Wagner, C. (2016). Folate deficiency affects histone methylation. *Med Hypotheses*, *88*, 63–7.

Garrow, T., Brenner, A., Whitehead, V., Chen, X., Duncan, R., Korenberg, J., & Shane, B. (1993). Cloning of human cDNAs encoding mitochondrial and cytosolic serine hydroxymethyltransferases and chromosomal localization. *J Biol Chem. 1993 Jun 5;268(16):11910-6*, *16*, 11910–6.

Gaspar, L., McNamara, E., Gay, E., Putnam, J., Crawford, J., Herbst, R., & Bonner, J. (2012). Small-cell lung cancer: prognostic factors and changing treatment over 15 years. *Clin Lung Cancer.*, *13*(2), 115–22.

Gazzali, A. M., Lobry, M., Colombeau, L., Acherar, S., Aza??s, H., Mordon, S., … Frochot, C. (2016). Stability of folic acid under several parameters. *European Journal of Pharmaceutical Sciences*, *93*, 419–430. https://doi.org/10.1016/j.ejps.2016.08.045

Genestier, L., Paillot, R., Quemeneur, L., Izeradjene, K., & Revillard, J. (2000). Mechanisms of action of methotrexate. *Immunopharmacology*, *47*(2–3), 247–57.

Ghoshal, K., & Jacob, S. (1994). Brief Specific Inhibition of Pre-Ribosomal RNA Processing in Extracts from the Lymphosarcoma Cells Treated with 5-Fluorouracil. *Cancer Reasearch*, *54*, 632–636.

Giardina, G., Brunotti, P., Fiascarelli, A., Cicalini, A., Costa, M. G. S., Buckle, A. M., … Paone, A. (2015). cytosolic and mitochondrial serine hydroxymethyltransferase oligomeric state. *FEBS Journal*, *282*, 1225–1241. https://doi.org/10.1111/febs.13211

Gibbons, D., Byers, L., & Kurie, J. (2014). Smoking, p53 Mutation, and Lung Cancer. *Mol Cancer Res. 2014*, *12*(1), 3–13. https://doi.org/10.1158/1541-7786.MCR-13-0539.Smoking

Gillison, M., D'Souza, G., Westra, W., Sugar, E., Xiao, W., Begum, S., & Viscidi, R. (2008). Distinct risk factor profiles for human papillomavirus type 16-positive and human papillomavirus type 16-negative head and neck cancers. *J Natl Cancer Inst.*, *100*(6), 407–20.

Gillison, M., Koch, W., Capone, R., Spafford, M., Westra, W., Wu, L., … Sidransky, D. (2000). Evidence for a causal association between human papillomavirus and a subset of head and neck cancers. *J Natl Cancer Inst.*, *92*(9), 709–20.

Girgis, S., Nasrallah, I., Suh, J., Oppenheim, E., Zanetti, K., Mastri, M., & Stover, P. (1998). Molecular cloning, characterization and alternative splicing of the human cytoplasmic serine hydroxymethyltransferase gene. *Gene. 1998 Apr 14;210(2):315-24.*, *210*(2), 315–24.

Goldin, A., Venditti, J., Humphreys, S., Dennis, D., Mantel, N., & Greenhouse, S. (1955). A quantitative comparison of the antileukemic effectiveness of two folic acid antagonists in mice. *J Natl Cancer Inst.*, *15*(6), 1657–64.

Gonen, N., & Assaraf, Y. G. (2012). Antifolates in cancer therapy: Structure, activity and mechanisms of drug resistance. *Drug Resistance Updates*, *15*(4), 183–210. https://doi.org/10.1016/j.drup.2012.07.002

Gotanda, K., Hirota, T., Matsumoto, N., & Ieiri, I. (2013). MicroRNA-433 negatively regulates the expression of thymidylate synthase (TYMS) responsible for 5-fluorouracil sensitivity in HeLa cells. *BMC Cancer.*, *13*.

Graham, J., Kaye, S., & Brown, R. (2009). The promises and pitfalls of epigenetic therapies in solid tumours. *Eur J Cancer.*, *45*(7), 1129–36.

Grimminger, P., Schneider, P., Metzger, R., Vallböhmer, D., Hölscher, A., Danenberg, P., & Brabender, J. (2010). Low thymidylate synthase, thymidine phosphorylase, and dihydropyrimidine dehydrogenase mRNA expression correlate with prolonged survival in resected non-small-cell lung cancer. *Clin Lung Cancer*, *11*(5), 328–34.

Grosso, A., Martins, S., & Carmo-Fonseca, M. (2008). The emerging role of splicing factors in cancer. *EMBO Rep.*, *9*(11), 1087–93.

Guo, S., Jiang, C., Wang, G., Li, Y., Wang, C., Guo, X., … Zhang, X. (2013). MicroRNA-497 targets insulin-like growth factor 1 receptor and has a tumour suppressive role in human colorectal cancer. *Oncogene.*, *32*(15), 1910–20.

Gupta, R., Yang, Q., Dogra, S. K., & Wajapeyee, N. (2017). Serine hydroxymethyl transferase 1

stimulates pro-oncogenic cytokine expression through sialic acid to promote ovarian cancer tumor growth and progression. *Oncogene*, (December 2016), 1–11. https://doi.org/10.1038/onc.2017.37

Gustafsson, B. I., Kidd, M., Chan, A., Malfertheiner, M. V, & Modlin, I. M. (2008). Bronchopulmonary Neuroendocrine Tumors. *American Cancer Society*, *113*(1). https://doi.org/10.1002/cncr.23542

Hagner, N., & Joerger, M. (2010). Cancer chemotherapy: targeting folic acid synthesis. *Cancer Management and Research*, *2*, 293–301.

Hanahan, D., & Weinberg, R. A. (2011). Hallmarks of cancer: The next generation. *Cell*, *144*(5), 646–674. https://doi.org/10.1016/j.cell.2011.02.013

Hayes, J., Peruzzi, P. P., & Lawler, S. (2014). MicroRNAs in cancer: biomarkers, functions and therapy. *Trends in Molecular Medicine, August*, *20*(8).

Heidelberger, C., Chaudhuri, N., Danneberg, P., Mooren, D., Griesbach, L., Duschinsky, R., … Scheiner, J. (1957). Fluorinated pyrimidines, a new class of tumour-inhibitory compounds. *Nature*, *179*(4561), 663–6.

Heinmöller, P., Gross, C., Beyser, K., Schmidtgen, C., Maass, G., Pedrocchi, M., & Rüschoff, J. (2003). HER2 status in non-small cell lung cancer: results from patient screening for enrollment to a phase II study of herceptin. *Clinical Cancer Research : An Official Journal of the American Association for Cancer Research*, *9*(14), 5238–43. Retrieved from http://www.ncbi.nlm.nih.gov/pubmed/14614004

Heller, G., Babinsky, V. N., Ziegler, B., Weinzierl, M., Noll, C., Altenberger, C., … Zöchbauer-Müller, S. (2013). Genome-wide CpG island methylation analyses in non-small cell lung cancer patients. *Carcinogenesis*, *34*(3), 513–521. https://doi.org/10.1093/carcin/bgs363

Heller, G., Zielinski, C., & Zöchbauer-Müller, S. (2010). Lung cancer: from single-gene methylation to methylome profiling. *Cancer Metastasis Rev.*, *29*(1), 95–107.

Hellmich, M., Coletta, C., Chao, C., & Szabo, C. (2014). The Therapeutic Potential of Cystathionine β-Synthetase/Hydrogen Sulfide Inhibition in Cancer. *Antioxidants & Redox Signaling*, *22*(5), 424–448. https://doi.org/10.1089/ars.2014.5933

Herbig, K., Chiang, E. P., Lee, L. R., Hills, J., Shane, B., & Stover, P. J. (2002). Cytoplasmic serine hydroxymethyltransferase mediates competition between folate-dependent deoxyribonucleotide and S-adenosylmethionine biosyntheses. *Journal of Biological Chemistry*, *277*(41), 38381–38389. https://doi.org/10.1074/jbc.M205000200

Holliday, R., & Pugh, J. (1975). DNA modification mechanisms and gene activity during development. *Science*, *187*(4173), 226–32.

Hooijberg, J. H., Jansen, G., Kathmann, I., Peters, R., Laan, A. C., Zantwijk, I. van, … Peter, G. J. (2014). Folates provoke cellular efflux and drug resistance of substrates of the multidrug resistance protein 1 (MRP1). *Cancer Chemother Pharmacol*, *73*, 911–917.

Horie, N., Aiba, H., Oguro, K., Hojo, H., & Takeishi, K. (1995). Functional analysis and DNA polymorphism of the tandemly repeated sequences in the 5'-terminal regulatory region of the human gene for thymidylate synthase. *Cell Struct Funct*, *20*(3), 191–7.

Houghton, J., Tillman, D., & Harwood, F. (1995). Ratio of 2'-Deoxyadenosine-5'-triphosphate/Thymidine-5'triphosphate Influence the Commitment of Human Colon Carcinoma Cells to Thymineless Death. *Clinical Cancer Reasearch*, *1*, 723–730.

Hryniuk, W. (1975). The mechanism of action of methotrexate in cultured L5178Y leukemia cells. *Cancer Res.*, *35*(4), 1085–92.

Humeniuk, R., Mishra, P., Bertino, J., & Banerjee, D. (2009). Epigenetic reversal of acquired resistance to 5-fluorouracil treatment. *Mol Cancer Ther.*, *8*(5), 1045–54.

Hung, R. J., Mckay, J. D., Gaborieau, V., Boffetta, P., Hashibe, M., Zaridze, D., … Field, J. K. (2008). A susceptibility locus for lung cancer maps to nicotinic acetylcholine receptor subunit genes on 15q25. *Nature*, *452*(April), 633–637. https://doi.org/10.1038/nature06885

Hurst, C. K., & Chetty, I. J. (2014). Improving radiotherapy planning, delivery accuracy, and normal tissue sparing using cutting edge technologies. *Journal of Thoracic Disease*, *6*(4), 303–318. https://doi.org/10.3978/j.issn.2072-1439.2013.11.10

Hurvitz, S., Shatsky, R., & Harbeck, N. (2014). Afatinib in the treatment of breast cancer. *Expert Opinion on Investigational Drugs*, *23*(7), 1039–1047. https://doi.org/10.1517/13543784.2014.924505

Ichinose, Y., Yoshimori, K., Sakai, H., Nakai, Y., Sugiura, T., Kawahara, M., & Niitani, H. (2004). S-1 plus cisplatin combination chemotherapy in patients with advanced non-small cell lung cancer: a multi-institutional phase II trial. *Clin Cancer Res.*, *10*(23), 7860–4.

Inoue, M., Sawabata, N., & Okumura, M. (2012). Surgical intervention for small-cell lung cancer: What is the surgical role? *General Thoracic and Cardiovascular Surgery*, *60*(7), 401–405. https://doi.org/10.1007/s11748-012-0072-9

Irizarry, R., Ladd-Acosta, C., Wen, B., Wu, Z., Montano, C., Onyango, P., … Feinberg, A. (2009). The human colon cancer methylome shows similar hypo- and hypermethylation at conserved tissue-specific CpG island shores. *Nat Genet.*, *41*(2), 178–86.

Issa, J. (2007). DNA methylation as a therapeutic target in cancer. *Clin Cancer Res.*, *13*(6), 1634–7.

Iwahashi, S., Ishibashi, H., Utsunomiya, T., Morine, Y., Ochir, T. L., Hanaoka, J., … Shimada, M. (2011). Effect of histone deacetylase inhibitor in combination with 5-fluorouracil on pancreas cancer and cholan- giocarcinoma cell lines. *The Journal of Medical Investigation*, *58*, 106–109.

James, S. J., Pogribny, I. P., Pogribna, M., Miller, B. J., Jernigan, S., & Melnyk, S. (2003). Mechanisms of DNA Damage , DNA Hypomethylation , and Tumor. *The Journal of Nutrition*, (7), 3740–3747.

Jansen, G., Barr, H., Kathmann, I., Bunni, M., Priest, D., Noordhuis, P., … Assaraf, Y. (1999). Multiple mechanisms of resistance to polyglutamatable and lipophilic antifolates in mammalian cells: role of increased folylpolyglutamylation, expanded folate pools, and intralysosomal drug sequestration. *Mol Pharmacol.*, *55*(4), 761–9.

Jansson, M., & Lund, A. (2012). MicroRNA and cancer. *Mol Oncol.*, *6*(6), 590–610.

Jhee, K.-H., & Kruger, W. D. (2005). The role of cystathionine beta-synthase in homocysteine metabolism. *Antioxidants & Redox Signaling*, *7*(5–6), 813–822. https://doi.org/10.1089/ars.2005.7.813

Jia, L., Osada, M., Ishioka, C., Gamo, M., Ikawa, S., Suzuki, T., … Kuroki, T. (1997). Screening the p53 Status of Human Cell Lines Using a Yeast Functional Assay. *MOLECULAR CARCINOGENESIS 19:243–253*, *19*, 243–253.

Jin, G., Huang, J., Hu, Z., Dai, J., Tang, R., Chen, Y., … Shen, H. (2010). Genetic variants in one-carbon metabolism-related genes contribute to NSCLC prognosis in a Chinese population. *Cancer*, *116*(24), 5700–5709. https://doi.org/10.1002/cncr.25301

Johnston, P., Lenz, H., Leichman, C., Danenberg, K., Allegra, C., Danenberg, P., & Leichman, L. (1995). Thymidylate synthase gene and protein expression correlate and are associated with response to 5-fluorouracil in human colorectal and gastric tumors. *Cancer Res.*, *55*(7), 1407–12.

Jones, P. A., & Baylin, S. B. (2007). The Epigenomics of Cancer. *Cell*, *128*(4), 683–692. https://doi.org/10.1016/j.cell.2007.01.029

Jones, P. A., & Liang, G. (2009). Rethinking how DNA Methylation Patterns are Maintained Peter. *Nat Rev Genet.*, *10*(11), 805–811. https://doi.org/10.1038/nrg2651.Rethinking

Kabil, O., Zhou, Y., & Banerjee, R. (2006). Mar. *Biochemistry.*, *45*(45), 13528–36.

Kanda, T., Tada, M., Imazeki, F., Yokosuka, O., Nagao, K., & Saisho, H. (2005). 5-aza-2'-deoxycytidine sensitizes hepatoma and pancreatic cancer cell lines. *Oncol Rep.*, *14*(4), 975–9.

Kastrup, I., Worm, J., Ralfkiaer, E., Hokland, P., Guldberg, P., & Grønbaek, K. (2008). Genetic and epigenetic alterations of the reduced folate carrier in untreated diffuse large B-cell lymphoma. *Eur J Haematol.*, *80*(1), 61–6.

Kato, H., Ichinose, Y., Ohta, M., Hata, E., Tsubota, N., Tada, H., … Chemotherapy, J. L. C. R. G. on P. A. (2004). A randomized trial of adjuvant chemotherapy with uracil-tegafur for adenocarcinoma of the lung. *N Engl J Med.*, *350*(17), 1713–21.

Kawahara, M., Furuse, K., Segawa, Y., Yoshimori, K., Matsui, K., Kudoh, S., … Group), S.-1 C. S. G. (Lung C. W. (2001). Phase II study of S-1, a novel oral fluorouracil, in advanced non-small-cell lung cancer. *Br J Cancer.*, *85*(7), 939–43.

KIM, J., HONG, S. J., PARK, J. H., PARK, S. Y., KIM, S. W., CHO, E. Y., … 1CbsBioscience. (2009). Expression of cystathionine ß-synthase is downregulated in hepatocellular carcinoma and associated with poor prognosis. *Oncology Reports*, *21*, 1449–1454. https://doi.org/10.3892/or

Kim, S., Jung, W., & Koo, J. (2014). Differential expression of enzymes associated with serine/glycine metabolism in different breast cancer subtypes. *PLoS One*, *9*(6).

Kim, Y. (2005). Nutritional epigenetics: impact of folate deficiency on DNA methylation and colon cancer susceptibility. *J Nutr.*, *135*(11), 2703–9.

Kim, Y. (2007a). Folate and colorectal cancer: an evidence-based critical review. *Mol Nutr*

Food Res, *51*(3), 267–92.

Kim, Y. (2007b). Folate and colorectal cancer: An evidence-based critical review. *Molecular Nutrition and Food Research*, *51*(3), 267–292. https://doi.org/10.1002/mnfr.200600191

Kim, Y., Christman, J., Fleet, J., Cravo, M., Salomon, R., Smith, D., … Mason, J. (1995). Moderate folate deficiency does not cause global hypomethylation of hepatic and colonic DNA or c-myc-specific hypomethylation of colonic DNA in rats. *Am J Clin Nutr.*, *61*(5), 1083–90.

Kneip, C., Schmidt, B., Seegebarth, A., Weickmann, S., Fleischhacker, M., Liebenberg, V., … Dietrich, D. (2011). SHOX2 DNA methylation is a biomarker for the diagnosis of lung cancer in plasma. *J Thorac Oncol.*, *6*(10), 1632–8.

Kodera, Y., Ito, S., Fujiwara, M., Mochizuki, Y., Nakayama, G., Ohashi, N., … Nakao, M. (2007). Gene expression of 5-fluorouracil metabolic enzymes in primary gastric cancer: Correlation with drug sensitivity against 5-fluorouracil. *Cancer Letters*, *252*, 307–313.

Kodidela, S., Suresh Chandra, P., & Dubashi, B. (2014). Pharmacogenetics of methotrexate in acute lymphoblastic leukaemia: Why still at the bench level? *European Journal of Clinical Pharmacology*, *70*(3), 253–260. https://doi.org/10.1007/s00228-013-1623-4

Koontongkaew, S. (2013). The Tumor Microenvironment Contribution to Development, Growth, Invasion and Metastasis of Head and Neck Squamous Cell Carcinomas. *Journal of Cancer*, *4*(41). https://doi.org/10.7150/jca.5112

Kotoula, V., Krikelis, D., Karavasilis, V., Koletsa, T., Eleftheraki, A. G., Televantou, D., … Fountzilas, G. (2012). Expression of DNA repair and replication genes in non-small cell lung cancer (NSCLC): a role for thymidylate synthetase (TYMS). *BMC Cancer.*, *12*.

Koumarianou, A., Tzeveleki, I., Mekras, D., Eleftheraki, A., Bobos, M., Wirtz, R., … Fountzilas, G. (2014). Prognostic markers in early-stage colorectal cancer: significance of TYMS mRNA expression. *Anticancer Res.*, *34*(9), 4949–62.

Kozomara, A., & Griffiths-jones, S. (2014). miRBase : annotating high confidence microRNAs using deep sequencing data. *Nucleic Acids Research*, *42*(November 2013), 68–73. https://doi.org/10.1093/nar/gkt1181

Krushkal, J., Zhao, Y., Hose, C., Monks, A., Doroshow, J. H., & Simon, R. (2016). Concerted changes in transcriptional regulation of genes involved in DNA methylation, demethylation, and folate-mediated one-carbon metabolism pathways in the NCI-60 cancer cell line panel in response to cancer drug treatment. *Clinical Epigenetics*, *8*, 73. https://doi.org/10.1186/s13148-016-0240-3

Kulis, M., & Esteller, M. (2010). DNA Methylation and Cancer. *Advances in Genetics*, *70*(10), 27–56. https://doi.org/10.1016/B978-0-12-380866-0.60002-2

Lacko, M., Braakhuis, B. J. M., Sturgis, E. M., Boedeker, C. C., Suárez, C., Rinaldo, A., … Takes, R. P. (2014). Genetic susceptibility to head and neck squamous cell carcinoma. *International Journal of Radiation Oncology Biology Physics*, *89*(1), 38–48. https://doi.org/10.1016/j.ijrobp.2013.09.034

Langevin, S. M., & Kelsey, K. T. (2013). The fate is not always written in the genes: Epigenomics in epidemiologic studies. *Environmental and Molecular Mutagenesis*, *54*(7), 533–541.

https://doi.org/10.1002/em.21762

Langevin, S. M., Kratzke, R. A., & Kelsey, K. T. (2015). Epigenetics of Lung Cancer. *Transl Res*, *165*(1), 74–90. https://doi.org/10.1038/jid.2014.371

Latz, J., Chaudhary, A., Ghosh, A., & Johnson, R. (2006). Population pharmacokinetic analysis of ten phase II clinical trials of pemetrexed in cancer patients. *Cancer Chemother Pharmacol.*, *57*(4), 401–11.

Lazo, P. (2017). Reverting p53 activation after recovery of cellular stress to resume with cell cycle progression. *Cellular Signalling*, *33*, 49–58. https://doi.org/10.1016/j.cellsig.2017.02.005

Leclerc, G., Mou, C., Leclerc, G., Mian, A., & Barredo, J. (2010). Histone deacetylase inhibitors induce FPGS mRNA expression and intracellular accumulation of long-chain methotrexate polyglutamates in childhood acute lymphoblastic leukemia: implications for combination therapy. *Leukemia.*, *24*(3), 552–62.

Lee, J., Park, J., Jung, Y., Kim, J., Jong, H., Kim, T., & Bang, Y. (2006). Histone deacetylase inhibitor enhances 5-fluorouracil cytotoxicity by down-regulating thymidylate synthase in human cancer cells. *Mol Cancer Ther.*, *5*(12), 3085–3095. https://doi.org/10.1158/1535-7163.MCT-06-0419

Leemans, C. R., Braakhuis, B. J. M., & Brakenhoff, R. H. (2011). The molecular biology of head and neck cancer. *Nature Reviews. Cancer*, *11*(1), 9–22. https://doi.org/10.1038/nrc2982

Leichman, C., Lenz, H., Leichman, L., Danenberg, K., Baranda, J., Groshen, S., … Danenberg, P. (1997). Quantitation of intratumoral thymidylate synthase expression predicts for disseminated colorectal cancer response and resistance to protracted-infusion fluorouracil and weekly leucovorin. *J Clin Oncol.*, *15*(10), 3223–9.

Levy, A., Sather, H., Steinherz, P., Sowers, R., La, M., Moscow, J., … Study, C. C. G. (2003). Reduced folate carrier and dihydrofolate reductase expression in acute lymphocytic leukemia may predict outcome: a Children's Cancer Group Study. *J Pediatr Hematol Oncol.*, *25*(9), 688–95.

Li, B., Lu, Q., Song, Z.-G., Yang, L., Jin, H., Li, Z.-G., … Xu, Z.-Y. (2013). Functional analysis of DNA methylation in lung cancer. *European Review for Medical and Pharmacological Sciences*, *17*(9), 1191–1197.

Li, Q., Lambrechts, M. J., Zhang, Q., Liu, S., Ge, D., Yin, R., … You, Z. (2013). Glyphosate and AMPA inhibit cancer cell growth through inhibiting intracellular glycine synthesis. *Drug Design, Development and Therapy*, *7*, 635–643.

Li, T., Gao, F., & Zhang, X. (2015). miR-203 enhances chemosensitivity to 5-fluorouracil by targeting thymidylate synthase in colorectal cancer. *Oncol Rep.*, *33*(2), 607–14.

Liani, E., Rothem, L., Bunni, M., Smith, C., Jansen, G., & Assaraf, Y. (2003). Loss of folylpoly-gamma-glutamate synthetase activity is a dominant mechanism of resistance to polyglutamylation-dependent novel antifolates in multiple human leukemia sublines. *Int J Cancer.*, *103*(5), 587–99.

Libbus, B. L., Borman, L. S., Ventrone, C. H., & Branda, R. F. (1990). Nutritional folate-

deficiency in Chinese hamster ovary cells. Chromosomal abnormalities associated with perturbations in nucleic acid precursors. *Cancer Genetics and Cytogenetics*, *46*(2), 231–242. https://doi.org/10.1016/0165-4608(90)90108-M

Liloglou, T., Bediaga, N. G., Brown, B. R. B., Field, J. K., & Davies, M. P. A. (2014). Epigenetic biomarkers in lung cancer. *Cancer Letters*, *342*(2), 200–212. https://doi.org/10.1016/j.canlet.2012.04.018

Lin, S. H., Wang, J., Saintigny, P., Wu, C.-C., Giri, U., Zhang, J., … Heymach, J. V. (2014). Genes suppressed by DNA methylation in non-small cell lung cancer reveal the epigenetics of epithelial–mesenchymal transition. *BMC Genomics*, *15*(1), 1079. https://doi.org/10.1186/1471-2164-15-1079

Liu, H., Jin, G., Wang, H., Wu, W., Liu, Y., Qian, J., … Lu, D. (2008). Association of polymorphisms in one-carbon metabolizing genes and lung cancer risk: a case-control study in Chinese population. *Lung Cancer*, *61*(1), 21–29. https://doi.org/10.1016/j.lungcan.2007.12.001

Liu, J., & Ward, R. L. (2010). *Folate and One-Carbon Metabolism and Its Impact on Aberrant DNA Methylation in Cancer*. *Advances in Genetics* (1st ed., Vol. 71). Elsevier Inc. https://doi.org/10.1016/B978-0-12-380864-6.00004-3

Liu, S., Fabbri, M., Gitlitz, B., & ILaird-Offringa, I. (2013). Epigenetic therapy in lung cancer. *Frontiers in Oncology*, *3*.

Liu, X., Szebenyi, D. M. E., Thiel, D. J., & Stover, P. J. (2001). Lack of Catalytic Activity of a Murine mRNA Cytoplasmic Serine Hydroxymethyltransferase Splice Variant : Evidence against Alternative Splicing as a Regulatory Mechanism †. *Biochemistry*, *10*, 4932–4939.

Liu, Z.-B., Wang, L.-P., Shu, J., Jin, C., & Lou, Z.-X. (2013). Methylenetetrahydrofolate reductase 677TT genotype might be associated with an increased lung cancer risk in Asians. *Gene*, *515*(1), 214–9. https://doi.org/10.1016/j.gene.2012.11.036

Longley, D., Harkin, D., & Johnston, P. (2003). 5-fluorouracil: mechanisms of action and clinical strategies. *Nat Rev Cancer.*, *3*(5), 330–8.

Lopez-Serra, L., & Esteller, M. (2008). Proteins that bind methylated DNA and human cancer: reading the wrong words. *British Journal of Cancer*, *98*(12), 1881–1885. https://doi.org/10.1038/sj.bjc.6604374

Lucock, M. (2000). Folic acid: nutritional biochemistry, molecular biology, and role in disease processes. *Molecular Genetics and Metabolism*, *71*(1–2), 121–38. https://doi.org/10.1006/mgme.2000.3027

Luka, Z., Moss, F., Loukachevitch, L., Bornhop, D., & Wagner, C. (2011). Histone demethylase LSD1 is a folate-binding protein. *Biochemistry*, *50*(21), 4750–6.

MacFarlane, A. J., Anderson, D. D., Flodby, P., Perry, C. A., Allen, R. H., Stabler, S. P., & Stover, P. J. (2011a). Nuclear localization of de Novo thymidylate biosynthesis pathway is required to prevent uracil accumulation in DNA. *Journal of Biological Chemistry*, *286*(51), 44015–44022. https://doi.org/10.1074/jbc.M111.307629

MacFarlane, A. J., Anderson, D. D., Flodby, P., Perry, C. A., Allen, R. H., Stabler, S. P., & Stover,

P. J. (2011b). Nuclear Localization of de Novo Thymidylate Biosynthesis Pathway Is Required to Prevent Uracil Accumulation in DNA *. https://doi.org/10.1074/jbc.M111.307629

Marcus, M., Chen, Y., Liloglou, T., & Field, J. (2013). New perspectives to respiratory tract cancers. *Oncol Feb*, *275*(3).

Marcus, M. W., Chen, Y., Raji, O. Y., Duffy, S. W., & Field, J. K. (2015). LLPi : Liverpool Lung Project Risk Prediction Model for Lung Cancer Incidence. *Cancer Prevention Research*, *8*(6). https://doi.org/10.1158/1940-6207.CAPR-14-0438

Marignani, P. A. (2005). LKB1, the multitasking tumour suppressor kinase. *Journal of Clinical Pathology*, *58*(1), 15–9. https://doi.org/10.1136/jcp.2003.015255

Markovic, J., Borrás, C., Ortega, Á., Sastre, J., Viña, J., & Pallardó, F. V. (2007). Glutathione Is Recruited into the Nucleus in Early Phases of Cell Proliferation. *THE JOURNAL OF BIOLOGICAL CHEMISTRY*, *282*(28), 20416–20424.

Marsh, S. (2005). Thymidylate synthase pharmacogenetics. *Investigational New Drugs*, *23*(6), 533–537. https://doi.org/10.1007/s10637-005-4021-7

Martin, D. I. K., Cropley, J. E., & Suter, C. M. (2011). Epigenetics in disease: Leader or follower? *Epigenetics*, *6*(7), 843–848. https://doi.org/10.4161/epi.6.7.16498

Marur, S., & Forastiere, A. A. (2016). Head and Neck Squamous Cell Carcinoma: Update on Epidemiology, Diagnosis, and Treatment. *Mayo Clinic Proceedings*, *91*(3), 386–396. https://doi.org/10.1016/j.mayocp.2015.12.017

Matherly, L. H., Hou, Z., & Deng, Y. (2007). Human reduced folate carrier: Translation of basic biology to cancer etiology and therapy. *Cancer and Metastasis Reviews*, *26*(1), 111–128. https://doi.org/10.1007/s10555-007-9046-2

Matsumoto, S., Iwakawa, R., Takahashi, K., Kohno, T., Nakanishi, Y., Matsuno, Y., … Yokota, J. (2007). Prevalence and specificity of LKB1 genetic alterations in lung cancers. *Oncogene. 2007 August 30; 26(40): 5911–5918. doi:10.1038/sj.onc.1210418.*, *40*(26), 5911–5918. https://doi.org/10.1016/j.immuni.2010.12.017.Two-stage

Mauritz, R., Peters, G., Priest, D., Assaraf, Y., Drori, S., Kathmann, I., … Jansen, G. (2002). Multiple mechanisms of resistance to methotrexate and novel antifolates in human CCRF-CEM leukemia cells and their implications for folate homeostasis. *Biochem Pharmacol.*, *63*(2), 105–15.

McBurney, M., & Whitmore, G. (1975). Mechanism of growth inhibition by methotrexate. *Cancer Res.*, *35*(3), 586–90.

McElnay, P., & Lim, E. (2014). Adjuvant or neoadjuvant chemotherapy for NSCLC. *Journal of Thoracic Disease*, *6*(SUPPL.2), 224–227. https://doi.org/10.3978/j.issn.2072-1439.2014.04.26

Mehta, A., Dobersch, S., Romero-Olmedo, A. J., & Barreto, G. (2015). Epigenetics in lung cancer diagnosis and therapy. *Cancer and Metastasis Reviews*, *34*(2), 229–241. https://doi.org/10.1007/s10555-015-9563-3

Mentch, S. J., & Locasale, J. W. (2016). One-carbon metabolism and epigenetics: understanding the specificity. *Annals of the New York Academy of Sciences*, *1363*(1), 91–8. https://doi.org/10.1111/nyas.12956

Merlo, A., Herman, J., Mao, L., Lee, D., Gabrielson, E., Burger, P., … Sidransky, D. (1995). 5' CpG island methylation is associated with transcriptional silencing of the tumour suppressor p16/CDKN2/MTS1 in human cancers. *Nat Med*, *1*(7), 686–92.

Meulendijks, D., Henricks, L., Sonke, G., Deenen, M., Froehlich, T., Amstutz, U., … Schellens, J. (2015). Clinical relevance of DPYD variants c.1679T>G, c.1236G>A/HapB3, and c.1601G>A as predictors of severe fluoropyrimidine-associated toxicity: a systematic review and meta-analysis of individual patient data. *Lancet Oncol.*, *16*(16), 1639–50.

Milano, G. A. (2015). Targeted therapy in non-small cell lung cancer: a focus on epidermal growth factor receptor mutations. *Chin Clin Oncol*, *4*(4), 47. https://doi.org/10.3978/j.issn.2304-3865.2015.12.04

Miles, E. W., & Kraus, J. P. (2004). Cystathionine B-synthase: Structure, function, regulation, and location of homocystinuria-causing mutations. *Journal of Biological Chemistry*, *279*(29), 29871–29874. https://doi.org/10.1074/jbc.R400005200

Mirza, S., Sharma, G., & Pandya, P. (2010). Demethylating agent 5-aza-2-deoxycytidine enhances susceptibility of breast cancer cells to anticancer agents. *Mol Cell Biochem*, *342*, 101–109. https://doi.org/10.1007/s11010-010-0473-y

Mitchell, K., Snell, E., & Williams, J. (1941). The concentration of "folic acid". *Journal of the American Chemical Society.*, *63*, 2284. https://doi.org/10.1021/ja01853a512

Mojard, L., Botet, J., Quintales, L., Moreno, S., & Salas, M. (2013). New Insights into the RNA-Based Mechanism of Action of the Anticancer Drug 5 9 -Fluorouracil in Eukaryotic Cells. *PLoS One*, *8*(11). https://doi.org/10.1371/journal.pone.0078172

Momparler, R., Bouffard, D., Momparler, L., Dionne, J., Belanger, K., & Ayoub, J. (1997). Pilot phase I-II study on 5-aza-2'-deoxycytidine (Decitabine) in patients with metastatic lung cancer. *Anticancer Drugs.*, *8*(4), 358–68.

Morales, C., García, M., Ribas, M., Miró, R., Muñoz, M., Caldas, C., & Peinado, M. (2009). Dihydrofolate reductase amplification and sensitization to methotrexate of methotrexate-resistant colon cancer cells. *Mol Cancer Ther.*, *8*(2), 424–32.

Moran, D., Trusk, P. B., Pry, K., Paz, K., Sidransky, D., & Bacus, S. S. (2014). KRAS Mutation Status Is Associated with Enhanced Dependency on Folate Metabolism Pathways in Non-Small Cell Lung Cancer Cells. *Molecular Cancer Therapeutics*, *13*(6), 1611–24. https://doi.org/10.1158/1535-7163.MCT-13-0649

Moran, R., Mulkins, M., & Heidelberger, C. (1979). Role of thymidylate synthetase activity in development of methotrexate cytotoxicity. *Proc Natl Acad Sci U S A.*, *76*(11), 5924–8.

Morita, S., Iida, S., Kato, K., Takagi, Y., Uetake, H., & Sugihara, K. (2006). The synergistic effect of 5-aza-2'-deoxycytidine and 5-fluorouracil on drug-resistant tumors. *Oncology.*, *71*(5–6), 437–45.

Mudd, S. H., Brosnan, J. T., Brosnan, M. E., Jacobs, R. L., Stabler, S. P., Allen, R. H., … Wagner,

C. (2007). Methyl balance and transmethylation fluxes in humans. *American Journal of Clinical Nutrition*, *85*(1), 19–25. https://doi.org/85/1/19 [pii]

Muhale, F. A., Wetmore, B. A., Thomas, R. S., & McLeod, H. L. (2011). Systems pharmacology assessment of the 5-fluorouracil pathway. *Pharmacogenomics*, *12*(3), 341–350. https://doi.org/10.2217/pgs.10.188.Systems

Mutze, K., Langer, R., Schumacher, F., Becker, K., Ott, K., Novotny, A., … Keller, G. (2011). DNA methyltransferase 1 as a predictive biomarker and potential therapeutic target for chemotherapy in gastric cancer. *European Journal of Cancer*, *47*(12), 1817–1825. https://doi.org/10.1016/j.ejca.2011.02.024

Nakano, M., Fukami, T., Gotoh, S., & Nakajima, M. (2017). A-to-I RNA Editing Up-regulates Human Dihydrofolate Reductase in Breast Cancer. *J Biol Chem.*, *292*(12), 4873–4884.

Navada, S. C., Steinmann, J., Lübbert, M., & Silverman, L. R. (2014). Clinical development of demethylating agents in hematology. *The Journal of Clinical Investigation*, *124*(1), 40–46.

Ndiaye, C., Mena, M., Alemany, L., Arbyn, M., Castellsagué, X., Laporte, L., … Trottier, H. (2014). HPV DNA, E6/E7 mRNA, and p16INK4a detection in head and neck cancers: a systematic review and meta-analysis. *Lancet Oncol.*, *15*(12), 1319–31.

Noro, R., Miyanaga, A., Minegishi, Y., Okano, T., Seike, M., Soeno, C., … Gemma, A. (2010). Histone deacetylase inhibitor enhances sensitivity of non-small-cell lung cancer cells to 5-FU／S-1 via down-regulation of thymidylate synthase expression and up-regulation of p21. *Cancer Science*, *101*(6), 1424–30. https://doi.org/10.1111/j.1349-7006.2010.01559.x

Ocker, M., Alajati, A., Ganslmayer, M., Zopf, S., Lu, M., Neureiter, D., … Herold, C. (2005). The histone-deacetylase inhibitor SAHA potentiates proapoptotic effects of 5-fluorouracil and irinotecan in hepatoma cells. *J Cancer Res Clin Oncol*, *131*, 385–394. https://doi.org/10.1007/s00432-004-0664-6

Oguri, T., Achiwa, H., Bessho, Y., Muramatsu, H., Maeda, H., Niimi, T., … Ueda, R. (2005). The role of thymidylate synthase and dihydropyrimidine dehydrogenase in resistance to 5-fluorouracil in human lung cancer cells. *Lung Cancer*, *49*(3), 345–351. https://doi.org/10.1016/j.lungcan.2005.05.003

Okano, M., Xie, S., & Li, E. (1998). Cloning and characterization of a family of novel mammalian DNA (cytosine-5) methyltransferases. *Nat Genet.*, *19*(3), 219–20.

Olaussen, K. A., & Postel-Vinay, S. (2016). Predictors of chemotherapy efficacy in non-small-cell lung cancer: a challenging landscape. *Ann Oncol.*, *27*(11).

Ong, T. P., Moreno, F. S., & Ross, S. A. (2012). Targeting the epigenome with bioactive food components for cancer prevention. *Journal of Nutrigenetics and Nutrigenomics*, *4*(5), 275–292. https://doi.org/10.1159/000334585

Osada, H., & Takahashi, T. (2002). Genetic alterations of multiple tumor suppressors and oncogenes in the carcinogenesis and progression of lung cancer. *Oncogene*, *21*(48), 7421–7434. https://doi.org/10.1038/sj.onc.1205802

Oshiro, Y., & Sakurai, H. (2013). The use of proton-beam therapy in the treatment of non-

small-cell lung cancer. *Expert Review of Medical Devices*, *10*(2), 239–245. https://doi.org/10.1586/erd.12.81

Ozasa, H., Oguri, T., Uemura, T., Miyazaki, M., Maeno, K., Sato, S., & Ueda, R. (2010). Significance of thymidylate synthase for resistance to pemetrexed in lung cancer. *Cancer Sci*, *101*(1), 161–166.

Package, V., Lorenz, R., Bernhart, S. H., Höner, C., Tafer, H., & Flamm, C. (2011). ViennaRNA Package 2.0. *Algorithms Mol Biol*, *6*(26).

Pagliara, V., Saide, A., Mitidieri, E., Bianca, V., Sorrentino, R., Russo, G., & Russo, A. (2016). 5-FU targets rpL3 to induce mitochondrial apoptosis via cystathionine-β-synthase in colon cancer cells lacking p53, *7*(31).

Pai, S. I., & Westra, W. H. (2009). Moleccular Pathology of Head and Neck Cancer:Implications for Diagnosis, Prognosis and Treatment. *Annu. Rev. Pathol.*, *4*, 49–70. https://doi.org/10.1146/annurev.pathol.4.110807.092158.Molecular

Pandey, S., Garg, P., Lee, S., Choung, H., Choung, Y., Choung, P., & Hoon, J. (2014). Nucleotide biosynthesis arrest by silencing SHMT1 function via vitamin B 6 -coupled vector and effects on tumor growth inhibition. *Biomaterials*, *35*(34), 9332–9342. https://doi.org/10.1016/j.biomaterials.2014.07.045

Paone, A., Marani, M., Fiascarelli, A., Rinaldo, S., Giardina, G., Contestabile, R., … Cutruzzolà, F. (2014). SHMT1 knockdown induces apoptosis in lung cancer cells by causing uracil misincorporation, 1–11. https://doi.org/10.1038/cddis.2014.482

Parajuli, K. R., Zhang, Q., Liu, S., & You, Z. (2016). Aminomethylphosphonic acid inhibits growth and metastasis of human prostate cancer in an orthotopic xenograft mouse model. *Oncotarget*, *7*(9).

Passetti, F., Ferreira, C., & Costa, F. (2009). The impact of microRNAs and alternative splicing in pharmacogenomics. *Pharmacogenomics J.*, *9*(1), 1–13.

Pastuszak-Lewandoska, D., Kordiak, J., Migdalska-Sęk, M., Czarnecka, K., Antczak, A., Górski, P., … Brzeziańska-Lasota, E. (2015). Quantitative analysis of mRNA expression levels and DNA methylation profiles of three neighboring genes: FUS1, NPRL2/G21 and RASSF1A in non-small cell lung cancer patients. *Respir Res.*, *16*(76).

Piskac-Collier, A. L., Monroy, C., Lopez, M. S., Cortes, A., Etzel, C. J., Greisinger, A. J., … El-Zein, R. A. (2011). Variants in Folate Pathway Genes as Modulators of Genetic Instability and Lung Cancer Risk. *Genes, Chromosomes & Cancer*, *50*, 1–12. https://doi.org/10.1002/gcc

Ponomaryova, A., Rykova, E., Cherdyntseva, N., Skvortsova, T., Dobrodeev, A., Zav'yalov, A., … Laktionov, P. (2011). RARβ2 gene methylation level in the circulating DNA from blood of patients with lung cancer. *Eur J Cancer Prev.*, *20*(6), 453–5.

Portela, A., & Esteller, M. (2010). Epigenetic modifications and human disease. *Nature Biotechnology*, *28*(10), 1057–1068. https://doi.org/10.1038/nbt.1685

Price, K. A. R., & Cohen, E. E. (2012). Current treatment options for metastatic head and neck cancer. *Current Treatment Options in Oncology*, *13*(1), 35–46. https://doi.org/10.1007/s11864-011-0176-y

Protiva, P., Mason, J., Liu, Z., Hopkins, M., Nelson, C., Marshall, J., … Holt, P. (2011). Altered folate availability modifies the molecular environment of the human colorectum: implications for colorectal carcinogenesis. *Cancer Prev Res (Phila)*, *4*(4), 530–43.

Prudova, A., Albin, M., Bauman, Z., Lin, A., Vitvitsky, V., & Banerjee, R. (2007). Testosterone regulation of homocysteine metabolism modulates redox status in human prostate cancer cells. *Antioxid Redox Signal.*, *9*(11), 1875–81.

Pulte, D., & Brenner, H. (2010). Changes in survival in head and neck cancers in the late 20th and early 21st century: a period analysis. *The Oncologist*, *15*(9), 994–1001. https://doi.org/10.1634/theoncologist.2009-0289

Qiu, A., Jansen, M., Sakaris, A., Min, S. H., Chattopadhyay, S., Tsai, E., … Goldman, I. D. (2006). Identification of an Intestinal Folate Transporter and the Molecular Basis for Hereditary Folate Malabsorption. *Cell*, *127*(5), 917–928. https://doi.org/10.1016/j.cell.2006.09.041

Quinlivan, E. P., Davis, S. R., Shelnutt, K. P., Henderson, G. N., Ghandour, H., Shane, B., … Gregory, J. F. (2005). Methylenetetrahydrofolate reductase 677C->T polymorphism and folate status affect one-carbon incorporation into human DNA deoxynucleosides. *The Journal of Nutrition*, *135*(3), 389–96. https://doi.org/135/3/389 [pii]

Raz, S., Stark, M., & Assaraf, Y. G. (2016). Folylpoly-gamma-glutamate synthetase: A key determinant of folate homeostasis and antifolate resistance in cancer. *Drug Resistance Updates*, *28*, 43–64.

Refsum, H., Smith, A., Ueland, P., Nexo, E., Clarke, R., McPartlin, J., … Scott, J. (2004). Facts and recommendations about total homocysteine determinations: an expert opinion. *Clin Chem. 2004 Jan;50(1):3-32*, *50*(1), 3–32.

Rekhtman, N. (2010). Neuroendocrine Tumors of the Lung An Update. *Arch Pathol Lab Med*, *134*, 1628–1638. https://doi.org/10.1043/2009-0583-RAR.1

Rieke, D. T., Klinghammer, K., & Keilholz, U. (2016). Targeted Therapy of Head and Neck Cancer. *Oncology Research and Treatment*, *39*(12), 780–786. https://doi.org/10.1159/000452432

Rijavec, E., Biello, F., Genova, C., Barletta, G., Maggioni, C., Dal Bello, M. G., … Grossi, F. (2013). Pemetrexed for the treatment of non-small cell lung cancer. *Expert Opin. Pharmacother.*, *14*(11), 1545–1558. https://doi.org/https://dx.doi.org/10.1517/14712598.2015.1073709

Risch, A., & Plass, C. (2008). Lung cancer epigenetics and genetics. *International Journal of Cancer*, *123*(1), 1–7. https://doi.org/10.1002/ijc.23605

Robertson, K. D. (2001). DNA methylation, methyltransferases, and cancer. *Oncogene*, *20*, 3139–3155.

Robertson, K. D. (2005). DNA methylation and human disease. *Nature Reviews Genetics*, *6*. https://doi.org/10.1038/nrg1655

Robien, K., Boynton, A., & Ulrich, C. M. (2005). Pharmacogenetics of folate-related drug targets in cancer treatment. *Pharmacogenomics*, *6*(7), 673–689. https://doi.org/10.2217/14622416.6.7.673

Russo, A., Saide, A., Cagliani, R., Cantile, M., Botti, G., & Russo, G. (2016). rpL3 promotes the apoptosis of p53 mutated lung cancer cells by down- regulating CBS and NF κ B upon 5-FU treatment. *Scientific Reports*, *6*, 1–13. https://doi.org/10.1038/srep38369

Russom, A., Tooke, N., Andersson, H., & Stemme, G. (2005). Pyrosequencing in a Microfluidic Flow-Through Device. *Anal. Chem.*, *77*(23), 7505–7511. https://doi.org/10.1021/ac0507542

Sacco, A. G., & Cohen, E. E. (2015). Current Treatment Options for Recurrent or Metastatic Head and Neck Squamous Cell Carcinoma. *Journal of Clinical Oncology : Official Journal of the American Society of Clinical Oncology*, *33*(29), 3305–13. https://doi.org/10.1200/JCO.2015.62.0963

Safdari, Y., Khalili, M., Farajnia, S., Asgharzadeh, M., Yazdani, Y., & Sadeghi, M. (2014). Recent advances in head and neck squamous cell carcinoma - A review. *Clinical Biochemistry*, *47*(13–14), 1195–1202. https://doi.org/10.1016/j.clinbiochem.2014.05.066

Salbaum, J. M., & Kappen, C. (2012). Genetic and epigenomic footprints of folate. *Progress in Molecular Biology and Translational Science*, *108*, 129–158. https://doi.org/10.1016/B978-0-12-398397-8.00006-X

Salonga, D., Danenberg, K., Johnson, M., Metzger, R., Groshen, S., Tsao-Wei, D., … Danenberg, P. (2000). Colorectal tumors responding to 5-fluorouracil have low gene expression levels of dihydropyrimidine dehydrogenase, thymidylate synthase, and thymidine phosphorylase. *Clin Cancer Res.*, *6*(4), 1322–7.

Sandoval, J., Mendez-gonzalez, J., Nadal, E., Chen, G., Carmona, F. J., Sayols, S., … Beer, D. G. (2013). A Prognostic DNA Methylation Signature for Stage I Non – Small-Cell Lung Cancer. *Journal of Clinical Oncology*, *31*(32). https://doi.org/10.1200/JCO.2012.48.5516

Sandoval, J., Peiró-Chova, L., Pallardó, F. V, & García-Giménez, J. L. (2013). Epigenetic biomarkers in laboratory diagnostics: emerging approaches and opportunities. *Expert Review of Molecular Diagnostics*, *13*(5), 457–471. https://doi.org/10.1586/erm.13.37

Santi, D., & McHenry, C. (1972). 5-Fluoro-2'-deoxyuridylate: covalent complex with thymidylate synthetase. *Proc Natl Acad Sci U S A.*, *69*(7), 1855–7.

Santi, D., McHenry, C., & Sommer, H. (1974). Mechanism of interaction of thymidylate synthetase with 5-fluorodeoxyuridylate. *Biochemistry.*, *13*(3), 471–81.

Saxonov, S., Berg, P., & Brutlag, D. L. (2006). A genome-wide analysis of CpG dinucleotides in the human genome distinguishes two distinct classes of promoters. *Proceedings of the National Academy of Sciences*, *103*(5), 1412–1417. https://doi.org/10.1073/pnas.0510310103

Scaglione, F., & Panzavolta, G. (2014). Folate, folic acid and 5-methyltetrahydrofolate are not the same thing. *Xenobiotica*, *44*(5), 480–488. https://doi.org/10.3109/00498254.2013.845705

Scartozzi, M., Maccaroni, E., Giampieri, R., Pistelli, M., Bittoni, A., Del Prete, M., … Cascinu, S. (2011). 5-Fluorouracil Pharmacogenomics: Still Rocking After All These Years? *Pharmacogenomics*, *12*(2), 251–265. https://doi.org/10.2217/pgs.10.167

Schmid, K., Oehl, N., Wrba, F., Pirker, R., Pirker, C., & Filipits, M. (2009). EGFR/KRAS/BRAF mutations in primary lung adenocarcinomas and corresponding locoregional lymph node metastases. *Clin Cancer Res*, *15*(14), 4554–60.

Schrump, D., Fischette, M., Nguyen, D., Zhao, M., Li, X., Kunst, T., … Steinberg, S. (2006). Phase I study of decitabine-mediated gene expression in patients with cancers involving the lungs, esophagus, or pleura. *Clin Cancer Res.*, *12*(19), 5777–85.

Schubbert, S., Shannon, K., & Bollag, G. (2007). Hyperactive Ras in developmental disorders and cancer. *Nature Reviews. Cancer*, *7*(4), 295–308. https://doi.org/10.1038/nrc2109

Schuler, P., Trellakis, S., Greve, J., Bas, M., Bergmann, C., Bölke, E., … Hoffmann, T. (2010). In vitro chemosensitivity of head and neck cancer cell lines. *Eur J Med Res.*, *15*(8), 337–44.

Schwerk, C., & Schulze-Osthoff, K. (2005). Regulation of apoptosis by alternative pre-mRNA splicing. *Mol Cell.*, *19*(1), 1–13.

Scionti, I., Michelacci, F., Pasello, M., Hattinger, C., Alberghini, M., Manara, M., … Serra, M. (2008). Clinical impact of the methotrexate resistance-associated genes C-MYC and dihydrofolate reductase (DHFR) in high-grade osteosarcoma. *Ann Oncol.*, *19*(8), 1500–8.

Scotti, M., Stella, L., Shearer, E. J., & Stover, P. J. (2013). Modeling cellular compartmentation in one-carbon metabolism. *Wiley Interdisciplinary Reviews: Systems Biology and Medicine*, *5*(3), 343–365. https://doi.org/10.1002/wsbm.1209

Sen, S., Kawahara, B., Gupta, D., Tsai, R., Khachatryan, M., Roy-Chowdhuri, S., … Chaudhuri, G. (2015). Role of cystathionine B-synthase in human breast Cancer. *Free Radical Biology and Medicine*, *86*, 228–238. https://doi.org/10.1016/j.freeradbiomed.2015.05.024

Shafran, A., Ifergan, I., Bram, E., Jansen, G., Kathmann, I., Peters, G., … Assaraf, Y. (2005). ABCG2 harboring the Gly482 mutation confers high-level resistance to various hydrophilic antifolates. *Cancer Res.*, *65*(18), 8414–22.

Shah, A. A., Jeffus, S. K., & Stelow, E. B. (2014). Squamous cell carcinoma variants of the upper aerodigestive tract: a comprehensive review with a focus on genetic alterations. *Archives of Pathology & Laboratory Medicine*, *138*(6), 731–44. https://doi.org/10.5858/arpa.2013-0070-RA

Sharma, S., Kelly, T. K., & Jones, P. A. (2010). Epigenetics in cancer. *Carcinogenesis*, *31*(1), 27–36. https://doi.org/10.1093/carcin/bgp220

Shen, M., Rothman, N., Berndt, S. I., He, X., Yeager, M., Welch, R., … Lan, Q. (2005). Polymorphisms in folate metabolic genes and lung cancer risk in Xuan Wei, China. *Lung Cancer*, *49*(3), 299–309. https://doi.org/10.1016/j.lungcan.2005.04.002

Shi, L., Wu, L., Chen, Z., Yang, J., Chen, X., Yu, F., … Lin, X. (2015). MiR-141 Activates Nrf2-Dependent Antioxidant Pathway via Down-Regulating the Expression of Keap1 Conferring the Resistance of Hepatocellular Carcinoma Cells to 5-Fluorouracil. *Cell Physiol Biochem.*, *35*(6), 2333–48.

Shi, Q., Zhang, Z., Neumann, A. S., Li, G., Spitz, M. R., & Wei, Q. (2005). Case-control analysis of thymidylate synthase polymorphisms and risk of lung cancer. *Carcinogenesis*, *26*(3), 649–656. https://doi.org/10.1093/carcin/bgh351

Shimizu, T., Nakanishi, Y., Nakagawa, Y., Tsujino, I., Takahashi, N., Nemoto, N., & Hashimoto, S. (2012). Association between expression of thymidylate synthase, dihydrofolate reductase, and glycinamide ribonucleotide formyltransferase and efficacy of pemetrexed in advanced non-small cell lung cancer. *Anticancer Research*, *32*(10), 4589–4596. https://doi.org/32/10/4589 [pii]

Shookhoff, J., & Gallicano, G. (2010). A new perspective on neural tube defects: folic acid and microRNA misexpression. *Genesis.*, *48*(5), 282–94.

Shultz, D. B., Filippi, A. R., Thariat, J., Mornex, F., Loo, B. W., & Ricardi, U. (2014). Stereotactic Ablative Radiotherapy for Pulmonary Oligometastases and Oligometastatic Lung Cancer. *Journal of Thoracic Oncology*, *9*(10), 1426–1433. https://doi.org/10.1097/JTO.0000000000000317

Singh, S., & Banerjee, R. (2011). PLP-dependent H2S Biogenesis. *Biochim Biophys Acta*, *1814*(11), 1518–1527.

Sodani, K., Patel, A., Kathawala, R. J., & Chen, Z. S. (2012). Multidrug resistance associated proteins in multidrug resistance. *Chinese Journal of Cancer*, *3*(2).

Sommer, H., & Santi, D. (1974). PURIFICATION AND AMINO ACID ANALYSIS OF AN ACTIVE SITE PEPTIDE FROM THYMIDYLATE SYNTHETASE CONTAINING COVALENTLY BOUND 5-FLUORO-2'-DEOXYURIDYLATE AND METHYLENETETRAHYDROFOLATE. *BIOCHEMICAL AND BIOPHYSICAL RESEARCH COMMUNICATIONS.*, *57*(3).

Stead, L. M., Jacobs, R. L., Brosnan, M. E., & Brosnan, J. T. (2004). Methylation demand and homocysteine metabolism. *Advances in Enzyme Regulation*, *44*(1), 321–333. https://doi.org/10.1016/j.advenzreg.2003.11.012

Steinhardt, J. J., & Gartenhaus, R. B. (2013). Epigenetic approaches for chemo-sensitization of refractory diffuse large B-cell lymphomas. *Cancer Discov.*, *3*(9).

Stephan, L., & Momparler, R. L. (2015). Combination chemotherapy of cancer using the inhibitor of DNA methylation 5-aza-2'-deoxycytidine (decitabine). *Journal of Cancer Research & Therapy*, *3*(5), 56–65.

Stern, L. L., Mason, J. B., Selhub, J., Gene, M. R., Stern, L. L., Mason, J. B., … Choi, S. (2000). Genomic DNA Hypomethylation , a Characteristic of Most Cancers , Is Present in Peripheral Leukocytes of Individuals Who Are Homozygous for the C677T Polymorphism in the Methylenetetrahydrofolate Reductase Gene Genomic DNA Hypomethylation , a Characteristi, *9*(August), 849–853.

Stover, P., Chen, L., Suh, J., Stover, D., Keyomarsi, K., & Shane, B. (1977). Molecular cloning, characterization, and regulation of the human mitochondrial serine hydroxymethyltransferase gene. *J Biol Chem. 1997 Jan 17;272(3):1842-8.*, *272*(3), 1842–8.

Subramaniam, D., Thombre, R., Dhar, A., & Anant, S. (2014). DNA Methyltransferases: A Novel Target for Prevention and Therapy. *Frontiers in Oncology*, *4*(May), 1–13. https://doi.org/10.3389/fonc.2014.00080

Sun, S., Shi, W., Wu, Z., Zhang, G., Yang, B., & Jiao, S. (2015). Prognostic significance of the mRNA expression of ERCC1, RRM1, TUBB3 and TYMS genes in patients with non-small

cell lung cancer. *Experimental and Therapeutic Medicine*, *10*(3), 937–941. https://doi.org/10.3892/etm.2015.2636

Sun, W., Kim, H., Jung, W., & Koo, J. (2016). Expression of serine/glycine metabolism-related proteins is different according to the thyroid cancer subtype. *J Transl Med.*, *14*(1), 168.

Szabo, C., Coletta, C., Chao, C., Módis, K., Szczesny, B., & Papapetropoulos, A. (2013). Tumor-derived hydrogen sul fi de, produced by cystathionine- β -synthase, stimulates bioenergetics, cell proliferation, and angiogenesis in colon cancer, *110*(30). https://doi.org/10.1073/pnas.1306241110/-/DCSupplemental.www.pnas.org/cgi/doi/10.1073/pnas.1306241110

Szabo, E., Mao, J. T., Lam, S., Reid, M. E., & Keith, R. L. (2013). Chemoprevention of lung cancer: Diagnosis and management of lung cancer, 3rd ed: American college of chest physicians evidence-based clinical practice guidelines. *Chest*, *143*(5). https://doi.org/10.1378/chest.12-2348

Taddia, L., D'Arca, D., Ferrari, S., Marraccini, C., Severi, L., Ponterini, G., … Costi, M. P. (2015). Inside the biochemical pathways of thymidylate synthase perturbed by anticancer drugs: Novel strategies to overcome cancer chemoresistance. *Drug Resistance Updates*, *23*, 20–54. https://doi.org/10.1016/j.drup.2015.10.003

Tartarone, A., Giordano, P., Lerose, R., Rodriquenz, M., Conca, R., & Aieta, M. (2017). Progress and challenges in the treatment of small cell lung cancer. *Med Oncol.*, *34*(6), 110.

Tibbetts, A. S., & Appling, D. R. (2010). Compartmentalization of Mammalian folate-mediated one-carbon metabolism. *Annual Review of Nutrition*, *30*, 57–81. https://doi.org/10.1146/annurev.nutr.012809.104810

Tomasini, P., Barlesi, F., Mascaux, C., & Greillier, L. (2016). Pemetrexed for advanced stage nonsquamous non-small cell lung cancer: latest evidence about its extended use and outcomes. *Therapeutic Advances in Medical Oncology*, *8*(3), 198–208. https://doi.org/10.1177/1758834016644155

Travis, W. D., Brambilla, E., Nicholson, A. G., Yatabe, Y., M Austin, J. H., Beth Beasley, M., … Behalf of the WHO Panel, O. (2015). The 2015 World Health Organization Classification of Lung Tumors. *Journal of Thoracic Oncology*, *10*(9), 1243–1260. https://doi.org/10.1097/JTO.0000000000000630

Ulrich, C. M., & Robien, K. (2002). Pharmacogenetics and folate metabolism – a promising direction, *3*, 299–313.

Van Triest, B. (1999). Thymidylate Synthase: A Target for Combination Therapy and. *Oncology*, *57*(3).

Vermorken, J. B., Mesia, R., Rivera, F., Remenar, E., Kawecki, A., Rottey, S., … Hitt, R. (2008). Platinum based chemotherapy plus cetuximab in head and neck cancer. *N Engl J Med*, *359*, 1116–1127. https://doi.org/10.1056/NEJMoa0802656

Veronesi, G., Bottoni, E., Finocchiaro, G., & Alloisio, M. (2015). When is surgery indicated for small-cell lung cancer? *Lung Cancer*, *90*(3), 582–589. https://doi.org/10.1016/j.lungcan.2015.10.019

Vigneswaran, N., & Williams, M. (2014). Epidemiological Trends in Head and Neck Cancer and Aids in Diagnosis. *Oral Maxillofac Surg Clin North Am.*, *26*(2), 123–141.

Viktorsson, K., De Petris, L., & Lewensohn, R. (2005). The role of p53 in treatment responses of lung cancer. *Biochem Biophys Res Commun.*, *331*(3), 868–80.

Visentin, M., Zhao, R., & Goldman, I. D. (2012). The Antifolates. *Hematol Oncol Clin North Am.*, *26*(3), 629. https://doi.org/10.1016/j.hoc.2012.02.002.The

Wang, E., Sandberg, R., Luo, S., Khrebtukova, I., Zhang, L., Mayr, C., … Burge, C. (2008). Alternative isoform regulation in human tissue transcriptomes. *Nature.*, *456*(7221), 470–6.

Wang, H., Yang, T., & Wu, X. (2015). 5-Fluorouracil preferentially sensitizes mutant KRAS non-small cell lung carcinoma cells to TRAIL-induced apoptosis. *Molecular Oncology*, *9*(9), 1815–1824. https://doi.org/10.1016/j.molonc.2015.06.003

Wang, J., & Li, G. (2014). Relationship between RFC gene expression and intracellular drug concentration in methotrexate-resistant osteosarcoma cells. *Genet Mol Res.*, *13*(3), 5313–21.

Wang, L., Aakre, J., Jiang, R., Marks, R., Wu, Y., Chen, J., … Yang, P. (2010). Methylation markers for small cell lung cancer in peripheral blood leukocyte DNA. *J Thorac Oncol*, *5*(6), 778–85.

Wang, L., Lu, J., An, J., Shi, Q., Spitz, M. R., & Wei, Q. (2007). Polymorphisms of cytosolic serine hydroxymethyltransferase and risk of lung cancer: a case–control analysis. *Lung Cancer*, *57*(2), 143–151. https://doi.org/10.1038/jid.2014.371

Wang, L., Wang, R., Pan, Y., Sun, Y., Zhang, J., Chen, H., & (2014). The pemetrexed-containing treatments in the non-small cell lung cancer, is -/low thymidylate synthase expression better than +/high thymidylate synthase expression: a meta-analysis. *BMC Cancer.*, *14*(205).

Wang, T., Chuan Pan, C., Rui Yu, J., Long, Y., Hong Cai, X., De Yin, X., … Li Luo, L. (2013). Association between TYMS Expression and Efficacy of Pemetrexed-Based Chemotherapy in Advanced Non-Small Cell Lung Cancer: A Meta-Analysis. *PLoS ONE*, *8*(9). https://doi.org/10.1371/journal.pone.0074284

Wang, W.-B., Yang, Y., Zhao, Y.-P., Zhang, T.-P., Liao, Q., & Shu, H. (2014). Recent studies of 5-fluorouracil resistance in pancreatic cancer. *World J Gastroenterol.*, *20*(42), 15682–15690.

Wang, X., Yue, K., & Hao, L. (2015). Meta-analysis of methylenetetrahydrofolate reductase polymorphism and lung cancer risk in Chinese. *Int J Clin Exp Med*, *8*(1), 1521–1525.

Wills, L. (1931). Treatment of “Pernicious Anameia of Pregnancy” and “Tropical Anaemia.” *British Medical Journal*, *3676*, 1059–1064.

Wilson, A., Power, B., & Molloy, P. (2007). DNA hypomethylation and human diseases. *Biochim Biophys Acta.*, *1775*(1), 138–62.

Wilson, P., Danenberg, P., Johnston, P., Lenz, H., & Adner, R. (2014). Standing the test of time:

targeting thymidylate biosynthesis in cancer therapy. *Nat Rev Clin Oncol.*, *11*(5), 282–98.

Wohlhueter, R., Mclvor, R., & Plagemann, P. (1980). Facilitated Transport of Uracil and 5-Fluorouracil, and Permeation of Orotic Acid Into Cultured Mammalian Cells. *J Cell Physiol.*, *104*(3), 309–19.

Wojtuszkiewicz, A., Raz, S., Stark, M., Assaraf, Y., Jansen, G., Peters, G., … Cloos, J. (2016). Folylpolyglutamate synthetase splicing alterations in acute lymphoblastic leukemia are provoked by methotrexate and other chemotherapeutics and mediate chemoresistance. *Int J Cancer.*, *138*(7), 1645–56.

Wright, D. L., & Anderson, A. C. (2012). Antifolate Agents: A Patent Review (2006–2010). *Expert Opin Ther Pat*, *21*(9), 1293–1308. https://doi.org/10.1517/13543776.2011.587804.Antifolate

Wu, S., Zhang, G., Li, P., Chen, S., Zhang, F., Li, J., … Zhao, G. (2016). miR-198 targets SHMT1 to inhibit cell proliferation and enhance cell apoptosis in lung adenocarcinoma. *Tumor Biology*, *37*(4), 5193–5202. https://doi.org/10.1007/s13277-015-4369-z

Xiao, J., Peng, F., Yu, C., Wang, M., Li, X., Li, Z., … Sun, C. (2014). microRNA-137 modulates pancreatic cancer cells tumor growth, invasion and sensitivity to chemotherapy. *Int J Clin Exp Pathol.*, *7*(11), 7442–50.

Yang, M., Fan, W. F., Pu, X. L., Liu, F. Y., Meng, L. J., & Wang, J. (2014). Significance of thymidylate synthase expression for resistance to pemetrexed in pulmonary adenocarcinoma. *Oncology Letters*, *7*(1), 227–232. https://doi.org/10.3892/ol.2013.1688

Yang, X., Lay, F., Han, H., & Jones, P. A. (2010). Targeting DNA methylation for epigenetic therapy. *Trends in Pharmacological Sciences*, *31*(11), 536–546. https://doi.org/10.1016/j.tips.2010.08.001

Yang, Y., Yang, L. J., Deng, M. Z., Luo, Y. Y., Wu, S., Xiong, L., … Liu, H. (2016). MTHFR C677T and A1298C polymorphisms and risk of lung cancer: a comprehensive evaluation. *Genet Mol Res.*, *15*(2).

Yi, P., Melnyk, S., Pogribna, M., Pogribny, I. P., Hine, R. J., & James, S. J. (2000). Increase in plasma homocysteine associated with parallel increases in plasma S-adenosylhomocysteine and lymphocyte DNA hypomethylation. *Journal of Biological Chemistry*, *275*(38), 29318–29323. https://doi.org/10.1074/jbc.M002725200

Yilmaz, M., Kacan, T., Sari, I., & Kilickap, S. (2014). Lack of Association between the MTHFR C677T Polymorphism and Lung Cancer in a Turkish Population. *Asian Pac J Cancer Prev, 15 (15), 6333-6337*, *15*(15), 6333–6337.

Yip, P. Y., Yu, B., Cooper, W. A., Selinger, C. I., Ng, C. C., Kennedy, C. W., … O'Toole, S. A. (2013). Patterns of DNA mutations and ALK rearrangement in resected node negative lung adenocarcinoma. *Journal of Thoracic Oncology : Official Publication of the International Association for the Study of Lung Cancer*, *8*(4), 408–414. https://doi.org/10.1097/JTO.0b013e318283558e

Yoshida, T., Okamoto, T., Yano, T., Takada, K., Kohno, M., Suda, K., … Maehara, Y. (2016). Molecular Factors Associated with Pemetrexed Sensitivity According to Histological Type

in Non-small Cell Lung Cancer. *Anticancer Res.*, *36*(12), 6319–6326.

Zeller, C., & Brown, R. (2010). Therapeutic modulation of epigenetic drivers of drug resistance in ovarian cancer. *Therapeutic Advances in Medical Oncology*, *2*(5), 319–329. https://doi.org/10.1177/1758834010375759

Zhang, N., Yin, Y., Xu, S.-J., & Chen, W.-S. (2008). 5-Fluorouracil: Mechanisms of Resistance and Reversal Strategies. *Molecules*, *13*, 1551–1569.

Zhang, W., Braun, A., Bauman, Z., Olteanu, H., Madzelan, P., & Banerjee, R. (2005). Expression Profiling of Homocysteine Junction Enzymes in the NCI60 Panel of Human Cancer Cell Lines. *Cancer Res*, *65*(4), 1554–60.

Zhang, Y., Chen, G., Ji, Y., Huang, B., Shen, W., Deng, L., … Cao, X. (2012). Quantitative assessment of the effect of MTHFR polymorphisms on the risk of lung carcinoma. . *Mol Biol Rep.*, *39*(5), 6203–11.

Zhang, Z., Shi, Q., Sturgis, E., Spitz, M., & Wei, Q. (2005). Polymorphisms and haplotypes of serine hydroxymethyltransferase and risk of squamous cell carcinoma of the head and neck: a case-control analysis. *Pharmacogenet Genomics*, *15*(8), 557–64.

Zhao, R., Gao, F., & Goldman, I. (2001). Marked suppression of the activity of some, but not all, antifolate compounds by augmentation of folate cofactor pools within tumor cells. *Biochem Pharmacol.*, *61*(7), 857–65.

Zhao, R., & Goldman, I. D. (2003). Resistance to antifolates. *Oncogene*, *22*(47), 7431–7457. https://doi.org/10.1038/sj.onc.1206946

Zhao, R., Larry, M., & Goldman, I. D. (2013). Membrane Transporters and Folate Homeostasis; Intestinal Absorption, Transport into Systemic Compartments and Tissues. *Exp Rev Mol Med*. https://doi.org/10.1017/S1462399409000969.Membrane

Zhao, Y., Zhao, L., Ischenko, I., Bao, Q., Schwarz, B., Nieß, H., … Camaj, P. (2015). Antisense inhibition of microRNA-21 and microRNA-221 in tumor-initiating stem-like cells modulates tumorigenesis, metastasis, and chemotherapy resistance in pancreatic cancer. *Target Oncol.*, *10*(4), 535–48.

Zhou, Q., Agoston, A., Atadja, P., Nelson, W., & Davidson, N. (2008). Inhibition of histone deacetylases promotes ubiquitin-dependent proteasomal degradation of DNA methyltransferase 1 in human breast cancer cells. *Mol Cancer Res.*, *6*(5), 873–83.

Web References

1- Cancer research UK. (2014) Lung cancer incidence statistics: (Accessed 03.03.2017).

2- Cancer research UK. (2014) Cancer incidence for common cancers: (Accessed 03.03 2017).

3- Cancer research UK. (2014) Lung cancer mortality statistics: (Accessed 05.03.2017).

4- Cancer research UK. (2014) Cancer mortality for common cancers: (Accessed 05.03.2017).

5- Cancer research UK. (2014) Oral cancer incidence statistics: (Accessed 09.03.2017).

6- Cancer research UK. (2014) Oral cancer mortality statistics: (Accessed 09.03.2017).

7- Genetic Perturbation Platform. (2017) GPP Web Portal: (Accessed 06.05.2017).

8- Kaplan-Meier Plotter. (2017) Lung cancer: (Accessed 08.09.2017).

9- ViennaRNA Web Services. (2017) Institute for Theoretical Chemistry. *RNAfold* WebServer: (Accessed 07.06.2017).

10- NCBI Reference sequences. (2016) CBS cystathionine-beta-synthase [Homo sapiens (human)]: (Accessed 07.06.2017).

11- NCBI Reference sequences. (2013) SHMT1 serine hydroxymethyltransferase 1 [*Homo sapiens* (human)]: (Accessed 10.06.2017).

12- Ensembl. Gene: (2016) CBS ENSG00000160200: (Accessed 10.06.2017).

13- Ensembl. Gene: (2016) SHMT1 ENSG00000176974: (Accessed 10.06.2017).

14- The microRNA database. (2017) Search miRBase: (Accessed 09.12.2017).

15- Genomics of Drug Sensitivity in Cancer. (2017) Compound: 5-Fluorouracil: (Accessed 20.11.2017).

16- Genomics of Drug Sensitivity in Cancer. (2017) Compound: Methotrexate: (Accessed 20.11.2017).